

RESEARCH PAPER

Physiological predictions and the role of IL-10 -819 promoter polymorphism in preeclampsia

Shno Sabah Tahir^{1,3} and Mudhir Sabir Shekha^{1,2,3}

1 Department of Biology, College of Science, Salahaddin University-Erbil, 44001 Erbil, Kurdistan-Region, Iraq

2 Department of Pathological Analysis, College of Science, Knowledge University, Erbil 074016, Kurdistan-Region of Iraq, Iraq

3 Research Centre, Salahaddin University-Erbil, 44001 Erbil, Kurdistan-Region, Iraq

ABSTRACT:

Preeclampsia is a multisystem pregnancy-specific syndrome that affects some of pregnancies, which remains a leading cause of maternal and perinatal morbidity and mortality worldwide. Preeclampsia primarily provokes life-threatening, especially to the fetus. The aim of this study was to estimate some physiological and biochemical markers of preeclampsia and investigate the association between IL-10 -819 polymorphism and preeclampsia.

A total of 52 pregnant women with preeclampsia and 35 women with normal pregnancy attended the high-risk unit of Erbil Maternity and Pediatric Governmental Hospital, KRG, Iraq, were considered in the present study. During the regular pregnancy check-ups, blood pressure, occurrence of gestational hypertension (early or late onset), preeclampsia, were also documented. Remarkably, serum Urea, Creatinine, Alkaline Phosphatase (ALP) and Mean Platelet Volume (MPV) were significantly increased in preeclampsia patients. In contrast, Direct Bilirubin, Glucose, GPT, GOT and Platelet count were not significant between preeclampsia and control women. Additionally, Mean Arterial Pressure (MAP) and Systolic Blood Pressure (SBP) were significantly elevated. Furthermore, genotyping of IL-10 T-819 C promoter polymorphism was carried out for all participants using a standard Amplification Refractory Mutation System (ARMS) PCR. Genotypic distribution of the control and patient groups were compared with values predicted by Hardy-Weinberg equilibrium using χ^2 test. Interestingly, there were significant differences in (IL)-10 (-819) T/C genotype distribution frequency between preeclampsia and control groups. **Conclusion** The present study suggests that the IL-10 T-819 C gene promoter polymorphism might be a major genetic regulator in the etiology of increased risk of preeclampsia.

KEY WORDS: Physiological markers, IL-10 -819, polymorphism and preeclampsia

DOI: <http://dx.doi.org/10.21271/ZJPAS.33.1.1>

ZJPAS (2021) , 33(1);1-10 .

INTRODUCTION:

Preeclampsia is the most commonly confronted medical complication of pregnancy, which has an adverse impact on 3% to 5% of all pregnancies (Wang et al., 2002). It is characterized by a complex hypertensive disorder ($\geq 140/\geq 90$ mmHg) along with proteinuria (≥ 0.3 g/24 h), which leads to maternal and fetal mortality/ morbidity. Preeclampsia takes place after 20 weeks of gestation as far as 6 weeks postpartum, also leads to perinatal death, preterm birth, intrauterine growth restriction (IUGR) and in a number of cases, intrauterine death (IUD) of the fetus (Salimi et al., 2014, Tannetta et al., 2013).

Preeclampsia is a multisystem disorder that may trigger eclampsia, renal failure, pulmonary edema, stroke and death. The first preclinical phase comprises deficient remodeling of the uteroplacental circulation during the 8th-18th week of gestation, results in dysfunctional perfusion and placental oxidative stress. The second clinical phase, which initiates after the 20th week, includes systemic vascular inflammation. This has been shown to be an extension of a broader maternal systemic inflammatory response intrinsic to normal pregnancies, but more severe in preeclampsia, including endothelial dysfunction, clotting, and complement disturbances (Tannetta et al., 2013). Despite the thorough studies, the underlying pathophysiology of preeclampsia is still indistinct (Wang et al., 2002).

* Corresponding Author:

Shno Sabah Tahir

E-mail: mudhir.shekha@su.edu.krd

Article History:

Received: 11/10/2019

Accepted: 23/12/2020

Published: 20/02 /2021

Previous studies have shown the role of various cytokines in defective placental invasion and endothelial damage in preeclampsia (Udenze et al., 2015). Wegmann *et al.* have reported that T-helper type 2 (Th2) cell is responsible for a successful pregnancy, nevertheless the survival rate of the fetus is secured by the inhibition of T-helper type 1 (Th1) cell responses. Therefore, a Th1/Th2 ratio is required for a decent placentation. Th1 cells produce proinflammatory cytokines such as interleukin (IL)-2, interferon (IFN)- γ and tumour necrosis factor (TNF)- α that are engaged in cell-mediated responses and delayed type hypersensitivity reactions. Conversely, the anti-inflammatory cytokines such as IL-4, IL-5, IL-10 and IL-13 are generated by Th2 cells that elicitate humoral immunity (Mosmann and Sad, 1996). Th1 and Th2 coordinate their functions in a regular way to generate a balance in the immune system (Lieberman et al., 2003, Matsuzaki et al., 2005). Interleukin-10 (IL-10) is a potent pleiotropic cytokine, plays a crucial role in Th2 immunity, which is located on human chromosome 1 (1q31–1q32) (Eskdale et al., 1997, Kim et al., 1992). IL-10 plays a vital role in maintaining equilibrium of anti-inflammatory and proinflammatory setting at the fetal-maternal interface (Kalkunte et al., 2011). Numerous single nucleotide polymorphisms (SNPs) positioned in the IL-10 both of proximal (-1082A/G, -819T/C, and -592A/C) and distal regions of promoter control the transcriptional rate of propagating IL-10 (Eskdale et al., 1998, D'Alfonso et al., 2000, Mörmann et al., 2004).

Genotypic modifications in the human IL-10 promoter justify remarkable inter-individual differences in IL-10 production and may conduct individual susceptibility to autoimmune diseases. Sowmya *et al.* have suggested that IL-10 T-819 C gene promoter polymorphism can be a major genetic regulator in the etiology of preeclampsia (Sowmya et al., 2014a). The T/C polymorphism at position -819 has been related to high/low IL-10 production rank. With this in mind, the current study is designed to assess the role of IL-10 (-819 T/C) gene promoter polymorphism in the etiology of preeclampsia.

Materials and methods

Selection of cases and controls

A total of 52 pregnant women with early-onset preeclampsia and 35 of age-matched women

with normal pregnancy attended the high-risk unit of Erbil Maternity and Pediatric Governmental Hospital were considered in the present study during the year 2019. Women with no complications throughout their gestational period, such as infections, fetal anomalies, hypertension and diabetes were considered as the control subjects. Information regarding the demographic features such as age, parity, systolic blood pressure, diastolic blood pressure, smoking status, gestational age, family history and consanguinity, etc. were obtained from all the subjects with the help of a standard structured questionnaire. The study was approved by the general director of Health.

Criteria for patients

Inclusion criteria A case was defined as follows: preeclampsia was diagnosed with minimum criteria of blood pressure $>130/90$ mm Hg on two occasions, 6 h apart, and onset of proteinuria $>2+$ by dipstick test in urine samples, and those who showed blood pressure $>150/100$ mm Hg and proteinuria $>3+$ by dipstick test in urine samples were considered to be patients with severe pre-eclampsia.

Exclusion criteria. Patients with a previous history of intrauterine fetal deaths and other complications were not considered for the study.

Criteria for controls

Inclusion criteria The inclusion criteria were pregnant women with a gestational age of more than 20 weeks, normal blood pressure, normal fetal growth and with no other physiological abnormalities. Controls were selected randomly at the same time as the case selection. The controls were administered the same questionnaire.

Exclusion criteria. Pregnant women with heart problems, with previous history of eclampsia or blood pressure were not included, as per the normal standard, in the study.

Sample collection

Five milliliters of the venous blood was collected from all the subjects for biochemical and molecular analysis and aliquoted in plain and EDTA vacutainers. Serum and plasma was separated after centrifugation at 1,500 rpm for 10 min. All the samples were stored at -20°C for further analysis.

Determination of IL-10 Polymorphism (DNA extraction and genotyping)

The genomic DNA was extracted from blood according to the protocol of Primeprep Genomic DNA extraction Kit/Korea. Twenty microliter of proteinase K was added to 1.5ml tube then 200 μ L of whole blood sample mixed with it. Two hundred microliter of GB buffer was added and mixed well by vortex. The samples were incubated at 56C° around 10 minutes. After incubation 200 μ L of Absolute ethanol was added with well pulse vortexing. Then transfer the lysate to the spin column. The samples were centrifuged at 10,000 rpm for 1 minute. Five hundred microliter of GW1 buffer was added then centrifuged at 10,000 rpm for 1 minute. The flow through was discarded and transfer the spin column to new collection tube. The excess ethanol was removed by more centrifugation at 12,000 rpm for 1 to 2 minutes. Two hundred microliter of GE buffer was added and incubated at room temperature for 1 minute. Eventually DNA was eluted by centrifugation 10,000 rpm for 1 minute. The extracted DNA samples were stored at -20C° (Sowmya et al., 2014). The isolated DNA was subjected to a standard amplification refractory mutation system polymerase chain reaction (ARMS-PCR) (Perrey et al., 1999). Briefly, two complementary reactions were established for each allele consisting of target DNA: allele-specific ARMS primers and a common primer (CR). A 223-bp region in the IL-10 gene promoter was targeted for amplification. The primers used are as follows: common reverse AGG ATG TGT TCC AGG CTC CT; C forward CCC TTG TACAGG TGA TGT AAC; and T forward ACC CTT GTA CAG GTG ATG TAA T. The optimized reaction conditions for the amplification was performed in 10 μ l with 25–50 ng of DNA sample, 20 mM Tris–HCl (pH 8.4), 50 mM KCl, 2 mM MgCl₂, 0.2 mM of each dNTP, 2 μ M of each specific/common primers, and 0.25 units of Taq DNA polymerase. The cycling conditions were as follows: an initial denaturation at 95 °C for 5 min, followed by 35 cycles at 95 °C for 30 s, 64.2 °C for 50 s, and 72 °C for 1 min 30 s. The final extension step was at 72 °C for 5 min. The PCR products were separated by electrophoresis on an agarose gel (2 %) stained with ethidium bromide. The gel was visualized under ultraviolet light with a 100-bp ladder. Results were crosschecked with internal positive (410 bp of β globin gene) and negative controls

(Millipore water). Ten percent of the samples were randomly taken, and the assay was repeated, and no bias in the genotyping was found. The findings were similar on a replicative study with the results being 100 % concordant.

Statistical analysis

Genotype distribution in the control and case groups were compared with values predicted by Hardy-Weinberg equilibrium using χ^2 test. Discrete variables were expressed as counts (%) and were compared by the χ^2 test. Odds ratios (OR) and their 95% confidence intervals were used to measure the strength of association between IL-10 gene polymorphism and preeclampsia. Data of the physiological and biochemical were described as percentages and mean \pm SD (standard deviation) for parametric. Level of significance between preeclampsia and normal women was analyzed using independent t-test

Results

Demographics between preeclampsia and control groups

In total 87 patients' data was analyzed. The mean age was approximately similar between the two groups, being 26.6 \pm 6.93 for control group and 30.14 \pm 7.48 for Preeclampsia group. There were no significant differences in age between preeclampsia patient and control groups.

The mean of diastolic blood pressure in the preeclamptic women was (104.4 \pm 13.0 mmHg); while in the control group was (79.17 \pm 12.01 mmHg); with P.value (<0.0001). The mean of systolic blood pressure in the preeclamptic women was (166.3 \pm 20.08 mmHg); while in the control group was (116.7 \pm 28.75 mmHg); with P.value (<0.0001). The mean of arterial pressure in the women with pre-eclampsia was (123.3 \pm 18.49 mmHg) versus (91.67 \pm 17.35 mmHg) in the women with normal pregnancy with very high significant difference P. Value (0.0004) (P < 0.001; Table 1.

The mean of serum urea in the women with pre-eclampsia was (32.52 \pm 7.883 mg/dl) versus (19 \pm 11.11 mg/dl) in the women with normal pregnancy with very high significant difference. Serum creatinine in the women with pre-eclampsia was (0.676 \pm 0.199 mg/dl) versus

(0.524±0.134 mg/dl) in the women with normal pregnancy with P.value (0.0405) Table 1.

The mean of serum ALP in the women with pre-eclampsia was (331.6±67.75 mg/dl) versus (249.1±19.95mg/dl) in the women with normal pregnancy with P.value (0.047) Table 1.

The mean of S. Glucose in the women with pre-eclampsia was (0.247±0.190 g/dl) versus (84.16±19.58 g/dl) in the women with normal pregnancy with no significant difference. The mean of S. Direct Bilirubin in the women with pre-eclampsia was (0.247±0.190) versus (0.170±0.112) in the women with normal pregnancy with no significant difference. Table 1.

The mean of S. GOT and GPT in the women with pre-eclampsia were (14.78±9.266) and (21.05±7.829) versus (10.96±1.686 and 20.02±3.345) in the women with normal pregnancy with no significant difference respectively as shown in Table 1.

The mean of PLTs in the women with pre-eclampsia was (233.9±53.33 X 10⁹/l) versus (210.7±78.76 X 10⁹/l) in the women with normal pregnancy; with no significant difference. The mean of MPV in the women with pre-eclampsia was (8.981± 0.9537) versus (8.981± 0.9537) in the women with normal pregnancy; with P. value (0.0365), as seen in Table 1.

Furthermore, the allele and genotype frequencies of the IL-10 promoter polymorphisms at positions -819 T/C were detected by T-ARMS-PCR method and were compared between preeclampsia cases and healthy control women. The data reported in Table 3 illustrate allele and genotype distributions of different promoter polymorphisms of IL-10.

The frequencies of the genotypes in Co-dominant CC, CT, and TT were 41.18, 37.25, and 21.57 % in women with preeclampsia and 22.86, 28.57 and 48.57 % in control subjects, respectively. The frequencies of the genotypes in dominant were 41.18 and 58.82 % in women with preeclampsia and 22.86 and 77.14 % in control

subjects, respectively. The IL-10 -819 T/C recessive genotype distribution frequencies were 62.07 and 37.93% in women with preeclampsia and 70.18 and 29.82 % in control groups, respectively. The IL-10 -819 T/C over-dominant genotype distribution frequencies were 62.75 and 37.25 % in women with preeclampsia and 71.43 and 28.57 % in control groups, respectively while the distribution frequencies of interleukin (IL)-10 (-819) T/C alleles were 57.75 and 42.25 % in women with preeclampsia patients and 48.72 and 51.28 % in control groups.

There were significant differences in (IL)-10 (-819) T/C genotype distribution frequency between preeclampsia and control groups. There were statistical differences in the distribution of genotypic frequencies between the patient and control groups when compared with different models: over-dominant model: CT vs. CC+TT (OR=1.484, 95 % CI= 0.5646-3.712, P= 0.4027) and recessive model: TT vs. CT+CC (OR= 1.438, 95 % CI= 0.5426-3.577, P= 0.4482). In contrast, there were no significant differences in the distribution of genotypic frequencies between the preeclampsia and control groups when compared with different models: codominant model: CC vs. TT (OR=0.2465, 95 % CI=0.087-0.71) and CC vs. CT (OR=0.724, 95 % CI=0.2582-2.262); and dominant model: CC vs. CT+TT (OR=0.4233, 95 % CI=0.1589-1.158).

Regarding to allele frequency of the IL-10-1082 T/C allele between preeclampsia and healthy control groups (X²= 0.8276, P= 0.3630) there was no statistical difference in allele frequency of IL-10-819 C/T and it was not associated with preeclampsia patients.

Genotypes expressed as CC (C) and TT (T) in the homozygote alleles while TC in the heterozygous allele. Using the two pairs primers to the homozygous CC and TT the genotypes and the heterozygote genotype, a single band of 233 bp was produced.

Table 1. Demographic features in women with preeclampsia during pregnancy and women with normal pregnancy

Parameters	Control n(35)	Preeclampsia n(52)	P-Value
Mean age(years)	26.6±6.93	30.14±7.48	NS
SBP (mmHg)	116.7±28.75	166.3±20.08	<0.0001 ***
DBP (mmHg)	79.17±12.01	104.4±13.0	<0.0001 ***
MAP (mmHg)	91.67±17.35	123.3±18.49	0.0004 ***

Table 2. Biochemical and hematological characteristics in controls and patients

Parameters	Control n(35)	Preeclampsia n(52)	t-test	P-Value
S. Urea	19±11.11	32.52±7.883	t=3.703	0.0007 ***
S. Creatinine	0.524±0.134	0.676±0.199	t=2.125	0.0405 *
S. ALP	249.1±19.95	331.6±67.75	t=2.072	0.047 *
S. Direct Bilirubin	0.170±0.112	0.247±0.190	t=0.5748	0.570
S. Glucose	84.16±19.58	93.88±22.54	t=1.177	0.2463
S. GPT	10.96±1.686	14.78±9.266	t=0.9048,	0.3746
S. GOT	20.02±3.345	21.05±7.829	t=0.2863	0.7765
Platelet count	210.7±78.76	233.9±53.33	t=1.281	0.2057
MPV	8.981± 0.9537	9.605± 0.9839	t=2.147	0.0365*

Table 3. Distribution Frequencies of interleukin (IL)-10 (-819) Genotypes and Alleles in control and patients

Genotypes and alleles	Control group <i>n</i> (%)	Patient group <i>n</i> (%)	OR (95% CI)	X ² -test P-value
Co-dominant				
C/C	8 (22.86%)	21 (41.18%)		
C/T	10 (28.57%)	19 (37.25%)	0.724 (0.2582-2.262)	X ² =7.178
T/T	17(48.57%)	11 (21.57%)	0.2465 (0.087-0.71)	P=0.0276*
Dominant				
C/C	8 (22.86%)	21 (41.18%)		X ² =3.117
C/T + T/T	27 (77.14%)	30 (58.82%)	0.4233 (0.1589-1.158)	P=0.0775
Recessive				
C/C+ C/T	40 (70.18%)	18 (62.07%)		X ² = 0.5752
T/T	17 (29.82%)	11 (37.93%)	1.438 (0.5426-3.577)	P= 0.4482
Over-dominant				
C/C+ T/T	25 (71.43%)	32 (62.75%)		X ² = 0.7002
C/T	10 (28.57%)	19 (37.25%)	1.484 (0.5646-3.712)	P= 0.4027
Alleles				
C	19 (48.72%)	41 (57.75%)	0.6951 (0.3061-1.554)	X ² = 0.8276
T	20 (51.28%)	30 (42.25%)		P= 0.3630

*P value < 0.05. OR = odds ratio; CI = confidence interval.

Discussion

Preeclampsia is the most widespread pregnancy specific complication that yet situates as one of the considerable obstetric disorders. Preeclampsia is a placenta- dependent pregnancy disorder. Preeclampsia disease is characterized as exaggerated response to maternal inflammation, maybe destine against foreign fetal antigens that induce a series proceedings including: defection in the spiral artery remodeling, placental infarction and release of pro-inflammatory cytokines, invasion of surface trophoblast, and placental fragments in the systemic circulation (Gupte and Wagh, 2014, Neiger, 2017, Sabnavis et al., 2013).

Present research was assumed to estimate some physiological and biochemical parameters in pre-eclampsia.

Our observations are in agreement with the work of (Macdonald-Wallis et al., 2012) they present that increased SBP, DBP and MAP in patients with pre-eclampsia. Preeclampsia causes an increment in peripheral vascular resistance and vasoconstriction (Roberts et al., 1991, Schobel et al., 1996a). An increase in the activity of

sympathetic vasoconstrictor has been demonstrated with measurements of muscle sympathetic nerve tone, which may lead to endothelial dysfunction (Greenwood et al., 2003, Savvidou et al., 2003, Schobel et al., 1996b). Endothelial dysfunction that is known to occur in preeclampsia as this is an important step in the development of atherosclerosis in patients with chronic hypertension (Cipolla, 2007).

Creatinine, urea and uric acid are non-protein nitrogenous metabolites that are cleared from the body by the kidney following glomerular filtration. Measurements of plasma or serum concentration of these metabolites are commonly used as indicators of kidney function and other conditions (Gowda et al., 2010). Therefore, their determination in serum during pregnancy is of a major importance to diagnose kidney function especially in women with preeclampsia signs (Müller-Deile and Schiffer, 2014, Tangren et al., 2018). This would be used to evaluate kidney function as well as the possibility of a secondary source of urea or of the nitrogen part of urea

increase (Blood urea nitrogen) in plasma (Weiner et al., 2015).

In the present study, the serum urea and creatinine levels were higher in pre-eclamptic when compared to the normotensives. Our observation was similar to the previous study by Hassan et al and Vyakaranm et al as they describe raised blood urea and creatinine during pregnancy as a known feature of pre-eclampsia (Hassan et al., 1991, Vyakaranam et al., 2015).

One of the most commonly accepted explanations of elevated Serum Urea and Creatinine has been thought to be due to increase reabsorption and decrease excretion in proximal tubules, similar to the physiologic response to hypovolemia.

In the present study, the serum ALP was significantly higher in preeclampsia, which was similar to those seen in other studies (Dabare et al., 1999, Okesina et al., 1995, Rajagambeeram et al., 2014).

Alkaline phosphatase is an important enzyme involved in the transport of sugar and phosphate across the trophoblast cell membranes (She et al., 2000). The elevated levels of serum ALP in preeclampsia may be attributed to placental dysfunction, which results in increased serum levels of this enzyme. Shedding of syncytiotrophoblast into the maternal circulation is a normal part of pregnancy, but is increased during pre-eclampsia. In pre-eclampsia, this process of syncytio-trophoblast renewal is overactive and complicated by necrosis and apo necrosis of the syncytio-trophoblast particles (Hutchinson et al., 2009)

Bilirubin comes from haemoglobin (Hgb) as red blood cells (RBCs) breakdown either through physiological regeneration at the end of normal lifespan or as a consequence of pathologic hemolysis. Hgb releases heme and is converted inside macrophages to biliverdin, which is then converted into unconjugated bilirubin (indirect bilirubin) that travels through the liver, where, it combines with glucuronic acid to form conjugated bilirubin (also known as bilirubin diglucuronide or direct bilirubin (Odhiambo et al., 2015). In relation to direct bilirubin level, the result was confirmed that direct bilirubin level in preeclamptic pregnant women had not obvious difference compared to normotensive pregnant women our results are compatible with results of

(Hassanpour and Karami, 2018, Kasraeian et al., 2018)

In this study, there were a non-significant increase in serum AST and ALT concentration in preeclampsia compared to normal pregnant women. There is no agreement on the effect of preeclampsia on serum AST and ALT. In a few studies, AST and/ or ALT levels slightly increase in the third trimester (Mutua et al., 2018). However, in most studies, AST and ALT levels remain within the normal range for non-pregnant state (Westbrook et al., 2016).

Mean platelet volume is a routinely measured marker of platelet size, with established predictive value in a variety of cardiovascular disorders (Choi et al., 2016). The present research demonstrated that preeclampsia is associated with a significant increase of MPV. Our results are in consistent with study of (Monteith et al., 2018) they detailed that there is a significant increase in MPV at time of diagnosis preeclampsia therefore the mean platelet volume can represents a promising biomarker for the detection and follow-up of patients that develop preeclampsia (Bellos et al., 2018).

The results of the data analysis showed platelet count non significantly changed in preeclampsia comparing with control. Our data are compatible with work of (Bellos et al., 2018) and incompatible with experiment of (Neiger et al., 1992) their findings suggest the existence of subclinical thrombocytopenia in preeclamptic women whose platelet values are within normal range.

The mean of S. Glucose in the women with preeclampsia was not significant compared to women with normal pregnancy. The current results are compatible with previous study that has shown no significant alteration in fasting blood glucose between preeclampsia and control (Babu et al., 2014).

The IL-10 gene promoter is highly polymorphic with multiple single nucleotide polymorphic sites. The three most important ones are -819 (C/T), -1082 (A/G), and -592 (C/A) (Jiang et al., 2015). In the present study (our case – control study), established that the genotype distribution of the IL-10 gene promoter -819 (C/T) to pregnant women with preeclampsia in of Erbil Maternity and Pediatric Governmental Hospital is reliable with the results of a previous study

(Perrey et al., 1999) Therefore, this gene might conceivably be a candidate susceptibility gene in pre-eclampsia (Sowmya et al., 2014b).

According to the result of our study, as shown in figure 1. promoter gene -819 (C/T) polymorphism represented a statistically significant positive association with pre-eclampsia. The polymorphic CT-genotype and TT frequencies as an over-dominant and recessive model were significantly greater while polymorphic CC-genotype frequency was not significant in pregnant women with preeclampsia compared to control women. These positive associations of over-dominant and recessive models indicate that this C>T polymorphisms might increase the predisposition possibility of preeclampsia women. Our results agree with previous reports which correlate women with CT genotype are at high risk to develop preeclampsia in pregnant women. The conflicting results from different populations were reported. Our observation is in concordance with the study by Sowmya et al (Sowmya et al., 2014a) in an Indian population, which revealed high association with the promoter gene -819 (C/T) polymorphism of preeclampsia in pregnant women to high production of IL-10.

Additionally, our data showed that the promoter -819 locus CC genotype frequency and the polymorphic CT genotype and TT frequencies

were statistically not significant association with pre-eclampsia under condition of co-dominant, dominant and alleles C and T models. On the other hand, Kamali-Sarvestani et al. have demonstrated that the genotype of IL-10 promoter genotype and allele frequency in an Iranian population has no significant difference of the polymorphism between the patient and the control group (Kamali et al., 2007). Likewise, some studies have investigated the correlation of promoter polymorphisms with the circulating levels and placental levels of IL-10. Moreover, have shown that the genotype of IL-10 promoter may not play a significant role in the circulating of IL-10 levels, but has an effect on the placental levels of IL-10, suggesting that IL-10 plays an important role in proper placentation (Makris et al., 2006, Sowmya et al., 2014b).

Conclusion

The present research suggests that the IL-10 T-819 C gene promoter polymorphism can be a major genetic regulator in the etiology of increased risk of preeclampsia.

Acknowledgment

The authors acknowledge Mr. Govand Musa for his help in designing ARMS-PCR, Dr Mukhlis Hamad and other contributors who made the study possible.

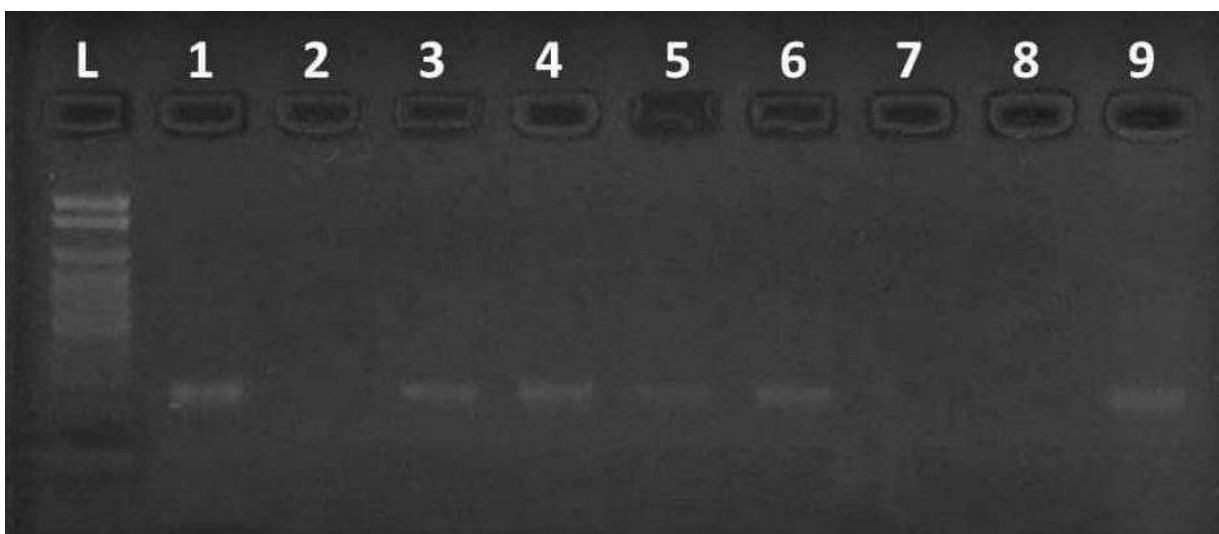


Figure 1: Genotyping of interleukin 10 promoter region -819 locus. L:DNA Ladder of 1kb, Lane: 1,3,4, homozygous C/C; Lane:2 Patient sample not amplified with allele C primer; Lane :5,6, homozygous T/T, Lane:7-8 Preclampsia samples not amplified with allele T primer; Lane:9,heterozygous C/T.

Footnotes

Disclosure: No conflict of interest is reported at the current time.

References

- BABU, M. S., BOBBY, Z., HABEEBULAH, S., SRILATHA, K., LALITHA, V. & NIRANJAN, G. K. 2014. Fasting insulin levels, lipid profile and proteinuria an index of cardiovascular risk in euglycemic preeclampsia. *Conference Proceedings*.
- BELLOS, I., FITROU, G., PERGIALIOTIS, V., PAPANTONIOU, N. & DASKALAKIS, G. 2018. Mean platelet volume values in preeclampsia: A systematic review and meta-analysis. *Pregnancy Hypertens*, 13, 174-180.
- CHOI, D.-H., KANG, S.-H. & SONG, H. 2016. Mean platelet volume: a potential biomarker of the risk and prognosis of heart disease. *The Korean journal of internal medicine*, 31, 1009-1017.
- CIPOLLA, M. J. 2007. Cerebrovascular function in pregnancy and eclampsia. *Hypertension*, 50, 14-24.
- D'ALFONSO, S., RAMPI, M., ROLANDO, V., GIORDANO, M. & MOMIGLIANO-RICHIARDI, P. 2000. New polymorphisms in the IL-10 promoter region. *Genes Immun*, 1, 231-3.
- DABARE, A., NOURI, A., CANNELL, H., MOSS, T., NIGAM, A. & OLIVER, R. J. U. I. 1999. Profile of placental alkaline phosphatase expression in human malignancies: effect of tumour cell activation on alkaline phosphatase expression. 63, 168-174.
- ESKDALE, J., GALLAGHER, G., VERWEIJ, C. L., KEIJERS, V., WESTENDORP, R. G. & HUIZINGA, T. W. 1998. Interleukin 10 secretion in relation to human IL-10 locus haplotypes. *Proc Natl Acad Sci U S A*, 95, 9465-70.
- ESKDALE, J., KUBE, D., TESCH, H. & GALLAGHER, G. 1997. Mapping of the human IL10 gene and further characterization of the 5' flanking sequence. *Immunogenetics*, 46, 120-8.
- GOWDA, S., DESAI, P. B., KULKARNI, S. S., HULL, V. V., MATH, A. A. K. & VERNEKAR, S. N. 2010. Markers of renal function tests. *North American journal of medical sciences*, 2, 170-173.
- GREENWOOD, J. P., SCOTT, E. M., WALKER, J. J., STOKER, J. B. & MARY, D. A. J. A. J. O. H. 2003. The magnitude of sympathetic hyperactivity in pregnancy-induced hypertension and preeclampsia. 16, 194-199.
- GUPTA, S. & WAGH, G. 2014. Preeclampsia-eclampsia. *J Obstet Gynaecol India*, 64, 4-13.
- HASSAN, T. J., SADARUDDIN, A. & JAFAREY, S. N. 1991. Serum calcium, urea and uric acid levels in pre-eclampsia. *J Pak Med Assoc*, 41, 183-5.
- HASSANPOUR, S. & KARAMI, S. 2018. Evaluation of Hepatic Biomarkers in Pregnant Women with Preeclampsia. *Gynecology & Obstetrics*, 08.
- HUTCHINSON, E. S., BROWNBILL, P., JONES, N. W., ABRAHAMS, V. M., BAKER, P. N., SIBLEY, C. P. & CROCKER, I. P. 2009. Utero-placental haemodynamics in the pathogenesis of pre-eclampsia. *Placenta*, 30, 634-41.
- JIANG, X.-H., LIN, K.-X., ZHANG, Y.-X., CHEN, R.-H. & LIU, N. 2015. Correlating interleukin-10 promoter gene polymorphisms with human cerebral infarction onset. *Neural regeneration research*, 10, 1809-1813.
- KALKUNTE, S., NEVERS, T., NORRIS, W. E. & SHARMA, S. 2011. Vascular IL-10: a protective role in preeclampsia. *J Reprod Immunol*, 88, 165-9.
- KAMALI, E., KIANY, S., GHARESI-FARD, B. & ROBATI, M. 2007. Association study of IL-10 and IFN- γ gene polymorphisms in Iranian women with preeclampsia. *Journal of reproductive immunology*, 72, 118-26.
- KASRAEIAN, M., ASADI, N., VAFAEI, H., ZAMANPOUR, T., SHAHRAKI, H. R. & BAZRAFESHAN, K. 2018. Evaluation of serum biomarkers for detection of preeclampsia severity in pregnant women. *Pakistan journal of medical sciences*, 34, 869-873.
- KIM, J. M., BRANNAN, C. I., COPELAND, N. G., JENKINS, N. A., KHAN, T. A. & MOORE, K. W. 1992. Structure of the mouse IL-10 gene and chromosomal localization of the mouse and human genes. *J Immunol*, 148, 3618-23.
- LIBERMAN, A. C., REFOJO, D. & ARZT, E. 2003. Cytokine signaling/transcription factor cross-talk in T cell activation and Th1-Th2 differentiation. *Arch Immunol Ther Exp (Warsz)*, 51, 351-65.
- MACDONALD-WALLIS, C., LAWLOR, D. A., FRASER, A., MAY, M., NELSON, S. M. & TILLING, K. 2012. Blood pressure change in normotensive, gestational hypertensive, preeclamptic, and essential hypertensive pregnancies. *Hypertension (Dallas, Tex. : 1979)*, 59, 1241-1248.
- MAKRIS, A., XU, B., YU, B., THORNTON, C. & HENNESSY, A. 2006. Placental deficiency of interleukin-10 (IL-10) in preeclampsia and its relationship to an IL10 promoter polymorphism. *Placenta*, 27, 445-51.
- MATSUZAKI, J., TSUJI, T., IMAZEKI, I., IKEDA, H. & NISHIMURA, T. 2005. Immunostimulatory as a regulator for Th1/Th2 balance: its possible role in autoimmune diseases. *Autoimmunity*, 38, 369-75.
- MONTEITH, C., EGAN, K., O'CONNOR, H., MAGUIRE, P., KEVANE, B., SZKLANNA, P. B., COOLEY, S., MALONE, F. & AINLE, F. N. 2018. Early onset preeclampsia is associated with an elevated mean platelet volume (MPV) and a greater rise in MPV from time of booking compared with pregnant controls: results of the CAPE study. *J Perinat Med*, 46, 1010-1015.
- MOSMANN, T. R. & SAD, S. 1996. The expanding universe of T-cell subsets: Th1, Th2 and more. *Immunol Today*, 17, 138-46.
- MUTUA, D., NJAGI, E. & ORINDA, G. 2018. Liver Function Tests in Normal Pregnant Women. *Journal of Liver*, 07.
- MÖRMANN, M., RIETH, H., HUA, T. D., ASSOHO, C., ROUPELIEVA, M., HU, S. L., KREMSNER, P.

- G., LUTY, A. J. & KUBE, D. 2004. Mosaics of gene variations in the Interleukin-10 gene promoter affect interleukin-10 production depending on the stimulation used. *Genes Immun*, 5, 246-55.
- MÜLLER-DEILE, J. & SCHIFFER, M. 2014. Preeclampsia from a renal point of view: Insides into disease models, biomarkers and therapy. *World journal of nephrology*, 3, 169-181.
- NEIGER, R. 2017. Long-Term Effects of Pregnancy Complications on Maternal Health: A Review. *J Clin Med*, 6.
- NEIGER, R., CONTAG, S. A. & COUSTAN, D. R. 1992. Preeclampsia effect on platelet count. *Am J Perinatol*, 9, 378-80.
- ODHIAMBO, C., OYARO, B., ODIPO, R., OTIENO, F., ALEMNJI, G., WILLIAMSON, J. & ZEH, C. 2015. Evaluation of Locally Established Reference Intervals for Hematology and Biochemistry Parameters in Western Kenya. *PLoS ONE*, 10, e0123140.
- OKESINA, A., DONALDSON, D., LASCELLES, P., MORRIS, P. J. I. J. O. G. & OBSTETRICS 1995. Effect of gestational age on levels of serum alkaline phosphatase isoenzymes in healthy pregnant women. 48, 25-29.
- PERREY, C., TURNER, S. J., PRAVICA, V., HOWELL, W. M. & HUTCHINSON, I. V. 1999. ARMS-PCR methodologies to determine IL-10, TNF-alpha, TNF-beta and TGF-beta 1 gene polymorphisms. *Transpl Immunol*, 7, 127-8.
- RAJAGAMBEERAM, R., ABU RAGHAVAN, S., GHOSH, S., BASU, S., RAMASAMY, R. & MURUGAIYAN, S. B. 2014. Diagnostic utility of heat stable alkaline phosphatase in hypertensive disorders of pregnancy. *Journal of clinical and diagnostic research : JCDR*, 8, CC10-CC13.
- ROBERTS, J. M., TAYLOR, R. N. & GOLDFIEN, A. 1991. Clinical and biochemical evidence of endothelial cell dysfunction in the pregnancy syndrome preeclampsia. *Am J Hypertens*, 4, 700-8.
- SABNAVIS, S., RAMAIAH, A., SUNITHA, T., NALLARI, P., JYOTHY, A. & VENKATESHWARI, A. 2013. Evaluation of Interleukin-10 (G-1082A) Promoter Polymorphism in Preeclampsia %J JRI. *Journal of Reproduction & Infertility*, 14, 62-67.
- SALIMI, S., FARAJIAN-MASHHADI, F., NAGHAVI, A., MOKHTARI, M., SHAHRAKIPOUR, M., SARAVANI, M. & YAGHMAEI, M. 2014. Different profile of serum leptin between early onset and late onset preeclampsia. *Dis Markers*, 2014, 628476.
- SAVVIDOU, M. D., HINGORANI, A. D., TSIKAS, D., FRÖLICH, J. C., VALLANCE, P. & NICOLAIDES, K. H. J. T. L. 2003. Endothelial dysfunction and raised plasma concentrations of asymmetric dimethylarginine in pregnant women who subsequently develop pre-eclampsia. 361, 1511-1517.
- SCHOBEL, H. P., FISCHER, T., HEUSZER, K., GEIGER, H. & SCHMIEDER, R. E. 1996a. Preeclampsia -- a state of sympathetic overactivity. *N Engl J Med*, 335, 1480-5.
- SCHOBEL, H. P., FISCHER, T., HEUSZER, K., GEIGER, H. & SCHMIEDER, R. E. J. N. E. J. O. M. 1996b. Preeclampsia—a state of sympathetic overactivity. 335, 1480-1485.
- SHE, Q.-B., MUKHERJEE, J. J., HUANG, J.-S., CRILLY, K. S. & KISS, Z. J. F. L. 2000. Growth factor-like effects of placental alkaline phosphatase in human fetus and mouse embryo fibroblasts. 469, 163-167.
- SOWMYA, S., RAMAIAH, A., SUNITHA, T., NALLARI, P., JYOTHY, A. & VENKATESHWARI, A. 2014a. Role of IL-10 -819(t/c) promoter polymorphism in preeclampsia. *Inflammation*, 37, 1022-7.
- SOWMYA, S., SRI MANJARI, K., RAMAIAH, A., SUNITHA, T., NALLARI, P., JYOTHY, A. & VENKATESHWARI, A. 2014b. Interleukin 10 gene promoter polymorphisms in women with early-onset pre-eclampsia. *Clin Exp Immunol*, 178, 334-41.
- TANGREN, J. S., WAN MD ADNAN, W. A. H., POWE, C. E., ECKER, J., BRAMHAM, K., HLADUNEWICH, M. A., ANKERS, E., KARUMANCHI, S. A. & THADHANI, R. 2018. Risk of Preeclampsia and Pregnancy Complications in Women With a History of Acute Kidney Injury. *Hypertension*, 72, 451-459.
- TANNETTA, D. S., DRAGOVIC, R. A., GARDINER, C., REDMAN, C. W. & SARGENT, I. L. 2013. Characterisation of syncytiotrophoblast vesicles in normal pregnancy and pre-eclampsia: expression of Flt-1 and endoglin. *PLoS One*, 8, e56754.
- UDENZE, I., AMADI, C., AWOLOLA, N. & MAKWE, C. C. 2015. The role of cytokines as inflammatory mediators in preeclampsia. *Pan Afr Med J*, 20, 219.
- VYAKARANAM, S., BHONGIR, A. V., PATLOLLA, D., CHINTAPALLY, R. J. I. J. O. M. S. & HEALTH, P. 2015. Study of serum uric acid and creatinine in hypertensive disorders of pregnancy. 4, 1424.
- WANG, J. X., KNOTTNERUS, A. M., SCHUIT, G., NORMAN, R. J., CHAN, A. & DEKKER, G. A. 2002. Surgically obtained sperm, and risk of gestational hypertension and pre-eclampsia. *Lancet*, 359, 673-4.
- WEINER, I. D., MITCH, W. E. & SANDS, J. M. 2015. Urea and Ammonia Metabolism and the Control of Renal Nitrogen Excretion. *Clinical journal of the American Society of Nephrology : CJASN*, 10, 1444-1458.
- WESTBROOK, R. H., DUSHEIKO, G. & WILLIAMSON, C. 2016. Pregnancy and liver disease. *Journal of Hepatology*, 64, 933-945.

RESEARCH PAPER

Isolation, Antimicrobial activities, Antioxidant Scavenging activities and Trace Element Investigation of Isolated Actinomycetes spp. in Kalar, Iraqi Kurdistan Region

Saman Mohammad Mohammad Amin

Department of Biology College of Education, University of Garmian, Kurdistan Region Governorate

ABSTRACT:

The poor prognosis of the most microbial pathogenic diseases, due to acquiring resistance against the most convenient antimicrobial medication, encourages researchers to find out a new approach to obtain a novel medication. The current study was aimed to obtain new actinomycetes strains or their novel bioactive metabolites. Eleven isolates were found from 45 distinct non-farming soils in Kalar, Iraqi Kurdistan Region. The non-farming soil 2 (NFS2) isolate was demonstrated as the most effective isolate among all other isolates when tested for primary antimicrobial screening. In addition, in case of crude extract, the NFS2 confers great antimicrobial activities particularly against Gram-positive bacteria *Staphylococcus aureus* ATCC 25923 and *Micrococcus luteus* ATCC 9341, as well as, against *Candida albicans* ATCC 10231, with inhibition zones diameters, 25.5, 33.5 and 30.5 mm respectively. However, the isolate has no any antibacterial responses against Gram-negative bacteria, using all types of extracts including crude extract and organic solvent extracts. The crude extract exhibited the powerful antioxidant and H₂O₂ scavenging activities recording 93.46% with 30mg/ml and 43.94% with 1.25 mg/ml respectively. Investigating the trace elements concentration in broth cultures yeast malt extract broth (ISP2) by inductively coupled plasma (ICP), for confirming the value of these elements particularly (Ca, Fe, K, Na, P, Sr, Mg, and Zn). Primarily, these elements were either exhausted or produced during the fermentation process. Furthermore, manipulating the trace elements concentration will play a crucial role in enhancing or diminishing the final secondary metabolites products in actinomycetes isolates.

KEY WORDS: Isolation, Actinomycetes, Antimicrobial, Antioxidant, Trace elements

DOI: <http://dx.doi.org/10.21271/ZJPAS.33.1.2>

ZJPAS (2021) , 33(1);11-20 .

1.INTRODUCTION:

The screening for obtaining new bioactive metabolites from microbial sources including novel antimicrobial compounds, potentially used in industrial, agricultural and pharmaceutical applications, has become an important field for investigating the impact of the metabolites against currently isolated multi-drug resistance microbial pathogens. The researchers have been deeply focusing in their searching process to achieve novel potent, sustainable, as well as broad-spectrum antimicrobial compounds from different sources especially microbial population and more closely actinomycetes (Berdy, 2005; Praveen *et al.*, 2008; Singh and Tripathi, 2011; Singh *et al.*, 2016).

Actinomycetes are Gram-positive bacteria, spore-forming, free-living and having a filamentous structure with DNA that have high GC content. Also the bacteria spread over all ecological habitat including water, soil and different niche, therefore; the investigators attempt in their searching for obtaining new strains or novel bioactive compounds through playing an extensive role in the pharmaceutical uses as well as in medical application and industry (Janardhan *et al.*, 2014). According to the published and reviewed articles, there are more than 10000 bioactive secondary metabolites which are produced by the group of bacteria called actinomycetes that represent about 45% of all discovered bioactive microbial secondary

* Corresponding Author:

Saman Mohammad Mohammad Amin
E-mail: saman.amin@garmian.edu.krd

Article History:

Received: 20/04/2020

Accepted: 07/09/2020

Published: 20/02 /2021

metabolites. Most of these discovered bioactive compounds, isolated and characterized by researchers, have currently been well studied and developed for making novel medications in treating a wide range of common disease in human, animal and agricultural fields (Subathra *et al.*, 2013). In fact, novel metabolites provide antibacterial, anticancer, antifungal, antiviral, anti-infective and anti-parasitic properties, as well as immunosuppressive and enzyme inhibitory (Kekuda *et al.*, 2010). In Iraq, previously, several researches have been attempted to isolate actinomycetes and recording some bioactive metabolites (Abbas, 2009, Jaralla, 2014; Burghal, 2015 and AL-Mawlah, 2018). Although in the Kalar district Iraqi Kurdistan Region, there were few studies have been documented for exploring biological activities of the metabolites (Risan, *et al.*, 2016). Therefore, the aim of the current study was to screen different soils in the Kalar soil for isolating novel actinomycetes strain for investigating their antimicrobial, antioxidant prosperities as well as evaluating the amount of trace elements concentration consumed or produced during the entire fermentation process.

2. Material and Methods

2.1 Soil Sample collecting and treatment

Forty-five soil samples were collected in Kalar district which located between latitudes 34° 37' 45" N and longitudes 45° 19' 20" E. Elevation 231 m (758 ft) above the sea level, Iraqi Kurdistan Region (Figure 1). Fifteen gm of soils were collected, each soil sample was collected from 10 to 15 cm depth, and the sample directed placed in polyether bags 15*25 cm. The collected soil samples well crushed, sieved and supplemented with calcium carbonate at a ratio 10:1 (soil: calcium carbonate) in order to reduce the growth of fungi and mold, this was done inside the autoclave for 3 days at 40 °C, the soil sample ready to use for isolation purpose. One gram of dried and pretreatment soil sample was suspended in 99ml of sterilized distal water and making serial dilution up to 10⁻³. 100µl of each dilution was taken and spread over the surface of yeast malt extract agar (ISP2) medium in triplicate, supplemented with streptomycin and nystatin (50µg/ml from each one). The inoculated plate incubated at 28°C for seven days, after the incubation period. The whitish pin-point colonies, with a clear zone of inhibition around them, indicate the most outstanding characteristic of

actinomycetes bacterial population. Via a sterilized needle the colonies with the previous characters transferred to a new plate, which then purified and stored at 4°C for further study (Saadoun *et al.*, 1999; Rahman *et al.*, 2011; Waksman, 1961; Hopwood *et al.*, 1985)

2.2 Primary Screening for Antimicrobial Activity

The purified and isolated colonies of actinomycetes were used to determining the primary antimicrobial screening assay. The protocol was carried out via cross streak method on yeast malt extract agar medium (ISP2) against human microbial pathogens (obtained from media medical center in Irbil, Iraqi Kurdistan Region). The human microbial pathogens were used for conducting the antimicrobial activities include *Staphylococcus aureus* ATCC 25923, *Escherichia coli* ATCC 25922, *Pseudomonas aeruginosa* ATCC27853, *Micrococcus luteus* ATCC 9341 and *Candida albicans* ATCC 10231. The isolated strains were grown on yeast malt extract agar (ISP2) plate by streak it as a parallel line across the entire plate. After 3 days of incubation at 28°C were all of them fully cultured, the tested microbial pathogens streaked at 90° to the originally grown isolate, and then incubated for 24hours at 37°C (Salim *et al.*, 2017).

2.3 Secondary Antimicrobial Screening and Fermentation Condition

The pure isolated actinomycetes used to make bacterial suspension by transferring a loop full of the grown isolate on ISP2 agar to 50ml of yeast malt extract broth and incubating it at 28°C for 4days making stock solution. 1.5ml of the stock solution used to inoculated 150 ml of yeast malt extract broth (ISP2) and incubating it in shaking incubator at 28°C, 150 rpm for seven days. The culture broth was centrifuged at 6000rpm for 10 minutes. The supernatant was filtered through Whatman filter paper No.1, collected and treated as a crude extract. This used for investigating antimicrobial activity against microbial pathogens were grown on Muller Hinton agar plates (20 ml agar medium per plate). The agar wells diffusion techniques was used conduct secondary antimicrobial activates. Sterilized pasture pipette were used for making the wells (5mm); the wells were filled with 75±5 µl of the filtered crude extract supernatant and incubated at 37°C for 24 hours. The diameter of the growth zones of

inhibition was measured in (mm) (Gebreyohannes *et al.*, 2013).

2.4 Extracellular Antimicrobial Metabolites Extraction

In order to extract extracellular antimicrobial metabolites different organic solvents (ethyl acetate, n-butanol and, n-hexane) were used. Equal amounts (1:1 volume) of crude extract supernatant with above solvents were taken, shaking for one hour and were spun at 12000rpm for 12 minutes. After centrifugation, the upper phase was containing the dissolved extracellular antimicrobial metabolites collected in sterilized plates; the plates were kept in the autoclave at 45°C for evaporating the organic solvents. After solvents were completely dried out the sediments (remaining) re-suspended with 500 ul of sterilized distal water; the obtained mixture treated as solvent extracellular extract against tested microbial pathogens, the diameter of the growth zone of inhibition were measured in (mm) (Gurung *et al.*, 2009).

2.5 Comparing Antibacterial Activities between Crude Extract and Synthetic Antibiotic Discs

Different synthetic antibiotic discs were used to compare the antibacterial activities with the crude extract of NFS2 against human microbial pathogens *S aureus* ATCC 25923, *E coli* ATCC 25922, *P aeruginosa* ATCC ATCC27853, *M luteus* ATCC 9341. The microbial pathogens were grown on Muller Hinton agar. Five different types of the antibiotic susceptibility discs from Bioanalyse were used include (Tobramycin 10 µg; ToB 10, Gentamicin 10 µg; CN 10, Cefriaxono 10 µg; CRO 10, Amoxicillin/Clavulanic acid 30 µg; AMC 30 and Ciprofloxacin 10 µg; Cip 10). Inhibition zones were measured after 24 hours after incubation on 37°C.

2.6 Evaluating Antioxidant Properties of Crude Extract

The standard solution was prepared by dissolving 50 mg of ascorbic acid in 50ml methanol. Different concentrations of ascorbic acid (1, 0.5, 0.25, 0.125, 0.64, 0.32 mg/ml) were prepared, then mixed with Diphenyl Picryl Hydrazil solution (DPPH) (0.002mg/100ml), and then kept for 30 minutes at room temperature in dark. Absorbance was read by spectrophotometer at 517nm after 30minutes of reaction, to obtain a standard curve for calculating DPPH radical scavenging activity.

1,1-diphenyl-2-picryl hydrazyl free radical scavenging assay was performed to evaluate radical scavenging activities of the NFS2 crude extract. Exactly 0.002gm of DPPH dissolved in 100ml methanol and kept in darkness. The crude extract concentration mixed with methanol to obtain final dilution concentration as (0.1, 0.5, 1.0, 3.0, 5.0, 10.0, 20.0 and 30.0 mg/ml). A mixture of 2.5ml of DPPH solution and 0.5ml of the crude extract of NFS2 were mixed, and then kept at room temperature in a dark place for 30 minutes. The absorbance was read at 517 nm by using visible spectrophotometer after 30min of reaction. The ability to scavenge the DPPH radicals (antioxidant activity) was calculated as follow:

DPPH radical scavenging activity% = $(A_0 - A_1) / A_0 * 100$; Where A_0 is the absorbance of the control after 30 minutes and A_1 is the absorbance of the sample after 30 minutes. All concentration was analyzed in duplicates (Khalaf *et al.*, 2008).

2.7 Hydrogen Peroxide Radical Scavenging Activity

According to (Patel *et al.*, 2016) and (Dholakiya *et al.*, 2017) hydrogen peroxide solution (40mmol/L) was prepared in phosphate buffer (pH 7.4). Different concentrations of NFS2 crude extract after drying it was prepared in the same phosphate buffer ranging from (5 to 0.08 mg/ml). 4ml of the NFS2 extract was mixed with 0.6 ml of H₂O₂ solution, and incubated at room temperature for 10 minutes. The optical density (OD) after 10 minutes was calculated at 230nm by the UV-visible spectrometer. All concentration was analyzed in duplicates. The percentage of H₂O₂ scavenging activity was determined as follow;

H₂O₂ Scavenging activity (%) = $[(OD_{320} \text{ of control} - OD_{320} \text{ of Extract}) / OD_{320} \text{ of control}] * 100$

2.8 Trace Elements Contain Analyzing by Inductively Coupled Plasma (ICP)

According to (Hsiung *et al.*, 1997) protocol with little modification; several elements in the yeast malt extract broth (ISP2) contained were detected using Inductively Coupled Plasma (ICP). The assay was conducted by comparing 18 trace elements concentrations (mg/l) include (Ba, Ca, Co, Cu, Fe, Hg, K, Li, Mn, Mo, Na, Ni, P, Se, Sr, Ti, Zn and Mg). The comparing carried out between only broth (negative control) at the zero points without the NFS2 isolate and the supernatant of crude extract inoculated with NFS2

isolate after 7 days of incubation in shaking incubator. Taking 1ml of both broth and diluted with 4 ml of the sterilized distilled water to make final dilution 5 times. 18 trace elements included in the analysis through using ICP (Spectro Arcos, Germany). The instrument conditions were used: Spray chamber is Scott spray; Nebulizer: cross-flow; RF power/W: 1400; pump speed: 30 RPM; Coolant flow (L/min): 14; Auxiliary flow (L/min): 0.9; nebulizer gas flow (L/min): 0.8; Preflush (s): 40; Measure time (s): 28; replicate measurement: 3; multi-elements stock solutions containing 1000 mg/L were obtained from Bernd Kraft (Bernd Kraft GmbH, Duisburg, Germany); standard solutions were diluted by several dilution into 0.1, 0.5, 2 ppm in 0.5% nitric acid.

3.Results and Discussions

Eleven different isolates were obtained from non-farming soil (NFS), (NFS 1,2,3,4,5,6, 7,14,19,34 and 36) out of 45 collected samples in Kalar district, by plate diluting techniques on yeast malt extract agar ISP2 depending on the most general characters of actinomycetes isolation guidelines. The result was in agreement with that described by (Portillo *et al.*, 2009) that the colony number may represent from two to four per each plate and the number will be reduced when similar habitat or soils are present. At the first step, all obtained colonies were screened using Gram stain method (Figure 2 A), and the results showed that all isolates are Gram positive filamentous bacteria. The primary screening assay via cross streak method was carried out for determining the most powerful antimicrobial isolate as shown in (Figure 2 B and C). Among all eleven isolated actinomycetes, the isolate NFS2 was presented on ISP2 medium before adding the microbial pathogens after 3 days (Figure 2 B) and seven days (Figure 2D) of incubations. Following incubation of the actinomycetes microbial pathogens, *E coli* ATCC 25922 (E), *S aureus* ATCC 25923 (S), *Micrococcus luteus* ATCC 9341 (M), *C albicans* ATCC 10231 (C) and *P aeruginosa* ATCC27853 (P) were added, the results showed that the NFS2 isolate presented powerful antimicrobial activities against the most used microbial pathogens especially *S aureus*, *M luteus* and *C albicans* (Figure 2 C).

The results for secondary metabolites activities against all microbial pathogens as crude extract and extracellular antimicrobial metabolites such

(n-hexan, n- butanol and ethyl acetate) are presented in (Table 1). The crude extract exhibits powerful antimicrobial activity against both Gram-positive bacteria (*S aureus* and *M luteus*) and *C albicans*. The inhibition zones were 25.5 and 33.5 mm for *S aureus* ATCC 25923 and *M luteus* ATCC 9341 respectively, while 30.5 mm was recorded for *Candida albicans* ATCC 10231. On the other side, the crude extract does not exhibit any inhibition zone against the Gram-negative bacteria used including *E coli* ATCC 25922 and *P aeruginosa* ATCC 27853. These results indicate that the crude extract from the bacterial fermentation only has an effective antimicrobial against both Gram-positive bacteria and *C albicans*. The extracellular secondary metabolites extracted from all organic solvents also showed antimicrobial activities (Table 1). For instance, the result for n-hexane extract was 28 mm zones of inhibition against *S aureus* ATCC 25923. In the case of *M luteus* ATCC 9341, both n-hexane and n-butanol have the same antimicrobial activities which are 21 mm zones of inhibitions. In addition, the difference in the antibacterial powerful activity by using different organic solvent extracts may be due to their difference in the solubility of bioactive compounds in various solvents and variation in the cell wall structure of tested bacteria (Aali *et al.*, 2018). Finally the result for *C albicans* ATCC 10231 for n-hexane extract was 29 mm zones of inhibition. The results for Gram-positive bacteria were in agreement with that obtained and described by (Kim *et al.*, 1994; Singh *et al.*, 2016), as they demonstrate that the Gram negative bacterial cell wall structure is mainly composed of lipopolysaccharide (LPS). However, the Gram-positive bacteria lack this structure, and this causes the bacteria to become more susceptible to our extracted metabolites.

Comparing antibacterial activities between NFS2 crude extract and synthetic antibiotic discs were presented in (Figure 3). Panel (A) represents the activity of NFS2 crude extract and synthetic antibiotic discs against *S aureus* ATCC 25923. The results indicated that the NFS2 crude extract records higher inhibition zone overall used synthetic except Gentamicin 10 µg (CN 10), while in case of *M luteus* ATCC 9341, Panel (B), NFS2 recorded the best inhibition zone overall used synthetic zone except Ciprofloxacin 10 µg (Cip

10). In contrast, in the case of both Gram-negative bacteria *E. coli* ATCC 25922, *P. aeruginosa* ATCC 27853 as presented in Panel (C and D) respectively, there were no any results recorded, which point out the NFS2 extract only effects on Gram-positive bacteria.

The antioxidant scavenge activity of NFS2 isolate crude extract was summarized in (Figure 4). The result was gradually increased depending on the crude extract concentration for scavenging free radical presented in the solution till recording the maximum activity with 30mg/ml which record 93.46% scavenging activity with the standard deviation ($SD \pm 8.43$). The presented result was in agreement with that obtained and recorded by (Mbwambo *et al.*, 2007; Mohammad-Amin *et al.*, 2016; Maikhan *et al.*, 2018). On the other hands, the result for H_2O_2 scavenging activities presented in (Figure 5), indicate that the crude extract of NFS2 isolate has the potent for scavenging the great amount of H_2O_2 in the solution, the highest scavenging activity result was recorded 43.94% scavenging activity which obtained by 1.25 mg/ml of crude extract with standard deviation ($SD \pm 1.8$). Hydrogen peroxide easily penetrates across the cell membrane, producing the ROS (reactive oxygen species) after reacting with (Fe^{2+} and Cu^{2+}) which having more toxic affects such hydroxyl free radical (Sawant *et al.*, 2009). The results for both antioxidant activity and H_2O_2 scavenging activity indicate the presence of active compounds in the crude extract with the

competence of reducing Fe^{+3} ions as described by (Kekuda *et al.*, 2010). As well as, perform the preventing the progress of various oxidative stress-related disorders (Poongodi *et al.*, 2012).

The results for comparing trace elements concentration between the non-inoculated ISP2 broth as a negative control, with inoculated ISP2 broth by NFS2 after 7 days of fermentation was presented in (Table 2), the results indicate that were trace elements in the culture broth highly changed, some of them decreased while a little of them increased, this fluctuation of the trace elements concentration (especially decreased elements) due to their consumed during the fermentation process by the bacteria, and other increased trace elements concentration due to their production by the bacterial cell in response to the fermentation process. Some of the tested trace elements play a vital role in the bacterial life cycle such (Ca, Fe, K, Na, P, Sr, Mg, and Zn) for enhancing or inhibiting the bacterial secondary metabolites production as in the study of (Chesters and Rolinson, 1951), they investigate that some trace elements are essential for growth such zinc and copper, as well as, other required for production of antibiotics as for grown alone such iron, therefore, manipulating these trace elements in the broth culture during fermentation process will give the new results differ widely from steadily running standard or internationally pre-described medium.

Table1: Secondary antimicrobial activities of crude extract alone and extracellular metabolites activities against microbial pathogens (mm zones of inhibition)

Microbial pathogens	Inhibition zone (mm)			
	Crude extract	n-hexan extract	n- butanol extract	Ethyl acetate extract
<i>Escherichia coli</i> (ATCC 25922)	0	0	0	0
<i>Staphylococcus aureus</i> (ATCC 25923)	25.5	28	25	18
<i>Pseudomonas aeruginosa</i> (ATTC27853)	0	0	0	0
<i>Micrococcus luteus</i> (ATTC 9341)	33.5	21	21	14
<i>Candida albicans</i> (ATCC 10231)	30.5	29	25	20

Table 2: trace elements concentration comparison (mg/l) of ISP2 broth media, between negative control starting point and inoculating broth with NFS2 after 7 days incubation

Trace elements	Negative control starting point mg/l	ISP2 after fermentation mg/l	Notes
Ba	1.17	1.015	-
Ca	24.785	20.49	-
Co	0.01	0.005	-
Cu	ND	ND	
Fe	0.045	0.02	-
Hg	0.145	0.135	-
K	121.85	95.09	-
Li	0.095	0.075	-
Mn	0.005	0	-
Mo	ND	ND	
Na	184.695	127.85	-
Ni	0.025	0.03	+
P	14.125	6.285	-
Se	0.165	0.25	+
Sr	3.95	3.555	-
Ti	0.07	0.055	-
Zn	0.12	0.085	-
Mg	9.945	7.96	-

ND: note detected; -: Decreased; +: increased



Figure 1: Kalar district location and their border on Iraqi map, 45 soil samples were collected from non-farming soil. The picture was get from the Google map

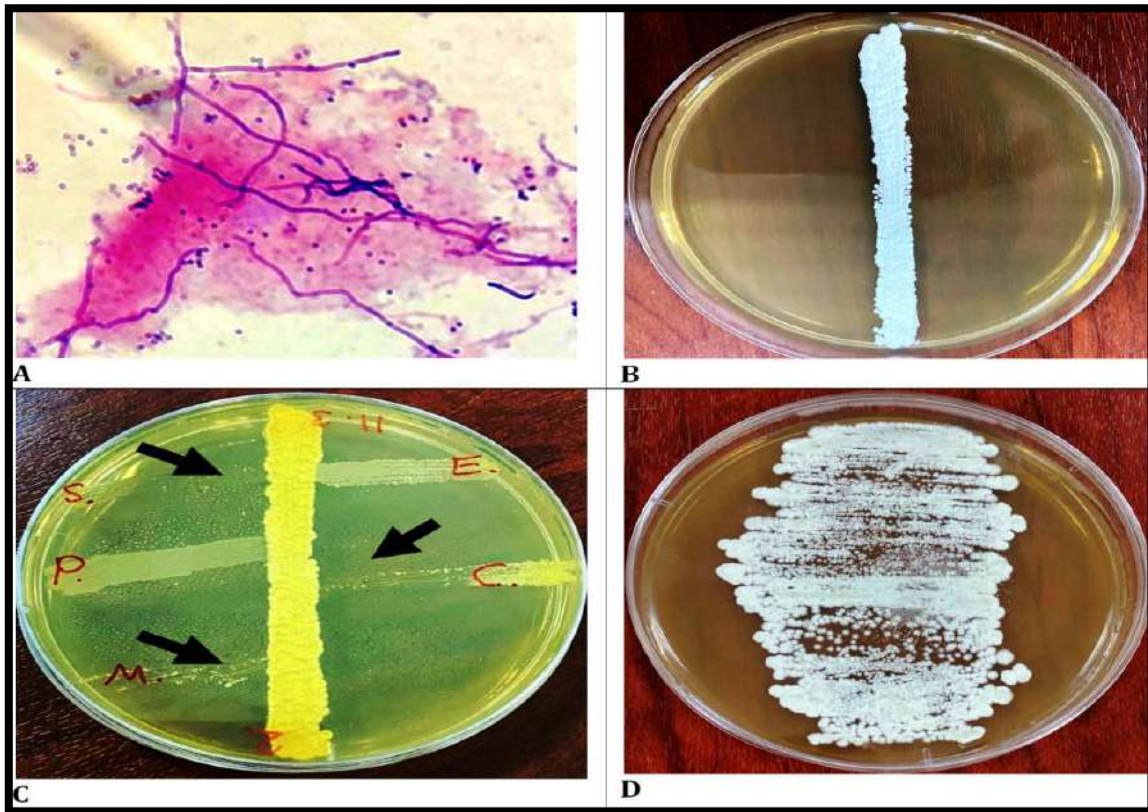


Figure 2: **A** Gram stain for all isolates (positive results; NFS2); **B** primary screening assay, cross streak assay after 3 days of incubations without the microbial pathogens; **C**, Primary screening assay results for NFS2 on all microbial pathogens; **D**, pure culture colonies of NFS2 on ISP2 after 7 days of incubation.

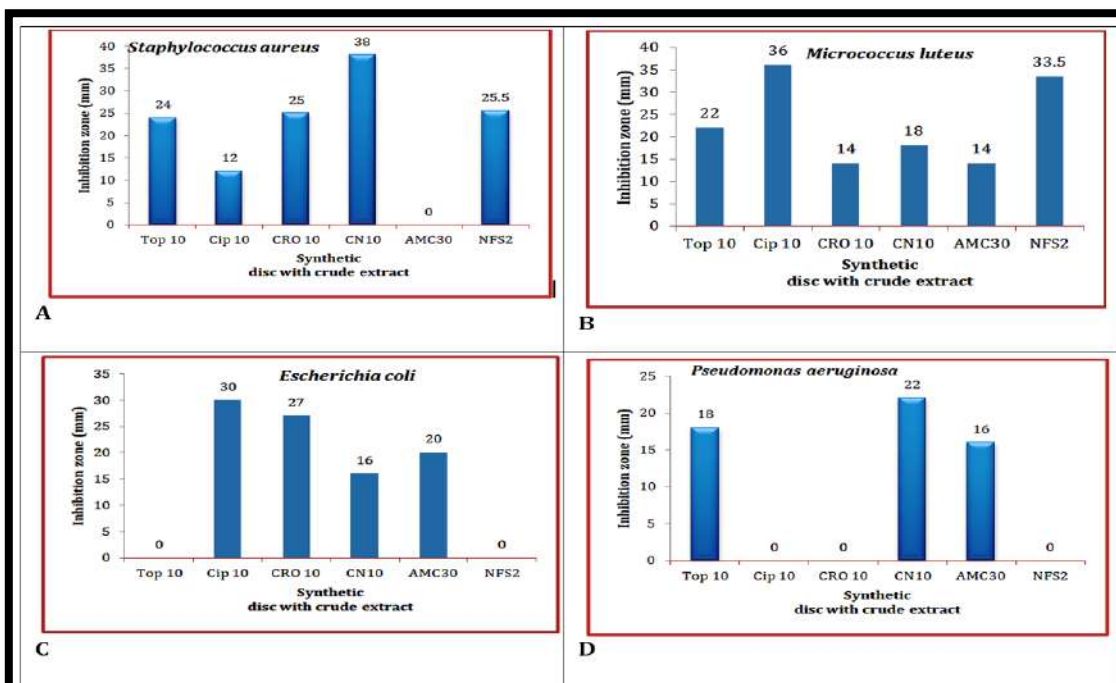


Figure 3: Comparing antibacterial activity of different synthetic antibiotic discs with NFS2 crude extract on microbial pathogen; **A:** *Staphylococcus aureus*, **B:** *Micrococcus luteus*, **C:** *Escherichia coli*, **D:** *Pseudomonas aeruginosa*. n=1

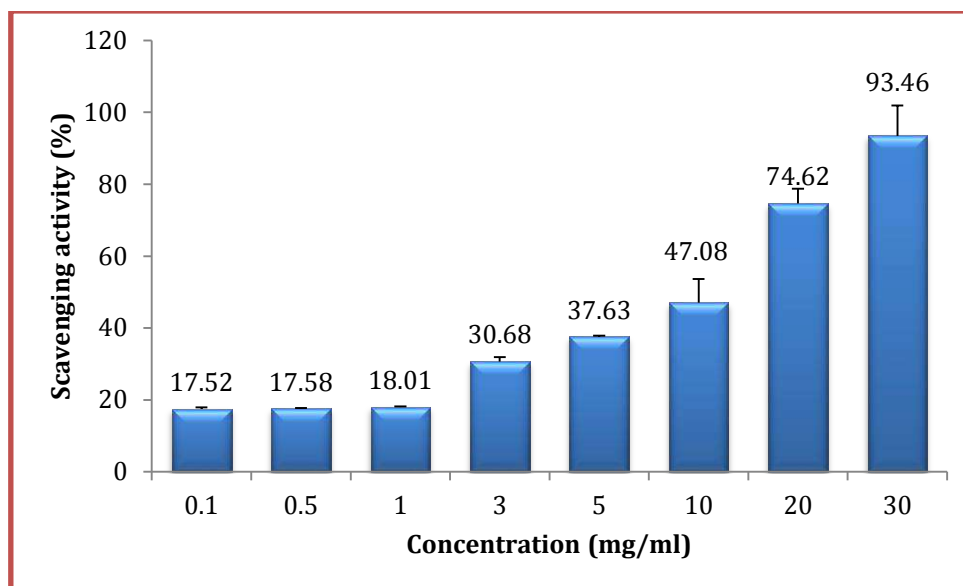


Figure 4: Antioxidant scavenging activities of NFS2 crude extract by DPPH radical scavenging activity assay, mean of the antioxidant scavenging activity with standard deviation, n=2

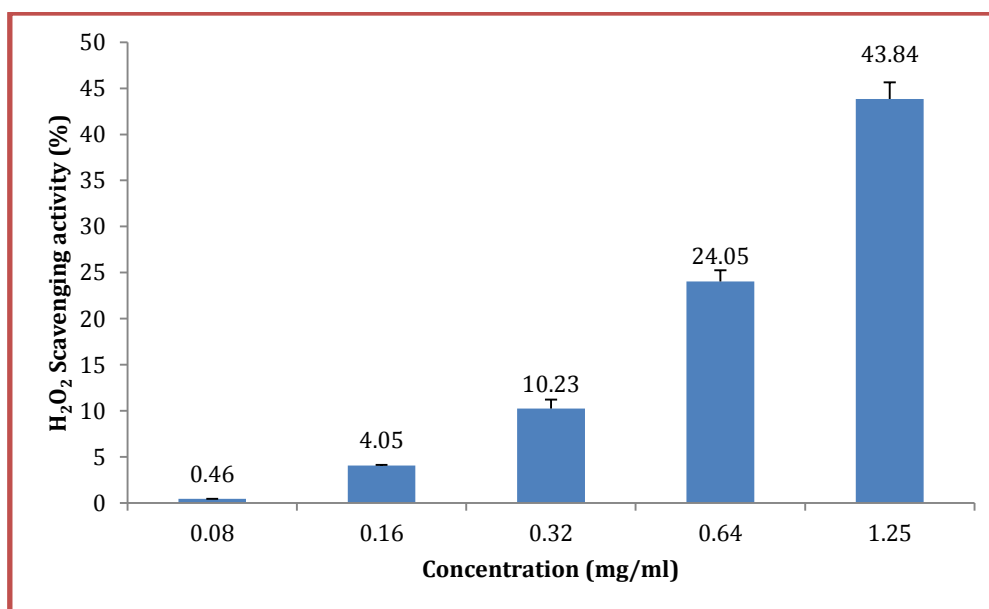


Figure 5: H₂O₂ scavenged activity of NFS2 crude extract with different concentration, mean of the scavenging activity with standard deviation, n=2

4. Conclusion

Eleven isolates of actinomycetes were obtained from forty five soil samples in Kalar district. NFS2 isolate had the most potent antimicrobial metabolites against Gram positive and Candida. Furthermore, this isolate showed antioxidant activity through scavenging the free radicals. Different trace elements concentrations in ISP2 were detected throughout the fermentation process by ICP. This suggests that the NFS2 isolate may use some of these trace elements in their growth process.

Recommendation

The screening protocol for isolating novel isolates from different habitats needs more soil types with different depth. Manipulating the trace element concentrations in the ISP2 broth media will exhibit different results especially relating with antagonistic or antioxidant activities. Future study should focus on separating the bioactive compounds which can be used for discovering new antibiotics.

Acknowledgment

This work was conducted in the research center of Garmian University; I thank all efforts from assist prof. Dr. Ayad Palani and Mr. Azad Hama Ali for helping me for conducting antioxidant activity and trace elements analyzing respectively.

5.References

- Aali, M.H., Ismaiel, N.J. and Majid, F.A.A. 2018. Antioxidant, and Antimicrobial Activities of Phenolic and Flavonoid Rich Medicinal Plants (Fritillaria Zagrica and Tulipa Kurdica) Bulbs Collected in Kurdistan Region of Iraq, *ZANCO Journal of Pure and Applied Sciences*, 30 (5) 1-16.
- Abbas, A.K. 2009. Antifungal activities of actinomycetes isolated from a sample of Iraqi soils, *Iraqi Journal of Community Medicine*, 22(3) 179-183.
- AL-Mawlah, Y.H., 2018. Antibacterial Activity of Streptomyces sp. Isolated from High Tolerant Ecosystem in Babylon Province, Iraq, *Journal of University of Babylon for Pure and Applied Sciences*, 26 (7) 303-308.
- Berdy, J. 2005. Bioactive microbial metabolites, *The Journal of antibiotics*, 58(1) 1-26.
- Burghal, A.A., Mahdi, K.H. and Al-Mudaffar, N.A. 2015. Isolation and identification of actinomycetes strains from oil refinery contaminated soil, Basrah-Iraq, *International Journal of Innovations in Engineering and Technology*, 2, 20-27.
- Chesters, C.G.C. and Rolinson, G.N. 1951. Trace elements and streptomycin production, *Microbiology*, 5(3) 559-565.
- Dholakiya, R.N., Kumar, R., Mishra, A., Mody, K.H. and Jha, B. 2017. Antibacterial and antioxidant activities of novel actinobacteria strain isolated from Gulf of Khambhat, Gujarat, *Frontiers in microbiology*, 8, 2420, 1-16.
- Gebreyohannes, G., Moges, F., Sahile, S. and Raja, N. 2013. Isolation and characterization of potential antibiotic producing actinomycetes from water and sediments of Lake Tana, Ethiopia. *Asian pacific journal of Tropical biomedicine*, 3(6) 426-435.
- Gurung, T.D., Sherpa, C., Agrawal, V.P. and Lekhak, B. 2009. Isolation and characterization of antibacterial actinomycetes from soil samples of Kalapatthar, Mount Everest Region, *Nepal Journal of science and Technology*, (10) 173-182.
- Hopwood DA, Bibb MJ, Chater KF, Kieser T, Bruton CJ, Kieser HM, et al. Norwich, UK: The John Innes Foundation. 1985. Genetic Manipulation of Streptomyces. *A Laboratory Manual*.
- Hsiung, C.S., Andrade, J.D., Costa, R. and Ash, K.O. 1997. Minimizing interferences in the quantitative multielement analysis of trace elements in biological fluids by inductively coupled plasma mass spectrometry, *Clinical chemistry*, 43(12)2303-2311.
- Janardhan, A., Kumar, A.P., Viswanath, B., Saigopal, D.V.R. and Narasimha, G. 2014. Production of bioactive compounds by actinomycetes and their antioxidant properties, *Biotechnology research international*, 1-8.
- Jaralla, E.M., Al-Dabbagh, N.N., Hameed, N. and Abdul-Hussain, N. 2014. Screening for enzymatic production ability and antimicrobial activity of actinomycetes isolated from soil in Hillah/Iraq, *Journal of Pharmacy and Biological Sciences*, 9 (5) 42-47.
- Kekuda, P.T.R., Shobha, K.S. and Onkarappa, R. 2010. Studies on antioxidant and anthelmintic activity of two Streptomyces species isolated from Western Ghat soils of Agumbe, Karnataka, *Journal of Pharmacy Research*, 3(1)26-29.
- Khalaf, N.A., Shakya, A.K., Al-Othman, A., El-Agbar, Z. and Farah, H. 2008. Antioxidant activity of some common plants, *Turkish Journal of Biology*, 32(1)51-55.
- Kim, C.J., Lee, K.H., Kwon, O.S., Shimazu, A. and Yoo, I.D. 1994. Selective isolation of actinomycetes by physical pretreatment of soil sample, *Microbiology and Biotechnology Letters*, 22(2) 222-225.
- Maikhan, H.K., Mohammad-Amin, S.M. and Tawfeeq, H.M. 2018. Morphological and Molecular Identification of Trichophyton Mentagrophytes Isolated from Dermatophytes Patients in Garmian Area, *ZANCO Journal of Pure and Applied Sciences*, 30(4)1-10.
- Mbwambo, Z.H., Moshi, M.J., Masimba, P.J., Kapingu, M.C. and Nondo, R.S., 2007. Antimicrobial activity and brine shrimp toxicity of extracts of Terminalia brownii roots and stem, *BMC complementary and Alternative Medicine*, 7 (1) 9.
- Mohammad-Amin, S. M, Rasin, M. H. Abdulmohimin, N. 2016. Antimicrobial and Antioxidant Activities of Biologically Active Extract from Locally Isolated Actinomycetes in Garmian Area, *Journal of Garmian University*, (1)1-10
- Patel, M.K., Mishra, A. and Jha, B. 2016. Non-targeted metabolite profiling and scavenging activity unveil the nutraceutical potential of psyllium (Plantago ovata Forsk), *Frontiers in plant science*, 7 (431) 1-17.
- Poongodi, S., Karuppiyah, V., Sivakumar, K. and Kannan, L. 2012. Marine actinobacteria of the coral reef environment of the gulf of mannar biosphere reserve, India: a search for antioxidant property, *International Journal of Pharmacy and Pharmaceutical Sciences*, 4(5) 316-321.
- Portillo, M.C.; Saiz-Jimenez, C. and Gonzalez, J.M. 2009. Molecular characterization of total and metabolically active bacterial communities of "white colonizations" in the Altamira Cave, Spain, *Research in Microbiology*, 160 (1) 41-47.
- Praveen, V., Tripathi, D., Tripathi, C.K.M. and Bihari, V. 2008. Nutritional regulation of actinomycin-D production by a new isolate of Streptomyces sindensis using statistical methods, *Indian Journal of Experimental Biology*, 46(2) 138-144.
- Rahman, M., Islam, M.Z., Islam, M. and Ul, A. 2011. Antibacterial activities of Actinomycete isolates

- collected from soils of Rajshahi, Bangladesh, *Biotechnology research international*, 2011 ID 857925, 1-6
- Risan, M.H., Abdulmohimin, N. and Mohammad-Amin, S.M. 2016. Production, Partial Purification and Antitumor Properties of Bioactive Compounds from Locally Isolated Actinomycetes (KH14), *Iraqi journal of biotechnology*, 15(3) 51-64.
- Saadoun, I., Hameed, K.M. and Moussauui, A. 1999. Characterization and analysis of antibiotic activity of some aquatic actinomycetes, *Microbios*, 99 (394) 173-179.
- Salim, F.M., Sharmili, S.A., Anbumalarmathi, J. and Umamaheswari, K. 2017. Isolation, molecular characterization and identification of antibiotic producing actinomycetes from soil samples, *Journal of Applied Pharmaceutical Science*, 7(09) 069-075.
- Sawant, O., Kadam, V.J. and Ghosh, R. 2009. In vitro free radical scavenging and antioxidant activity of *Adiantum lunulatum*, *Journal of Herbal medicine and Toxicology*, 3(2) 39-44.
- Singh V, Haque S, Singh H, Verma J, Vibha K, Singh R, Jawed A and Tripathi CKM. 2016. Isolation, Screening, and Identification of Novel Isolates of Actinomycetes from India for Antimicrobial Applications, *Frontier Microbiology*, (7) 1921.
- Singh, V. and Tripathi, C.K.M., 2011. Olivanic acid production in fed batch cultivation by *Streptomyces olivaceus* MTCC 6820. *Research Journal of Pharmaceutical, Biological and Chemical Sciences*, 2 (4)726-731.
- Subathra, D.C., Amrita, K., Nitin, J., Jemimah, N.S., Mohana, S.V. 2013. Screening of actinomycetes isolated from soil samples for antibacterial and antioxidant activity, *International Journal of Pharmacy and Pharmaceutical Science*, 5(4) 483-489.
- Waksman, S.A. 1961. Classification, identification and descriptions of genera and species, *The actinomycetes*, (2) 61-292.

RESEARCH PAPER

Molecular Study of *IL-7R* Gene Polymorphism and their Associations with Male Multiple Sclerosis Patients in Erbil Province.

Shukur W. Smail¹, Mukhlis H. Aali¹, Fikry A. Qadir¹, Ahmed O. Pirdawid², Abdulla A. Shareef¹, Abdulkarim Y. Karim¹, Roza T. Yaseen³, Mohammed Q. Mustafa³, Kovan F. Jalal³ and Abbas Salihi^{1,3}

¹ Department of Biology, College of Science, Salahaddin University-Erbil, Kurdistan Region, Iraq

² Department of Biology, College of Science - University of Duhok, Kurdistan Region, Iraq

³ Department of Medical Analysis, Tishk International University, Erbil, Kurdistan Region, Iraq

ABSTRACT:

Multiple sclerosis (MS) is an autoimmune disease in which immune cells attacks the body cells mistakenly; it is characterized by chronic inflammation that leads to demyelination and conduction of nerve impulse is affected negatively. The cause of the disease is unknown, but it may be partially under the control of genetics, including interleukin 7 receptor alpha (*IL7Rα*). In this case-control study, 40 relapsing-remitting MS (RRMS) male patients, which fulfills McDonald criteria and 40 healthy controls, with matched sex, were compared depending on the rs6897932 polymorphism within the exon 6 of *IL7Rα* gene by Tetra-amplification refractory mutation system polymerase chain reaction (Tetra-ARMS-PCR) method. The frequency of T allele of *IL7Rα* rs6897932 was considerably higher in male MS patients than healthy control males (31.25 vs 17.5%). Genotype distributions of the single nucleotide polymorphism (SNP) rs6897932 deviated from Hardy-Weinberg equilibrium with a p-value of 0.80. Both homozygous (TT) and Heterozygous (CT) were non-significantly positively associated with MS male patients (OR = 6.75, 95%CI = 0.73-62.4, p = 0.059, OR = 1.68, 95%CI = 0.64-4.38, p = 0.28) respectively. The distribution of the rs6897932 polymorphism is not significantly different in our case/control study in the Erbil province.

KEY WORDS: Multiple Sclerosis, Interleukin 7 Receptor, Polymorphism, Relapsing-Remitting Multiple Sclerosis

DOI: <http://dx.doi.org/10.21271/ZJPAS.33.1.3>

ZJPAS (2021) , 33(1);21-26 .

1. INTRODUCTION

Multiple sclerosis (MS) is a long-standing autoimmune disease that occurs by the inflammation in the central nervous system (CNS) and results in demyelination and impairment of axons (Valcarcel *et al.*, 2018, Gold *et al.*, 2012). It can be classified as an autoimmune disease that impacts CNS and distinguished by numerous brain and spinal cord lesions (Rosati, 2001, Hafler, 2004, Wilkins, 2018).

The disease is expected to influence approximately two and a half million people in the world (Rosati, 2001). Furthermore, MS is more common in females than in males. Currently, the rate of females with this disease to males is 2–1 (Ascherio and Munger, 2016).

MS etiology is unclear, but several studies have already shown that causative agents of MS is reliant on a strong genetic factor (Akkad *et al.*, 2009). Several different methods have been used to determine the genetic bases of MS, such as genetic linkage, gene expression and candidate

* Corresponding Author:

Shukur Wasman Smail

E-mail: shukur.smail@su.edu.krd

Article History:

Received: 16/03/2020

Accepted: 08/09/2020

Published: 20/02 /2021

gene association (Gregory *et al.*, 2007, Rizvi *et al.*, 2020).

Amongst the association study is a viable approach toward recognizing the risk genetic loci of genes as a marker such as SNP. Among these was reported the relationship of many *IL-7* receptor SNPs with MS in various ethnic groups (Sahami-Fard *et al.*, 2020, Zhang *et al.*, 2019). The position of *IL7R* is chromosome 5 short arm 13 (5p13). This gene consists of γ chain (*IL7R γ*) and α chain (*IL7R α*) usually recognized as CD132 and CD127 respectively. The SNPs throughout the alpha chain of *IL7R* gene have a big role in the impairment of immune system homeostasis and this prone to MS easily (Zhang *et al.*, 2005, Čierny *et al.*, 2015).

Appropriately, association studies for the variants of *IL7R α* gene revealed that rs6897932 in the exon 6 might be a causative factor for MS evolving in many Japanese and European communities (Gregory *et al.*, 2007, Weber *et al.*, 2008, Fang *et al.*, 2011).

In the exon number 6 of *IL7R α* gene there is SNP called rs6897932 induces non-conservative amino acid transition at location 244 in which isoleucine shifted to threonine 244 (Ile \rightarrow Thr) (ATC / ACC) (Teutsch *et al.*, 2003). This amino acid shift affects the expression product of *IL7R α* which results in the variation amount of membrane-bound isoform and soluble form. Such modifications are accompanied by the regulation of the *IL7* signaling pathway and a direct association MS with this SNP (Gregory *et al.*, 2007).

Before many types of researches have been done, most of them have assessed the relationship of T244I variant, rs6897932 with MS pathology, while other researches couldn't find any connection between them. Studies that recently done have shown that the C allele is slightly more prevalent than the T allele. Also, it has been suggested in region rs6897932 the C allele will lead to a higher threat of MS in some population (Gregory *et al.*, 2007, Weber *et al.*, 2008, Fang *et al.*, 2011). Therefore, the opportunity to have MS will increase by 1.5 and 1.3 folds for the genotypes CC and CT respectively, if we deliberated that genotype TT as a normal risk. Dependent on many types of researches with varied results about the polymorphism rs6897932, it is difficult to know for sure concerning the

interaction of this SNP with MS (Čierny *et al.*, 2015).

To arrive at a definite conclusion, we decided to have this study in Erbil province-Iraq to evaluate the importance of the *IL7R α* gene polymorphisms, rs6897932 in such community and investigate their influence on *IL7R α* gene expression concerning MS pathogenesis.

2. MATERIALS AND METHODS

2.1. Sample Collection

Forty males with MS patients enrolled in this study who visited department of neurology, Rzgari hospital in Erbil city-Iraq from April to June of 2015, and they were diagnosed according to 2005 revised McDonald criteria. Forty control males who were age-matched with MS patients.

2.2. Molecular Technique Analysis

2.2.1. Genomic DNA Extraction from Human Blood Samples

Human Blood samples were taken from peripheral veins using the five-milliliter syringe. The blood put into K₂EDTA (5.4mg) tube for direct DNA extraction. The Genomic DNA extracted from whole blood samples by using spin column method (AccPrep Genomic DNA extraction Kit-Bioneer, South Korea), depending on the manufacturer's instructions. Then the concentration and purity of genomic DNA extracted from each human blood samples were determined using Nano-Drop™ (Thermo Scientific, USA) spectrophotometer by recording the concentration ranged (11.05-61.60 ng/ μ l) and purity (1.69-2.27) for each sample.

2.2.2. Genotyping *IL7R α* Gene Polymorphism (PCR Amplification)

Genotyping of the SNP rs6897932 C>T that located in exon 6 of *IL7R α* gene performed by a rapid and cost-effective technique called the Tetra-ARMS-PCR method in Tishk International University. In this polymorphism one sequence-specific forward primers: 5'-AAGAAGGAAGAGAGCATTGG-3', and three sequence-specific reverse primers that two of them: 5'-GAAAAAACTCAAATGCTGATGG-3' (for C allele) and 5'-AGAAAAAACTCAAATGCTGATGA-3' (for T allele) and one reverse were a primer for internal control 5' TTA CTTTGGGGACAGCGTTT-3' used (Majdinasab *et al.*, 2014).

The total of 25 μ l volume of PCR master mix reaction achieved containing 3 μ l of genomic

DNA, 12.5 μ l of Taq DNA Polymerase 2x Master Mix RED (Ampliqon, Danish) and 1 μ l was added for each of the forward and reverse primers for *IL7Ra* gene. Then the mixture was completed by adding 3.5 μ l of nuclease-free water (Čierny et al., 2015).

The program of PCR amplification consisted of an initial denaturation at 94 °C for 5 minutes followed by the next 35 cycles 94 °C for 30 seconds (denaturation), 62 °C for 30 seconds (annealing), 72 °C for 30 seconds (elongation) and the final step at 72 °C for 5 minutes to extend all PCR fragments (Majdinasab et al., 2014). After PCR amplification, the PCR DNA amplicons separated on 1.5% agarose gel (after applying 5 V/cm) (Magdeldin, 2012), then the separated bands were stained with ethidium bromide to visualize under UV light (Bio-Rad UV-transilluminator) (Brown, 2016). The 301 bp mean the appearance of *IL-7R* gene polymorphism in exon 6 (Figure 1).

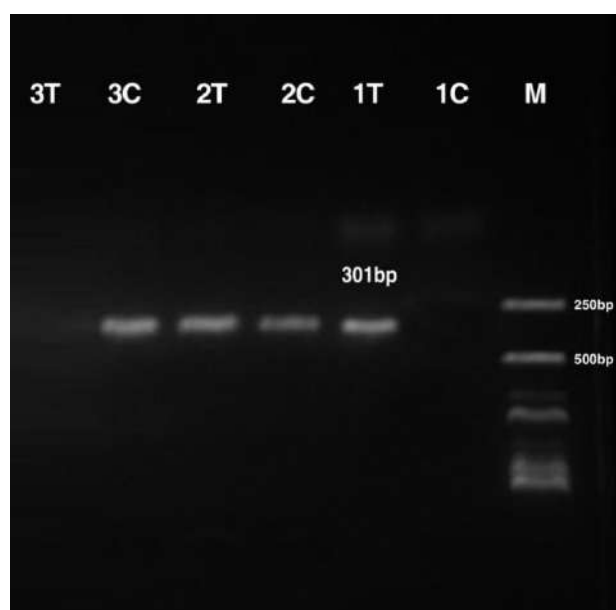


Figure 1. Gel electrophoresis for the *IL7Ra* rs6897932 gene showing the T and C alleles in some MS patients. Band 301bp indicates the presence of T or C alleles. Sample 1 (lane 1C and

1T) has TT genotypes, sample 2 (lane 2C and 2T) has CT genotype and sample 3 (lane 3C and 3T) has CC genotype, M= 250 bp DNA ladder.

2.3. Statistical Analysis

GraphPad Prism 6 statistical software used for statistical analysis. A student t-test used to compare the ages between MS patients and healthy controls. Genotype and allele frequencies of MS patients and healthy controls were analyzed using the Chi-square (χ^2) test. Both genotype and allelic odds ratio (ORs) and 95% confidence interval (CI) calculated to determine the association of the SNP in exon 6 of the *IL7Ra* receptor gene polymorphisms with MS. A *p*-value of less than 5% ($p < 0.05$) set to be statistically significant.

3. RESULTS

Demographic profiles of both male MS patients and healthy control males had shown in table 1. The mean age of MS patients was 34.85 ± 1.442 years, and of the control group was 32.25 ± 1.375 years; yielding no statistically significant difference in their ages. In this case-control study, 40 MS patients and 40 healthy controls compared depending on the rs6897932 polymorphism within the exon 6 of *IL7Ra* gene by Tetra-ARMS-PCR method. The genotype and allele frequencies of *IL7Ra* rs6897932 are given in (Table 2). The frequency of the T allele of *IL7Ra* rs6897932 was not significantly changed in male MS patients than healthy control males (31.25 vs 17.5%). Genotype distributions of the SNP rs6897932 deviated from Hardy-Weinberg equilibrium with a *p*-value of 0.80. The significance association was not found in both homozygous (TT) and Heterozygous (CT) in MS male patients (OR = 6.75, 95%CI = 0.73-62.4, $p = 0.059$, OR = 1.68, 95%CI = 0.64-4.38, $p = 0.28$) respectively (Table 2).

Table 1. Age of MS patients and controls

Variable	Age Range (years)	Mean Age \pm SE
MS Patients	20-50	34.85 \pm 1.442
Controls	20-50	32.25 \pm 1.375

Table 2. Association of MS with carriage of alleles/genotypes of *IL7Ra* rs6897932 SNP

Polymorphism	MS (n=40)		Control (n=40)		OR	95% CI	p-value	HWE
	No.	%	No	%				
CC	20	50.0	27	67.5	1.0	-	-	0.80
CT	15	37.5	12	30.0	1.688	0.64-	0.28	
						4.38		
TT	5	12.5	1	2.5	6.75	0.73-	0.059	
						62.4		
C-Allele	55	68.75	66	82.5	2.143	1.016-	0.0428	
T-Allele	25	31.25	14	17.5		4.518		

4. DISCUSSION

Multiple sclerosis (MS) is an autoimmune disease, which is characterized by demyelination of the axon of neurons in the CNS and predominant of inflammation. The etiology of the disease is not well known, but it may be under genetics and environmental factors (Dyment *et al.*, 1997). The genes, which are involved and increased susceptibility to the disease, are divided into two groups: *HLA* genes (Sawcer *et al.*, 2011) and non-*HLA* genes (Rounachi *et al.*, 2009). The most *HLA* gene which is related to MS is *HLA-DRB1*1501* class II allele (Alcina *et al.*, 2010), it is located on chromosome 6p21. Besides *HLA* genes there are many genes which are proposed by GWAS that candidates be involved in the

development and severity of the MS. Non-*HLA* genes have a role in regulation and modulation of cytokine, cytokine receptor, transcription factor and T lymphocyte receptor (Rounachi *et al.*, 2009). Non-*HLA* genes that are usually involved in MS are *CD 25*, *EVI5*, *CD58*, *CD154* and *IL7Ra*.

Interleukin 7 receptor alpha (*IL7Ra*, also known as *CD127*), is one of the most critical genes which has a role in developing MS. It located on chromosome 5p13.2. It expressed on B and T lymphocytes, it has essential in maturation, developing and survival of them (Manolio *et al.*, 2009). There are many SNP of *IL7Ra* but, the most critical SNP in MS is (rs6897932, p.T244I) which is vital for developing *IL7Ra* in the form of membrane-bound or the way of the soluble

receptor, in this manner it is involved in developing MS (Booth *et al.*, 2005, Zuvich *et al.*, 2009). Since, rs6897932 polymorphism of *IL7Ra* controlling post-transcription modification and alternative splicing the exon 6 of pre-mature mRNA of *IL7Ra* (Booth *et al.*, 2005). The allele of "C" has a role in skipping alternative splicing the exon 6, and developing a soluble form of *IL7Ra* while, The allele of "T" has a role alternative splicing the exon 6 and developing a membrane-bound type of *IL7Ra* (Gregory *et al.*, 2007). The carriers of the "T" allele believed to be a predisposing factor for developing MS because it leads to the formation of the more membrane-bound form of *IL7Ra* and the creation of more auto-reactive T and B lymphocyte (Gregory *et al.*, 2007).

Another explanation for the role of *IL7Ra* in the pathogenesis of RRMS is that *IL7Ra* down-regulates the forkhead box P3 (FoxP3) which is, in turn, is the transcription factor for developing CD4+CD25+ regulatory T (T reg) cells, T reg cells is crucial in promoting tolerance and suppress autoreactive T lymphocyte. *IL7Ra* by decreasing FoxP3 can breakdown tolerance and developing an autoimmune disease, e.g. MS. The results of the current analysis are inconsistent with O'Doherty *et al.* (2008), Alcina *et al.* (2008) and Majdinasab *et al.* (2014) who found that rs6897932 polymorphism of *IL7Ra* was related with MS in UK, Spain and Iran, respectively.

CONCLUSIONS

In summary, there is no association between rs6897932 polymorphism of *IL7Ra* and RRMS patients in the Erbil province, by comparing this variant in control and MS groups. This study confirmed that rs6897932 polymorphism of *IL7Ra* is not a predisposing factor for developing the disease in the Erbil province.

Acknowledgment

We thank MS center in Rzgari hospital in Erbil city-Iraq for their support for taking permission from MS patients to give blood for conducting the research.

REFERENCES

AKKAD, D., HOFFJAN, S., PETRASCH-PARWEZ, E., BEYGO, J., GOLD, R. & EPPLIN, J. 2009.

Variation in the *IL7RA* and *IL2RA* genes in German multiple sclerosis patients. *Journal of autoimmunity*, 32, 110-115.

ALCINA, A., FEDETZ, M., NDAGIRE, D., FERNÁNDEZ, O., LEYVA, L., GUERRERO, M., ARNAL, C., DELGADO, C. & MATESANZ, F. 2008. The T244I variant of the interleukin-7 receptor- α gene and multiple sclerosis. *Tissue Antigens*, 72, 158-61.

ALCINA, A., FERNÁNDEZ, Ó., GONZALEZ, J. R., CATALÁ-RABASA, A., FEDETZ, M., NDAGIRE, D., LEYVA, L., GUERRERO, M., ARNAL, C. & DELGADO, C. 2010. Tag-SNP analysis of the *GFI1-EVI5-RPL5-FAM69* risk locus for multiple sclerosis. *European journal of human genetics*, 18, 827-831.

ASCHERIO, A. & MUNGER, K. L. 2016. Epidemiology of Multiple Sclerosis: From Risk Factors to Prevention-An Update. *Seminars in Neurology*, 36, 103-14.

BOOTH, D., ARTHUR, A., TEUTSCH, S., BYE, C., RUBIO, J., ARMATI, P., POLLARD, J., HEARD, R., STEWART, G. & CONSORTIUM, S. M. G. 2005. Gene expression and genotyping studies implicate the interleukin 7 receptor in the pathogenesis of primary progressive multiple sclerosis. *Journal of molecular medicine*, 83, 822-830.

BROWN, T. A. 2016. *Gene cloning and DNA analysis: an introduction*. New York, United States: John Wiley & Sons.

ČIERNY, D., HÁNYŠOVÁ, S., MICHALIK, J., KANTOROVÁ, E., KURČA, E., ŠKEREŇOVÁ, M. & LEHOTSKÝ, J. 2015. Genetic variants in interleukin 7 receptor α chain (*IL-7Ra*) are associated with multiple sclerosis risk and disability progression in Central European Slovak population. *Journal of neuroimmunology*, 282, 80-84.

DYMENT, D., SADOVNICK, A. & EBERS, G. 1997. Erratum: Genetics of multiple sclerosis (Human Molecular Genetics (1997) 6 (1693-1698)). *Human Molecular Genetics*, 6.

FANG, L., ISOBE, N., YOSHIMURA, S., YONEKAWA, T., MATSUSHITA, T., MASAKI, K., DOI, H., OCHI, K., MIYAMOTO, K. & KAWANO, Y. 2011. Interleukin-7 receptor α gene polymorphism influences multiple sclerosis risk in Asians. *Neurology*, 76, 2125-2127.

GOLD, R., KAPPOS, L., ARNOLD, D. L., BAR-OR, A., GIOVANNONI, G., SELMAJ, K., TORNATORE, C., SWEETSER, M. T., YANG, M. & SHEIKH, S. I. 2012. Placebo-controlled phase 3 study of oral

- BG-12 for relapsing multiple sclerosis. *New England Journal of Medicine*, 367, 1098-1107.
- GREGORY, S. G., SCHMIDT, S., SETH, P., OKSENBERG, J. R., HART, J., PROKOP, A., CAILLIER, S. J., BAN, M., GORIS, A. & BARCELLOS, L. F. 2007. Interleukin 7 receptor α chain (IL7R) shows allelic and functional association with multiple sclerosis. *Nature genetics*, 39, 1083-1091.
- HAFLER, D. A. 2004. More MS news articles for April 2004. *Journal of Clinical Investigation*, 113, 788-794.
- HENINGER, A. K., THEIL, A., WILHELM, C., PETZOLD, C., HUEBEL, N., KRETSCHMER, K., BONIFACIO, E. & MONTI, P. 2012. IL-7 abrogates suppressive activity of human CD4+CD25+FOXP3+ regulatory T cells and allows expansion of alloreactive and autoreactive T cells. *Journal of Immunology*, 189, 5649-58.
- MAGDELDIN, S. 2012. *Gel electrophoresis: Principles and basics*. Deutschland: BoD–Books on Demand.
- MAJDINASAB, N., HOSSEINI BEHBAHANI, M., GALEHDARI, H. & MOHAGHEGH, M. 2014b. Association of interleukin 7 receptor gene polymorphism rs6897932 with multiple sclerosis patients in Khuzestan. *Iranian journal of neurology*, 13, 168-171.
- MANOLIO, T. A., COLLINS, F. S., COX, N. J., GOLDSTEIN, D. B., HINDORFF, L. A., HUNTER, D. J., MCCARTHY, M. I., RAMOS, E. M., CARDON, L. R. & CHAKRAVARTI, A. 2009. Finding the missing heritability of complex diseases. *Nature*, 461, 747-753.
- O'DOHERTY, C., KANTARCI, O. & VANDENBROECK, K. 2008. IL7RA polymorphisms and susceptibility to multiple sclerosis. *New England Journal of Medicine*, 358, 753-754.
- RIZVI, S. A., STONE, J. A., CHAUDHRY, S. T., HADDAD, N., WONG, B. & GRIMES, J. O. 2020. Clinical Decision-Making in the Management of Multiple Sclerosis. *Clinical Neuroimmunology*. Springer.
- ROSATI, G. 2001. The prevalence of multiple sclerosis in the world: an update. *Neurological sciences*, 22, 117-139.
- RONAGHI, M., VALLIAN, S., & ETEMADIFAR, M. (2009). CD24 gene polymorphism is associated with the disease progression and susceptibility to multiple sclerosis in the Iranian population. *Psychiatry Research*, 170(2-3), 271-272.
- SAHAMI-FARD, M. H., MOZHDEH, M., IZADPANA, F., KASHANI, H. H. & NEZHADI, A. 2020. Interleukin 7 receptor T244I polymorphism and the multiple sclerosis susceptibility: a meta-analysis. *Journal of Neuroimmunology*, 577166.
- SAWCER, S., HELLENTHAL, G., PIRINEN, M., SPENCER, C. C., PATSOPOULOS, N. A., MOUTSIANAS, L., DILTHEY, A., SU, Z., FREEMAN, C. & HUNT, S. E. 2011. Genetic risk and a primary role for cell-mediated immune mechanisms in multiple sclerosis. *Nature*, 476, 214.
- TEUTSCH, S. M., BOOTH, D. R., BENNETTS, B. H., HEARD, R. N. & STEWART, G. J. 2003. Identification of 11 novel and common single nucleotide polymorphisms in the interleukin-7 receptor- α gene and their associations with multiple sclerosis. *European journal of human genetics*, 11, 509-515.
- VALCARCEL, A. M., LINN, K. A., KHALID, F., VANDEKAR, S. N., TAUHID, S., SATTERTHWAITE, T. D., MUSCHELLI, J., BAKSHI, R. & SHINOHARA, R. T. MIMoSA: An Approach to Automatically Segment T2 Hyperintense and T1 Hypointense Lesions in Multiple Sclerosis. International MICCAI Brainlesion Workshop, 2018. New York City: Springer.
- WEBER, F., FONTAINE, B., COURNU-REBEIX, I., KRONER, A., KNOP, M., LUTZ, S., MÜLLER-SARNOWSKI, F., UHR, M., BETTECKEN, T. & KOHLI, M. 2008. IL2RA and IL7RA genes confer susceptibility for multiple sclerosis in two independent European populations. *Genes & Immunity*, 9, 259-263.
- WILKINS, A. 2018. *Mechanisms of disease progression. Progressive Multiple Sclerosis*. New York City: Springer.
- ZHANG, Y., ZHANG, J., LIU, H., HE, F., CHEN, A., YANG, H. & PI, B. 2019. Meta-analysis of FOXP3 gene rs3761548 and rs2232365 polymorphism and multiple sclerosis susceptibility. *Medicine*, 98.
- ZHANG, Z., DUVEFELT, K., SVENSSON, F., MASTERMAN, T., JONASDOTTIR, G., SALTER, H., EMAHAZION, T., HELLGREN, D., FALK, G. & OLSSON, T. 2005. Two genes encoding immune-regulatory molecules (LAG3 and IL7R) confer susceptibility to multiple sclerosis. *Genes & Immunity*, 6, 145-152.
- ZUVICH, R., MCCAULEY, J., PERICAK-VANCE, M. & HAINES, J. *Genetics and pathogenesis of multiple sclerosis. Seminars in immunology, 2009*. Netherlands: Elsevier.

RESEARCH PAPER

The Association Study between Tumor Necrosis Factor- Receptor 1 36 A/G (TNFR1 36 A/G) Gene Polymorphism and Azoospermic Infertile Men in Erbil City

Ashti Mohammad Amin Said

Department of Molecular Biology, Medical Research Center/ Hawler Medical University, Kurdistan Region, Iraq

ABSTRACT:

Tumor necrosis factor-alpha (TNF- α) is a multifunctional cytokine that controls cellular activities related to spermatogenesis. (TNFR1) affects TNF- α activity and also may leads to gene dysfunction and male infertility. This retrospective study was done to assess the linkage of TNFR1 36 A/G gene polymorphism with idiopathic azoospermia in Erbil City. The present study was carried out on 98 infertile, 109 fertile males as healthy control. TNFR1 36 A/G gene polymorphisms were detected in all study subjects, and their seminal fluids were analyzed. Polymerase chain reaction-restriction fragment length polymorphism (PCR-RFLP) method is used for identify polymorphism in both cases and control groups. MspAII restriction enzyme were digested PCR products. Digested and PCR products were analyzed by 3% gel electrophoresis for 45 minutes at 97 V. . The results of the present study showed that the incidence of AG genotype in azoospermia male higher than control groups (OR=2.069(1.154-3.708), P=0.014, this study found that G allele frequency in azoospermia men had a significant difference compared to the control group (OR=1.487 (0.992-2.170). Moreover, AG genotype and G allele associated with an increased risk of non-obstructive azoospermia in Erbil City.

KEY WORDS: Male infertility, Tumor necrosis factor-alpha, allele. Azoospermia, Genotype.

DOI: <http://dx.doi.org/10.21271/ZJPAS.33.1.4>

ZJPAS (2021) , 33(1);27-34 .

1. INTRODUCTION

Infertility in males is usually due to disturbance in the process of spermatogenesis, which cause no or incompetent spermatozoa (Rajender *et al.*, 2010; Sikka,2001). Some spermatogenic factors cause infertility, such as decreased sperm motility, low sperm count, destruction of sperm DNA, or poor semen quality.

Quality of seminal fluid may be compromised due to some factors like high levels of reactive oxygen species (ROS) and oxidative stress (OS) (Harchegani *et al.*, 2019; Aitken, 1999; Armstrong *et al.*, 1999).

The world's population is increasing and may reach nine billion in 2050. In addition to that, 15% of couples world-wide remain childless due to infertility. Only a few of these due to genetic causes, also genetic factors are thought to underlie many causes of idiopathic infertility (Bracke *et al.*, 2018). About 30-40% of the male in the reproductive age group have a defect in sperm production. In quality or quantity, 50% of them due to low sperm motility (asthenozoospermia)

* Corresponding Author:

Ashti Mohammad Amin Said

E-mail: ashtihmu1@gmail.com

Article History:

Received: 28/02/2020

Accepted: 12/09/2020

Published: 20/02 /2021

and low sperm count (oligospermia) Shamsi *et al.* (2008).

Azoospermia means a lack of sperm in at least two ejaculate samples (including the centrifuged sediment) (World Health Organization, 2010; Corea *et al.*, 2005). Generally, 40 to 50 % of couple infertile. About 50% of them are male, and 10-20% of these (or 1% of all men in the general population) suffer from azoospermia (Pashaei *et al.* 2020).

Chromosomal diseases are mostly founded in infertile compared with fertile population (Signore *et al.* 2020). These chromosomal changes found in 20% of azoospermic and the Klinefelter syndrome (47,XXY) is most frequent genetic causes of azoospermia (or severe oligozoospermia) (Röpke. and Tüttelmann, 2017). Therefore, it is better these men doing genetic testing before the use of their sperm for assisted reproductive techniques ART.

Tumor necrosis factor-alpha (TNF- α) is a protein with molecular weight's around (17KDa) and produced mostly by activated T cells, monocytes, macrophages, and a few non-lymphoid cells such as male germ cells and Sertoli. TNF- α binding to a TNF transmembrans receptor, which recruits cytosolic proteins and transduces the signal. TNF- α is causing Leydig cell steroidogenesis, Sertoli cell-germ cell junction dynamics, and regulates germ cell apoptosis (Xia *et al.*, 2005). TNF- α due to activation of nuclear factor kappa B represses gene expression of the steroidogenic enzyme in Leydig cells (Siu *et al.*, 2003; Hong *et al.*, 2004; Pentikäinen *et al.*, 2001). Both Sertoli and Leydig cells produce a lot of the immunoregulatory cytokine, IL-6, driven by IL-1. Both these cytokines control Sertoli cell and germ cell development (Hedger *et al.*, 2003).

Current studies are yet to show direct connections among cytokines and male infertility. Furthermore, cytokines might be helpful markers for analysis and observing treatment in patients with urogenital infection/inflammation (Sengupta *et al.*, 2020)

Fertility in men relies upon the best possible creation of sperm cells, by means of spermatogenesis, which is extremely intricate and includes the synchronization of numerous components. The nearness of proinflammatory cytokines, TNF- α , interleukin (IL)- 1 α and IL1 β in the male reproductive system, explicitly in testes, epididymis and spermatozoa, have a few critical physiological capacities including

immunoregulation in the male reproductive tract.(Azenabor *et al.*, 2015).

The steroidogenic enzymes are causing a decrease in the production of testosterone (Rebourcet *et al.*, 2020). High levels of testosterone hormone cause the depletion of germ cells from the epithelium (Mealy *et al.* 1990). Increase levels of TNF- α also found in the semen of sub-fertile and infertile men. Some studies reported a high TNF- α level in the seminal fluid in cases of leukocyte infiltration of sperm and also found that inflammation-mediated azoospermia is directly related to TNF- α in the seminal fluid (Martínez *et al.*, 2010; Seshadri *et al.*, 2009).

The location of *TNFR1* gene is on chromosome 12p13.2 (Hong *et al.* 2004). There are many polymorphisms in *TNFR1* gene which have a huge effect on the performance of receptor; one of these is 36 A/G, and this receptor has important role in the activity of TNF- α . Because of that it is better to investigate the polymorphisms associated with this gene. The present study found the association of alleles and genotypes of *TNFR1* 36 A/G polymorphism with azoospermia. The present case-control study was undertaken to identify the Gene polymorphism in male with azoospermia in Erbil City.

2.MATERIALS AND METHODS

2.1 Subjects

The present study performed on 98 non-obstructive azoospermic infertile men (age range 20-50 years) and 109 healthy fertile men as a control groups, from February 2018 to May 2019. This study performed on human subjects that are selected from patients who are attending the infertility center in Erbil City. Those Patients that are married for about one year and having unprotected intercourse were considered for this study. Those patients that have chronic diseases, history of pelvic /spinal injuries, and karyotype abnormalities are excluded in this study. And from all patients, informed verbal consent was obtained, and the ethics committees approved the research of the Medical Research Center/ Hawler Medical University. Assessment of seminal fluid of studied groups were done after 3-5 days of sexual abstinence according to the guideline of the World Health Organization (WHO) to diagnose their infertility status and to know the quality and quantity of sperm. See (Table 3)

2.2 Detection of TNFR1 Gene Polymorphism

Venous blood samples (3ml) were collected via atraumatic antecubital venipuncture into vacutainer tubes containing EDTA. The samples were either used immediately for study of polymorphism or kept at about -20 °C until further analysis. The identification of *TNFR1* gene polymorphism assessed by using polymerase chain reaction and PCR-RFLP, techniques that are used at the Medical Research Center/Hawler Medical University in Erbil City/ IRAQ. Briefly, DNA was isolated from blood samples (by using 100 prep DNA extraction kit (Fermentas company)), and the polymorphic region is amplified by PCR (Boiron/ Genekam Biotechnology ready to use PCR master mix), concentration and volume of the solutions in PCR reaction were: (15µl Master mix, 5µl DNA sample, 2µl Forward primer, 2µl Reverse primer and 26µl ddH₂O).

PCR thermal profile for amplification of single nucleotide 36A/G polymorphisms of TNFR1 gene was: (5min initiation denaturation at 95 °C, 30s denaturation at 95 °C, 30s annealing at 69 °C, 30s extension at 72 °C and 5 min final extension at 72°C) with primers 5-GAGCCCAAATGGGGGAGTGAGAGG-3 and 5-ACCAGGCCCGGGCAGGAGAG-3. The PCR products were analyzed by 2% agarose gel electrophoresis (Genekam Biotechnology AG, Germany) to amplify the TNFR1 gene fragment, that 183-bp band was observed. PCR products were subsequently digested with restriction enzyme endonucleases MspII (BioLabs inc. NEW ENGLAND), then the samples were analyzed on 3% agarose gel for 45 minutes at 97 °C.

2.3 Digestion By MSPAII Restriction Enzyme

The PCR-RFLP method was used after a PCR reaction, also by using the MSPAII restriction enzyme for both case and control samples. After optimizing the enzymatic digestion conditions, 8µl PCR products (for each sample) were cut by mixed with 1µl MSPAII restriction enzyme, 5µl NE Buffer (1X), and 26µl ddH₂O. For activation of this enzyme, this 40µl (total volume) was incubated overnight for 37°C. After that, the restriction enzyme inactivated at 65°C for 20min. Through 3% agarose gel, the mixtures were electrophoresed. The polymorphism within amplified products has a length of 183 bp. In this research, it is expected to find three different

bands on gel electrophoresis, including homozygous individuals (AA): a fragment in 183-bp region, heterozygous individuals (AG): three fragments in 183-bp, 108-bp, and 75-bp regions, as well as homozygous individuals (GG): two fragments in 108-bp and 75-bp regions.

3. STATISTICAL ANALYSIS

Through the chi-square test using the statistical package, version 20 SPSS, assessment done and found the difference between infertile men and control groups and their relationships with azoospermia. The Odds Ratio (OR), P-value, and confidence interval were calculated for the frequencies and parameters, while quantitative variables were expressed as the mean standard deviation (SD). Differences were considered statistically significant at $p \leq 0.05$.

4. RESULTS

The participants are divided into two groups: infertility (n=98) and fertility (n=109) subjects. On 3% gel electrophoresis, three different bands were observed. Including AA genotype (183bp). AG genotype (183bp, 108bp, and 75bp) and GG genotype (108bp, and 75bp). Figure 1 indicating digested products on 3% agarose gel.

The results demonstrated that the frequencies of AA (183bp), AG (183bp, 108bp, and 75bp), and GG (108bp, and 75bp) genotypes were 17.34%, 42.8%, and 39.7% respectively in cases and 34.86%, 26.60%, and 38.53% in control groups. Table 1.

Besides, the frequencies of A and G alleles were 38.3% and 60.6% respectively in the case group, and 48.16% and 51.83% in the control group (Table 2). The present study indicated that the frequency of AG genotype in cases and controls was significantly different ($p=0.014$). The frequency of AG genotype was higher in cases when compared with controls. The risk of non-obstructive azoospermia was more in men with AG genotype (OR=2.069) (1.154-3.708). The difference in A and G alleles frequency was significant between the two groups ($P=0.054$), and the risk of azoospermia people with G allele was higher 1.487 (0.992-2.170) when compared with A allele (0.682(0.461=1.008). Table 2.

Chi-square test showed significant differences between genotypes frequencies in cases and controls OR=2.069, CI; 95%, 1.154-3.708. Chi-square test showed significant

differences between alleles frequencies in cases and controls OR=1.487, CI; 95%, 0.992-2.170.

Regarding semen quality, especially volume of sperm, concentration, total count, motility (motile, and immotile), and morphology

of sperm (normal, and abnormal) , a highly significant change among fertile men, was defined compared with infertile men (azoospermia) (p=0.000). Table 3.

Table (1) : Frequency distribution of TNFR1 36A/G polymorphism genotypes in infertile men with azoospermia

Genotypes	Azoospermic men n=98	Controls n=109	P-value	OR (CL;95%)
AA	17 (17.34%)	38 (34.86%)	0.004	0.387(0.201-0.744)
AG	42 (42.8%)	29 (26.60%)	0.014	2.069(1.154-3.708))
GG	39 (39.7%)	42 (38.53%)	0.894	1.039(0.594-1.818)

Table (2): Frequency distribution of TNFR1 36 A/G polymorphism alleles in patients with azoospermia.

Genotypes	Azoospermic men n=196 n= (%)	Controls (n=218) n= (%)	P- value	OR (CL;95%)
A	76(38.3%)	105(48.16%)	0.054	0.682(0.461=1.008)
G	120(60.6%)	113(51.83%)	0.054	1.487 (0.992-2.170)

Table(3): Seminal Fluid Analysis of fertile and infertile men (Azoospermia men .

Variable		Fertile men No (109) (Mean±SD)	Infertile men(Azoospermic men) No(98) (Mean±SD)	p. value
Volume (ml)		4.55±0.95	2.014±0.667	0.000 ^S
Concentration (10 ⁶ / ml)		58.48±18.99	0.0 00±0.000	0.000 ^S
Total count (10 ⁶ /ejaculate)		2.692 ±100.700	0.0 00±0.000	0.000 ^S
Motility	Motile	79.17±13.57	0.0 00±0.000	0.000 ^S
	Immotile	21.055±10.23	0.0 00±0.000	0.000 ^S
Morphology	Normal	68.55±10.99	0.0 00±0.000	0.000 ^S

	Abnormal	31.75±4.99	0.0 00±0.000	0.000 ^S
--	----------	------------	--------------	--------------------

5. DISCUSSION

Azoospermia, which means discharge free of sperm, that influences 1% of all men and up to 15% of men with infertility (Gudeloglu, 2013). Our research was led to survey *TNFR1* 36 A/G Gene Polymorphism, and it is predominance among patients with idiopathic azoospermia and found that the G allele and AG genotype of *TNFR1* 36 A/G polymorphism is significantly higher in azoospermic infertile men when compared to control group. However, polymorphism of *TNFR1* 36 A/G gene, can change in function of the type 1 receptor of TNF- α cytokine, resulting in cytokine dysfunction.

It has been claimed in an Iranian study that the GG genotype associated with non-obstructive azoospermia and they clarified that the increased risk of non-obstructive azoospermia associated with G allele (Ashrafzadeh *et al.*, 2017). NOA happens due to defects in spermatogenesis. However, the etiology of most patients' testicular dysfunction stays obscure (Han *et al.*, 2020).

According to the study in Erbil City the single nucleotide polymorphism (SNP) rs12086634 (T>G) of the HSD11B1 gene is associated with polycystic ovary syndrome (PCOS) significantly, and the G allele of this SNP rs12086634 (T>G) was associated with obesity. (Shareef, *et al.*, 2019)

Lazaros *et al.*, 2012 in Greece population investigated the relationship between 36 A/G polymorphism of *TNFR1* with male infertility and sperm concentration and motility using PCR-RFLP. Their study showed that the allele A of *TNFR1* is associated with increased sperm concentration and motility, and supporting the significance of the *TNFR1* gene is semen quality. The study in Kurdistan region demonstrated a significant association between TT genotype of mir-125a G >T polymorphism and In Vitro Fertilization (IVF) failure (Dizay *et al.*, 2019).

The genetic factors and environmental have a role in infertility, and the genetic factors are confirmed in men with idiopathic infertility (Tanoomand *et al.*, 2019). Table 1, showed that the odds ratio for AG groups was more than one and the p-value was 0.014; it means that this group has increased risk to azoospermia. But the odds ratio for GG, AA

groups was less than one, and the p-value was non-significant, and according to these values, the two groups have decreased risk to azoospermia.

Men with NOA have high rates of DNA repair mechanisms defects and irregularities in cell cycle control. (Gunes *et al.*, 2015). The infertility issues in 15% of couples are identified with male factors in 40% of them (Zaimy *et al.*, 2013).

Spermatogenesis is depend on a huge number of cellular signals causing coordination and connection between various cells of the testes. Cytokines, including TNF- α , control this relationship and capacity among the cells and, subsequently it could be related with sperm variations for example, changes in morphology, number, and motility. TNF- α receptors, for example, TNFR1 and TNFR2 exist in sertoli and leydig cells. The capacity of these cells can be balanced by binding the cytokine to them (Tronchon *et al.*, 2008; Zalata *et al.*, 2013).

Figure 1, determined digested PCR products on 3% agarose gel at 45 minutes for 97 V: And three different patterns were observed on this gel, including homozygous individuals (AA): a fragment in 183-bp region: One may argue that no mutation found on this region, heterozygous individuals (AG): three bands in 183-bp, 108-bp, and 75-bp areas, it means that the variation could be observed on one strand of DNA but cannot be detected in other once. As well as homozygous individuals (GG): two bands in 108-bp and 75-bp regions, it means that mutation should be observed on both strands of DNA.

According to the Table 1 and 2: The PCR-RFLP was used by the help of restriction *Msp*I enzyme for the 98 blood samples (cases) and 109 blood samples (control groups), and the results demonstrated that the frequency AG genotype and G allele were less in controls than cases.

Primary infertilities' prevalence is accounted for to be 10% to 12% (World Health Organization 2004). Also, the rate of fertility and number of children is steady decreasing globally (World Health Organization, 2004). Incremental population growth, caused by low fertility rates, is an existential problem for the developing countries in Asia. The northern and western parts of Europe first encountered the risk of low fertility rates, but now Asian countries are haunted by it. Marriage is strongly embodied in the Asian social

systems as a habit or tradition; hence the rates of children born to single mothers are limited. This phenomenon immensely contributed to low fertility rates and the number of children (Matsuda S., 2020).

Kotowicz *et al.* (2010) determined that increasing the serum levels of Cancer A-125

recommends the need for applying progressively forceful types of treatment. Soluble TNF receptor type I might be of significance in diagnosing patients at the early clinical phases of adenocarcinoma, particularly those with Cancer A-125 focus inside.

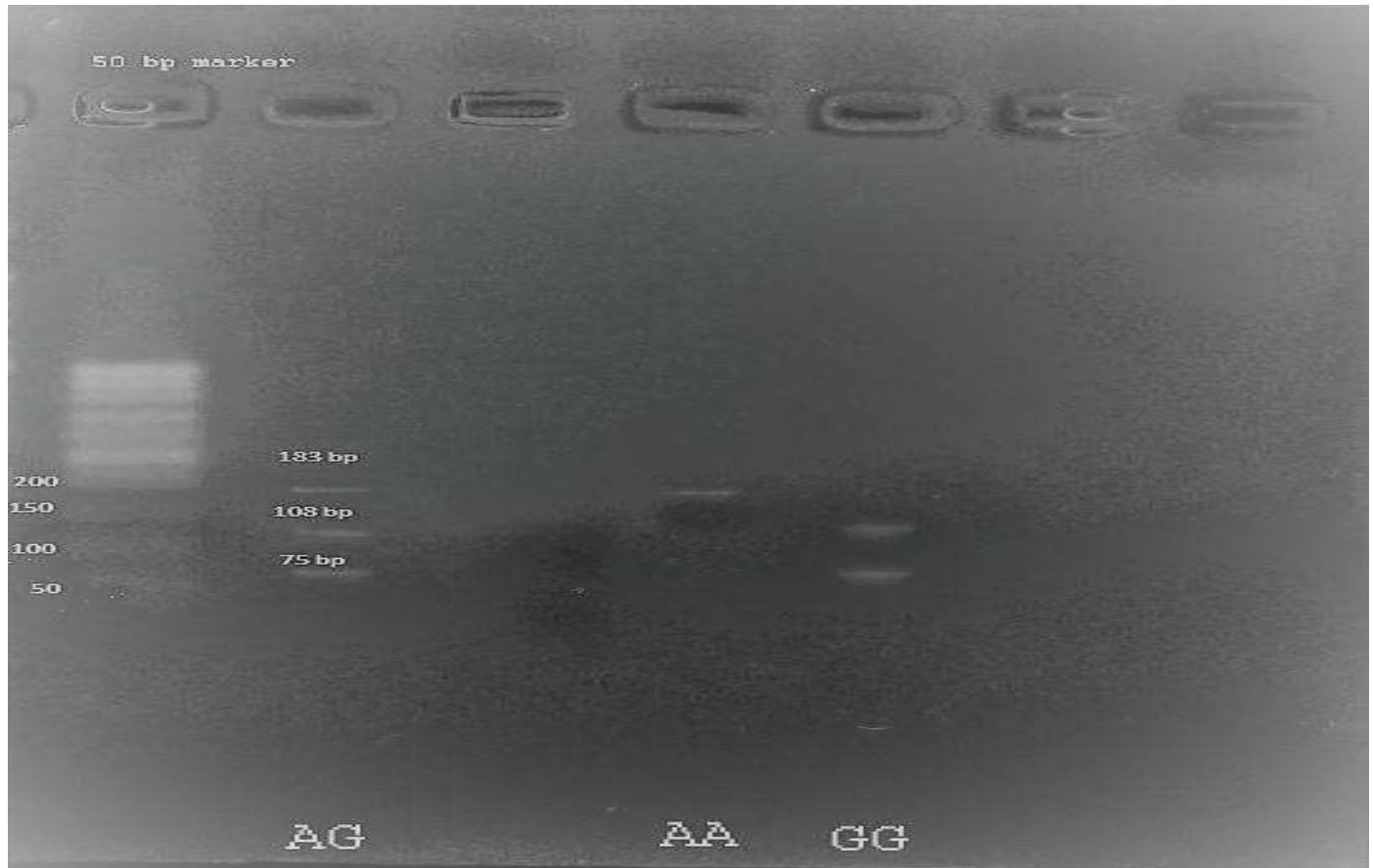


Figure 1: 3% agarose gel electrophoresis pattern of some RFLP products of *TNFR1* gene polymorphism. Line (1) indicates DNA markers with a 50 bp. Lane (2) is (AG) heterozygous individuals: three bands in 183-bp, 108-bp, and 75-bp areas, it means that the variation could be observed on one strand of DNA but cannot be detected in other once. Lanes (3 and 6, 7) are negative and don't have the mutation. Lane (4) is homozygous individuals (AA): a fragment in 183-bp region, and no mutation found on this region, As well as lane (5) is homozygous individuals (GG): two bands in 108-bp and 75-bp regions, it means that mutation should be observed on both strands of DNA.

6.CONCLUSION

In conclusion, the study showed that the AG genotype and G allele of 36 AG *TNFR1* might be a risk factor for non-obstructive azoospermia in a population of Erbil City

Acknowledgment

This study has been supported by the Infertility Center in Erbil City and Medical Research Center/Hawler Medical University, Kurdistan, Iraq.

CONFLICT OF INTERESTS

There are no conflicts of interest regarding this study.

REFERENCES

- Aitken, R. J., 1999. The Amoroso Lecture The human spermatozoon—a cell in crisis?. *Reproduction*, 115(1), 1-7.
- Armstrong, J. S., Rajasekaran, M., Chamulitrat, W., Gatti, P., Hellstrom, W. J., & Sikka, S. C., 1999. Characterization of reactive oxygen species

- induced effects on human spermatozoa movement and energy metabolism. *Free Radical Biology and Medicine*, 26(7-8), 869-880.
- Ashrafzadeh, H.R., Nazari, T., Tezerjani, M.D., Bami, M.K., Ghasemi-Esmailabad, S., and Ghasemi, N. 2017. Frequency of TNFR1 36 A/G gene polymorphism in azoospermic infertile men: A case-control study. *International Journal of Reproductive BioMedicine*, 15(8), 521.
- Azenabor, A., Ekun, A.O. and Akinloye, O., 2015. Impact of inflammation on male reproductive tract. *Journal of reproduction & infertility*, 16(3), p.123.
- Bracke, A., Peeters, K., Punjabi, U., Hoogewijs, D. and Dewilde, S., 2018. A search for molecular mechanisms underlying male idiopathic infertility. *Reproductive biomedicine online*, 36(3), 327-339.
- Corea, M., Campagnone, J., and Sigman, M.. 2005. The diagnosis of azoospermia depends on the force of centrifugation. *Fertility and sterility*, 83(4), 920-922.
- Dizay, R.K. and Mustafa, S.A., 2019. Polymorphism of miRNA and its Impact on IVF Failure. *ZANCO Journal of Pure and Applied Sciences*, 31(6), 84-91.
- Gudeloglu, A., & Parekattil, S. J., 2013. Update in the evaluation of the azoospermic male. *Clinics*, 68, 27-34.
- Gunes, S., Al-Sadaan, M. and Agarwal, A., 2015. Spermatogenesis, DNA damage and DNA repair mechanisms in male infertility. *Reproductive biomedicine online*, 31(3), 309-319.
- Harchegani, A.B., Rahmani, H., Tahmasbpour, E. and Shahriary, A., 2019. Hyperviscous semen causes poor sperm quality and male infertility through induction of oxidative stress. *Current urology*, 13(1),1-6.
- Hong, C.Y., Park, J.H., Ahn, R.S., Im, S.Y., Choi, H.S., Soh, J., Mellon, S.H., and Lee, K. 2004. Molecular mechanism of suppression of testicular steroidogenesis by proinflammatory cytokine tumor necrosis factor- α . *Molecular and Cellular Biology*, 24(7), 2593-2604.
- Han, F., Jiang, X., Li, Z.M., Zhuang, X., Zhang, X., Ouyang, W.M., Liu, W.B., Mao, C.Y., Chen, Q., Huang, C.S. and Gao, F., 2020. Epigenetic Inactivation of SOX30 Is Associated with Male Infertility and Offers a Therapy Target for Non-obstructive Azoospermia. *Molecular Therapy-Nucleic Acids*, 19, 72-83.
- Hedger, M.P. and Meinhardt, A., 2003. Cytokines and the immune-testicular axis. *Journal of reproductive immunology*, 58(1), 1-26.
- Kotowicz, B., Kaminska, J., Fuksiewicz, M., Kowalska, M., Jonska-Gmyrek, J., Gawrychowski, K., ... & Bidzinski, M. 2010. Clinical significance of serum CA-125 and soluble tumor necrosis factor receptor type I in cervical adenocarcinoma patients. *International Journal of Gynecologic Cancer*, 20(4), 588-592.
- Lazaros, L. A., Xita, N. V., Chatzikyriakidou, A. L., Kaponis, A. I., Grigoriadis, N. G., Hatz, E. G., ... & Georgiou, I. A. 2012. Association of TNF α , TNFR1, and TNFR2 polymorphisms with sperm concentration and motility. *Journal of andrology*, 33(1), 74-80.
- Matsuda, S., 2020. Progress of Low Fertility in Japan and Other Asian Countries: A Theoretical Framework. In *Low Fertility in Advanced Asian Economies* (1-20). Springer, Singapore.
- Mealy, K.E.N.N.E.T.H., Robinson, B.R.U.C.E., Millette, C.F., Majzoub, J.O.S.E.P.H. and Wilmore, D.W. 1990. The testicular effects of tumor necrosis factor. *Annals of Surgery*, 211(4), 470.
- Martínez-Prado, E., and Camejo Bermúdez, M.I. 2010. Expression of IL-6, IL-8, TNF- α , IL-10, HSP-60, Anti-HSP-60 Antibodies, and Anti-sperm Antibodies, in Semen of Men with Leukocytes and/or Bacteria. *American Journal of Reproductive Immunology*, 63(3), 233-243.
- Pashaei, M., Bidgoli, M.M.R., Zare-Abdollahi, D., Najmabadi, H., Haji-Seyed-Javadi, R., Fatehi, F. and Alavi, A., 2020. The second mutation of SYCE1 gene associated with autosomal recessive nonobstructive azoospermia. *Journal of assisted reproduction and genetics*, 37(2), 451-458.
- Pentikäinen, V., Erkkilä, K., Suomalainen, L., Ojala, M., Pentikäinen, M.O., Parvinen, M., and Dunkel, L. 2001. TNF α down-regulates the Fas ligand and inhibits germ cell apoptosis in the human testis. *The Journal of Clinical Endocrinology & Metabolism*, 86(9), 4480-4488.
- Rebourcet, D., Mackay, R., Darbey, A., Curley, M.K., Jørgensen, A., Frederiksen, H., Mitchell, R.T., O'Shaughnessy, P.J., Nef, S. and Smith, L.B., 2020. Ablation of the canonical testosterone production pathway via knockout of the steroidogenic enzyme HSD17B3, reveals a novel mechanism of testicular testosterone production. *The FASEB Journal*.
- Röpke, A. and Tüttelmann, F., 2017. Mechanisms in endocrinology: Aberrations of the X chromosome as cause of male infertility. *European Journal of Endocrinology*, 177(5), R249-R259.
- Rajender, S., Rahul, P. and Mahdi, A.A., 2010. Mitochondria, spermatogenesis and male infertility. *Mitochondrion*, 10(5), 419-428.
- Shamsi, M. B., Kumar, R., Bhatt, A., Bamezai, R. N. K., Kumar, R., Gupta, N. P., ... & Dada, R. 2008. Mitochondrial DNA mutations in the etiopathogenesis of male infertility. *Indian Journal of Urology: IJU: Journal of the Urological Society of India*, 24(2), 150.
- Shareef, A.A. and Al-Attar, M.S., 2019. Association Study of HSD11B1 rs12086634 (T> G) Gene Polymorphism with Polycystic Ovarian Syndrome

- in Erbil Province. *ZANCO Journal of Pure and Applied Sciences*, 31(5), pp.36-43.
- Siu, M.K., Mruk, D.D., Lee, W.M. and Cheng, C.Y. 2003. Adhering junction dynamics in the testis are regulated by an interplay of $\beta 1$ -integrin and focal adhesion complex-associated proteins. *Endocrinology*, 144(5), 2141-2163.
- Seshadri, S., Bates, M., Vince, G., and Jones, D.L., 2009. The role of cytokine expression in different subgroups of subfertile men. *American Journal of Reproductive Immunology*, 62(5), 275-282.
- Signore, F., Gulia, C., Votino, R., De Leo, V., Zaami, S., Putignani, L., Gigli, S., Santini, E., Bertacca, L., Porrello, A. and Piergentili, R., 2020. The role of number of copies, structure, behavior and copy number variations (CNV) of the Y chromosome in male infertility. *Genes*, 11(1), 40.
- Sengupta, P., Dutta, S., Alahmar, A.T. and D'souza, U.J.A., 2020. Reproductive tract infection, inflammation and male infertility. *Chemical Biology Letters*, 7(2), 75-84.
- Sikka, S. C., 2001. The relative impact of oxidative stress on male reproductive function. *Current medicinal chemistry*, 8(7), 851-862.
- Tanoomand, A., Hajibemani, A. and Abouhamzeh, B., 2019. Investigation of the association of idiopathic male infertility with polymorphisms in the methionine synthase (MTR) gene. *Clinical and experimental reproductive medicine*, 46(3), 107.
- Tronchon, V., Vialard, F., El Sirkasi, M., Dechaud, H., Rollet, J., Albert, M., Bailly, M., Roy, P., Mauduit, C., Fenichel, P. and Selva, J., 2008. Tumor necrosis factor-alpha-308 polymorphism in infertile men with altered sperm production or motility. *Human reproduction*, 23(12), 2858-2866.
- World Health Organization, 2010. WHO laboratory manual for the examination and processing of human semen.
- World Health Organization .2004. Demographic and Health Surveys (DHS)Comparative reports No. 9: Infecundity, infertility, and childlessness in developing countries.
- Xia, W., Mruk, D.D., Lee, W.M. and Cheng, C.Y. 2005. Cytokines and junction restructuring during a spermatogenesis-a lesson to learn from the testis. *Cytokine & growth factor reviews*, 16(4-5), 469-493.
- Zaimy, M. A., Kalantar, S. M., Sheikha, M. H., Jahaninejad, T., Pashaiefar, H., Ghasemzadeh, J., & Zahraei, M., 2013. The frequency of Yq microdeletion in azoospermic and oligospermic Iranian infertile men. *Iranian Journal of reproductive medicine*, 11(6), 453.
- Zalata, A., Atwa, A., Badawy, A.E.N., Aziz, A., El-Baz, R., Elhanbly, S. and Mostafa, T., 2013. Tumor necrosis factor- α gene polymorphism relationship to seminal variables in infertile men. *Urology*, 81(5), 962-966.

RESEARCH PAPER

Green Synthesis, Characterization and Antimicrobial Activity of Silver Nanoparticles Using Locally Growing *Allium Sativum* Extract

Twana Mohammed M.Shafea, Kamal M. Mahmoud

¹Department of chemistry, College of Science, Salahaddin University-Erbil, Kurdistan Region, Iraq

ABSTRACT:

In the present paper, a green synthesis of silver nanoparticles (AgNPs) have been prepared using *Allium sativum* (garlic) extract(GE) (growing in Kurdistan-Iraq) at 60 – 65 C°, The synthesized silver nanoparticles were characterized by UV-Visible absorption spectroscopy, Fourier transform infrared spectroscopy (FTIR), Scanning Electron microscopy (SEM), X-ray diffraction (XRD) and Energy-Dispersive X-ray spectroscopy(EDX). The UV-Visible spectroscopy of synthesized AgNPs showed absorption maxima at 433 nm. The XRD examination implied that AgNPs support the equalizer with an average crystallite size of 15 nm. Antimicrobial activity of prepared nanoparticles (two different concentrations) and extracted garlic was done. It has an effect on the growth of three microorganisms (*Micrococcus* sp. (gram positive bacteria); *Pseudomonas aeruginosa* (gram negative bacteria) and *Candida albicans* (fungus)). The most important interests of this preparation are safe, fast and it has activity against bacterias and fungus.

KEYWORDS: Green synthesis; Silver nanoparticles; Garlic (*Allium sativum* L.);antibacterial and antifungal activity.

DOI: <http://dx.doi.org/10.21271/ZJPAS.33.1.5>

ZJPAS (2021) , 33(1);35-41 .

1. INTRODUCTION :

Among all noble metal nanoparticles, AgNPs have obtained an individual interest. There are many methods for producing nanoparticles among these methods is chemical method by using chemicals like reducing agents, which afterward become responsible for a range of biological hazards due to their universal toxicity.

This problem can be solved by using green methods such as plants which contain biological molecules in the extracts demonstrating excellences more than chemical and physical methods (Ahmed *et al.* 2016).

Garlic (*Allium sativum* L.) globally known as a food, spice and classical medicine. Variety of investigations have previously established that garlic may be useful for the protection of cardiovascular, carcinogenesis and age-related diseases (Abbas *et al.* 2019; Rahman 2003). The beneficial and medicinal properties are refers to specific organosulfur compounds (Agarwal 1996; Lawson 1993; Sendl *et al.* 1992; Yanagita *et al.* 2003; Yeh and Liu 2001). Garlic extract is a rich source of phenolics and flavonoids which has an essential role in the reduction process for synthesis of metal nanoparticles (El-Refai *et al.* 2018).

*Corresponding Author:

Twana Mohammed Mohammed Shafea

E-mail : twanamohammed1990@gmail.com

Article History:

Received: 24/05/2020

Accepted: 12/09/2020

Published: 20/02 /2021

Nanoparticles (NPs) display size and shape-dependent characteristics which are of avails for applications ranging from antimicrobial activity, bio sensing and catalysts to optics, chemical sensors, electrometers, and computer transistors (Qadir *et al.* 2019). These particles have also many applications in different fields such as drug delivery, medical imaging, filters, and Nano composites (Andra *et al.* 2019; Sun *et al.* 2008).

Silver nanoparticles have dragged the concern of researchers due to their wide applications such as sensors (Guozhong 2004), cell electrodes (Klaus-Joerger *et al.* 2001), photonics (Jebril *et al.* 2020), antimicrobials (Elumalai *et al.* 2010), pharmaceutical products (Nguyen *et al.* 2020), etc.

The aim of this study is to prepare AgNPs, using simple solution-based green approach using garlic extract growing in Kurdistan Region-Iraq. In consequence according to the commenced results, the most important differences of this preparation from the previous study which is about green synthesis of robust and biocompatible AgNPs using garlic extract (Von White *et al.* 2012) are low cost, simplicity, moreover, the produced AgNPs recommend a possible application as an antibacterial and antifungal activities.

2. Experimental

2.1. Chemicals and Reagents

All chemicals were purchased at the highest grade available and used directly without any further purification. Silver nitrate (AgNO_3) (99.9% w/w) was acquired from Sigma-Aldrich USA. Bulbs of Garlic were grown and collected from a farm in Soran, Erbil city, Kurdistan- Iraq. It was peeled and rinsed with deionized water to remove contaminants. All glasswares was washed with deionized water, followed by next drying.

2.2. Preparation of Garlic Extract

The outer covering of the Garlic bulbs was peeled off manually, and then washed with deionized water. About 30.0 g of peeled garlic was chopped (not crushed) into small pieces, and boiled in 100ml of deionized water for 10 minute at 70°C (Ahamed *et al.* 2011). After that the extract was cooled and filtered, finally the extract

was kept in refrigerator at about 4°C until further usage.

2.3. Preparation of Silver Nanoparticles Using Garlic Extract

Add 20.0 mL of GE drop wise to 50.0 mL of AgNO_3 (0.05 M) with constant stirring at $60-65^\circ\text{C}$ for two hours (Ahamed *et al.* 2011). The brown color indicates that the silver nanoparticles were formed. The obtained precipitate washes out with deionized water and methanol to take out possible precipitation. Finally calcination was done by putting in a furnace at 350°C for 2 hours to remove any residues of extract. Figure (1) shows the steps of this preparation.



Figure (1): Synthesis steps of silver nanoparticle by green method.

2.4. Characterization Techniques

The UV-Vis. absorption spectra were recorded on a double-beam spectrophotometer (Koya University) (model) for AgNPs to make certain that the NPs are formed. The functional groups present in the extract and AgNPs were gathered by Fourier transform infrared spectrometer (FTIR) (Perkin Elmer FTIR spectroscopy model 1725 from $400-4000\text{ cm}^{-1}$). X-ray diffraction (XRD) measurements were carried out (Scientific Research Centre, Soran University) using a PAN analytical X'pert PRO ($\text{Cu K}_\alpha = 1.5406\text{ \AA}$). The rate of scanning was $0.5^\circ/\text{min}$. in the 2θ range from $20-80^\circ$. Scanning electron microscopy (SEM) (Quanta 4500) was employed for the study of morphological and particle dispersion. The elemental analysis of the synthesized NPs was

analyzed by energy dispersive X-ray spectrometer (EDX) performed in SEM.

3. Results and Discussion

3.1. Physicochemical Characterization

3.1.1. UV-Vis. Spectroscopy

The reduction of silver ions to silver nanoparticles was confirmed by UV-Visible spectroscopy analysis and it is shown in figure (2). It is known that the silver nanoparticles shows brown colour due to the observable fact of surface plasmon resonance in the metal nanoparticles. The absorption spectra of silver nanoparticles formed in the reaction mixture was obtained by the UV-Vis analysis at the range between 200-700 nm, the AgNPs has an absorbance with highest peak at about 433 nm.

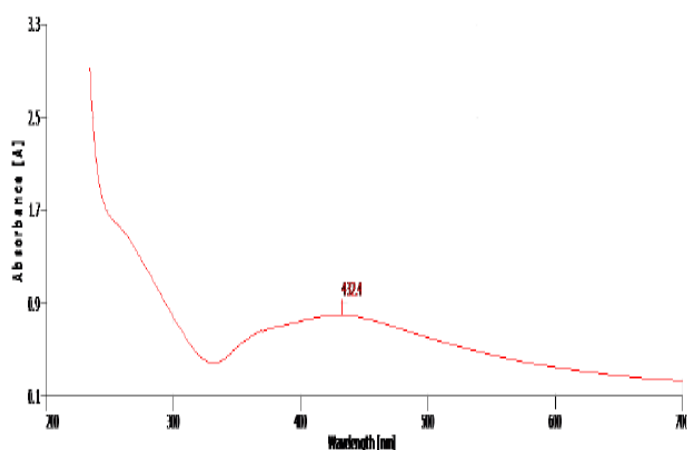


Figure (2): Uv- visible spectra of AgNPs

3.1.2. FTIR analysis of GE and AgNPs

The FTIR analysis was used to identify the possible biomolecules responsible for the capping and stabilizing of silver nanoparticles synthesized by the plant extracts. The FT-IR spectra of garlic extract in figure (3) show several major peaks at 3304, 2931, 2889, 1635, 1411, 1132, and 1022 cm^{-1} and some other peaks approximately at around 536 to 929 cm^{-1} . The broad and intense peak at 3304 cm^{-1} represents the -OH stretching vibration from phenolic compounds in the extract. The peaks observed at 2931, 2889, and 599 cm^{-1} are due to C-H stretching of alkanes. Furthermore, the FT-IR of AgNPs shows some differences in the shape and location of peaks indicating the interaction between AgNO_3 and involved sites of

biomolecules for production of nanoparticles figure (4). Biomolecules could be adsorbed on the surface of metal nanoparticles, possibly by interaction through π -electrons.

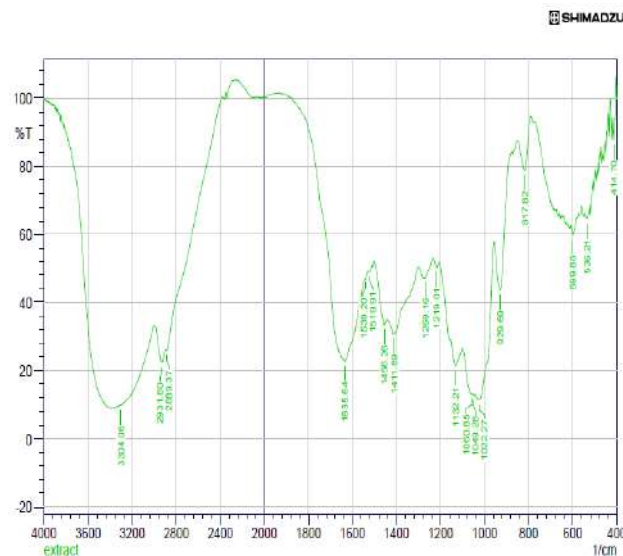


Figure (3): FTIR spectrum of garlic extract.

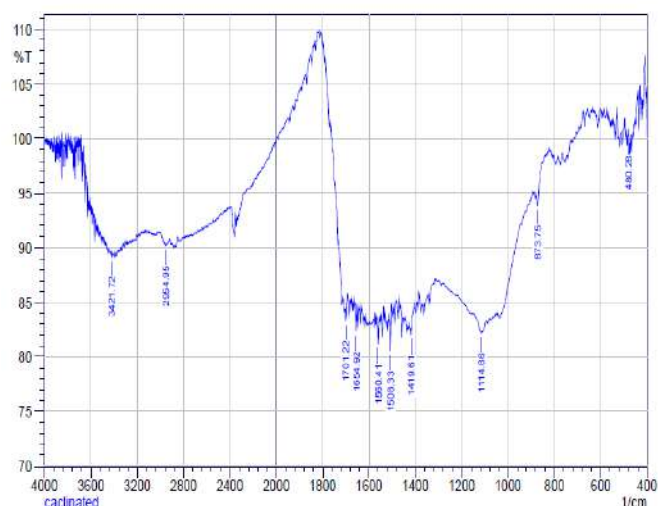


Figure (4): FTIR spectrum of AgNPs.

3.1.3. XRD studies of AgNPs

X-ray crystallography was used to examine the crystallite nature of nanoparticles, the XRD patterns of the synthesized AgNPs from silver nitrate (AgNO_3) and Garlic (*Allium Sativum*) extract as the capping and reducing agent which is in the range of 2θ from 20° to 80° is shown in figure (5). Two peaks of nanoparticles (111) and (200) are appeared, which can be indexed as centered cubic phase of crystalline silver which are corresponding to 2θ values of (37.9211) and

(44.1013) respectively (JCPDS No. 98-005-3761). The strength of peaks imitated means the high grade of crystallinity of the AgNPs.

The Debye - Scherrer formula ($D = K\lambda / \beta \cos\theta$) can be used to calculate the overall particle size of AgNPs, where K is the Scherrer constant (shape factor) with values 0.9 - 1.0, λ is the wavelength (1.54060 Å), β is the full width at half maximum (FWHM) of the XRD peak, θ is the Bragg's angle and D is the crystalline size. The XRD characteristic shows that the synthesized AgNPs have the average crystalline size around 15 nm.

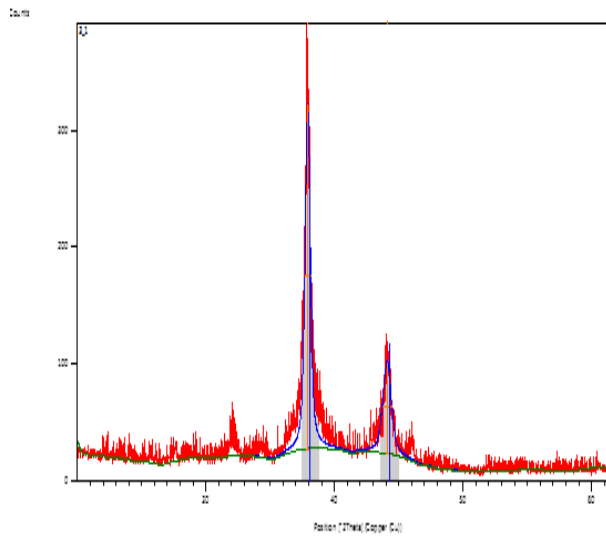
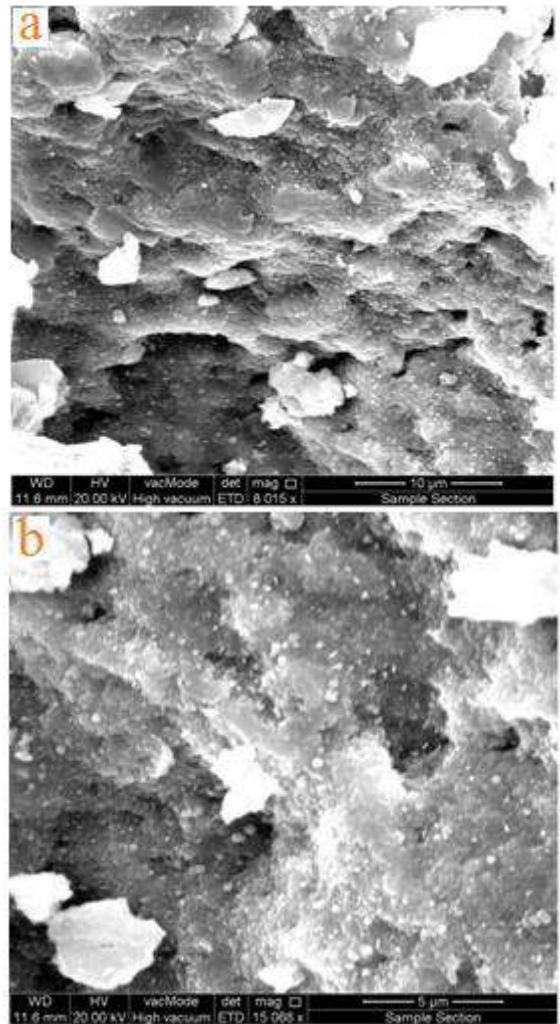
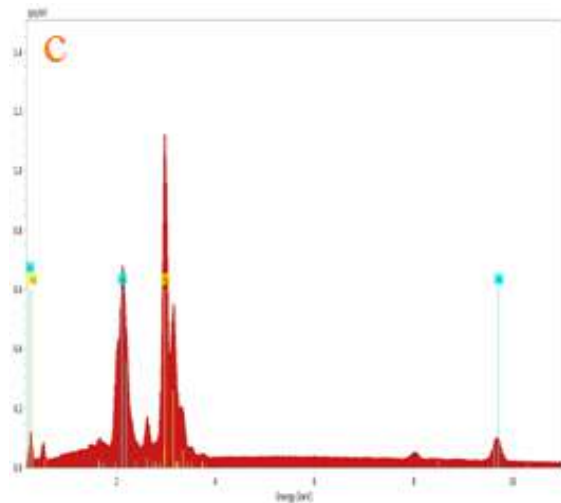


Figure (5): XRD spectra of AgNPs



3.1.4. SEM and EDX analysis

The AgNPs synthesized by the assist of extracted garlic was scanned by SEM as shown in Figure (6a,b). It was shown that silver nanoparticles appeared to be morphologically spherical and small. EDX study provides quantitative and qualitative status of the elements that is involved in the nanoparticle formation. From the EDX spectra figure (6c), the strong signal confirms the AgNPs formation. The optical absorption peaks of the nanocrystals of metallic silver typically had shown around 3.0 KeV. The attendance of gold (Au) in EDX analysis is an outcome of gold covering to get better image of SEM. Figure (6d) shows the distribution of silver in silver nanoparticles.



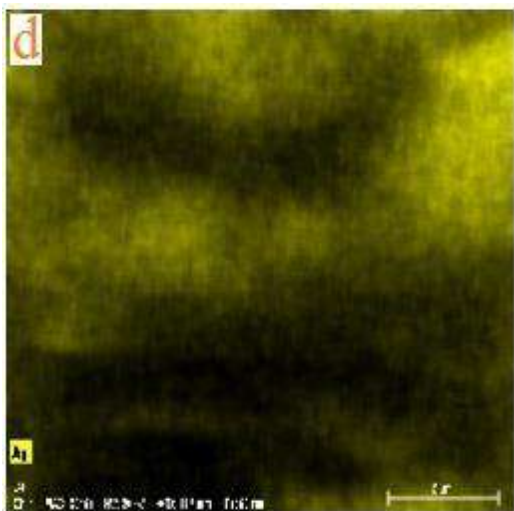


Figure (6): (a)SEM micrograph of AgNPs magnified 8015x;(b) magnified 15068x;(c)EDX image of synthesized AgNPs;(d)corresponding mapping image of Ag in AgNPs.

3.1.5. Evaluation of antimicrobial activity of prepared Nano-particles

1- Yeast:

Candida albicans sensitivity to different concentration of prepared nanoparticles, garlic extract and nystatin (ASIA pharmacological Syria, used as positive control) was tested by using agar well diffusion method (Saeed and Saadullah 2019). The sterile sabouraud's dextrose agar (SDA) were poured in Petri dishes, allowed to solidify, followed by a hole with a diameter of 6.0 mm is punched objectively with a sterile cork borer, Yeast suspension prepared from 24 hours colony by using phosphate buffer saline (PBS) in compare with standard control with concentration 41.5×10^6 Cell/mL of yeast suspension. 0.1 mL of yeast suspension were inoculated on SDA then spread using sterilized L shaped glass rod, then incubated at 37°C for 15 minutes, a volume (80 µL) of the tested antimicrobial agent and extract solutions were poured into the well, then incubated at 37°C for 24-48 hours (AL-REFAI 2006; Ismael 2009). Zones of inhibition were achieved by measuring the radius of the disc from the center to the edge of the inhibition of growth. Measurements were done from both the average accepted and the slope sides.

Nystatin sensitivity test:

The stock solution (20mg/mL) of nystatin was prepared by dissolving a nystatin disc (Al

Kanawati medical products /Syria) that contained (500 000 I.U. of nystatin) in 10 mL of deionized water.

2- Bacteria

The prepared silver Nanoparticle, garlic extract and (Chloramphenicol) were evaluated for its antibacterial activity. The tested bacteria were *Micrococcus* sp. (gram-positive bacteria) and *Pseudomonas aeruginosa* (gram-negative bacteria). The media of Muller Hinton agar (MHA) were poured into plates, allowed to solidify, after that, a hole with a width of 6.0 mm is punched objectively with a sterile cork borer, The suspension for each bacterium was prepared from 24 hours colony by using PBS in compare with standard control with concentration (1.5×10^4 cells /mL). Then 0.1 mL of each suspension were inoculated on MHA then spread using sterilized L shaped glass rod, then incubated at 37°C for 15 minutes, a volume (80 µL) of the tested antimicrobial agent and extract solutions were poured into the well, then incubated at 37°C for 24-48 hours (Holder and Boyce 1994). Zones of inhibition were getting by measuring the radius of the disc from the center to the edge of the growth inhibition. Measurements were done from the average accepted side and its sides of slope.

Table (1) shows the effect of prepared nanoparticles and garlic extracts on the growth of three tested microorganisms including two bacteria: *Micrococcus* sp. (gram positive bacteria), *Pseudomonas aeruginosa* (gram negative bacteria) and *Candida albicans* (fungus). After 48 hours of incubation, the results shows that garlic extracts have the highest effects on the *C. Albicans* and *Micrococcus* sp. with inhibition zones of (23 and 19.5 mm), followed by Nanoparticle 1 (N1) (AgNPs- garlic extracted without water) which showed the highest effect on *P.aeruginosa*, and moderate effects on both *Micrococcus* sp. and *C. albicans*, with inhibition zones of (12, 14 and 9 mm) respectively. While Nanoparticle 2 (N2) (AgNPs- garlic extracted with water) showed the lowest rate of inhibition on the *Micrococcus* sp. and *P.aeruginosa* and *C. Albicans* with inhibition zones of (9, 6 and 6 mm) respectively, Figure (7) shows the results.

Table (1): The effect of nanoparticles and garlic extract on the microorganisms

Tested Microorganisms	Nano 1 (mm)	Nano2 (mm)	Garlic (mm)	Control (mm)
<i>Micrococcus</i> sp.	14	9	17.5	22
<i>Pseudomonas aeruginosa</i>	12	6	4.00	0
<i>Candida albicans</i>	9	6	23.0	0

**Figure (7):(a) *Pseudomonas aeruginosa*;(b) *Micrococcus* sp. ;(c) *C. Albicans*(N1:AgNPs- garlic extracted without water; N2 AgNPs- garlic extracted with water; G: Garlic extract; C: Control).**

4. Conclusions

In summary, we verified a low cost, non-toxic, simple and environmentally friendly synthesis of Ag NPs using garlic extract as reducing, capping and stabilizing agent. The presence of different biomolecules in the extract such as flavonoids and phenolics makes silver nanoparticle formation easier and these biomolecules are responsible in reducing silver ions (Ag^+) to silver particles in nanosize. Presence of AgNPs was determined by change in colour from colourless to brown owing to the reduction of Ag ions and it is due to surface plasmon resonance. The results observed from UV-visible spectrum, SEM, XRD and EDX shows that Ag NPs were crystallite in nature with FCC phase and have an average crystalline size about 15 nm and sphere-shaped. The antifungal and antibacterial activity of prepared nanoparticles and garlic extract on the growth of three microorganisms *Micrococcus* sp. ; *Pseudomonas aeruginosa* and *Candida albicans* after 48 hours of incubation, is shown. The result shows that AgNPs have the highest effect on *P. aeruginosa*, and moderate effects on both *Micrococcus* sp. and *C. albicans*.

Acknowledgements

The authors would like to thank the Soran University – Scientific Research Centre, for their kind help during the analysis of (XRD, SEM and EDX). Authors have also thank the Biology Department – College of Science / Salahaddin University, for their facilitated through their biological activities.

References

- Abbas HMK, Kong X, Wu J, Ali M, Dong W (2019) Antimicrobial Potential of Genes from Garlic (*Allium sativum* L.) Medicinal Plants-Use in Prevention and Treatment of Diseases. IntechOpen
- Agarwal KC (1996) Therapeutic actions of garlic constituents. Medicinal research reviews 16(1):111-124

- Ahamed M, Khan MM, Siddiqui M, AlSalhi MS, Alrokayan SA (2011) Green synthesis, characterization and evaluation of biocompatibility of silver nanoparticles. *Physica E: Low-dimensional Systems and Nanostructures* 43(6):1266-1271
- Ahmed S, Ahmad M, Swami BL, Ikram S (2016) A review on plants extract mediated synthesis of silver nanoparticles for antimicrobial applications: a green expertise. *Journal of advanced research* 7(1):17-28
- AL-REFAI F (2006) Isolation and identification of fungi from cosmetic using some plant extracts as preservative agents. Ph. D. Thesis. College of Science. Mosul Univ. Iraq
- Andra S, Balu S, Ramoorthy R, Muthalagu M, Manisha VS (2019) Terminalia bellerica Fruit Extract Mediated Synthesis of Silver Nanoparticles and Their Antimicrobial Activity. *Materials Today: Proceedings* 9:639-644
- El-Refai AA, Ghoniem GA, El-Khateeb AY, Hassaan MM (2018) Eco-friendly synthesis of metal nanoparticles using ginger and garlic extracts as biocompatible novel antioxidant and antimicrobial agents. *Journal of Nanostructure in Chemistry* 8(1):71-81
- Elumalai E, Prasad T, Hemachandran J, Therasa SV, Thirumalai T, David E (2010) Extracellular synthesis of silver nanoparticles using leaves of *Euphorbia hirta* and their antibacterial activities. *J Pharm Sci Res* 2(9):549-554
- Guozhong C (2004) Nanostructures and nanomaterials: synthesis, properties and applications. *World scientific*
- Holder I, Boyce S (1994) Agar well diffusion assay testing of bacterial susceptibility to various antimicrobials in concentrations non-toxic for human cells in culture. *Burns* 20(5):426-429
- Ismael H (2009) Prevalence of dermatophytes and non dermatophyticfungi in a rural village of Iraqi Kurdistan with special reference to their inhibition by some natural plant extract. M. Sc. Thesis.. College of science. Salahaddin University-Erbil
- Jebri S, Jenana RKB, Dridi C (2020) Green synthesis of silver nanoparticles using *Melia azedarach* leaf extract and their antifungal activities: In vitro and in vivo. *Materials Chemistry and Physics* 248:122898
- Klaus-Joerger T, Joerger R, Olsson E, Granqvist C-G (2001) Bacteria as workers in the living factory: metal-accumulating bacteria and their potential for materials science. *TRENDS in Biotechnology* 19(1):15-20
- Lawson LD (1993) Bioactive organosulfur compounds of garlic and garlic products: role in reducing blood lipids. ACS Publications
- Nguyen DH, Lee JS, Park KD, et al. (2020) Green Silver Nanoparticles Formed by *Phyllanthus urinaria*, *Pouzolzia zeylanica*, and *Scoparia dulcis* Leaf Extracts and the Antifungal Activity. *Nanomaterials* 10(3):542
- Qadir RW, Qadir KW, Aziz SB (2019) Effect of Various Shapes of Silver Nanoparticles on the Performance of Plasmonic Solar Cells Active Layer. *ZANCO Journal of Pure and Applied Sciences* 31(s4):44-48
- Rahman K (2003) Garlic and aging: new insights into an old remedy. *Ageing research reviews* 2(1):39-56
- Saeed AS, Saadullah AA (2019) Isolation, Identification and Antifungal Susceptibility Testing of *Candida* Species from Dermatologic Specimens in Duhok Province. *ZANCO Journal of Pure and Applied Sciences* 31(4):1-8
- Sendl A, Elbl G, Steinke B, Redl K, Breu W, Wagner H (1992) Comparative pharmacological investigations of *Allium ursinum* and *Allium sativum*. *Planta medica* 58(01):1-7
- Sun C, Lee JS, Zhang M (2008) Magnetic nanoparticles in MR imaging and drug delivery. *Advanced drug delivery reviews* 60(11):1252-1265
- Von White G, Kerscher P, Brown RM, et al. (2012) Green synthesis of robust, biocompatible silver nanoparticles using garlic extract. *Journal of nanomaterials* 2012
- Yanagita T, Han S-y, Wang Y-M, Tsuruta Y, Anno T (2003) Cycloalliin, a cyclic sulfur imino acid, reduces serum triacylglycerol in rats. *Nutrition* 19(2):140-143
- Yeh Y-Y, Liu L (2001) Cholesterol-lowering effect of garlic extracts and organosulfur compounds: human and animal studies. *The journal of nutrition* 131(3):989S-993S
- Yeh Y-Y, Liu L (2001) Cholesterol-lowering effect of garlic extracts and organosulfur compounds: human and animal studies. *The journal of nutrition* 131(3):989S-993S

RESEARCH PAPER

Impact of Diabetes and obesity on Human Fertility and Semen Quality

¹ Mohsin Hussein Sheikh Mohammad,² Edrees Mohammad Ameen

^{1,2} Department of Biology, College of Science, Salahaddin University, Erbil, Kurdistan Region, Iraq

ABSTRACT:

The present study was done to assist the effect of obesity and diabetes on semen quality and fertility of adult males in Erbil city. For this purpose, one hundred twenty adult males were used in this study. The subjects were divided into four groups. The control group included 30 healthy males, the obese group included 30 males with BMI ≥ 30 . The diabetes group included 30 males with diabetes mellitus type 2 (T2 DM) and obese and the diabetes group included 30 males with both BMI ≥ 30 and T2 DM. Semen analysis and sex hormones were determined to evaluate semen quality and fertility. The incidence of abnormal viscosity in patient groups is significantly higher than that of the control group. Semen volume, sperm concentration, normal morphology, total motility, and grade activity in the control group is significantly higher than that of the other 3 groups. Lower sex hormones LH, FSH, and testosterone were recorded in a group of obese with diabetes group. A lower concentration of the serum malondialdehyde (MDA) is recorded in the control group. Despite the decreasing of the semen volume, sperm concentration, normal morphology, and motility in the patient's groups, all these values are not threshold and within the normal ranges which were recommended by World Health Organization (WHO). In our results concluded that obesity and diabetes have a minor effect and not detrimental to the fertility of males.

KEY WORDS: Semen quality; Fertility; Sex hormones; Obesity; Diabetes; Spermatozoa.

DOI: <http://dx.doi.org/10.21271/ZJPAS.33.1.6>

ZJPAS (2021), 33(1);42-54 .

1.INTRODUCTION:

Infertility remains a global public health problem and a major clinical issue concern which affects 15% of reproductive-age couples (Mascarenhas *et al.*, 2012, Jiang *et al.*, 2015). Low quality of semen is well known as a large disorder causing male infertility (Radwan *et al.*, 2016, Levine *et al.*, 2017).

An estimated 70 million people are Worldwide, couples suffer subfertility or infertility, and around 40% of the reasons for the cases are a male (Légaré *et al.*, 2014, Salas-Huetos *et al.*, 2017).

A rigorous and comprehensive meta-analysis recent of studies carried out between 1973 and 2011, that was reported a decrease of the sperm counts by more than 50%. The same goes for several other studies that have also recorded a continuous decline in semen quality (Li *et al.*, 2016, Sengupta *et al.*, 2017).

Now the epidemic of obesity is spreading across the world and according to the latest World Health Organization estimates that 650 million people worldwide were obese and more than 1.9 billion were overweight in 2016 (Moussa *et al.*, 2016). Obesity has been related to an increased risk for many medical conditions include cardiovascular disorders, osteoarthritis, diabetes, liver, kidney disease, depression, and infertility (Bieniek *et al.*, 2016, Dubeux *et al.*, 2016). Recent studies have looked at the relationships between abnormal BMI and semen quality but contradictory findings remain (Sermondade *et al.*, 2013, Eisenberg *et al.*, 2014, Tsao *et al.*, 2015). Chavarro *et al.* (2010) for example, proposed that the BMI of approximately 35 kg/m² was associated with lower ejaculate volume and sperm count among 483 men attending the clinic for infertility. Wang *et al.* (2017a) also observed an increase in BMI appeared to be linked to sperm count among 2384 subfertile men in northern China. In contrast, 31 studies have a pooled meta-

* Corresponding Author:

Edrees Mohammad Ameen
E-mail: edrees.ameen@su.edu.krd

Article History:

Received: 04/08/2020

Accepted: 13/09/2020

Published: 20/02 /2021

analysis, proved there were no significant associations between the BMI and volume of semen, and sperm concentration (MacDonald *et al.*, 2010).

Diabetes mellitus (DM), a chronic non-communicable illness, was deemed one of the most important health risks, impacting 9% (422 million) of the world's population as of 2014. Diabetes mellitus is considered to cause multiple medical complications; impotence-based male infertility, retrograde ejaculation, and hypogonadism are not commonly accepted as one of these. In recent years, definitive findings from multiple research have disputed the views that DM has adverse effects on the male reproductive system (Omolaoye and Du Plessis, 2018).

Of the 21 research studies in a total of 1218 cases and 1171 controls, the results indicated that semen volume, sperm concentration, total sperm motility, progressive sperm motility, and normal sperm morphology were significantly lower in DM patients than in nondiabetic controls (Zhu *et al.*, 2017). Reportedly, DM affects male reproductive function through various pathways and mechanisms. Several studies have studied and identified the adverse effects of reactive oxygen species and the subsequent production of oxidative stress that occurs due to DM (Omolaoye and Du Plessis, 2018).

Due to no data about the effect of obesity and diabetes on male fertility in Erbil city. The present study was done and aimed to evaluate the influence of obesity and diabetes type 2 on semen quality and fertility of adult males by performing of semen analysis, and measurement of sex hormones and oxidative stress in the serum of patients groups.

2.MATERIALS AND METHODS

2.1Subjects

The study included 120 male persons and divided into four groups:

- 1- Control group: Included 30 healthy males.
- 2- Obese group: included 30 males with BMI \geq 30.
- 3- Diabetes group: included 30 males with T2 DM.
- 4- Obese and diabetes group. Included 30 males with both BMI \geq 30 and T2 DM.

The study was carried out between April 2019 and February 2020 in the college of Science, Biology department, Salahaddin University-Erbil. The samples were taken and collected in Leila Qasim Diabetes hospital. Before starting the evaluation of semen analysis, other information was taken from the male persons. This information was recorded in a prepared data form. The ages of all individuals in all groups ranged between 35-45 years. The mean ages of the control group were (37.26 ± 4.56); obese group (40.34 ± 3.56), diabetes group (42.75 ± 3.87), and obese and diabetic group (43.24 ± 2.45) with no significant differences between them.

2.2 Semen and serum collection

Semen samples were collected after 3 days of abstinence via masturbation and sexual container, in wide mouth disposable plastic containers. The semen samples were incubated at 37 °C for 30 minutes to liquefy (Pal *et al.*, 2006). In the liquefied semen samples, the following routine parameters were evaluated according to the methods described in the WHO (WHO, 2009, 2010). The parameters were including; the volume, pH, viscosity, and, appearance of the semen, sperm (count, motility, and morphology). Also, the blood samples were obtained from the individuals and centrifuged at 3000 (rpm) for 15 minutes to obtain the serum. The serum was stored in -20 °C for further examinations, such as determination of sex hormones and malondialdehyde.

2.3 Semen analysis

Upon liquefaction, the sample's viscosity can be measured by aspirating gently in a wide-boring plastic disposable pipette (about 1.5 mm in diameter), enabling the semen to drop by gravity and to follow the length of every thread. The standard sample leaves a small discrete decrease in the pipette. Where viscosity is anomalous, a thread greater than 2 cm long can shape the drop. A typical sample of liquefied semen has a homogeneous, grey-opalescent look. If the sperm concentration is very small, it can appear less opaque; color alternatively, red-brown can be different when red blood cells are present

(haemospermia), Or yellow in jaundice, or taking other vitamins or medications. The volume of the ejaculate was measured with a graduated cylinder tube (WHO, 2010). The semen sample pH was estimated using a 6.1-10 pH paper range. Whatever form of pH paper is used for this analysis, its accuracy should be tested before being used in routine semen analysis according to established requirements (Comhaire and Vermeulen, 1995).

The sperm concentration was estimated by multiply the mean of sperm number in ten fields with 10^6 . Total sperm count = Sperm concentration \times volume. Sperm motility was assessed by examining a drop of ejaculate, covered with a cover glass, under a microscope 400x equipped with heat plate 37 °C. A minimum of around 200 spermatozoa should be counted; both motile and immotile sperms are counted in at least 5 separate fields (WHO, 2009). Motility % = number of motile spermatozoa/total number of spermatozoa (motile and immotile) $\times 100$. Progressive motility was measured by counting the spermatozoa with straight-line forward movement only in percent of motile spermatozoa. In each sample, sperm motility is graded to 0, 1, 2, 3, or 4, depending on whether it shows:

- 0 = no movement
- 1 = movement but not forward progression
- 2 = movement with slow forward progression
- 3 = movement in an almost straight line with good speed
- 4 = movement in a straight line with high speed. (Seaman *et al.*, 1994). The sperm motility index was calculated by multiplying the grading activity with the percentage of motility (Makler *et al.*, 1979).

The normal morphology of spermatozoa was determined by using the hematoxylin and eosin staining procedure (Jequier and Crich, 1986).

2.4 Sex hormones

Serum FSH, LH, and Testosterone hormones were measured by using (Cobas e 411 Roche/Hitachi) in the advanced laboratory of Malaekat Al-Rahma in Erbil city.

2.5 Malondialdehyde

The Serum MDA level was determined by a modified procedure described by (Guidet and Shah, 1989). In short; apply the following to 150 μ l of serum: 1 ml of trichloroacetic acid 17.5%, 1 ml of 0.6% thiobarbituric acid, combined well with vortex, incubated for 15 minutes in a boiling

water bath, and then allowed to cool. Then add 1 ml of 70% trichloroacetic acid TCA, then let the mixture stand at room temperature for 20 minutes, centrifuged for 15 minutes at 2000 rotation per minute, and remove the supernatant for spectrophotometric scanning (Muslih *et al.*, 2002).

The conc. of MDA = absorbance at 532 nm \times D/L $\times E_o$.

L: light bath (1 cm)

E_o : extinction coefficient $1.56 \times 10^5 \text{ M}^{-1} \cdot \text{cm}^{-1}$

D: dilution factor = 1 ml volume. used in Ref./0.15=6.7

2.6 Statistical analysis

Data were observed as means \pm standard errors of means. Fishers' Chi-square test is used to compare the semen viscosity and appearance between control, obese, and diabetes groups. Analysis of variance (ANOVA) and Duncan post-hoc test was used for the comparison of semen volume, sperm (concentration, motility, and morphology), sex hormones, and malondialdehyde between different groups. The level of statistical significance established was 0.05. The data were analyzed using the Statistical Package for Social Science (SPSS), version 17.

3.RESULTS

3.1 Semen analysis

The results presented in Table 1 illustrate the comparison of the semen viscosity and appearance between control, obese, and diabetes groups. A significant difference $p \leq 0.05$ of semen viscosity has appeared between the groups. Males with both obesity and diabetes have a high incidence of the abnormal semen viscosity 33.33% compared with the other groups, while the control group has lower abnormal viscosity 3.33%. No significant differences in semen appearance were observed between control and other patients group. The volume of the semen in the control group (4.22 ± 0.14 ml) is significantly $p \leq 0.05$ higher than that of the obese (3.19 ± 0.42 ml), diabetes (2.70 ± 0.45 ml), and males with obesity and diabetes (2.34 ± 0.26 ml), Table 2.

As shown in Table 3, a significantly higher concentration of the sperm and total sperm count was observed in the control group (88.86×10^6 /ml and 374.98×10^6 /ejaculate respectively), while lower sperm concentration count and total sperm count is recorded in the males with both obesity and diabetes (46.85×10^6 /ml and 109.63

$\times 10^6$ /ejaculate respectively). Regards the sperm morphology, significantly lower concentration of the normal morphology was found in diabetes ($50.45 \pm 3.22\%$) and males with both obesity and diabetes ($45.67 \pm 3.77\%$) as compared with control ($70.67 \pm 2.87\%$) and

males with obesity only ($68.32 \pm 4.32\%$), Table 4.

The results presented in Table 5, compare the motility between the groups and which are considered the most important factors in semen analysis and fertility of males. The results found significant differences ($p \leq 0.001$) in the total sperm count, sperm grade activity, and sperm motility index between the groups. Significantly higher total sperm count, sperm grade, and sperm motility index was observed in the control group ($56.34 \pm 1.45\%$, 3.90 ± 0.14 , and 219.72 ± 10.42) was compared with a lower value in the obese ($48.43 \pm 2.52\%$, 3.34 ± 0.05 and 161.75 ± 12.67), diabetes ($40.22 \pm 1.7676\%$, 2.50 ± 0.07 , and 100.55 ± 8.55), and males with both obesity and diabetes ($38.21 \pm 2.33\%$, 2.22 ± 0.09 , and 84.82 ± 9.26).

3.2 Sex hormones

As shown in Table 6, the concentration of the serum sex hormones LH and FSH, are significantly ($p \leq 0.05$) higher in control ($6.56 \pm 0.27 \mu\text{IU/ml}$ and $7.26 \pm \mu\text{IU/ml}$) and diabetes groups ($5.65 \mu\text{IU/ml}$ and $6.78 \mu\text{IU/ml}$) as compared with obese ($4.21 \mu\text{IU/ml}$ and $5.34 \mu\text{IU/ml}$) and males with both obesity and diabetes ($3.36 \pm 0.24 \mu\text{IU/ml}$ and $4.35 \pm 0.37 \mu\text{IU/ml}$). While the concentration of the testosterone is significantly higher ($p \leq 0.001$) in control ($6.77 \pm 0.43 \text{ ng/ml}$) as compared with the other 3 groups ($4.21 \pm 0.08 \text{ ng/ml}$ in obese, 4.00 ± 0.64 in diabetes and $2.65 \pm 0.09 \text{ ng/ml}$ in males with both obesity and diabetes).

3.3 Malondialdehyde

Significantly higher concentration ($p \leq 0.001$) of the serum MDA is recorded in males with both obesity and diabetes ($6.45 \pm 0.88 \mu\text{mol/L}$), while the lower concentration of it is found in the control group ($2.14 \pm 0.05 \mu\text{mol/L}$), Table 7.

Table 1. Viscosity and appearance of semen of control, obese and diabetic men.

Groups	Viscosity		Appearance	
	Normal viscosity	Abnormal high viscosity	Normal appearance	Abnormal appearance
Control	29 (96.66%)	1 (3.33%)	28 (93.33%)	2 (6.66%)
Obese	23 (76.66%)	7 (23.33%)	28 (93.33%)	2 (6.66%)
Diabetes	23 (76.66%)	7 (23.33%)	28 (93.33%)	2 (6.66%)
Obese and Diabetes	20 (66.66%)	10 (33.33%)	27 (90.00%)	3 (10%)
Calculated χ^2	6.46		3.27	
Tabulated χ^2	4.32		3.34	
p-value	0.05		0.87	

Table 2. The pH and volume of semen (Mean \pm SEM) of control, obese and diabetic men.

Groups	pH	Semen volume (ml)
Control	7.64 \pm 0.13 ^a	4.22 \pm 0.14 ^a
Obese	7.82 \pm 0.34 ^a	3.19 \pm 0.42 ^b
Diabetes	7.72 \pm 0.21 ^a	2.70 \pm 0.45 ^b
Obese and Diabetes	7.78 \pm 0.12 ^a	2.34 \pm 0.26 ^b
p-value	0.20	0.05

P- value \leq 0.05 considered significant

Post Hoc Duncan-test, no differences between groups with the same letter

SEM = standard error of the mean

Table 3. Sperm concentration and total sperm count (Mean \pm SEM) of control, obese, and diabetes men.

Groups	Sperm concentration ($\times 10^6$ /ml)	Total sperm count ($\times 10^6$ /ejaculate)
Control	88.86 \pm 5.89 ^a	374.98 \pm 20.35 ^a
Obese	56.66 \pm 3.76 ^b	180.74 \pm 12.26 ^b
Diabetes	51.57 \pm 5.46 ^b	139.23 \pm 10.87 ^c
Obese and Diabetes	46.85 \pm 8.77 ^b	109.63 \pm 10.34 ^d
p-value	0.001	0.001

P- value \leq 0.05 considered significant

Post Hoc Duncan-test, no differences between groups with the same letter

SEM = standard error of the mean

Table 4. Sperm morphology (Mean \pm SEM) of control, obese, and diabetes men.

Groups	Normal morphology (%)	Abnormal morphology (%)	
Groups	Total sperm motility (%)	Grade activity	Sperm motility index
Control	56.34 \pm 1.45 ^a	3.90 \pm 0.14 ^a	219.72 \pm 10.42 ^a
Obese	48.43 \pm 2.52 ^b	3.34 \pm 0.05 ^b	161.75 \pm 12.67 ^b
Diabetes	40.22 \pm 1.76 ^c	2.50 \pm 0.07 ^c	100.55 \pm 8.55 ^c
Obese and Diabetes	38.21 \pm 2.33 ^c	2.22 \pm 0.09 ^c	84.82 \pm 9.26 ^c
p-value	0.001	0.001	0.001

P- value \leq 0.05 considered significant

Post Hoc Duncan-test, no differences between groups with the same letter

SEM = standard error of the mean

Table 5. Sperm motility (Mean \pm SEM) of control, obese, and diabetes men.

Groups	Total sperm motility (%)	Grade activity	Sperm motility index
Control	56.34 \pm 1.45 ^a	3.90 \pm 0.14 ^a	219.72 \pm 10.42 ^a
Obese	48.43 \pm 2.52 ^b	3.34 \pm 0.05 ^b	161.75 \pm 12.67 ^b
Diabetes	40.22 \pm 1.76 ^c	2.50 \pm 0.07 ^c	100.55 \pm 8.55 ^c
Obese and Diabetes	38.21 \pm 2.33 ^c	2.22 \pm 0.09 ^c	84.82 \pm 9.26 ^c
p-value	0.001	0.001	0.001

P- value \leq 0.05 considered significant

Post Hoc Duncan-test, no differences between groups with the same letter

SEM = standard error of the mean

Table 6. Sex hormones (Mean ± SEM) of control, obese, and diabetes men.

Sex hormones	LH (μIU/ml)	FSH (μIU/ml)	Testosterone (ng/ml)
Control	6.56 ± 0.27 ^a	7.26 ± 0.88 ^a	6.77 ± 0.43 ^a
Obese	4.21 ± 0.08 ^b	5.34 ± 0.64 ^b	4.21 ± 0.25 ^b
Diabetes	5.65 ± 0.74 ^a	6.78 ± 0.78 ^a	4.00 ± 0.64 ^b
Obese and Diabetes	3.36 ± 0.24 ^b	4.35 ± 0.37 ^b	2.65 ± 0.09 ^c
p-value	0.05	0.05	0.001

P- value ≤ 0.05 considered significant

Post Hoc Duncan-test, no differences between groups with the same letter

SEM = standard error of the mean

Table 7. Malondialdehyde (Mean ± SEM) of control, obese, and diabetes men.

Groups	MDA (μmol/L)
Control	2.14 ± 0.05 ^c
Obese	4.32 ± 0.24 ^b
Diabetes	4.56 ± 0.76 ^b
Obese and Diabetes	6.45 ± 0.88 ^a
p-value	0.001

P- value ≤ 0.05 considered significant

Post Hoc Duncan-test, no differences between groups with the same letter

SEM = standard error of the mean

4.DISCUSSION

Overweight and obesity are well known to affect female fertility, their effects on male fertility and semen parameters are less clear (Alshahrani *et al.*, 2016). There are inconsistent data on the effect of obesity on seminal fluid and

men's fertility (Alahmar *et al.*, 2018). Some studies showed a correlation between obesity and low sperm concentration, motility, morphology, and integrity of the DNA (Bieniek *et al.*, 2016, Sermondade *et al.*, 2013, Wang *et al.*, 2017b). However, other studies have not recorded any link between obesity and poor quality of semen

(Hadjkacem Loukil et al., 2015, Dubeux et al., 2016). The decrease in the semen volume and sperm concentration of obese males in our results are consistent with the results of (Hammoud et al., 2008, Chavarro et al., 2010, Wang et al., 2017b). While it differs from (MacDonald et al., 2010, M. Al-Ali et al., 2014, Alshahrani et al., 2016), who observed no significant differences in semen volume and sperm concentration between obese and normal weight. A negative correlation between BMI and sperm concentration was found in both fertile and infertile men (Anderson et al., 2015).

As with sperm concentration, data are inconsistent on the impact of obesity on sperm morphology and motility. The study of (Macdonald et al., 2013) in New Zealand revealed no effect of BMI on sperm motility, but sperm morphology was decreased with increasing BMI. Current results agreed with the findings of (Lazaros et al., 2012, Belloc et al., 2014), that observed a negative correlation between BMI and sperm motility. While the results of other studies differ from the present results, which revealed no association between obesity and sperm motility (Eisenberg et al., 2014, Alshahrani et al., 2016). Jensen et al. (2004) recorded no link between obesity a motility percentage. The results of the study of (Hammoud et al., 2008) revealed a lower sperm grade activity in overweight and obese men. In population-based researches, obesity is the single most significant factor that results in a deficit of testosterone (Tajar et al., 2010). The pathophysiology behind the relationship between abnormal BMI and consistency of semen is uncertain and possibly complex. Overweight and obesity have been shown to affect the GnRH – FSH / LH pulse, which can disrupt the role of Leydig or Sertoli cells and interfere with sex hormone release and mature sperm production (Hammoud et al., 2008).

In current results, the concentration of the sex hormones, LH, FSH, and testosterone decrease in obese men, these results are in agreement with the findings of other investigations. Overweight and moderate obesity is primarily correlated with decreases in total testosterone, while free testosterone rates stay within the reference range, especially for younger men (Fui et al., 2014). Decreases in overall testosterone levels attributed to obesity-associated hyperinsulinemia are

primarily a result of decreases in sex hormone-binding globulin (SHBG). Nonetheless, although problematic, the calculation of free testosterone levels may provide a more precise androgen status evaluation than the (usually preferred) total testosterone calculation in circumstances where SHBG levels are below the reference range (Bhasin et al., 2010). Testosterone deficiency may cause increased adipogenesis and visceral obesity as evidenced by the rapid weight gain observed in men after androgen deprivation therapy or surgical castration (Tsai et al., 2000, Saylor and Smith, 2009). Weight loss achieved by pharmacologically improving testosterone and gonadotrophin levels with liraglutide (Jensterle et al., 2019) or bariatric surgery, and was able to reverse the hypogonadotropic hypogonadism caused by obesity (Pellitero et al., 2012, Escobar-Morreale et al., 2017).

Serum testosterone (total and free) and SHBG rates are decreased in obese male person (Diaz-Arjonilla et al., 2009). Epidemiological studies have shown that levels of both serum testosterone and, to a lesser extent, free testosterone is reduced in obese men (Allen et al., 2002, Gapstur et al., 2002, Jensen et al., 2004). The decline of overall and free testosterone is correlated not only with intra-abdominal fat but also with total body fat and body fat subcutaneously (Tsai et al., 2004). Obesity is correlated with reduced production of the luteinizing hormone (LH) (Diaz-Arjonilla et al., 2009). The increased levels of estrogen modulate the response of pituitary LH to the hormone-releasing gonadotropin (GnRH) (Castro-Fernandez et al., 2000). However, more obvious obesity is correlated with an unequivocal decrease of free testosterone rates, where rates of luteinizing hormone (LH) and follicle-stimulating hormone (FSH) are generally small or excessively high, indicating that the dominant repression happens at the hypothalamic-pituitary rate or level. This may be because adipose tissue expresses aromatase, which transforms testosterone to estradiol (E2), particularly in the inflamed, insulin-resistant state (Fui et al., 2014).

Obesity was confirmed to be triggering systemic oxidative stress (Ozata et al., 2002, Furukawa et al., 2017). The obese infertile males displayed fewer sperm motility as opposed to other classes, fewer sperm function tests values.

The concentration of Malondialdehyde (MDA) in seminal plasma of obese infertile subjects showed higher value compared with those of non-obese infertile men and controls (Najafi et al., 2012). Obesity may cause oxidative stress and decrease testosterone rates, it can modify testicular functions and therefore it can be hypothesized that obesity could be a significant causative factor in the male infertility etiology (Erdemir et al., 2012). Body mass index (BMI) was correlated positively with reactive oxygen species (ROS) and MDA (Han et al., 2018). There was a study done in 2016 showed that the fertile obese men had significantly higher seminal ROS compared to fertile normal-weight men and men with overweight (Taha et al., 2016), these results are in line with our results. A correlation has been identified between oxidative stress and obesity (Karaouzene et al., 2011), and a combination of increased sperm DNA fragmentation in obese men and poor quality of spermatogenesis has also been reported (Smit et al., 2010). Concentrations of seminal MDA are negatively associated with sperm concentration and motility which could offer an easy and effective method for predicting sperm parameters (Hsieh et al., 2006).

Regarding diabetes, our results found a negative impact of diabetes on semen parameters, other investigation approved these results. Studies of infertility prevalence in DM male partners of infertile couples showed decreased sperm motility and increased irregular sperm morphology (Li et al., 2004, Delfino et al., 2007). In a study conducted on 52 diabetic men, semen analysis revealed a significant decline in sperm motility, including the number of rapid progressive cells (Bhattacharya et al., 2014). Semen collected from men with diabetes showed significant sperm parameters decrease compared to men's groups with autoimmune disorders, kidney disease, ulcerative colitis, and cardiac disease (Ranganathan et al., 2002). A few further kinds of research have revealed a significant decline in semen volume, sperm motility, and morphology of diabetic men's semen (Agbaje et al., 2007, Ali and Rakkah, 2007). The findings showed that in DM patients, semen volume, sperm concentration, complete sperm motility, progressive sperm motility, and normal sperm morphology were considerably lower than in nondiabetic controls (Zhu et al., 2017). Semen in patients with T2 DM is of low volume, abnormal motility and

morphology compared with non-diabetic subjects (Ibrahim et al., 2018). Ali et al. (1993) reported a highly important increase in overall sperm count and sperm concentration in type 1 and type 2 DM patients. Sperm motility and volume of semen were, therefore, lower as for non-diabetics, though sperm morphology and sperm motility rate were not impaired. A high prevalence of irregular sperm motility and morphology in patients with DM was also identified (Amiri et al., 2011, ADA, 2014). Another research carried out in Sudanese males shows a substantial decrease in all parameters of semen (semen volume, sperm count, motility, and morphology) was found in patients with diabetes as opposed to non-diabetics (Abdullah et al., 2014).

There are inconsistent data on the effect of diabetes on sex hormones, A cross-sectional analysis of 355 men with type 2 diabetic aged > 30 in the United Kingdom found that testosterone rates with type 2 diabetes are frequently low, and most of these men have hypogonadism symptoms (Kapoor et al., 2007). Type 2 DM patients will be diagnosed with a moderate but not major decrease of testosterone relative to the regular subjects (Mohammed et al., 2018), these results are consistent with our results. The results of the (Chandel et al., 2008) found that the concentrations of LH and FSH were beyond acceptable limits in type 2 diabetic patients with small free testosterone concentrations. Ali and his colleges found high levels of serum and urinary FSH and LH in diabetics with low levels of total serum free testosterone (Ali et al., 1993).

In current results, a high concentration of MDA was found in diabetes patients. In diabetes patients, MDA is negatively associated with the main sperm parameters (La Vignera et al., 2012). Diabetes mellitus is associated with impaired sperm quality, which involves oxidative stress in pathogenesis, in particular with poor glycemic control (Omu et al., 2014). The semen parameters are reduced and the MDA standard for diabetics is raised whereas type 2 diabetes mellitus harms the capacity for male fertility relative to the non-diabetic (Singh et al., 2014). Excessive development of reactive oxygen species by mitochondria in hyperglycemia is the catalyst that propels these pathways. Excessive development of reactive oxygen species inhibits the activity of glyceraldehyde-3-phosphate dehydrogenase, which in effect stimulates all hyperglycaemic

harm pathways by diverting upstream glycolytic metabolites to these pathways. Also, where the highly potent ROS reaches the seminal antioxidant protection potential, several cascades of reactions can occur which can result in sperm DNA damage and degradation of mitochondrial DNA, then altered sperm parameters and ultimately male infertility (Ahmed, 2005).

5. CONCLUSIONS

In current results, concluded that patients with both obesity and diabetes have a negative impact on semen parameters and fertility than those with healthy control, obesity, or diabetes only. Despite decreasing the semen parameters and fertility in obese and diabetes males, the value of them within the normal ranges of the WHO guidelines. It is evident that in our study, obesity and diabetes have a minor effect and not detrimental to the fertility of males.

Acknowledgments

The authors would like to show sincere gratitude for all patients who participated in the study. The authors are also grateful for the Leila Qasim Diabetes hospital center for their help and collection of the samples.

Conflict of Interest

The authors declare no conflict of interest

REFERENCES

ABDULLAH, A. E., MORSI, A. N., ELHASSAN FARAGALLA, M. & ELSAYED, M. 2014. The Association Between Male Infertility And Diabetes Mellitus. *J Pharm Biomed Sci*, 4, 1097-1102.

ADA, A. D. A. 2014. Diagnosis and classification of diabetes mellitus. *Diabetes care*, 37, S81-S90.

AGBAJE, I., ROGERS, D., MCVICAR, C., MCCLURE, N., ATKINSON, A., MALLIDIS, C. & LEWIS, S. 2007. Insulin dependant diabetes mellitus: implications for male reproductive function. *Human Reproduction*, 22, 1871-1877.

AHMED, R. 2005. The physiological and biochemical effects of diabetes on the balance between oxidative stress and antioxidant defense system. *Med. J. Of Islamic Academy of Sci*, 15, 31-42.

ALAHMAR, A. T., ALI, Z., MUHSIN, Z. & QASIM, H. 2018. The impact of obesity on seminal fluid in men with infertility. *Middle East Fertility Society Journal*, 23, 346-349.

ALI, S., SHAIKH, R., ASHFAQSIDDIQI, N. & SIDDIQI, P. 1993. Serum and urinary levels of pituitary-gonadal hormones in insulin-dependent and non-

insulin-dependent diabetic males with and without neuropathy. *Archives of andrology*, 30, 117-123.

ALI, S. T. & RAKKAH, N. I. 2007. Neurophysiological role of sildenafil citrate (Viagra) on seminal parameters in diabetic males with and without neuropathy. *Pakistan journal of pharmaceutical sciences*, 20, 36-42.

ALLEN, N. E., APPLEBY, P. N., DAVEY, G. K. & KEY, T. J. 2002. Lifestyle and nutritional determinants of bioavailable androgens and related hormones in British men. *Cancer Causes & Control*, 13, 353-363.

ALSHAHRANI, S., AHMED, A. F., GABR, A., ABALHASSAN, M. & AHMAD, G. 2016. The impact of body mass index on semen parameters in infertile men. *Andrologia*, 48, 1125-1129.

AMIRI, I., KARIMI, J., PIRI, H., GOODARZI, M. T., TAVILANI, H., KHODADADI, I. & GHORBANI, M. 2011. Association between nitric oxide and 8-hydroxydeoxyguanosine levels in semen of diabetic men. *Systems biology in reproductive medicine*, 57, 292-295.

ANDERSON, Y. C., WYNTER, L. E., MOLLER, K. R., CAVE, T. L., DOLAN, G. M., GRANT, C. C., STEWART, J. M., CUTFIELD, W. S. & HOFMAN, P. L. 2015. The effect of a multi-disciplinary obesity intervention compared to usual practice in those ready to make lifestyle changes: design and rationale of Whanau Pakari. *BMC obesity*, 2, 1-10.

BELLOC, S., COHEN-BACRIE, M., AMAR, E., IZARD, V., BENKHALIFA, M., DALLÉAC, A. & DE MOUZON, J. 2014. High body mass index has a deleterious effect on semen parameters except morphology: results from a large cohort study. *Fertility and sterility*, 102, 1268-1273.

BHASIN, S., CUNNINGHAM, G. R., HAYES, F. J., MATSUMOTO, A. M., SNYDER, P. J., SWERDLOFF, R. S. & MONTORI, V. M. 2010. Testosterone therapy in men with androgen deficiency syndromes: an Endocrine Society clinical practice guideline. *The Journal of Clinical Endocrinology & Metabolism*, 95, 2536-2559.

BHATTACHARYA, S. M., GHOSH, M. & NANDI, N. 2014. Diabetes mellitus and abnormalities in semen analysis. *Journal of Obstetrics and Gynaecology Research*, 40, 167-171.

BIENIEK, J. M., KASHANIAN, J. A., DEIBERT, C. M., GROBER, E. D., LO, K. C., BRANNIGAN, R. E., SANDLOW, J. I. & JARVI, K. A. 2016. Influence of increasing body mass index on semen and reproductive hormonal parameters in a multi-institutional cohort of subfertile men. *Fertility and sterility*, 106, 1070-1075.

CASTRO-FERNANDEZ, C., OLIVARES, A., SODERLUND, D., LÓPEZ-ALVARENGA, J., ZAMBRANO, E., VELDHIJS, J. D., ULLOA-AGUIRRE, A. & MÉNDEZ, J. 2000. A preponderance of circulating basic isoforms is associated with decreased plasma half-life and biological to immunological ratio of gonadotropin-releasing hormone-releasable luteinizing hormone

- in obese men. *The Journal of Clinical Endocrinology & Metabolism*, 85, 4603-4610.
- CHANDEL, A., DHINDSA, S., TOPIWALA, S., CHAUDHURI, A. & DANDONA, P. 2008. Testosterone concentration in young patients with diabetes. *Diabetes care*, 31, 2013-2017.
- CHAVARRO, J. E., TOTH, T. L., WRIGHT, D. L., MEEKER, J. D. & HAUSER, R. 2010. Body mass index in relation to semen quality, sperm DNA integrity, and serum reproductive hormone levels among men attending an infertility clinic. *Fertility and sterility*, 93, 2222-2231.
- COMHAIRE, F. & VERMEULEN, L. 1995. Human semen analysis. *Human reproduction update*, 1, 343-362.
- DELFINO, M., IMBROGNO, N., ELIA, J., CAPOGRECO, F. & MAZZILLI, F. 2007. Prevalence of diabetes mellitus in male partners of infertile couples. *Minerva urologica e nefrologica= The Italian journal of urology and nephrology*, 59, 131-135.
- DIAZ-ARJONILLA, M., SCHWARCZ, M., SWERDLOFF, R. & WANG, C. 2009. Obesity, low testosterone levels and erectile dysfunction. *International journal of impotence research*, 21, 89-98.
- DUBEUX, V. T., RENOVATO, T., ESTEVES, A. C., ANDRÉ, L., DE OLIVEIRA, A. & PENNA, I. A. 2016. The impact of obesity on male fecundity: a Brazilian study. *JBRA assisted reproduction*, 20, 137-141.
- EISENBERG, M. L., KIM, S., CHEN, Z., SUNDARAM, R., SCHISTERMAN, E. F. & BUCK LOUIS, G. M. 2014. The relationship between male BMI and waist circumference on semen quality: data from the LIFE study. *Human reproduction*, 29, 193-200.
- ERDEMIR, F., ATILGAN, D., MARKOC, F., BOZTEPE, O., SUHA-PARLAKTAS, B. & SAHIN, S. 2012. The effect of diet induced obesity on testicular tissue and serum oxidative stress parameters. *Actas Urológicas Españolas (English Edition)*, 36, 153-159.
- ESCOBAR-MORREALE, H. F., SANTACRUZ, E., LUQUE-RAMÍREZ, M. & BOTELLA CARRETERO, J. I. 2017. Prevalence of 'obesity-associated gonadal dysfunction' in severely obese men and women and its resolution after bariatric surgery: a systematic review and meta-analysis. *Human Reproduction Update*, 23, 390-408.
- FUI, M. N. T., DUPUIS, P. & GROSSMANN, M. 2014. Lowered testosterone in male obesity: mechanisms, morbidity and management. *Asian journal of andrology*, 16, 223-231.
- FURUKAWA, S., FUJITA, T., SHIMABUKURO, M., IWAKI, M., YAMADA, Y., NAKAJIMA, Y., NAKAYAMA, O., MAKISHIMA, M., MATSUDA, M. & SHIMOMURA, I. 2017. Increased oxidative stress in obesity and its impact on metabolic syndrome. *The Journal of clinical investigation*, 114, 1752-1761.
- GAPSTUR, S. M., GANN, P. H., KOPP, P., COLANGELO, L., LONGCOPE, C. & LIU, K. 2002. Serum androgen concentrations in young men: A longitudinal analysis of associations with age, obesity, and race.: The CARDIA male hormone study. *Cancer Epidemiology and Prevention Biomarkers*, 11, 1041-1047.
- GUIDET, B. & SHAH, S. V. 1989. Enhanced in vivo H₂O₂ generation by rat kidney in glycerol-induced renal failure. *American Journal of Physiology-Renal Physiology*, 257, F440-F445.
- HADJKACEM LOUKIL, L., HADJKACEM, H., BAHLOUL, A. & AYADI, H. 2015. Relation between male obesity and male infertility in a Tunisian population. *Andrologia*, 47, 282-285.
- HAMMOUD, A. O., GIBSON, M., PETERSON, C. M., MEIKLE, A. W. & CARRELL, D. T. 2008. Impact of male obesity on infertility: a critical review of the current literature. *Fertility and sterility*, 90, 897-904.
- HAN, R., MA, J., LIU, W., AN, X., ZHANG, Z.-D. & WANG, S. 2018. Correlation of reproductive hormone levels and seminal plasma oxidative stress with semen quality in obese males. *Zhonghua nan ke xue= National journal of andrology*, 24, 419-424.
- HSIEH, Y.-Y., CHANG, C.-C. & LIN, C.-S. 2006. Seminal malondialdehyde concentration but not glutathione peroxidase activity is negatively correlated with seminal concentration and motility. *International Journal of Biological Sciences*, 2, 23-29.
- IBRAHIM, N. E., RIDA, M. & ABDRABO, A. A. 2018. Evaluation of Semen Quality in Type 2 Diabetes Mellitus Sudanese Patients Compared to Non-Diabetic Subjects. *The Open Clinical Biochemistry Journal*, 8, 20-25.
- JENSEN, T. K., ANDERSSON, A.-M., JØRGENSEN, N., ANDERSEN, A.-G., CARLSEN, E. & SKAKKEBÆK, N. E. 2004. Body mass index in relation to semen quality and reproductive hormones among 1,558 Danish men. *Fertility and sterility*, 82, 863-870.
- JENSTERLE, M., PODBREGAR, A., GORICAR, K., GREGORIC, N. & JANEZ, A. 2019. Effects of liraglutide on obesity-associated functional hypogonadism in men. *Endocrine connections*, 8, 195-202.
- JEQUIER, A. M. & CRICH, J. P. 1986. *Semen analysis: a practical guide*, Blackwell Scientific Publications; St. Louis, MO, USA. Distributors, USA, Blackwell Mosby Book Distributors.
- JIANG, W., SUN, H., ZHANG, J., ZHOU, Q., WU, Q., LI, T., ZHANG, C., LI, W., ZHANG, M. & XIA, X. 2015. Polymorphisms in Protamine 1 and Protamine 2 predict the risk of male infertility: a meta-analysis. *Scientific reports*, 5, 1-11.
- KAPOOR, D., ALDRED, H., CLARK, S., CHANNER, K. S. & JONES, T. H. 2007. Clinical and biochemical assessment of hypogonadism in men with type 2 diabetes: correlations with bioavailable testosterone and visceral adiposity. *Diabetes care*, 30, 911-917.
- KARAOUZENE, N., MERZOUK, H., ARIBI, M., MERZOUK, S., BERROUIGUET, A. Y., TESSIER, C. & NARCE, M. 2011. Effects of the association of aging and obesity on lipids, lipoproteins and oxidative stress biomarkers: a comparison of older with young men. *Nutrition*,

- Metabolism and Cardiovascular Diseases*, 21, 792-799.
- LA VIGNERA, S., CONDORELLI, R., VICARI, E., D'AGATA, R., SALEMI, M. & CALOGERO, A. 2012. High levels of lipid peroxidation in semen of diabetic patients. *Andrologia*, 44, 565-570.
- LAZAROS, L., HATZI, E., MARKOULA, S., TAKENAKA, A., SOFIKITIS, N., ZIKOPOULOS, K. & GEORGIU, I. 2012. Dramatic reduction in sperm parameters following bariatric surgery: report of two cases. *Andrologia*, 44, 428-432.
- LÉGARÉ, C., DROIT, A., FOURNIER, F. D. R., BOURASSA, S., FORCE, A., CLOUTIER, F., TREMBLAY, R. & SULLIVAN, R. 2014. Investigation of male infertility using quantitative comparative proteomics. *Journal of proteome research*, 13, 5403-5414.
- LEVINE, H., JØRGENSEN, N., MARTINO-ANDRADE, A., MENDIOLA, J., WEKSLER-DERRI, D., MINDLIS, I., PINOTTI, R. & SWAN, S. H. 2017. Temporal trends in sperm count: a systematic review and meta-regression analysis. *Human reproduction update*, 23, 646-659.
- LI, C.-J., TZENG, C.-R., CHEN, R.-Y., HAN, B.-C., YEH, C.-Y. & CHIEN, L.-C. 2016. Decline in semen quality in men in northern Taiwan between 2001 and 2010. *Chin J Physiol*, 59, 355-365.
- LI, W., ZHENG, H., BUKURU, J. & DE KIMPE, N. 2004. Natural medicines used in the traditional Chinese medical system for therapy of diabetes mellitus. *Journal of ethnopharmacology*, 92, 1-21.
- M. AL-ALI, B., GUTSCHI, T., PUMMER, K., ZIGEUNER, R., BROOKMAN-MAY, S., WIELAND, W., FRITSCH, H. & AZIZ, A. 2014. Body mass index has no impact on sperm quality but on reproductive hormones levels. *Andrologia*, 46, 106-111.
- MACDONALD, A., HERBISON, G., SHOWELL, M. & FARQUHAR, C. 2010. The impact of body mass index on semen parameters and reproductive hormones in human males: a systematic review with meta-analysis. *Hum Reprod Update*, 16, 293-311.
- MACDONALD, A., STEWART, A. & FARQUHAR, C. 2013. Body mass index in relation to semen quality and reproductive hormones in New Zealand men: a cross-sectional study in fertility clinics. *Human reproduction*, 28, 3178-3187.
- MAKLER, A., ITSKOVITZ, J., BRANDES, J. M. & PALDI, E. 1979. Sperm velocity and percentage of motility in 100 normospermic specimens analyzed by the multiple exposure photography (MEP) method. *Fertility and Sterility*, 31, 155-161.
- MASCARENHAS, M. N., FLAXMAN, S. R., BOERMA, T., VANDERPOEL, S. & STEVENS, G. A. 2012. National, regional, and global trends in infertility prevalence since 1990: a systematic analysis of 277 health surveys. *PLoS Med*, 9, e1001356.
- MOHAMMED, M., AL-HABORI, M., ABDULLATEEF, A. & SAIF-ALI, R. 2018. Impact of metabolic syndrome factors on testosterone and SHBG in type 2 diabetes mellitus and metabolic syndrome. *Journal of diabetes research*, 2018, 1-8.
- MOUSSA, H. N., ALRAIS, M. A., LEON, M. G., ABBAS, E. L. & SIBAI, B. M. 2016. Obesity epidemic: impact from pre-conception to postpartum. *Future science OA*, 2, 1-12.
- MUSLIH, R., AL-NIMER, O. & AL-ZAMELY, M. 2002. The level of Malondialdehyde after activation with H₂O₂ and CuSO₄ and inhibited by Desferoxamine and Molsidomine in the serum of patients with acute myocardial infection. *J. Chem*, 5, 148-149.
- NAJAFI, M., SREENIVASA, G., AARABI, M., DHAR, M., BABU, M. & MALINI, S. 2012. Seminal malondialdehyde levels and oxidative stress in obese male infertility. *Journal of Pharmacy Research*, 5, 3597-3600.
- OMOLAOYE, T. & DU PLESSIS, S. S. 2018. Diabetes mellitus and male infertility. *Asian Pacific Journal of Reproduction*, 7, 6-14.
- OMU, A., AL-BADER, M., AL-JASSAR, W., AL-AZEMI, M., OMU, F., MATHEW, T. & ANIM, J. 2014. Antioxidants attenuates the effects of insulin dependent diabetes mellitus on sperm quality. *Bioenergetics*, 3, 1-9.
- OZATA, M., MERGEN, M., OKTENLI, C., AYDIN, A., SANISOGLU, S. Y., BOLU, E., YILMAZ, M. I., SAYAL, A., ISIMER, A. & OZDEMIR, I. C. 2002. Increased oxidative stress and hypozincemia in male obesity. *Clinical biochemistry*, 35, 627-631.
- PAL, P., RAJALAKSHMI, M., MANOCHA, M., SHARMA, R., MITTAL, S. & RAO, D. 2006. Semen quality and sperm functional parameters in fertile Indian men. *Andrologia*, 38, 20-25.
- PELLITERO, S., OLAIZOLA, I., ALASTRUE, A., MARTÍNEZ, E., GRANADA, M. L., BALIBREA, J. M., MORENO, P., SERRA, A., NAVARRO-DÍAZ, M. & ROMERO, R. 2012. Hypogonadotropic hypogonadism in morbidly obese males is reversed after bariatric surgery. *Obesity surgery*, 22, 1835-1842.
- RADWAN, M., JUREWICZ, J., POLAŃSKA, K., SOBALA, W., RADWAN, P., BOCHENEK, M. & HANKE, W. 2016. Exposure to ambient air pollution-does it affect semen quality and the level of reproductive hormones? *Annals of human biology*, 43, 50-56.
- RANGANATHAN, P., MAHRAN, A. M., HALLAK, J. & AGARWAL, A. 2002. Sperm cryopreservation for men with nonmalignant, systemic diseases: a descriptive study. *Journal of andrology*, 23, 71-75.
- SALAS-HUETOS, A., BULLÓ, M. & SALAS-SALVADÓ, J. 2017. Dietary patterns, foods and nutrients in male fertility parameters and fecundability: a systematic review of observational studies. *Human reproduction update*, 23, 371-389.
- SAYLOR, P. J. & SMITH, M. R. 2009. Metabolic complications of androgen deprivation therapy for prostate cancer. *The Journal of urology*, 181, 1998-2008.
- SEAMAN, E., BAR-CHAMA, N. & FISCH, H. 1994. Semen analysis in the clinical evaluation of infertility. *Mediguide to Urology*, 7, 1-8.

- SENGUPTA, P., NWAGHA, U., DUTTA, S., KRAJEWSKA-KULAK, E. & IZUKA, E. 2017. Evidence for decreasing sperm count in African population from 1965 to 2015. *African health sciences*, 17, 418-427.
- SERMONDADE, N., FAURE, C., FEZEU, L., SHAYEB, A., BONDE, J. P., JENSEN, T. K., VAN WELY, M., CAO, J., MARTINI, A. C. & ESKANDAR, M. 2013. BMI in relation to sperm count: an updated systematic review and collaborative meta-analysis. *Human reproduction update*, 19, 221-231.
- SINGH, A. K., TOMARZ, S., CHAUDHARI, A. R., SINQH, R. & VERMA, N. 2014. Type 2 diabetes mellitus affects male fertility potential. *Indian J Physiol Pharmacol*, 58, 403-406.
- SMIT, M., ROMIJN, J. C., WILDHAGEN, M. F., WEBER, R. F. & DOHLE, G. R. 2010. Sperm chromatin structure is associated with the quality of spermatogenesis in infertile patients. *Fertility and sterility*, 94, 1748-1752.
- TAHA, E. A., SAYED, S. K., GABER, H. D., HAFEZ, H. K. A., GHANDOUR, N., ZAHRAN, A. & MOSTAFA, T. 2016. Does being overweight affect seminal variables in fertile men? *Reproductive biomedicine online*, 33, 703-708.
- TAJAR, A., FORTI, G., O'NEILL, T. W., LEE, D. M., SILMAN, A. J., FINN, J. D., BARTFAI, G. R., BOONEN, S., CASANUEVA, F. F. & GIWERCMAN, A. 2010. Characteristics of secondary, primary, and compensated hypogonadism in aging men: evidence from the European Male Ageing Study. *The Journal of Clinical Endocrinology & Metabolism*, 95, 1810-1818.
- TSAI, E., BOYKO, E., LEONETTI, D. & FUJIMOTO, W. 2000. Low serum testosterone level as a predictor of increased visceral fat in Japanese-American men. *International journal of obesity*, 24, 485-491.
- TSAI, E. C., MATSUMOTO, A. M., FUJIMOTO, W. Y. & BOYKO, E. J. 2004. Association of bioavailable, free, and total testosterone with insulin resistance: influence of sex hormone-binding globulin and body fat. *Diabetes care*, 27, 861-868.
- TSAO, C.-W., LIU, C.-Y., CHOU, Y.-C., CHA, T.-L., CHEN, S.-C. & HSU, C.-Y. 2015. Exploration of the association between obesity and semen quality in a 7630 male population. *PLoS One*, 10, 1-13.
- WANG, E.-Y., HUANG, Y., DU, Q.-Y., YAO, G.-D. & SUN, Y.-P. 2017a. Body mass index effects sperm quality: a retrospective study in Northern China. *Asian journal of andrology*, 19, 234-237.
- WANG, L., SOUTHERLAND, J., WANG, K., BAILEY, B. A., ALAMIAN, A., STEVENS, M. A. & WANG, Y. 2017b. Ethnic differences in risk factors for obesity among adults in California, the United States. *Journal of obesity*, 2017, 1-10.
- WHO 2009. World Health Organisation. Laboratory manual for the examination of human semen and sperm-cervical mucus interaction. Cambridge university press.
- WHO 2010. World Health Organization. Laboratory manual for the examination and processing of human semen. Fifth edititon. Geneva 27, Switzerland.
- ZHU, J.-Z., DONG, X.-Y., LIANG, J.-J., ZHANG, Z.-Q., HU, X.-Y. & LI, L.-K. 2017. Effects of diabetes mellitus on semen quality in adult men: a systematic review and meta-analysis. *Int J Clin Exp Med*, 10, 11290-303.

RESEARCH PAPER

Impact of vitamin D3 Nanoemulsion on spermatogenesis and antioxidant enzymes in Vitamin D deficient induced albino male rats.

Diyar Hamid Karim¹, Sulaf Mustafa Mohammed¹, Hoshyar Abdullah Azeez²

¹ Department of Biology, college of Science, University of Sulaimani, As-Sulaymaniyah, Kurdistan Region, Iraq.

² College of pharmacy, University of Sulaimani, As-Sulaymaniyah, Kurdistan Region, Iraq.

ABSTRACT:

Vitamin D deficiency is common with several effects that include nonskeletal impacts. Many studies showed associations between Vitamin D deficiency and oxidative statuses with disturbed testicles in male rats (*Rattus norvegicus*) which might be improved by vitamin D. The aim of this work is to find the effects of nanoemulsion pea protein isolates and novel vitamin D carrier, developed by sonication and pH shifting of pea protein isolate nanoemulsion on the spermatogenesis in induced vitamin D deficient male rats. Thirty male albino rats distributed into 5 groups, sufficient control was fed with normal diet, deficient control was treated with 100 mg/kg Rimfapicin and 50 mg/kg Isoniazid for three weeks, pea protein isolate group: vitamin D deficient rats treated daily with 60 mg/ml/kg nanoemulsion pea protean isolate, Vitamin D deficient rats were treated with vitamin D (54 mcg/ml/ kg), and pea protean isolate + vitamin D group: Vitamin D deficient rats were treated by nanoemulsion pea protein isolate (60 mg/dl/kg) plus Vitamin D (54 mcg/ml/ kg) for four weeks. The serum used for Vitamin D and total testosterone assay, after estimation of sperm count and morphology. Homogenized testes used for determination of Catalase and Glutathione peroxidase. The results revealed that vitamin D and supplementations each one alone have a positive significant effects on spermatogenesis. The nanoemulsion pea protein isolate +vitamin D resulted in a significant increase in the levels of vitamin D of total testosterone more than the supplementation of vitamin D and nanoemulsion pea protein isolate alone. Also sperm count, normal sperm morphology, as well as catalase and Glutathione peroxidase improved significantly in this group. In conclusion we demonstrated vitamin D nanoemulsion as more efficient formulation with more prominent effects on spermatogenesis in induced vitamin D deficient rats.

KEY WORDS: Vitamin D, Testosterone, Nanoemulsion, Catalase, Glutathione Peroxidase, Sperm morphology, Sperm count.
DOI: <http://dx.doi.org/10.21271/ZJPAS.33.1.7>
ZJPAS (2021), 33(1);55-67 .

1. INTRODUCTION:

The function of Vitamin D is not restricted in calcium metabolism homeostasis in skeletal and muscular system but vitamin D have many important roles in non-skeletomuscular system for example fertility (Spiro & Buttriss, 2014), (Farhangi et al., 2017), (Caprio et al., 2017). Many research findings have detected that vitamin D have beneficial effects on extraskeletal tissues as well (Forrest & Stuhldreher, 2011).

most common function of vitamin D proceeds many systems and organs which are include sexual reproductions, cardiovascular system, respiratory system, some immunological reactions, common health, as well as regulation of gene expression. (Jameson, 2018), (Prusik et al., 2018), (Pludowski et al., 2018), and (Karefylakis et al., 2018). Vitamin D receptors locate inside of nucleus, mostly abundant in more than 38 types of tissue, There are more than 200 genes have been found that vitamin D could affect them (Haussler et al., 2011) and (Sung et al., 2012). Leydig cells and Sertoli cells are two main endocrine cells in

* Corresponding Author:

Diyar Hamid Karim
E-mail: diyari_hami@gmail.com

Article History:

Received: 16/08/2020

Accepted: 13/09/2020

Published : 20/02/2021

testes that secrete and produce many sex hormones (O'Donnell et al., 2017). Many hormones and vitamin directly or indirectly interacts the normal function of testes (Mortimer et al., 2013). vitamin D receptor and vitamin D metabolizing enzymes have been existed in the testes this is the main evidence of effectiveness of vitamin D in male fertility (Jensen, 2014). Vitamin D deficiency implicates in various physiological abnormalities such as: asthma, impaired pregnancy consequence, osteoporosis, diabetes mellitus type two, cancer and cardiovascular disorder. In addition, vitamin deficiency could affect male reproductive system in many ways such as: deterioration growth of seminiferous tubules and decreased testicular weight, drops sperm count in caudal epididymis, damage testicular role, and disrupt Sertoli and Leydig cells. (Chen & Zhi, 2020) and (Sharma & Sharma, 1997). The reason behind the idea that vitamin D is close relationship with male fertility return to most reproductive parts of male and spermatozoa contain vitamin D receptor as well as vitamin metabolite enzymes. (Martin Blomberg Jensen et al., 2010). Moreover, some data showed that spermatogenesis is positively affected by Vit.D deficiency (Zanatta et al., 2011) and (O'sullivan et al., 2016)

Nanoemulsion acts as active system to carry of hydrophobic drug that have low solubility and poor absorption by gastrointestinal tract and keep them from low pH which increase cellular uptake. (Liu et al., 2019). Nanoemulsions can increase cellular absorption of the encapsulated drugs the reason behind this is micro sized and high stabilized. (He et al., 2011). In the last few years, because of less allergy, and good food make pea protein as a novel food ingredient has increasing attraction among researcher. Pea protein isolate has been modified and ameliorated in structure, physical and chemical characteristics by the combination of pH-shifting and ultrasonication. (Almajwal et al., 2019). In the last few years, authors expansively investigated that lipid and polymers act as a chemical carrier and deliver system for Vit.D (Park et al., 2017) (Hasanvand et al., 2018). Here are many problems related with these delivery systems for example short half-life, oxidation exposure, perhaps it will hydrolysis, allergy and others. (Sharma & Sharma, 1997) (Almajwal et al., 2019) improved serum Vit.D in vitamin D deficient rats by pea protein

isolate based vitamin D nanoemulsion. The aim of this study to know the effectiveness of nanoemulsion for bioavailability of Vit.D and increase oxidative enzymes activity in tests of male rats.

2. MATERIALS AND METHODS

2.1. Experimental Conditions

All Thirty male albino rats their weight were (300-350 g). The animals were kept in stainless steel cages with constant humidity, in a silent animal house with 12-h light /12-dark cycles; range of temperature was 22 ± 4 °C The rats obtain a typical diet with tap water ad libitum during all experimental time, before the start of the experiment; rats were permitted to acclimate one week to their situation. The animals were kept in animal house, after one week divided rats to five groups each group with 6 rats. During three days for each week, we monitored the rats both food stuff and their weight.

2.2. Preparation of pea protein isolates

The protein content of pea is 18-30%, which include albumins, globulins and prolamins, and rich in profile amino acids. (Shand et al., 2007). Ultrasound is a kind of mechanical wave that is used for formation of nanoemulsion (Kentish & Feng, 2014). Nanoemulsions are submicron sized colloidal particulate system (5-200 nm), thermodynamically unchangeable, transparent, and isotropic system, by mean an emulsifying factor both non-miscible fluids are integrated to form one phase. Biologically active substances such as drugs are carried and delivered by nanoemulsions and enhance the therapeutic efficacy of the drug. (Çımar, 2017), (Solans & Solé, 2012). (Jaiswal et al., 2015).

Pea protein isolate has been prepared according to (Boye et al., 2010), (Liang & Tang, 2013) and (Stone et al., 2015) methods, based on alkaline extraction and precipitation of acid procedure.

Pea protein isolate has been prepared according to (Boye et al., 2010), (Liang & Tang, 2013) and (Stone et al., 2015) methods, based on alkaline extraction and precipitation of acid procedure.

2.3. Preparation of pea protein isolates

The protein content of pea is 18-30%, which include albumins, globulins and prolamins, and rich in profile amino acids. (Shand et al., 2007). Ultrasound is a kind of mechanical wave that is used for formation of nanoemulsion (Kentish & Feng, 2014). Nanoemulsions are submicron sized colloidal particulate system (5-200 nm), thermodynamically unchangeable, transparent, and isotropic system, by mean an emulsifying factor both non-miscible fluids are integrated to form one phase. Biologically active substances such as drugs are carried and delivered by nanoemulsions and enhance the therapeutic efficacy of the drug. (Çimar, 2017), (Solans & Solé, 2012) (Jaiswal et al., 2015).

Pea protein isolate has been prepared according to (Boye et al., 2010), (Liang & Tang, 2013) and (Stone et al., 2015) methods, based on alkaline extraction and precipitation of acid procedure.

2.4. Preparation of nanoemulsion of pea protein isolate:

Ultrasound application was utilized using a Qsonica Q700 Sonicator processor at frequency 20 kHz (QSONICA,LLC 53 CHURCH RD.NEWTOWN,CT, USA). The sample has been exposed to acoustic energy, the acoustic power density (APD) was adjusted at 68 W/100 mL by using an ultrasonic probe the diameter was (13 mm). Snow bath has been applied to prevent protein denaturation by high temperature.

Three gram of pea protein isolate (PPI) was dissolved in (100 ml of deionized water) (30 mg/mL (w/v), pH 7.0. The dispersion was stirred at room temperature for 30 min then adjusted to pH 12.0 at 25 °C. Immediately, the protein dispersion was exposed to 5 min ultrasonication, followed by adjusting pH back to 7.0 for the treated solution and put at 25°C about one hour, then centrifuged at 8610 rpm for 15 min at 15 °C and collected supernatant then kept at 4 °C in a refrigerator.(S. Jiang, 2015)

2.5. Induction of vitamin D deficiency:

Vitamin D deficiency was induced experimentally by gavage of rats about three weeks with **Rifampicin capsules** (RIF) (100

mg/kg b.w.) and **Isoniazid** (INH) (50 mg/kg b.w.) (Brodie et al., 1982)

2.6. Experimental design

The rats were divided into five experimental groups, six rats for each one as following. sufficient control rats this group received 2 ml of 0.1N of HCl plus regular diet; the remaining vitamin D deficient rats were subdivided in to four groups; deficient control without treatment ; group pea protein isolate they received regular diet with nanoemulsion pea protein isolate (60 mg/ml/kg b.w. orally); group vitamin D they received regular diet with vitamin D was dissolved in olive oil (2160 IU/ml/ kg b.w. orally); group pea protein isolate +vitamin D they received regular diet plus vitamin D dissolved in olive oil (2160 IU/ml/ kg b.w. orally) with nanoemulsion pea protein isolation (60 mg/ml/kg b.w. orally). About four weeks for each group. Entire processes were done by involving sterilized laboratory condition.

2.7. Blood sample collection and biochemical analysis

All the rats has been fasted during the night at the end of four weeks, the experiment duration and anesthetized by using ketamine 10% (50 mg/kg/b.w) and xylazine 2% (10 mg/kg/b.w) via intraperitoneal. Blood samples were collected by heart puncture vacutainer tubes with silica clot activator. The samples were centrifuged at 4000 rpm for 10 min at 4 °C. The separated serum samples were frozen and kept at -80 °C until later analysis.

2.8. Testicular homogenization:

The testes have been removed surgically and washed by 1.15% KCL and homogenized in 0.01 M potassium buffer (pH 7.4), followed by centrifugation 13000x g for 10 min at -4 °C then supernatant of homogenized testes was collected and stored in refrigerator at -4 °C. Olayinka, E. T., & Ore, A. (2015)

2.9. Sperm count

200 mg of caudal epididymis mixed with NaCl till (2ml) in a Perti dish (30 mm). The

Macerated caudal epididymis has been divided by scissor into four parts then left the tissue for 30-60 seconds to let sperms leak from the tubules (the solution was tint whitish/grayish, similar to the diluted semen), and the resulted fluid will be handled exactly as the semen. Collected the fluid into an Eppendorf tube (1.5ml) for microscopical examination of sperm morphology and sperm cell count. The number of sperms was determined with an improved Neubauer hemocytometer with a cover glass. The measured sperm number was multiplied by the dilution factor to yield the total sperm count. The tissue suspension is diluted 10 times, and then it was further diluted in a NaCl + formalin (20 microL semen + 180 microL NaCl + formalin) to kill the sperms. So consider that two dilution factors ($\times 10^6$) in final calculation using the hemocytometer chamber, all steps have been done on hot stage at 37°C.

2.10. Sperm morphology:

Karanawska (1976) method has been used with few modifications to prepare sperms from epididymis and Vas deferens. The epididymis and Vas deferens were put in small Petri-dish containing 0.9% normal saline. The two organs have been placed on the glass and by press small needle slightly over them; the sperm has been extracted, then together with a drop of the normal saline has been smeared on the slide. The slide has been stained with 1% Eosin for 10 min, next it has been washed with tap water, later stained with Hematoxylin for 15 min, then it has been washed by tap water (Fattah & Mustafa, 2012). Smears were examined under an oil-immersion objective at $\times 100$. Four hundred sperm cells were examined per animal to determine the morphological abnormalities. Any disorders in the morphology and structure of either head or tail or both were considered as abnormal. Number of abnormal sperm divided to total sperm was defined as percentage of abnormal sperm (Mohammed, 2015). The presence of sperm without head, sperm without tail, abnormal neck, abnormal hook and abnormal head was assessed. We examined five different fields for each sample.

2.11. Statistical analysis

All results were expressed as mean \pm SEM using Graph Pad Prism software (version 2019) and then analyzed by one-way ANOVA and then

by Tukey's test. $P < 0.05$ was considered as statistically significance level.

3. RESULTS AND DISCUSSION

3.1. Serum Vitamin D3

Isoniazid and Rifampicin induced vitamin D deficient rats showed significant reduced of serum vitamin D (11.3 ± 0.7162 ng/ml) ($P < 0.05$) when compared with sufficient rats (17.5 ± 0.7662 ng/ml). Similar results were obtained by previous experimental vitamin D deficient study (Brodie et al., 1982), which revealed that oral supplementation of anti-TB drugs, such as isoniazid and rifampicin; decrease the level of serum Vit.D via various kinds of mechanisms. However, serum Vit.D level in sufficient control rats (17.5 ± 0.7662 ng/ml) and deficient control (11.3 ng/ml) showed significantly ($P < 0.05$) differences in comparison to Vit.D deficient treated with Vit.D and nanoemulsion PPI+ Vit.D (24.14 ± 0.9869 , 29.84 ± 2.045 ng/ml) respectively. Similar results were obtained by (Kadappan et al., 2018). Also (Grossmann & Tangpricha, 2010) showed that the nanoemulsion significantly increased the serum 25(OH)D3 by 73% when compared to the vehicle nanoemulsion without Vit.D. (S. Jiang et al., 2019) showed in their review Vit.D in an oil vehicle produced a greater 25(OH)D response than Vit.D in a powder or an ethanol vehicle in healthy subjects. Increased restoration of Vit.D3 in micelles via in vitro digestion significantly was displayed by modified PPI-prepared nanoemulsions. So they could use nanoemulsion PPI as good choice for sending and keeping medical substances. **Figure 1 and Table 1**

3.2. Serum total testosterone

Serum total testosterone level showed significantly ($P < 0.05$) reduction in Vit.D deficient rats (2.080 ± 0.1934 ng/ml) when compared with sufficient rat group (3.520 ± 0.2267 ng/ml). Similar result was supported by both (N.W. et al., 2017)(Guttoff et al., 2015) (Fu et al., 2017) separately they revealed that the level of testosterone decreased significantly in Vit.D deficient animals comparing to normal laboratory animals. The reason could be due to the expression of Vitamin D receptor in many reproductive organs. (Martin Blomberg Jensen et

al., 2010) found Vit.D receptor in testis, epididymis, and they suggested that the activity and survival of mature sperm depend on Vit.D, and (Elisabeth Lerchbaum & Obermayer-Pietsch, 2012), these led researchers to point of view of positive effects of Vit.D on spermatogenesis. Vit.D receptor is also exists on sperm head. However, it is lack in the midpiece and flagellum of human sperm that may be evidence about the effect of Vit.D on sperm quality (Aquila et al., 2009). In an observational study, (Menegaz et al., 2009) showed that patients suffered from azoospermic have lower serum Vit.D compared to those have normal sperm count. However, total testosterone level in serum in both Vit.D deficient rats treated with Vit.D (4.940 ± 0.3124 ng/mL) and nanoemulsion PPI+ Vit.D (6.470 ± 0.2278 ng/mL) was significantly ($P < 0.05$) increased rats in comparison with Vit.D deficient (2.080 ± 0.1934 ng/mL) and sufficient control (3.520 ± 0.2267 ng/mL). Similar results were obtained by previous experimental Vit.D deficient study. (N.W. et al., 2017). Vit.D may also affect spermatogenesis before sperm release (Kinuta et al., 2000). As well as the (Pilz et al., 2011) showed that Vit.D supplementation might increase testosterone levels. However, others could not establish this association between Vit.D and serum testosterone. (Yang et al., 2012) and (E Lerchbaum et al., 2014). **Figure and 2 and Table 1.**

3.3. Sperm count and sperm morphology

Vit.D deficient rats showed significant ($P < 0.05$) dropped in the percentage sperm count ($9.648 \pm 2.055 \times 10^6$ /ml), highly significant in the normal sperm morphology ($P < 0.05$) (29.38 ± 9.085 %) when compared to sufficient control rat group. Similar results were obtained by previous study (Kwiecinski et al., 1989), (Uhland et al., 1992) (Sood et al., 1995), and (Fu et al., 2017). Furthermore (Tartagni et al., 2015). And (Zhu et al., 2016) observed that Vit.D deficient rats suffered from default of spermatogenesis due to trouble in role of Leydig and Sertoli cell the current results are closely in accordance with two previous works. (Johnson et al., 1996) and (Merke et al., 1985) revealed that Vit.D have role spermatogenesis and mature sperm due existence of Vit.D receptor in epididymis, Seroli cell and

spermatogonia of male rodents.

Table (1) Effect of nanoemulsion PPI, vitamin-D3, nanoemulsion PPI plus and Vit.D3 in vitamin deficient rats on sex hormones (Vit.D and total testosterone) concentrations in Vit.D deficient male rats.

Groups	Parameters (ng/ml)	
	Serum Vit. D	Serum total Testosterones
SC	17.5 ± 0.7662^a	3.520 ± 0.2267^a
DC	11.3 ± 0.7162^b	2.080 ± 0.1934^b
PPI	15.04 ± 0.7692^{ab}	2.520 ± 0.4128^{ab}
VD	24.14 ± 0.9869^c	4.940 ± 0.3124^c
PPID	29.84 ± 2.045^d	6.470 ± 0.2278^d

Values expressed as mean \pm S.E. The different letters mean significant differences * $= p < 0.05$.

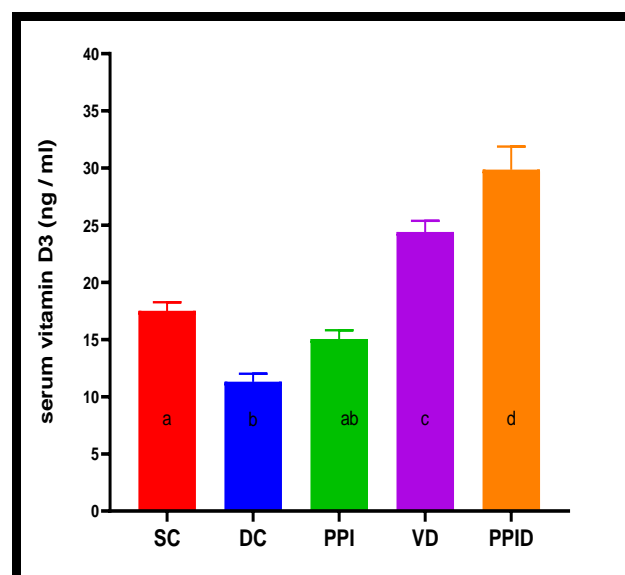


Figure (1) Effect of nanoemulsion PPI, Vit.D and Vit.D nanoemulsion on serum Vit.D (mean \pm S.E) ng/ml in Vit.D deficient male rats.

The different letters mean significant differences * $= p < 0.05$.

Furthermore, some medical research showed the relationship between Vit.D and sperm (Zhu et al., 2016) (Hammoud et al., 2012), (Martin Blomberg Jensen et al., 2011), (Ramlau-Hansen et al., 2011), (Dong et al., 2016), (Mahmoudi et al., 2013) (Schachter et al., 1973) and (Macchia et al., 2010)

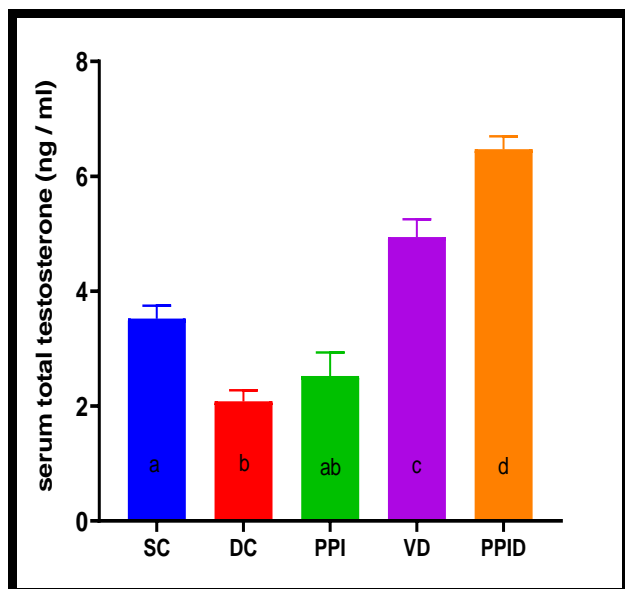


Figure (2) Effect of nanoemulsion PPI and Vit.D and Vit.D nanoemulsion on serum total testosterone (mean \pm S.E) ng/ml in Vit.D deficient male rats.

The different letters mean significant differences * $=p < 0.05$.

Eventually, (Martin Blomberg Jensen et al., 2011) and in (Yang et al., 2012), they demonstrated separately that Vit.D was an independent factor for sperm activity and normal feature of sperm in 300 and 559 fertile and infertile men respectively. In contrast, in this consideration, paradoxical results are exist.(Yang et al., 2012) and (M. Blomberg Jensen et al., 2012).

The treatment of Vit.D deficient rats with: Vit.D and nanoemulsion PPI + Vit.D showed significant ($P < 0.05$) increased in the percentage of sperm count ($38.70 \pm 5.490 \times 10^6/\text{ml}$) ($49.21 \pm 4.150 \times 10^6/\text{ml}$), normal sperm morphology ($92.95 \pm 1.598 \%$) ($92.95 \pm 1.598 \%$) in comparison with Vit.D deficient rats and ($9.648 \pm 2.055 \times 10^6/\text{ml}$), ($29.38 \pm 9.085 \%$). Similar result in different studies showed the same results like study of (Fu et al., 2017) who showed that the sperm count in the cauda epididymidis was significantly diminished in Vit.D deficient mice (from 24.75 million to 19.21 million).(Sood et al., 1995) showed that number of sperm was elevated significantly from 49.20 to 82.30 millions) in Vit.D deficient rats by injection of Vit.D. Sperm count and morphology in turn ability of fertilization have been rose by improving and adding amino acids to diets (Dong et al., 2016). (Mahmoudi et al., 2013) suggested that Vit.D has great role for spermatogenesis and

sperm development. Vit.D signaling has a positive increase on amount of semen(Jensen, 2014). Interestingly, the treatment of Vit.D deficient rats with nanoemulsion PPI showed significant ($P < 0.05$) elevation in the percentage of sperm count and normal sperm morphology ($49.21 \pm 4.150 \times 10^6/\text{ml}$) ($94.86 \pm 0.9863 \%$) respectively in comparison with Vit.D deficient rats and ($9.648 \pm 2.055 \times 10^6/\text{ml}$) (29.38%). The mechanism of the role of PPI on spermatogenesis, production normal sperm morphology and sex hormones is still not clear. However, PPI contains many types of amino acids (Overduin et al., 2015), some of these amino acids have positive effect on spermatogenesis. One of these amino acids is arginine. (Schachter et al., 1973) showed administration of Arginine to patients who suffered from deficiency of sperm in semen and low count with poor motility have been treated.

(Macchia et al., 2010) suggested that DL-aspartic acid integrates sperm production and development they showed that supplementation of DL-aspartic acid in bucks number of epididymis sperm have been increased. D-aspartic acid stimulates Leydig cell for making steroid hormone binding protein, in turn D-aspartic acid induces sperm motion (Sharpe et al., 1992). In addition the D-aspartic acid trigger cells of hypothalamus and pituitary gland to secret gonadotropic and FSH and LH hormones (Wang et al., 2002). A study revealed that testicle testosterone in rat has been increased by different concentration of d-aspartic acid (D'Aniello et al., 1996). D-aspartic acid is one of the most important components of pea protein (Overduin et al., 2015). Dietary that rich with high amount lysine contents increase live sperm concentration from 77.1 to 78.2% and methionine elevated the motility (72.7 vs 71.2%) in the second ejaculate of male rabbits(Nizza et al., 2000), (Luzi et al., 1996) showed no significant change in amount and concentration of semen from rabbits 19.7% and 14.5% crude protein.

It is difficult to comment on these results without further research on the effect of dilatory protein and amino acid. The protein level seems to have little effect on sperm quality. **Table 2, figure 3 and 4**

3.4. Catalase and GSH-PX activity:

The activities of Catalase and GSH-PX in homogenized testes of Vit.D deficient rats (14.96 ± 0.6849) (520.6 ± 46.96) were not significantly

($P < 0.05$) changed when compared to sufficient control rats (20.00 ± 1.751) (747.1 ± 97.90) respectively.

Table (2) Effect of nanoemulsion PPI, vitamin-D3, nanoemulsion and PPI plus Vit.D in vitamin deficient rats on sperm count and normal sperm morphology.

Groups	Parameters	
	Sperm count $\times 10^6$	Normal sperm morphology * %
SC	34.43 ± 5.428^b	82.92 ± 2.939^b
DC	9.648 ± 2.055^a	29.38 ± 9.085^a
PPI	49.21 ± 4.150^b	94.86 ± 0.9863^b
VD	38.70 ± 5.490^b	92.95 ± 1.598^b
PPID	49.29 ± 3.377^b	92.95 ± 1.598^b

Values expressed as mean \pm S.E. The different letters mean significant differences * = $p < 0.05$.

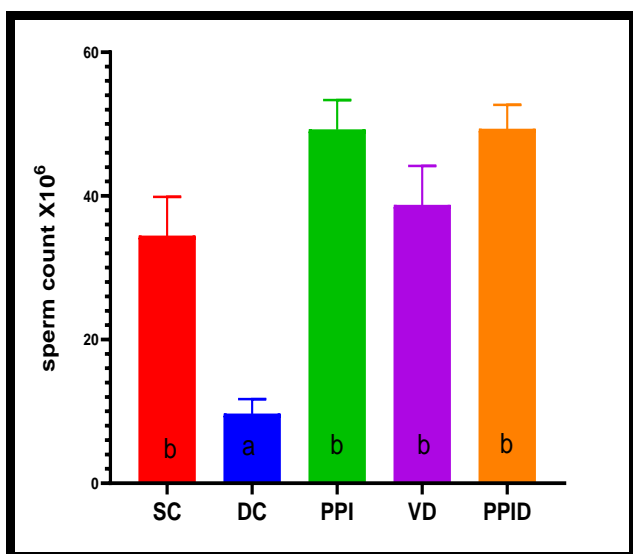


Figure (3) Effect of nanoemulsion PPI, Vit.D and Vit.D nanoemulsion on sperm count (mean \pm S.E) $\times 10^6$ in Vit.D deficient male rats.

The different letters mean significant differences * = $p < 0.05$.

Moreover, catalase and GSH-PX activities in homogenized testes of Vit.D deficient rats treated with nanoemulsion PPI (22.62 ± 1.271) (1053 ± 209.2), showed significantly ($P < 0.05$) increased in comparison to Vit.D deficient rats (14.96 ± 0.6849) (520.6 ± 46.96) respectively. Interestingly, there are similar significant differences in GSH-PX and catalase activities in

homogenized testes of Vit.D deficient rats treated with Vit. D

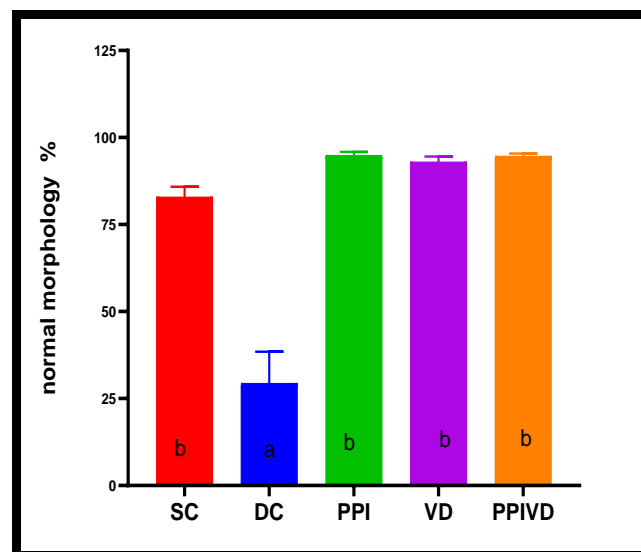


Figure (4) Effect of nanoemulsion PPI, Vit.D and Vit.D nanoemulsion on normal sperm morphology (mean \pm S.E) % in Vit.D deficient male rats.

The different letters mean significant differences * = $p < 0.05$.

Nanoemulsion PPI+ Vit.D (23.58 ± 2.488) (1023 ± 61.34), they are significantly ($P < 0.05$) increased in comparison to those of Vit.D deficient rats (14.96 ± 0.6849) (520.6 ± 46.96) respectively. However, catalase and GSH-PX activities in homogenized testes of sufficient control (20.00 ± 1.751) (747.1 ± 97.90) rats showed no significant ($P < 0.05$) changes in comparison to all treated groups in Vit.D deficient rats.

Many studies showed that Nanoemulsion PPI is a good diet and has high efficiency against oxidative stress. Hydrophobic and aromatic amino acids are high abundant in pea protein isolate and have antioxidant activity. furthermore PPI and look like to the modified PPI that have radical scavenging activities (Pownall et al., 2010), (S. Jiang et al., 2019), (J. Jiang et al., 2014), and (Dahl et al., 2012).

Arginine is one of the main amino acid that exists in PPI, which comprise about (4.3%) (Overduin et al., 2015). Many studies reported clearly that arginine has antioxidant activity due to a chemical moiety different from that serving as the substrate for NO biosynthesis, may lower the

amount of free oxygen radicals and reduce superoxide anion as well as drooping intensity of radical reactions or of antioxidative–enzyme. Thus affect the lowering of oxidative stress (Wallner et al., 2001), (Hosseini et al., 2012),(Lucotti et al., 2009) and(Korish, 2010). Lysine may have ability to keep cell membrane and proteins thus Lysine has efficient in stress state. Lysine suggested that an important role in antioxidant (Seminotti et al., 2008). Even though the PPI contain little amount of tryptophan (1.0%) (Overduin et al., 2015). Tryptophan has been reported to play an important role in the DPPH radical scavenging activity of purified patatin, perhaps as a hydrogen donor (Pownall et al., 2010).

Pea protein is rich in sulfhydryl amino acid cysteine; cysteine an effective cellular antioxidant, thus extracellular cysteine is the primary source of intracellular cysteine, which is necessary for GSH synthesis. (BELL, 2000) , (Atmaca, 2004), (Han et al., 1997).(Korhonen & Pihlanto, 2005) showed that protein hydrolysates possess antioxidant activity. The current results supported by the fact that PPI have antioxidant activity because it contains many other amino acids such as histidine, cysteine, tyrosine, phenylalanine and tryptophan, that make PPI have great antioxidant capacity (Pownall et al., 2011), (Peña-Ramos et al., 2004) and (Erdmann et al., 2008). **Table 3, figure 5 and 6.**

Table (3) Effect of nanoemulsion PPI, vitamin-D3, nanoemulsion and PPI plus Vit.D in vitamin deficient rats on the antioxidant parameters (CAT and GSH-PX activities)

Groups	(U/mgprot)*	
	CAT activity	CAT activity
SC	20.00 ± 1.751 ^{ab}	747.1± 97.90 ^{ab}
DC	14.96 ± 0.6849 ^a	520.6± 46.96 ^a
PPI	22.62 ± 1.271 ^b	1053± 209.2 ^b
VD	14.69 ±1.165 ^a	509.0 ± 41.21 ^a
PPID	23.58 ± 2.488 ^b	1023 ± 61.34 ^b

Values expressed as mean ± S.E. The differences letters mean significant differences * =p<0.05.

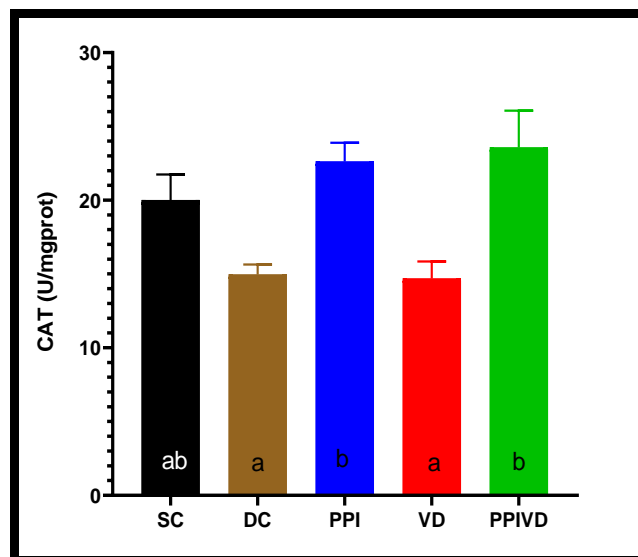


Figure (5) Effect of nanoemulsion PPI, Vit.D and Vit.D nanoemulsion on CAT activity (mean ± S.E) U/mg protein in Vit.D deficient male rats.

The different letters mean significant differences * =p<0.05.

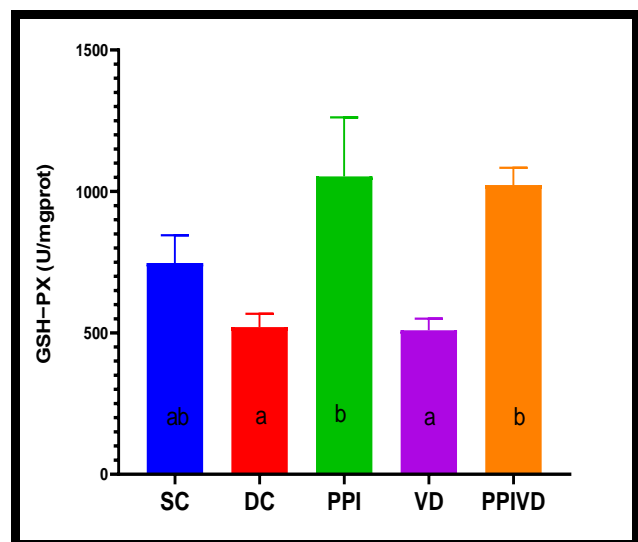


Figure (6) Effect of nanoemulsion PPI, Vit.D and Vit.D nanoemulsion on GSH–PX activity (mean ± S.E) U/mg protein in Vit.D deficient male rats.

The different letters mean significant differences * =p<0.05.

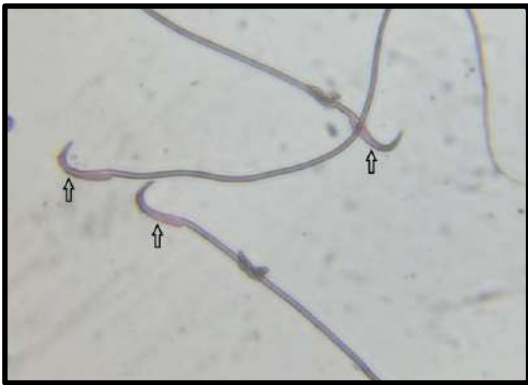


Figure 7: normal sperm morphology.



Figure 8: sperm abnormal head.



Figure 9: sperm without tail.



Figure 10: sperm without head.

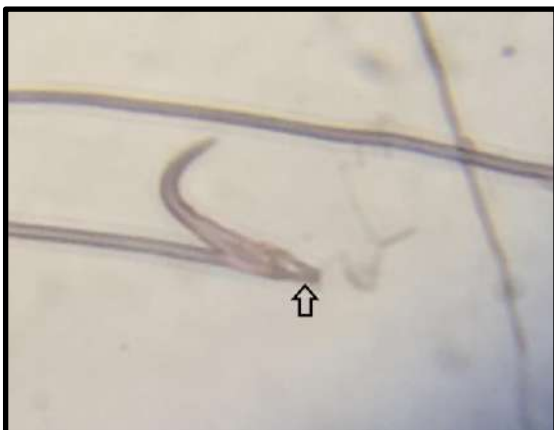


Figure 11: sperm with abnormal neck.

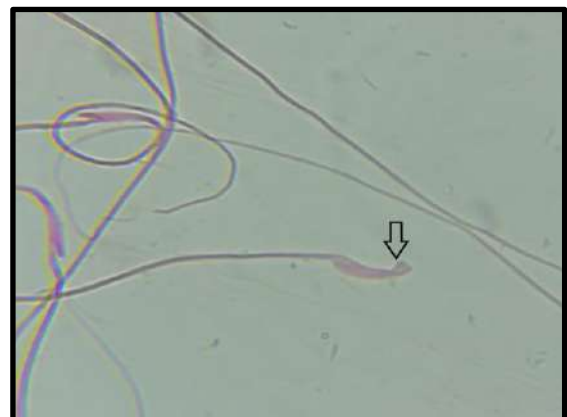


Figure 12: sperm with abnormal hook

4. CONCLUSIONS

The results of this study demonstrate that the supplementation of Vit.D deficient rats with Vit.D and nanoemulsion PPI may improve semen analysis, total testosterone and scavenger activity of testes. These findings show that Vit.D nanoemulsion supplementation resulted in a significant increase in the levels of sperm count, normal sperm morphology, as well as catalase and GSH-PX. The result showed that Vit.D nanoemulsion supplementation resulted in a significant increase in the levels of Total testosterone, sperm count, normal sperm morphology, as well as catalase and GSH-PX. Vitamin D nanoemulsion has a powerful effect on spermatogenesis in induced Vit.D deficient rats.

Reference:

- Almajwal, A. M., Abulmeaty, M. M. A., Feng, H., Alruwaili, N. W., Dominguez-Uscanga, A., Andrade, J. E., Razak, S., & Elsadek, M. F. (2019). Stabilization of vitamin D in pea protein isolate nanoemulsions increases its bioefficacy in rats. *Nutrients*, *11*(1). <https://doi.org/10.3390/nu11010075>
- Aquila, S., Guido, C., Middea, E., Perrotta, I., Bruno, R., Pellegrino, M., & Andò, S. (2009). Human male gamete endocrinology: 1 α , 25-dihydroxyvitamin D₃ (1, 25 (OH) 2D₃) regulates different aspects of human sperm biology and metabolism. *Reproductive Biology and Endocrinology*, *7*(1), 140.
- Atmaca, G. (2004). Antioxidant effects of sulfur-containing amino acids. In *Yonsei Medical Journal* (Vol. 45, Issue 5, pp. 776–788). <https://doi.org/10.3349/ymj.2004.45.5.776>
- BELL, S. J. (2000). Whey protein concentrates with and without immunoglobulins: a review. *Journal of Medicinal Food*, *3*(1), 1–13.
- Blomberg Jensen, M., Jørgensen, A., Nielsen, J. E., Bjerrum, P. J., Skalkam, M., Petersen, J. H., Egeberg, D. L., Bangsbøll, S., Andersen, A. N., Skakkebaek, N. E., Juul, A., Rajpert-De Meyts, E., Dissing, S., Leffers, H., & Jørgensen, N. (2012). Expression of the vitamin D metabolizing enzyme CYP24A1 at the annulus of human spermatozoa may serve as a novel marker of semen quality. *International Journal of Andrology*, *35*(4), 499–510. <https://doi.org/10.1111/j.1365-2605.2012.01256.x>
- Blomberg Jensen, Martin, Bjerrum, P. J., Jessen, T. E., Nielsen, J. E., Joensen, U. N., Olesen, I. A., Petersen, J. H., Juul, A., Dissing, S., & Jørgensen, N. (2011). Vitamin D is positively associated with sperm motility and increases intracellular calcium in human spermatozoa. *Human Reproduction*, *26*(6), 1307–1317. <https://doi.org/10.1093/humrep/der059>
- Blomberg Jensen, Martin, Nielsen, J. E., Jørgensen, A., Rajpert-De Meyts, E., Kristensen, D. M., Jørgensen, N., Skakkebaek, N. E., Juul, A., & Leffers, H. (2010). Vitamin D receptor and vitamin D metabolizing enzymes are expressed in the human male reproductive tract. *Human Reproduction*, *25*(5), 1303–1311. <https://doi.org/10.1093/humrep/deq024>
- Boye, J. I., Aksay, S., Roufik, S., Ribéreau, S., Mondor, M., Farnworth, E., & Rajamohamed, S. H. (2010). Comparison of the functional properties of pea, chickpea and lentil protein concentrates processed using ultrafiltration and isoelectric precipitation techniques. *Food Research International*, *43*(2), 537–546. <https://doi.org/10.1016/j.foodres.2009.07.021>
- Brodie, M. J., Boobis, A. R., Hillyard, C. J., Abeyasekera, G., Stevenson, J. C., MacIntyre, I., & Park, B. K. (1982). Effect of rifampicin and isoniazid on vitamin D metabolism. *Clinical Pharmacology and Therapeutics*, *32*(4), 525–530. <https://doi.org/10.1038/clpt.1982.197>
- Caprio, M., Infante, M., Calanchini, M., Mammi, C., & Fabbri, A. (2017). Vitamin D: not just the bone. Evidence for beneficial pleiotropic extraskeletal effects. *Eating and Weight Disorders-Studies on Anorexia, Bulimia and Obesity*, *22*(1), 27–41.
- Chen, Y., & Zhi, X. (2020). Roles of Vitamin D in Reproductive Systems and Assisted Reproductive Technology. *Endocrinology*, *161*(4). <https://doi.org/10.1210/endo/bqaa023>
- Çınar, K. (2017). A review on nanoemulsion: Preparation methods and stability. *Trakya Üniversitesi Mühendislik Bilimleri Dergisi*, *18*(1), 73–83.
- D’Aniello, A., Di Cosmo, A., Di Cristo, C., Annunziato, L., Petrucelli, L., & Fisher, G. (1996). Involvement of D-aspartic acid in the synthesis of testosterone in rat testes. *Life Sciences*, *59*(2), 97–104.
- Dahl, W. J., Foster, L. M., & Tyler, R. T. (2012). Review of the health benefits of peas (*Pisum sativum* L.). *British Journal of Nutrition*, *108*(SUPPL. 1). <https://doi.org/10.1017/S0007114512000852>
- de Angelis, C., Galdiero, M., Pivonello, C., Garifalos, F., Menafrà, D., Cariati, F., Salzano, C., Galdiero, G., Piscopo, M., Vece, A., Colao, A., & Pivonello, R. (2017). The role of vitamin D in male fertility: A focus on the testis. *Reviews in Endocrine and Metabolic Disorders*, *18*(3), 285–305. <https://doi.org/10.1007/s11154-017-9425-0>
- Dong, H.-J., Wu, D., Xu, S.-Y., Li, Q., Fang, Z.-F., Che, L.-Q., Wu, C.-M., Xu, X.-Y., & Lin, Y. (2016). Effect of dietary supplementation with amino acids on boar sperm quality and fertility. *Animal Reproduction Science*, *172*, 182–189.
- Erdmann, K., Cheung, B. W. Y., & Schröder, H. (2008). The possible roles of food-derived bioactive peptides in reducing the risk of cardiovascular disease. *Journal of Nutritional Biochemistry*, *19*(10), 643–654. <https://doi.org/10.1016/j.jnutbio.2007.11.010>
- Farhangi, M. A., Nameni, G., Hajiluan, G., & Mesgari-

- Abbasi, M. (2017). Cardiac tissue oxidative stress and inflammation after vitamin D administrations in high fat-diet induced obese rats. *BMC Cardiovascular Disorders*, 17(1), 1–7. <https://doi.org/10.1186/s12872-017-0597-z>
- Fattah, Y. M., & Mustafa, S. I. (2012). Effects of the pesticide cyren on chromosomes and sperms of albino males mice.
- Forrest, K. Y. Z., & Stuhldreher, W. L. (2011). Prevalence and correlates of vitamin D deficiency in US adults. *Nutrition Research*, 31(1), 48–54.
- Fu, L., Chen, Y. H., Xu, S., Ji, Y. L., Zhang, C., Wang, H., Yu, D. X., & Xu, D. X. (2017). Vitamin D deficiency impairs testicular development and spermatogenesis in mice. *Reproductive Toxicology*, 73, 241–249. <https://doi.org/10.1016/j.reprotox.2017.06.047>
- Grossmann, R. E., & Tangpricha, V. (2010). Evaluation of vehicle substances on vitamin D bioavailability: A systematic review. *Molecular Nutrition and Food Research*, 54(8), 1055–1061. <https://doi.org/10.1002/mnfr.200900578>
- Guttoff, M., Saberli, A. H., & McClements, D. J. (2015). Formation of vitamin D nanoemulsion-based delivery systems by spontaneous emulsification: Factors affecting particle size and stability. *Food Chemistry*, 171, 117–122. <https://doi.org/10.1016/j.foodchem.2014.08.087>
- Hammoud, A. O., Wayne Meikle, A., Matthew Peterson, C., Stanford, J., Gibson, M., & Carrell, D. T. (2012). Association of 25-hydroxy-vitamin D levels with semen and hormonal parameters. *Asian Journal of Andrology*, 14(6), 855–859. <https://doi.org/10.1038/aja.2012.77>
- Han, D., Sen, C. K., Roy, S., Kobayashi, M. S., Tritschler, H. J., & Packer, L. (1997). Protection against glutamate-induced cytotoxicity in C6 glial cells by thiol antioxidants. *American Journal of Physiology - Regulatory Integrative and Comparative Physiology*, 273(5 42-5), 1771–1778. <https://doi.org/10.1152/ajpregu.1997.273.5.r1771>
- Hasanvand, E., Fathi, M., & Bassiri, A. (2018). Production and characterization of vitamin D 3 loaded starch nanoparticles: effect of amylose to amylopectin ratio and sonication parameters. *Journal of Food Science and Technology*, 55(4), 1314–1324.
- Hausler, M. R., Jurutka, P. W., Mizwicki, M., & Norman, A. W. (2011). Vitamin D receptor (VDR)-mediated actions of 1 α ,25(OH) $_2$ vitamin D $_3$: Genomic and non-genomic mechanisms. *Best Practice and Research: Clinical Endocrinology and Metabolism*, 25(4), 543–559. <https://doi.org/10.1016/j.beem.2011.05.010>
- He, W., Tan, Y., Tian, Z., Chen, L., Hu, F., & Wu, W. (2011). Food protein-stabilized nanoemulsions as potential delivery systems for poorly water-soluble drugs: preparation, in vitro characterization, and pharmacokinetics in rats. *International Journal of Nanomedicine*, 6, 521.
- Hosseini, M., Pourganji, M., Khodabandehloo, F., Soukhtanloo, M., & Zabihi, H. (2012). Protective effect of l-arginine against oxidative damage as a possible mechanism of its Bene. cial properties on spatial learning in ovariectomized rats. *Basic and Clinical Neuroscience*, 3(5), 36–44.
- Jaiswal, M., Dudhe, R., & Sharma, P. K. (2015). Nanoemulsion: an advanced mode of drug delivery system. 3 *Biotech*, 5(2), 123–127. <https://doi.org/10.1007/s13205-014-0214-0>
- Jameson, J. L. (2018). *Harrison's principles of internal medicine*. McGraw-Hill Education,.
- Jensen, M. B. (2014). Vitamin D and male reproduction. *Nature Reviews Endocrinology*, 10(3), 175–186. <https://doi.org/10.1038/nrendo.2013.262>
- Jiang, J., Zhu, B., Liu, Y., & Xiong, Y. L. (2014). Interfacial structural role of pH-shifting processed pea protein in the oxidative stability of oil/water emulsions. *Journal of Agricultural and Food Chemistry*, 62(7), 1683–1691. <https://doi.org/10.1021/jf405190h>
- Jiang, S. (2015). *Enhanced physicochemical and functional properties of pea (Pisum sativum) protein by pH-shifting and ultrasonication combined process* [University of Illinois at Urbana-Champaign]. <http://hdl.handle.net/2142/88229>
- Jiang, S., Yildiz, G., Ding, J., Andrade, J., Rababah, T. M., Almajwal, A., Abulmeatyc, M. M., & Feng, H. (2019). Pea Protein Nanoemulsion and Nanocomplex as Carriers for Protection of Cholecalciferol (Vitamin D $_3$). *Food and Bioprocess Technology*, 12(6), 1031–1040. <https://doi.org/10.1007/s11947-019-02276-0>
- Johnson, J. A., Grande, J. P., Roche, P. C., & Kumar, R. (1996). Immunohistochemical detection and distribution of the 1,25-dihydroxyvitamin D $_3$ receptor in rat reproductive tissues. *Histochemistry and Cell Biology*, 105(1), 7–15. <https://doi.org/10.1007/BF01450873>
- Kadappan, A. S., Guo, C., Gumus, C. E., Bessey, A., Wood, R. J., McClements, D. J., & Liu, Z. (2018). The Efficacy of Nanoemulsion-Based Delivery to Improve Vitamin D Absorption: Comparison of In Vitro and In Vivo Studies. *Molecular Nutrition and Food Research*, 62(4), 1–24. <https://doi.org/10.1002/mnfr.201700836>
- Karefylakis, C., Särnblad, S., Ariander, A., Ehlersson, G., Rask, E., & Rask, P. (2018). Effect of Vitamin D supplementation on body composition and cardiorespiratory fitness in overweight men—A randomized controlled trial. *Endocrine*, 61(3), 388–397.
- Kentish, S., & Feng, H. (2014). Applications of power ultrasound in food processing. *Annual Review of Food Science and Technology*, 5(1), 263–284. <https://doi.org/10.1146/annurev-food-030212-182537>
- Kinuta, K., Tanaka, H., Moriwake, T., Aya, K., Kato, S., & Seino, Y. (2000). Vitamin D is an important factor in estrogen biosynthesis of both female and male gonads. *Endocrinology*, 141(4), 1317–1324. <https://doi.org/10.1210/endo.141.4.7403>
- Korhonen, H., & Pihlanto, A. (2005). Food-derived Bioactive Peptides - Opportunities for Designing Future Foods. *Current Pharmaceutical Design*, 9(16), 1297–1308.

- <https://doi.org/10.2174/1381612033454892>
- Korish, A. A. (2010). Multiple antioxidants and L-arginine modulate inflammation and dyslipidemia in chronic renal failure rats. *Renal Failure*, 32(2), 203–213.
- Kwieceński, G. G., Petrie, G. I., & DeLuca, H. F. (1989). Vitamin D is necessary for reproductive functions of the male rat. *The Journal of Nutrition*, 119(5), 741–744.
- Lerchbaum, E., Pilz, S., Trummer, C., Rabe, T., Schenk, M., Heijboer, A. C., & Obermayer-Pietsch, B. (2014). Serum vitamin D levels and hypogonadism in men. *Andrology*, 2(5), 748–754.
- Lerchbaum, Elisabeth, & Obermayer-Pietsch, B. (2012). Vitamin D and fertility: a systematic review. *Eur J Endocrinol*, 166(5), 765–778.
- Liang, H. N., & Tang, C. H. (2013). PH-dependent emulsifying properties of pea [*Pisum sativum* (L.)] proteins. *Food Hydrocolloids*, 33(2), 309–319. <https://doi.org/10.1016/j.foodhyd.2013.04.005>
- Liu, G., Zhou, Y., & Chen, L. (2019). Intestinal uptake of barley protein-based nanoparticles for β -carotene delivery. *Acta Pharmaceutica Sinica B*, 9(1), 87–96.
- Lucotti, P., Monti, L., Setola, E., La Canna, G., Castiglioni, A., Rossodivita, A., Pala, M. G., Formica, F., Paolini, G., & Catapano, A. L. (2009). Oral L-arginine supplementation improves endothelial function and ameliorates insulin sensitivity and inflammation in cardiopathic nondiabetic patients after an aortocoronary bypass. *Metabolism*, 58(9), 1270–1276.
- Luzi, F., Maertens, L., Mijten, P., & Pizzi, F. (1996). Effect of feeding level and dietary protein content on libido and semen characteristics of bucks. *Proc. 6. World Rabbit Congress, Toulouse, Proc. 2*, 87–92.
- Macchia, G., Topo, E., Mangano, N., D’Aniello, E., & Boni, R. (2010). dl-Aspartic acid administration improves semen quality in rabbit bucks. *Animal Reproduction Science*, 118(2–4), 337–343. <https://doi.org/10.1016/j.anireprosci.2009.07.009>
- Mahmoudi, A. R., Zarnani, A. H., Jeddi-Tehrani, M., Katouzian, L., Tavakoli, M., Soltanghoraei, H., & Mirzadegan, E. (2013). Distribution of vitamin D receptor and 1α -hydroxylase in male mouse reproductive tract. *Reproductive Sciences*, 20(4), 426–436.
- Menegaz, D., Rosso, A., Royer, C., Leite, L. D., Santos, A. R. S., & Silva, F. R. M. B. (2009). Role of $1\alpha,25(\text{OH})_2$ vitamin D₃ on α -[1-¹⁴C]MeAIB accumulation in immature rat testis. *Steroids*, 74(2), 264–269. <https://doi.org/10.1016/j.steroids.2008.11.015>
- Merke, J., Hügel, U., & Ritz, E. (1985). Nuclear testicular 1, 25-dihydroxyvitamin D₃ receptors in Sertoli cells and seminiferous tubules of adult rodents. *Biochemical and Biophysical Research Communications*, 127(1), 303–309.
- Mohammed, S. M. (2015). *Effect of Broccoli (Brassica oleracea) on Some Physiological Variables and Reproductive System on Lead Acetate Exposed Adult Male Albino (Rattus rattus)*. Tikrit University-Iraq.
- Mortimer, D., Barratt, C. L. R., Björndahl, L., De Jager, C., Jequier, A. M., & Muller, C. H. (2013). What should it take to describe a substance or product as ‘sperm-safe.’ *Human Reproduction Update*, 19(suppl_1), i1–i45.
- N.W., A., M.M.A., A., A.M., A., M.F., E., & S., R. (2017). Novel vitamin D-nanoemulsion improves testicular function of vitamin D deficient rats. In *FASEB Journal* (Vol. 31, Issue 1 Supplement 1). http://www.fasebj.org/content/31/1_Supplement/1b389.abstract?sid=53411162-021c-472f-9a4c-10f9113c3b2a%0Ahttp://ovidsp.ovid.com/ovidweb.cgi?T=JS&PAGE=reference&D=emed18&NEWS=N&AN=616959246
- Nizza, A., Di Meo, C., & Taranto, S. (2000). Effect of lysine and methionine on libido and semen characteristics of bucks. *World Rabbit Science*, 8(4), 181–184.
- O’Donnell, L., Stanton, P., & de Kretser, D. M. (2017). Endocrinology of the male reproductive system and spermatogenesis. In *Endotext [Internet]*. MDText.com, Inc.
- O’sullivan, J., Murray, B., Flynn, C., & Norton, I. (2016). The effect of ultrasound treatment on the structural, physical and emulsifying properties of animal and vegetable proteins. *Food Hydrocolloids*, 53, 141–154.
- Overduin, J., Guérin-Deremaux, L., Wils, D., & Lambers, T. T. (2015). NUTRALYS® pea protein: Characterization of in vitro gastric digestion and in vivo gastrointestinal peptide responses relevant to satiety. *Food and Nutrition Research*, 59, 1–9. <https://doi.org/10.3402/fnr.v59.25622>
- Park, S. J., Garcia, C. V., Shin, G. H., & Kim, J. T. (2017). Development of nanostructured lipid carriers for the encapsulation and controlled release of vitamin D₃. *Food Chemistry*, 225, 213–219.
- Peña-Ramos, E. A., Xiong, Y. L., & Arteaga, G. E. (2004). Fractionation and characterisation for antioxidant activity of hydrolysed whey protein. *Journal of the Science of Food and Agriculture*, 84(14), 1908–1918. <https://doi.org/10.1002/jsfa.1886>
- Pilz, S., Frisch, S., Koertke, H., Kuhn, J., Dreier, J., Obermayer-Pietsch, B., Wehr, E., & Zittermann, A. (2011). Effect of vitamin D supplementation on testosterone levels in men. *Hormone and Metabolic Research*, 43(3), 223.
- Pludowski, P., Holick, M. F., Grant, W. B., Konstantynowicz, J., Mascarenhas, M. R., Haq, A., Povorozyuk, V., Balatska, N., Barbosa, A. P., Karonova, T., Rudenka, E., Misiowski, W., Zakharova, I., Rudenka, A., Łukaszewicz, J., Marciniowska-Suchowierska, E., Łaszcz, N., Abramowicz, P., Bhattoa, H. P., & Wimalawansa, S. J. (2018). Vitamin D supplementation guidelines. *Journal of Steroid Biochemistry and Molecular Biology*, 175(2016), 125–135. <https://doi.org/10.1016/j.jsbmb.2017.01.021>
- Pownall, T. L., Udenigwe, C. C., & Aluko, R. E. (2010). Amino acid composition and antioxidant properties of pea seed (*Pisum sativum* L.) Enzymatic protein hydrolysate fractions. *Journal of Agricultural and Food Chemistry*, 58(8), 4712–4718. <https://doi.org/10.1021/jf904456r>
- Pownall, T. L., Udenigwe, C. C., & Aluko, R. E. (2011).

- Effects of cationic property on the in vitro antioxidant activities of pea protein hydrolysate fractions. *Food Research International*, 44(4), 1069–1074.
<https://doi.org/10.1016/j.foodres.2011.03.017>
- Prusik, K., Kortas, J., Prusik, K., Mieszkowski, J., Jaworska, J., Skrobot, W., Lipinski, M., Ziemann, E., & Antosiewicz, J. (2018). Nordic walking training causes a decrease in blood cholesterol in elderly women supplemented with Vitamin D. *Frontiers in Endocrinology*, 9, 42.
- Ramlau-Hansen, C. H., Moeller, U. K., Bonde, J. P., Olsen, J., & Thulstrup, A. M. (2011). Are serum levels of vitamin D associated with semen quality? Results from a cross-sectional study in young healthy men. *Fertility and Sterility*, 95(3), 1000–1004.
<https://doi.org/10.1016/j.fertnstert.2010.11.002>
- Schachter, A., Goldman, J. A., & Zukerman, Z. (1973). Treatment of oligospermia with the amino acid arginine. *The Journal of Urology*, 110(3), 311–313.
- Seminotti, B., Leipnitz, G., Amaral, A. U., Fernandes, C. G., da Silva, L. de B., Tonin, A. M., Vargas, C. R., & Wajner, M. (2008). Lysine induces lipid and protein damage and decreases reduced glutathione concentrations in brain of young rats. *International Journal of Developmental Neuroscience*, 26(7), 693–698.
- Shand, P. J., Ya, H., Pietrasik, Z., & Wanasundara, P. (2007). Physicochemical and textural properties of heat-induced pea protein isolate gels. *Food Chemistry*, 102(4), 1119–1130.
- Sharma, A., & Sharma, U. S. (1997). Liposomes in drug delivery: progress and limitations. *International Journal of Pharmaceutics*, 154(2), 123–140.
- Sharpe, R. M., Maddocks, S., Millar, M., Kerr, J. B., Saunders, P. T. K., & McKinnell, C. (1992). Testosterone and Spermatogenesis Identification of Stage- Specific, Androgen- Regulated Proteins Secreted by Adult Rat Seminiferous Tubules. *Journal of Andrology*, 13(2), 172–184.
- Solans, C., & Solé, I. (2012). Nano-emulsions: Formation by low-energy methods. *Current Opinion in Colloid and Interface Science*, 17(5), 246–254.
<https://doi.org/10.1016/j.cocis.2012.07.003>
- Sood, S., Reghunandan, R., Reghunandan, V., Marya, R. K., & Singh, P. I. (1995). Effect of vitamin D depletion on testicular function in vitamin D-deficient rats. *Annals of Nutrition and Metabolism*, 39(2), 95–98.
- Spiro, A., & Buttriss, J. L. (2014). Vitamin D: An overview of vitamin D status and intake in Europe. *Nutrition Bulletin*, 39(4), 322–350.
<https://doi.org/10.1111/nbu.12108>
- Stone, A. K., Karalash, A., Tyler, R. T., Warkentin, T. D., & Nickerson, M. T. (2015). Functional attributes of pea protein isolates prepared using different extraction methods and cultivars. *Food Research International*, 76(P1), 31–38.
<https://doi.org/10.1016/j.foodres.2014.11.017>
- Sung, C. C., Liao, M. T., Lu, K. C., & Wu, C. C. (2012). Role of vitamin D in insulin resistance. *Journal of Biomedicine and Biotechnology*, 2012(Figure 1).
<https://doi.org/10.1155/2012/634195>
- Tartagni, M., Matteo, M., Baldini, D., Tartagni, M. V., Alrasheed, H., De Salvia, M. A., Loverro, G., & Montagnani, M. (2015). Males with low serum levels of vitamin D have lower pregnancy rates when ovulation induction and timed intercourse are used as a treatment for infertile couples: Results from a pilot study. *Reproductive Biology and Endocrinology*, 13(1), 1–7.
<https://doi.org/10.1186/s12958-015-0126-9>
- Uhland, A. M., Kwiecinski, G. G., & DeLuca, H. F. (1992). Normalization of serum calcium restores fertility in vitamin D-deficient male rats. *The Journal of Nutrition*, 122(6), 1338–1344.
- Wallner, S., Hermetter, A., Mayer, B., & Wascher, T. C. (2001). The alpha- amino group of l- arginine mediates its antioxidant effect. *European Journal of Clinical Investigation*, 31(2), 98–102.
- Wang, H., Wolosker, H., Morris, J. F., Pevsner, J., Snyder, S. H., & Selkoe, D. J. (2002). Naturally occurring free D-aspartate is a nuclear component of cells in the mammalian hypothalamo-neurohypophyseal system. *Neuroscience*, 109(1), 1–4.
- Yang, B., Sun, H., Wan, Y., Wang, H., Qin, W., Yang, L., Zhao, H., Yuan, J., & Yao, B. (2012). Associations between testosterone, bone mineral density, vitamin D and semen quality in fertile and infertile Chinese men. *International Journal of Andrology*, 35(6), 783–792.
- Zanatta, L., Zamoner, A., Zanatta, A. P., Bouraïma-Lelong, H., Delalande, C., Bois, C., Carreau, S., & Silva, F. R. M. B. (2011). Nongenomic and genomic effects of 1 α ,25(OH) $_2$ vitamin D $_3$ in rat testis. In *Life Sciences* (Vol. 89, Issues 15–16, pp. 515–523).
<https://doi.org/10.1016/j.lfs.2011.04.008>
- Zhu, C. L., Xu, Q. F., Li, S. X., Wei, Y. C., Zhu, G. C., Yang, C., & Shi, Y. C. (2016). Investigation of serum vitamin D levels in Chinese infertile men. *Andrologia*, 48(10), 1261–1266.
<https://doi.org/10.1111/and.12570>

RESEARCH PAPER

A survey on the prevalence of some ectoparasite species infesting sheep and goats in Kalar district, Kurdistan region, Iraq

Sarkawt R. Kakabwa¹, Omer M. Amin¹, Noor N. Polus² and Nabeel A. Mawlood²

¹Department of Biology, College of Education, University of Garmian-Kalar, Kurdistan Region, Iraq

²College of Agricultural Engineering Sciences, University of Salahaddin-Erbil, Kurdistan Region, Iraq

ABSTRACT:

Tamed small ruminants such as sheep and goats are deemed important sources of people livelihood in Garmian area including Kalar district. Sustainability and prosperity of livestock resources are vigorously influenced by the heavy infestation of small ruminants with ectoparasites owing to the enormous economic loss caused by them, particularly in under-developed countries including Iraq. Hence, the present survey, carried out from March, 2019 to February, 2020 in Kalar district, intended to investigate the rampancy of external parasites among sheep and goats being reared in the aforementioned district. To meet the requirements of the survey, a total of 1700 sheep and 400 goats were arbitrarily sampled. The overall rate of ectoparasitosis in this study was 53.09%, in that, the infestation rate in goats (95%) was significantly higher than that of sheep (43.23%). Regarding sheep pediculosis, two species of lice; *Linognathus (L.) africanus* (35.58%), *Damalinia (D.) ovis* (24.11%), and two species of ticks; *Hyalomma (H.) anatolicum* (2.94%), *Rhipicephalus (R.) turanicus* (4.41%), in addition to the nasal bot fly, *Oestrus ovis* (12%) were identified. On the other hand, two species of lice; *D. caprae* (80%), *L. africanus* (30%), and two species of ticks; *H. anatolicum* (7.5%) and *R. turanicus* (3.75%) were detected in goats. Co-infections were significantly higher in sheep as compared to goats in this survey. Some of the aforementioned external parasites are known to transmit zoonotic diseases since sheep and goats are reared in close cohabitation with humans. For that reason, sustainable control of ectoparasitosis especially, tick infestations in domestic livestock is compulsory to prevent both economic loss and transmission of some serious diseases.

KEY WORDS: Ectoparasites, Sheep, Goats, Kalar, Prevalence

DOI: <http://dx.doi.org/10.21271/ZJPAS.33.1.8>

ZJPAS (2021) , 33(1);68-76 .

1.INTRODUCTION :

Over 80% of classified animal species belong to arthropods. These joint-legged invertebrates are found in all habitats on earth and

include varieties of classes such as insects, arachnids, myriapods, and crustaceans. Mode of living of some arthropods is parasitic on vertebral hosts feeding either on skin or blood. Ectoparasitosis has direct or indirect effects on the susceptible hosts (Seid et al., 2018). The chewing lice, *Damalinia (D.) ovis* and *D. caprae* are small (1.5-3 mm) yellowish brown ectoparasites feed on the cutaneous cells, lipids, sweat secretion and

* Corresponding Author:

Omer Mahmood Amin

E-mail: omer.mahmood@garmian.edu.krd

Article History:

Received: 07/06/2020

Accepted: 18/09/2020

Published: 20/02 /2021

skin bacteria of their vulnerable hosts (Ormazdi and Baker, 1979). Epidemiologically, chewing lice, also called biting lice, infest sheep and goats worldwide. The infectivity of these wingless insects has been studied in some districts of the Kurdistan region and some parts of Iraq (Zangana *et al.*, 2013; Pols and Mawlood, 2015; Mustafa, 2019). Moreover, domesticated small ruminants are also prone to infestation with sucking lice of the genus, *Linognathus*. For example, the obligate haematophagous blue louse, *Linognathus (L.) africanus* is capable of infesting both goats and sheep parasitizing on different parts of the body particularly the neck, back and the nape (Rashmi and Saxena, 2017). Usually, lice induce pruritic behavior in the host, and in response to that, the hosts rub, scratch, and bite their skins, which indirectly reduce the quality of the wool and hair (James and Moon, 1998).

Hard ticks (family: Ixodidae) are obligatory blood feeding ectoparasites comprise around 900 known species. Besides their blood feeding and skin damage, these acarines transmit many viral, bacterial and parasitic diseases, and they are reckoned second to mosquitoes in the transmission of infectious diseases (Parola and Raoult, 2001). Ovine and caprine similar to any other vertebrate hosts are exposed to infestation with hard ticks. Various ixodid ticks of sheep and goats were identified and reviewed in Iraq, including the Kurdistan region (Hussien and Yaqub, 2010; Mohammad and Jassim, 2011; Kadir *et al.*, 2012; Mohammad, 2016). In this regard, Zangana *et al.* (2013) have documented five species of ixodid ticks in ovine and caprine, viz. *Rhipicephalus (R.) sanguineus*, *R. turanicus*, *Hyalomma (H.) anatolicum anatolicum*, *H. marginatum*, and *Haemaphysalis spp.*

Larvae of the Dipteran bot fly, *Oestrus (O.) ovis* are cosmopolitan parasites which infest the nasal passages of sheep and goats. The viviparous females of *O. ovis* deposit first-stage larvae directly in the nasal orifices as a part of their life cycle. When the larva develops in the nasal sinus, it can cause a clinical picture termed, ovine oestrosis which characterized by difficulties in breathing, nasal discharge, myiasis of the nasal passages and frontal sinuses, frequent sneezing and dyspnea (Dorchies *et al.*, 1998). In addition to its effects on animals, this parasite is considered zoonotic and can infect human respiratory system

and eye causing ophthalmomyiasis (Abdellatif *et al.*, 2011).

Sheep and goat farming is one of the most important livestock husbandry activities in the Kurdistan region, including Kalar district. These domesticated animals significantly contribute to the provision of meat, milk, hide and skin, hair, horns, bones, manure and other materials that directly affect the economic growth of the area. Due to the significant impacts of ectoparasites on their hosts, the present study aimed to investigate the availability and intensity of sheep and goat ectoparasitosis in Kalar District and the surrounding villages.

2. MATERIALS AND METHODS

2.1. Study site

Kalar district is located in the southeast of Sulaymaniyah Province, the Kurdistan Region of Iraq. The weather of the area is hot and dry in the summer, and the temperature reaches over 50°C in July and August. The coldest months of the winter are December and January in which the temperature seldom reaches 0°C. Geographically, the district is located in between the latitude (34.6308° N) and the longitude (45.3276° E) of the eastern hemisphere. Kalar has a large area estimated of 438,317 km² with almost 250,000 populations. According to the annual report (issued in 2019) of the directorate of veterinary and animal resources in Kalar, there are nearly 100 flocks of sheep and 60 flocks of goats estimated with 45,000 sheep and 6,500 goats.

2.2. Collection of specimens

In the present study, 1700 sheep and 400 goats were examined randomly for the prevalence of ectoparasites between March 2019 and February 2020. The age of the animals was from six months to five years. The animals were selected randomly from 10 flocks of sheep and 6 flocks of goats from 10 locations in and around Kalar district (Fig 1). The samples were collected from different parts of the animal body (head, neck, flanks, front and rear legs, and abdomen). Regarding ticks, all the samples were collected from the body of the animals (fed ticks), tweezers were used carefully to remove the ticks. Lice were collected using brushing with fine comb (Yakhchali and Hosseine, 2006). Larvae of *O. ovis* were collected from the nasal cavity of

slaughtered sheep. Fifty heads of recently slaughtered sheep were purchased from local butchers. The heads were sawn at the sagittal

plane (Figure 2) and washed out with normal saline (Hidalgo *et al.*, 2015).



Figure 1: Map of the study area where samples of ectoparasites collected (1: Saida, 2: Shakal, 3: Punga, 4: Qarachil, 5: Qasm Agha, 6: Saykhalyl, 7: Barlut village, 8: Shorawa, 9: Rizgari, 10: Girda Gozina



Figure 2: Dissection of a sheep head at the sagittal plane showing larvae of *Oestrus ovis* in the nasal cavity

2.3. Laboratory examination of ectoparasites

After collection, samples were preserved in 70% ethanol and transferred to the laboratories of the College of Agricultural Engineering Sciences, University of Salahaddin. Samples were examined using a stereo microscope and images were taken using a digital Canon camera (Ucma series microscope camera). All samples were identified according to Kim and Ludwig (1978); Walker *et al.* (2003).

2.4. Statistical analysis

Chi-square test was applied in the present study for analyzing differences in infestation rates

using PRISM software version 6.1. Differences between variables were considered significant when the P value was less than 0.05.

3. RESULTS

The overall prevalence of ectoparasites in both sheep and goats was 53.09 %. Out of 1700 sheep investigated for ectoparasites, 735 were infested with at least one species of parasite. Whereas, out of the 400 inspected goats, 380 were infested. The prevalence of ectoparasites in sheep and goats in Kalar district is shown in table 1. The infestation rate in goats (95%) was significantly higher than those in sheep (43.23%) ($P < 0.05$).

Table 1
Prevalence of ectoparasites on sheep and goats in Kalar district

Host type	No. of samples	No. infested	Infestation rate %
Sheep	1700	735	43.23
Goats	400	380	95
Total	2100	1115	53.09
	Chi-square= 348.4	df=1	P=0.0001

In the present study, 6 different genera and species of parasites were identified in both sheep and goats. Regarding sheep, the sucking lice, *L. africanus* was the most dominant ectoparasites found in this study (35.58%). The chewing lice, *D. ovis* came next (24.11%). Two species of hard ticks were also identified in sheep; *R. turanicus* and *H. anatolicum* with infestation rates of 4.41% and 2.94% respectively. Larvae of *O. ovis* in the

nasal cavities of sheep were found to be 12% (Table 2).

The most common ectoparasites identified in goats in this study was the chewing lice, *B. caprae* (80%) followed by the sucking lice, *L. africanus* (30%) and the two hard ticks *H. anatolicum* and *R. turanicus* with infestation rates of 7.5% and 3.75% respectively. There were significant differences between infestation with different species of parasites in both sheep and goats (Table 2).

Table 2

Prevalence of different genera and species of ectoparasites in sheep and goats in Kalar district

Host type	Number of samples examined	Ectoparasites	Infestation rate %
Sheep	1700	<i>Linognathis africanus</i>	35.58 (605/1700)
		<i>Damalinia ovis</i>	24.11 (410/1700)
		<i>Hyalomma anatolicum</i>	2.94 (50/1700)
		<i>Rhipicephalus turanicus</i>	4.41 (75/1700)
		<i>Oestrus ovis</i>	12 (6/50)
Goats	400	<i>Damalinia caprae</i>	80 (320/400)
		<i>Linognathis africanus</i>	30 (120/400)
		<i>Rhipicephalus turanicus</i>	3.75 (15/400)

Most sheep were infested with more than one ectoparasite (co-infestation) at the same time (63.26%) as compared to the infestation with single parasite (36.73%). However, goats showed different results, in which the rate of infestation

with single parasite (71.05%) was higher than those with multiple infestations (28.94%). Statistical analysis showed a significant difference in multiple and single infestation between sheep and goats ($P < 0.05$), as shown in table 3.

Table 3
Single and multiple infestations with ectoparasites in sheep and goats in Kalar district

Host type	Samples examined	Single infestation rate %	Multiple infestation rate %
Sheep	1700	36.73 (270/735)	63.26 (465/735)
Goats	400	71.05 (270/380)	28.94 (110/380)
	Chi-square= 118.1	df=1	P=0.0001



Figure 3: Ectoparasites of sheep and goats detected in Kalar area: A- *Damalinia caprae*, B- *Damalinia ovis*, C- *Linognathus africanus*, D- *Rhipicephalus turanicus*, E- *Hyalomma anatolicum*, F- A larva of *Oestrus ovis*

4. DISCUSSION

The present survey was designed to investigate the diversity of ectoparasites of small ruminants in Kalar district. Based on previous published papers, this survey could be the first attempt to document and validate ectoparasites in Kalar area where livestock are being raised intensively. Parasites pose a great menace on the livestock productivity, which, in turn, causes an enormous economic loss. In this study, the overall prevalence of ectoparasites in sheep and goats collectively was 53.09%. Parasite infestation in goats (95%) was significantly higher as compared to that of sheep (43.23%). The same conclusion

was reported by Zangana *et al.* (2013) in Duhok Province when they found higher infestation rate in goats as compared to sheep. In contrast, the study of Mustafa (2019) in Sulaymaniyah province, which is close to Kalar district, recorded a higher rate of ectoparasite infestations in sheep as compared to goats. The reason behind the diversity of ectoparasite rampancy could be the difference in climatic conditions in different areas which might encourage the abundance of certain parasites over others (Yakhchali and Hosseine, 2006). Probably, another reason is related to the seriousness of the

farmers in treating their infested animals with antiparasitics. For example, sheep rearing is more common than goats in the district, so, according to the veterinary file in Kalar, the majority of livestock raisers are seeking treatment for their sheep. This habit leaves the infested goats untreated or intermittently treated, hence, the rate of ectoparasitosis in caprine will be elevated.

In sheep, the blue lice, *L. africanus* showed the highest parasitic rate 35.58% (605/1700), whereas 30% (120/400) of goats were infested with that parasite. The opposite was observed regarding the infestation with chewing lice, *Damalinia sp.* Eighty percent of the investigated goats were infested with *D. caprae*, however, 24.11% of the sheep were infested with *D. ovis*. Other studies in Iraq have also reported pediculosis in sheep and goats. Al-Saffar and Mohammad (2008) reported that sheep in the city of Mosul were infested with 5 species of lice among them *D. ovis* (6.4%) and *L. africanus* (0.2%). Zangana *et al.* (2013) reported that sheep were infested with *D. ovis* 75% and *L. stenopsis* 33.3% whereas goats were infested with 80.7% and 19.25% with the aforementioned parasites respectively. Mustafa (2019) reported two species of lice in sheep, namely, *D. ovis* 17.74% and *L. stenopsis* 13.63%, and two species in goats, vs. *D. caprae* 10.97% and *L. stenopsis* 6.22%. In a morphological study of goats' ectoparasites in Erbil province/Iraq, Pols and Mawlood (2015) have reported and described *D. caprae* and *L. africanus* from goats without mentioning the prevalence rate.

In the present study, two species of ticks were identified which were *H. anatolicum* and *R. turanicus* with prevalence rates of 2.94%, 4.41% and 7.5%, 3.75% in sheep and goats respectively. Mohammed (2016) reported 8 species of ticks from the middle and south of Iraq and the rate of sheep infestation with *H. anatolicum* was (28%) and with *R. turanicus* was (39%). In the same study, goats were also infested with *H. anatolicum* (24%) and *R. turanicus* (64%). The prevalence rate of ticks in this study was lower than what reported by Mustafa (2019) when he found that the infestation rate with *H. anatolicum* was 11.9% and 31.3% and *R. turanicus* was 7.5% and 15.96% in sheep and goats respectively.

Prevalence of *O. ovis* larvae in the present study was 12 (6/50). This was lower than most of the studies carried out in Iraq: 17.2% in Ninevah

governorate (Jarjees *et al.*, 2000), 33.4% in Baghdad (Al-Amery, 2007) and 68% in Erbil (Saad *et al.*, 1993).

Fluctuations in the prevalence rate of this parasite comparing to other studies could be attributed to several factors such as changes in climatic conditions which affect the activity of the adult fly in addition to the animal breeds (Saad *et al.*, 1993; Jacquet and Dorchie, 2002; Al-Ubeidi *et al.*, 2017)

5. CONCLUSIONS

Different species of ectoparasites were documented in this survey. The study of external parasites is not just important for animals themselves but rather more important for humans. Haematophagous ectoparasites particularly, ticks are known to transmit serious diseases to animals and humans.

Acknowledgements

We deeply thank personnel of the directorate of veterinary in Kalar for their continuous guidance and support. We also express our gratitude to the flock owners and shepherds for their help during sample collections.

6. Conflict of Interest

On behalf of the other co-authors in this article, I undertake that there is no conflict of interest among us.

References

- Abdellatif, M.Z., Elmazar H.M. and Essa A.B., 2011. *Oestrus ovis* as a cause of red eye in Aljabal Algharbi. Libya. *Middle East African Journal of Ophthalmology*, 18, 305-308.
- AL-Amery, A.M., 2007. Serepidemiological study of myasis caused by *Oestrus ovis* larvae. A thesis. Baghdad: Baghdad University.
- Al-Saffar T.M. and Muhammad B.A., 2008. Epidemiological and identification study of sheep lice in Al-Mosul city. *AL-Qadisiya Journal of Veterinary and Medicine Sciences*, 7, 7-11.
- Al-Ubeidi, N.H., Al-Ani, A.J. and Al-Kennany, E.R., 2017. Detection of nasal bot fly larvae in slaughtered sheep of Ninevah governorate – Iraq. *Basrah Journal of Veterinary Research*, 16, 240-247.
- Dorchies, P., Duranton, C. and Jacquet, P., 1998. Pathophysiology of *Oestrus ovis* infection in sheep and goats: a review. *Veterinary Record*, 142, 487-489.
- Hidalgo, A., Palma, H., Oberg, C. and Fonseca-Salamanca, F., 2015. *Oestrus ovis* infection of grazing sheep during summer in southern Chile. *Pesquisa Veterinária Brasileira*, 35, 497-500.
- Hussien, H.H. and Yaqub, A.Y., 2010. Distribution of ectoparasites among sheep in Baghdad. *Bulletin of Diyala Pure Sciences*, 6, 213-245.
- Jacquet, P. and Dorchies P., 2002. Towards a lower prevalence of *Oestrus ovis* infections in sheep in a temperate climate (south west France). *Veterinary Research*, 33, 449-453.
- James, P.J. and Moon, R.D., 1998. Pruritis and dermal response to insect antigens in sheep infested with *Bovicola ovis*. *International Journal for Parasitology*, 28, 419-427.
- Jarjees, M.T., Daoud, M.S. and Hassan, M.H., 2000. Natural occurrence of *Oestrus ovis* L (diptera) larvae in sheep in Ninevah province. *Iraqi Journal of Veterinary Sciences*, 13, 323-329.
- Kadir, M.A., Zangana, I.K. and Mustafa, B.H.S., 2012. A study on epidemiology of hard tick (Ixodidae) in sheep in Sulaimani governorate - Iraq. Proceedings of the 6th Scientific Conference, College of Veterinary Medicine, University of Mosul. *Iraqi Journal of Veterinary Sciences*, 26, Supplement III: 95-103.
- Kim, K.C. and Ludwig, H.W., 1978. The family classification of the Anoplura. *Systematic Entomology*, 3, 249-284.
- Mohammad M. K., 2016. Ixodid tick fauna infesting sheep and goats in the middle and south of Iraq. *Bulletin of the Iraq national History Museum*, 14, 43-50.
- Mohammad, M.K. and Jassim, S.Y., 2011. Distribution of hard tick species among sheep *Ovis aries* L. in Al-Anbar Province, western desert of Iraq. *Bulletin of the Iraq national History Museum*, 11, 7-31.
- Mustafa, B.H.S., 2019. Detection on ectoparasites on small ruminants and their impact on the tanning industry in Sulaimani province. *Iraqi Journal of Veterinary Sciences*, 33, 303-309.
- Oormazdi, H. and Baker, K.P., 1979. An examination of the dietary constituents of the cattle-biting louse, *Bovicola bovis*. *Annals of Tropical Medicine and Parasitology*, 73, 185-187.
- Parola, P. and Raoult, D., 2001. Ticks and Tickborne Bacterial Diseases in Humans: An Emerging Infectious Threat. *Clinical Infectious Diseases*, 32, 897-928.
- Pols, N.N. and Mawlood, N.A., 2015. Morphological Study of some ectoparasites of goats in Erbil Governorate Kurdistan Region-Iraq. *Zanco Journal of Pure and Applied Sciences*, 27, 39-44.
- Rashmi, A. and Saxena A.K., 2017. Population levels of phthirapteran ectoparasites on the goats in Rampur (U.P.). *Journal of Parasitic Diseases*, 41, 778-781.
- Saad, A.H., Muhamed, A.K. and Ismail, A.Y., 1993. Seasonal occurrence of *Oestrus* L (Diptera: oestridae) in goats in Arbil. *Iraqi Journal of Veterinary Sciences*, 16, 5-7.
- Seid, M., Zeryehun, T., Kemal, J. and Telahun, B., 2018. Ectoparasites of small ruminants in and around Kombolcha, northeastern Ethiopia. *Ethiopian Veterinary Journal*, 22, 81-93.
- Walker, A.R., Bouattour, A., Camicas, J.L., Estrada- Pena, A., Horak, I.G., Latif, A., Pegram, R.G. and Preston, P.M., 2003.

- Ticks of Domestic Animals in Africa. A Guide to Identification of Species. Bioscience Reports, London, UK. pp. 86-217.
- Yakhchali, M. and Hosseine, A., 2006. Prevalence and ectoparasites fauna of sheep and goats flocks in Urmia suburb, Iran. *Veterinarski Arhiv*, 76, 431-442.
- Zangana, I.K., Ali, B.A. and Naqid, I.A., 2013. Distribution of ectoparasites infested sheep and goats in Duhok province, north Iraq. *Basrah Journal of Veterinary Research*, 12, 54-64.

RESEARCH PAPER

Synthesis and characterization of palladium(II) and platinum(II) mixed ligand complexes of the type $[M(\text{bpoz})_2(\text{dppf})]\text{Cl}_2$, $\text{bpoz} = 2$ -(benzylthio)-5-phenyl-1,3,4-oxadiazole

Rezan A. Saleh*, Hikmat A. Mohammad

Department of Chemistry, College of Education, Salahaddin University-Erbil, Kurdistan Region, Iraq

ABSTRACT:

Treatment of $[\text{PdCl}_2(\text{dppf})].\text{CH}_2\text{Cl}_2$ or $[\text{PtCl}_2(\text{dppf})]$ with two moles of 2-(benzylthio)-5-phenyl-1,3,4-oxadiazole (bpoz) in (ethanol: chloroform) solvents for (2 h) afford $[\text{M}(\text{bpoz})_2(\text{dppf})]\text{Cl}_2$ in good yield. The synthesized ligand and complexes were identified using FT-IR, $^1\text{H-NMR}$, $^{13}\text{C-NMR}$, $^{31}\text{P-NMR}$, CHNS analysis, Uv-Visible spectra and conductivity measurements. The physicochemical data indicated that the prepared complexes have square planar geometries and the metal ions coordinate with the ligands through two phosphorous atoms of (dppf) and nitrogen atom of (bpoz).

KEY WORDS: palladium(II), platinum(II), diphosphine, oxadiazole.

DOI: <http://dx.doi.org/10.21271/ZJPAS.33.1.9>
ZJPAS (2021) , 33(1);77-90 .

INTRODUCTION:

In recent years, the interest of preparing coordination compounds with desired properties - functional compounds have been increased. One of the promising ligands for creating multifunctional complexes are compounds containing a 1,3,4-oxadiazole fragment (Pirimova *et al.*, 2020). Oxadiazoles are interesting class of five-membered heterocyclic compounds containing two atoms of nitrogen and one atom of oxygen (Paulo *et al.*, 2018). They exist in four different regioisomeric forms, namely 1,2,3-, 1,2,4-, 1,2,5-, and 1,3,4-oxadiazoles. In the past 40 years, oxadiazole-based ligands stimulated the curiosity of many researchers, creating a vast literature that spans from synthesis to different applications. In fact, oxadiazoles exhibit a broad range of uses: in medicinal chemistry they were employed as drug candidates for several diseases, in organic synthesis as useful intermediates,

and in material science as building blocks for new polymers (Giovanni and Alessio, 2019) (Zainab and Hameedi, 2020). Transition metal complexes of 1,3,4-oxadiazole derivatives are well known for their biological importance as well as their anticarcinogenic, antibacterial and antifungal properties (Adil, 2017).

A series of 1,1'-bis(diphenylphosphino)ferrocene possessing platinum(II) complexes depicting a novel series of tentative anticancer drug candidates. Compounds of this sort have already been displayed to illustrate both antineoplastic and antimicrobial activity (Puxty *et al.*, 2005). Metal complexes of bidentate phosphines have conceived considerable attention due to their possible use as antitumor agents (Al-Jibori *et al.*, 2013). Herein, we report the synthesis and identification of new mixed ligand Pd(II) and Pt(II) complexes including both 2-(benzylthio)-5-phenyl-1,3,4-oxadiazole (bpoz) and 1,1'-

* Corresponding Author:

Rezan A. Saleh

E-mail: rezan.saleh@su.edu.krd

Article History:

Received: 08/08/2020

Accepted: 04/10/2020

Published: 20/02/2021

bis(diphenylphosphino)ferrocene (dppf) as ligands.

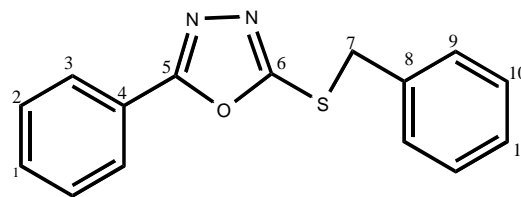
2. Materials and Methods

The (PdCl₂, PtCl₂, dppf, 2-Mercapto-5-phenyl-1,3,4-oxadiazole, materials were commercially available from Yahoo Chem. China. The [PdCl₂(dppf)].CH₂Cl₂ and [PtCl₂(dppf)] complexes were prepared according to the literature (Rezan *et. al.*, 2017). IR spectra were recorded on IR-Affinity-1, Shimadzu CORP-A21375003225 spectrophotometer in the range of 400-4000 cm⁻¹ using KBr discs. (¹H, ¹³C and ³¹P)-NMR spectra were recorded on a Bruker 400 MHZ Ultra-shield. Electronic spectra were recorded on a UV-Vis. spectrometer, AE-UV1609 (UK) CO., LTD. The conductivity was measured on a conductivity meter type Senz μSiemen conductivity tester. Elemental analysis was carried out on Euro EA 3000 Elemental Analyzer.

2.2. Synthesis of (bpozs) ligand

A solution of (4 mmole, 0.712 g) of 2-Mercapto-5-phenyl-1,3,4-oxadiazole (phozsH) in (10 ml) ethanol, was added to ethanol solution (10 ml) of NaOH (4 mmole, 0.16 g). The resultant mixture was refluxed for (15 min.) and (4 mmole, 0.474 ml) of benzyl bromide was added and refluxed for (4 h.). A white solid of (bpozs) was obtained after cooling of the solution in an ice bath. The formed precipitate was filtered off, dried and recrystallized from ethanol.

Yield = 0.85g, 60.93 %; mp: 95-96 °C; Color: White. C₁₅H₁₂N₂OS. IR (ν_{max}/cm⁻¹): ν(C-H) aromatic 3051, 2993; ν(C-H) aliphatic 2914, 2848; ν(C=N) 1608; ν(N-N) 1465; ν(C-O-C) 1080; ν(C-S) 704. ¹H-NMR (296K, ppm, d⁶-DMSO): d, 8.05 ppm, ³J(HH)=8 Hz. (2H, phenyl protons); m, 7.67-7.61 ppm (3H, phenyl protons); d, 7.56 ppm, ³J(HH)=8 Hz. (2H, phenyl protons); m, 7.44-7.35 ppm (3H, phenyl protons); s, 4.63 ppm (2H, CH₂ group), ¹³C-NMR (DMSO, δ, 400 MHz): 158 and 156 C_{5,6} (oxadiazole); 128.1 C₈; 123.8 C₂; 121.03 C_{1,10}; 120.8 C₉; 120.44 C₃; 119.75 C₁₁; 118.32 C₄; 39.88 C₇(CH₂).



2-(benzylthio)-5-phenyl-1,3,4-oxadiazole (bpozs)

2.3. Synthesis of complexes

2.3.1. Preparation of [Pd(bpozs)₂(dppf)]Cl₂ (1)

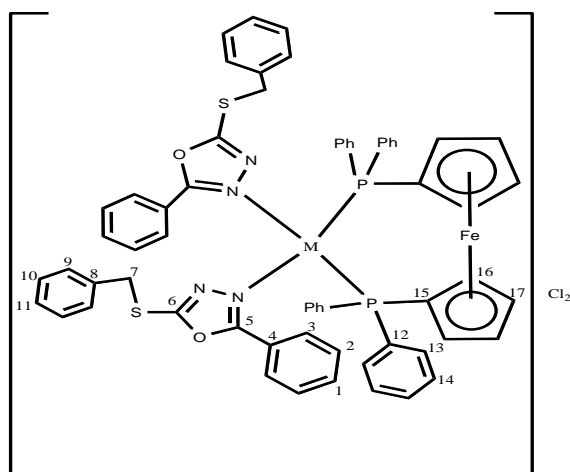
A warm solution of (bpozs) ligand (0.235 mmole, 0.066 g) in ethanol (10 ml) was added to a solution of [PdCl₂(dppf)].CH₂Cl₂ (0.117 mmole, 0.095 g) in CHCl₃ (20 ml). The mixture was refluxed for (2 h.) then filtered off. A brown precipitate was afforded after evaporation of the filtrate to dryness at room temperature.

Yield = 0.10 g, 66.2 %, mp: 91-92 °C; Color: brown. Anal. Calc. for C₆₄H₅₂FeCl₂ N₄PdO₂P₂S₂: C, 60.6; H, 4.10; N, 4.41; S, 5.05. Found: C, 59.98; H, 4.35; N, 3.62; S, 5.91 %. IR (ν_{max}/cm⁻¹): ν(C-H) aromatic 3051; ν(C-H) aliphatic 2924; ν(C=N) 1608; ν(N-N) 1465; ν(P-Ph) 1435; ν(C-O-C) 1091; ν(C-S) 692; ν(Pd-N) 528. ¹H-NMR (295K, ppm, CDCl₃): s, 7.93 ppm, m, 7.36 ppm (30H, phenyl protons); s, 4.47 ppm (2H, CH₂); s, 4.4, 4.34 (8H, Cp), ¹³C-NMR (CDCl₃, δ, 400 MHz): 165 and 163 C_{6,5}(oxadiazole); 136.05 C₁₂; 135.6 C₁₃; 132.10 C₈; 131.8 C₂; 129.49 C_{1,10,14}; 129.27 C₉; 128.57 C₃; 127.13 C₁₁; 124.02 C₄; 75, 73, 71 C₁₅₋₁₇(Cp); 37.33 C₇(CH₂), ³¹P-{¹H}-NMR; δP= 30.68 ppm.

2.3.2. Preparation of [Pt(bpozs)₂(dppf)]Cl₂ (2)

A warm solution of (bpozs) ligand (0.235 mmole, 0.066 g) in ethanol (10 ml) was added to a solution of [PtCl₂(dppf)] (0.117 mmole, 0.095 g) in CHCl₃ (20 ml). The mixture was refluxed for (2 h.) then filtered off. A yellow solid of the complex was appeared after evaporation of the filtrate to dryness at room temperature.

Yield = 0.12 g, 74.5 %, Decomposes at: 253°C; Color: Yellow. Anal. Calc. for $C_{64}H_{52}FeCl_2N_4PtO_2P_2S_2$: C, 56.64; H, 3.83; N, 4.13; S, 4.72. Found: C, 56.51; H, 4.55; N, 4.26; S, 4.00 %. IR (ν_{max}/cm^{-1}): $\nu(C-H)$ aromatic 3078; $\nu(C-H)$ aromatic 3078; $\nu(C-H)$ aliphatic 2966; $\nu(C=N)$ 1653; $\nu(N-N)$ 1465; $\nu(P-Ph)$ 1435; $\nu(C-O-C)$ 1097; $\nu(C-S)$ 690; $\nu(Pt-N)$ 518. 1H NMR (295K, ppm, $CDCl_3$): s, 7.86, m, 7.37 ppm (30H, phenyl protons); s, 4.36, 4.18 ppm (8H, Cp); s, 4.53 ppm (2H, CH_2), ^{13}C NMR ($CDCl_3$, δ , 400 MHz): 164 and 162 $C_{6,5}$ (oxadiazole); 136 C_{12} ; 135.31 C_{13} ; 132 C_8 ; 131.58 C_2 ; 129.41 $C_{1,10,14}$; 129.19 C_9 ; 128.28 C_3 ; 127.04 C_{11} ; 124.6 C_4 ; 75, 74, 72 C_{15-17} (Cp); 38 $C_7(CH_2)$, ^{31}P - $\{^1H\}$ -NMR; $\delta P = 9.79$ ppm; $J(Pt-P) = 3168$ Hz.



3. Results and discussion

3.1. FT-IR, 1H -NMR and ^{13}C -NMR Spectrum of (bpozS) ligand

In the IR spectrum of bpozS, the (SH) stretching band of phozsH compound at (2567 cm^{-1}) Fig. (1) was vanished and a new weak band at (2914 and 2848) cm^{-1} was appeared that corresponded to aliphatic (CH_2) group, this evidence for coordination of oxadiazole sulfur atom with benzyl group (Joshi *et al.*, 2015). The spectra exhibited bands at (1608 , 1465 , 1080 and 704) cm^{-1} , were respectively attributed to $\nu(C=N)$, $\nu(N-N)$, $\nu(C-O-C)$ and $\nu(C-S)$ of oxadiazole group Fig. (2)

(Kumar *et al.*, 2014)(Al-Azzawi and Hamd, 2013)(Rangappa Santosh *et al.*, 2019).

The 1H -NMR spectrum displayed a singlet band at (4.63) ppm, corresponded to the (CH_2) proton and disappearance of the thiol proton at (3) ppm was indicated for the formation of bpozS ligand.

The phenyl protons of bpozS ligand appeared as two doublets at (8.05) ppm; ($^3J(HH) = 8$ Hz.) and (7.56) ppm; ($^3J(HH) = 8$ Hz.), with two unresolved multiplets within ($7.67-7.61$ and $7.44-7.35$) ppm. Fig. (5) (Joshi *et al.*, 2015)(Kumar *et al.*, 2014)(Bhava *et al.*, 2013).

The ^{13}C -NMR spectrum showed peaks at (158 and 156) ppm, were attributed to C_6 and C_5 of oxadiazole ring, respectively (Almajan *et al.*, 2008). The aromatic carbon atoms (C_{1-4} and C_{8-11}) of bpozS ligand were observed at ($121.03, 123.8, 120.44, 118.32$ and $128.1, 120.8, 121.03, 119.75$) ppm respectively, furthermore, a new signal was detected at (39.88) ppm, attributed to carbon atom of (CH_2) group Fig. (6) (Tank and Acharya, 2013) (Aras and Hassan, 2018).

3.2. FT-IR, 1H -NMR, ^{13}C -NMR and ^{31}P - $\{^1H\}$ -NMR spectra of the synthesized complexes

The infrared spectra of Pd(II) and Pt(II) complexes Fig. (3, 4), displayed a weak intensity bands at (2924 and 2966) cm^{-1} , were respectively allocated to $\nu(CH_2)$ of benzyl group. Moreover, the $\nu(P-Ph)$ of dppe and $\nu(C=N)$, $\nu(N-N)$ and $\nu(C-S)$ stretching bands of bpozS ligand in (1 and 2) complexes occurred at (1435), (1608 , 1653), (1465) and (692 , 690) cm^{-1} , correspondingly (Jensen and Nielsen, 1963)(Zainab and Hameedi, 2020). Furthermore, a new weak intensity band was appeared at (528 and 518) cm^{-1} , were respectively attributed to the N-bound coordination of bpozS ligand to Pd and Pt metal (Al-Jibori *et al.*, 2002)(Al-Jibori *et al.*, 2015).

The ^1H -NMR, ^{13}C -NMR and $^{31}\text{P}\{-^1\text{H}\}$ -NMR spectra for both (1 and 2) complexes were measured in CDCl_3 solvent.

^1H NMR spectra were as expected, both (1 and 2) complexes displaying singlet and multiplets at $\delta(7.93, 7.36$ and $7.86, 7.37)$ ppm were respectively assigned to the phenyl protons and the two signals at $\delta(4.4, 4.34$ and $4.36, 4.18)$ ppm, were due to protons of cyclopentadienyl ligand, correspondingly (Al-Jibori *et al.*, 2012)(Riyadh, 2016). The aliphatic (CH_2) proton of bpozs in 1 and 2 complexes occurred as a singlet band at $\delta(4.47$ and $4.53)$ ppm, respectively. In the spectrum of complex 2 there is no $^3\text{J}(\text{Pt-H})$, which means that Pt is coordinated to bpozs through more basic N- atom not the S-atom (Lobana *et al.*, 2000)(Ivana and Marija, 2017)(Al-Jibori *et al.*, 2002).

The ^{13}C -NMR spectra of complex 1 and 2 Fig. (7, 8), exhibit signals at $\delta(165, 163$ and $164, 162)$ ppm, were assigned to the two oxadiazole carbon atoms, respectively. The phenyl carbon atoms of bpozs and dppf ligands appeared at $\delta(136.05 \text{ C}_{12}; 135.6 \text{ C}_{13}; 132.10 \text{ C}_8; 131.8 \text{ C}_2; 129.49 \text{ C}_{1,10,14}; 129.27 \text{ C}_9; 128.57 \text{ C}_3; 127.13 \text{ C}_{11}; 124.02 \text{ C}_4)$ in complex 1 and at $\delta(136 \text{ C}_{12}; 135.31 \text{ C}_{13}; 132 \text{ C}_8; 131.58 \text{ C}_2; 129.41 \text{ C}_{1,10,14}; 129.19 \text{ C}_9; 128.28 \text{ C}_3; 127.04 \text{ C}_{11}; 124.6 \text{ C}_4)$ in complex 2 (Almajan *et al.*, 2008). The carbon atoms of (Cp) groups (C_{15-17}) of phosphine ligand in 1 and 2 complexes occurred at $\delta(75, 73, 71$ and $75, 74, 72)$ ppm and existence of a peak at $\delta(37.33$ and $38)$ ppm, corresponded to the (CH_2) carbon atom (C_7) of bpozs ligand, respectively (Al-Jibori *et al.*, 2012)(Nur *et al.*, 2018)(Ivana and Marija, 2017).

The $^{31}\text{P}\{-^1\text{H}\}$ -NMR spectrum of complex (1 and 2) Fig. (9, 10), show a singlet band with platinum satellites, indicates that the electronic environment of both phosphorous atoms of dppf ligand are the same; both phosphorous are equivalent and trans to the same atom.

The spectrum of $[\text{Pt}(\text{bpozs})_2(\text{dppf})]\text{Cl}_2$ complex showed a singlet at $\delta(9.79)$ ppm with associated platinum satellites, $J(\text{Pt-P}) = 3168$ Hz. and the

$[\text{Pd}(\text{bpozs})_2(\text{dppf})]\text{Cl}_2$ complex exhibited a singlet band at $\delta(30.68)$ ppm, these suggests that dppf behaves as a bidentate chelating ligand that linked to metal ions through both phosphorous atoms and both P-atoms trans to N-atom of bpozs ligand (Al-Jibori *et al.*, 2012) (Al-Jibori *et al.*, 2007).

3.3. Elemental analysis for the prepared complexes

The elemental analysis (CHNS) data for the synthesized complexes are coherent with the recommended stoichiometries Table (1).

3.4. Electronic Spectra of the Prepared Complexes

The electronic spectrum of (bpozs) ligand Fig. (11) was measured in methanol and their synthesized mixed ligand complexes in DMSO solvent Fig. (12, 13). The spectrum of bpozs ligand illustrated two absorption bands in the Uv. region at $(41666$ and $37037)$ cm^{-1} , these transitions were respectively belonged to π - π^* and n - π^* transitions. The electronic spectrum of Pd(II) and Pt(II) complexes exhibited charge transfer band at (38461) cm^{-1} with two d-d bands in the uv. and visible regions at $(32258, 21276)$ and $(30303, 23255)$ cm^{-1} , were associated to $^1\text{A}_{1g} \rightarrow ^1\text{E}_g$ and $^1\text{A}_{1g} \rightarrow ^1\text{B}_{1g}$ transitions correspondingly Table (2), these electronic transitions indicated that the complexes are formed as a square planer geometry (Sutton, 1968).

3.5. Molar conductivity for the prepared complexes

The molar conductivity of bpozs ligand was surveyed for (10^{-3} M) solution in methanol and the prepared complexes in DMSO solvent at (25°C) . The conductivity measurements for both complexes are high, it was deduced that the prepared complexes are electrolyte that formed in the ratio of (1:2) as illustrated in Table 3.

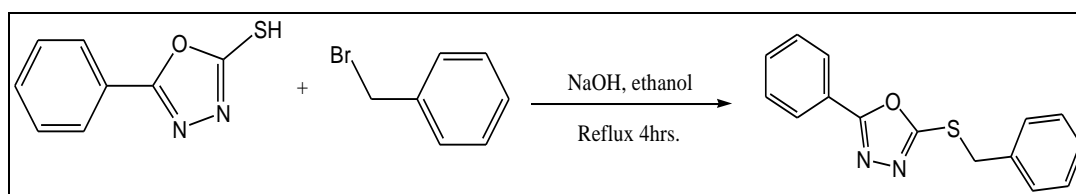
Conclusion

We have illustrated herein that palladium(II) and platinum(II) complexes of the type $[M(\text{bpoz})_2\text{dppf}]\text{Cl}_2$ are synthesized from the addition of two moles of (bpoz) ligand to the prepared $[\text{MCl}_2(\text{dppf})]$ complexes, where $\text{M}=\text{Pd}(\text{II})$ and $\text{Pt}(\text{II})$. Characterization was relatively straight-forward on the basis of spectroscopic and analytical data. According to the measurements data, we deduced that the prepared complexes have a square planer structure

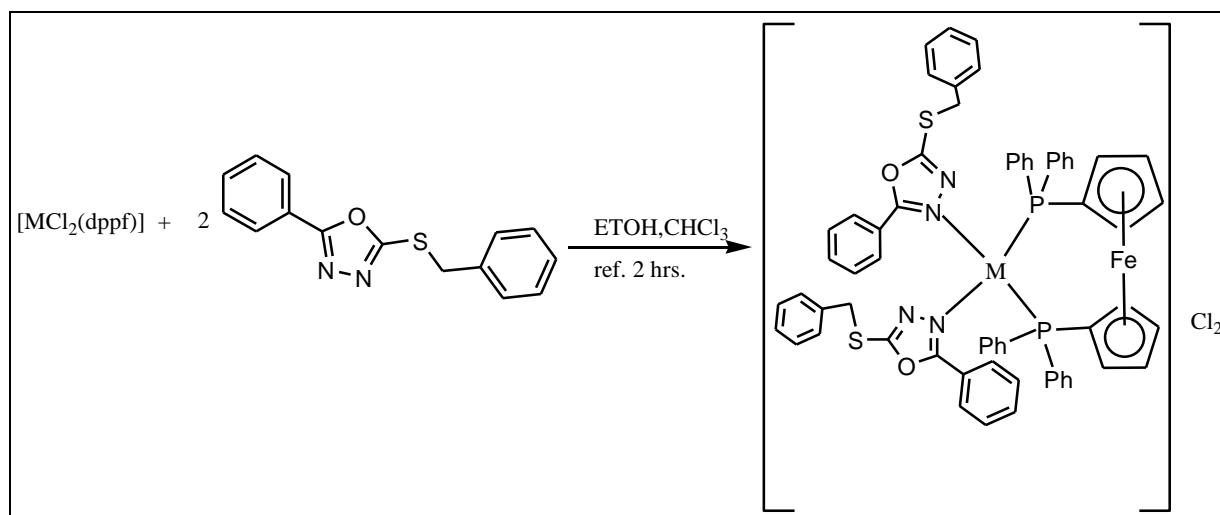
in which bpoz ligand bonded in a monodentate fashion through nitrogen atom, while the dppf ligand bind to metals centre through both P-atoms. Moreover, based on the molar conductivity data, it has been proposed that the synthesized complexes are ionic in the ratio of (1:2).

Acknowledgements

We would like to thank the University of Salahaddin, College of Education for partial support of this work.



Scheme 1. Synthesis of (bpoz) ligand



Scheme 2. Synthesis of $[\text{M}(\text{bpoz})_2(\text{dppf})]\text{Cl}_2$, where $\text{M}=\text{Pd}(\text{II})$ or $\text{Pt}(\text{II})$

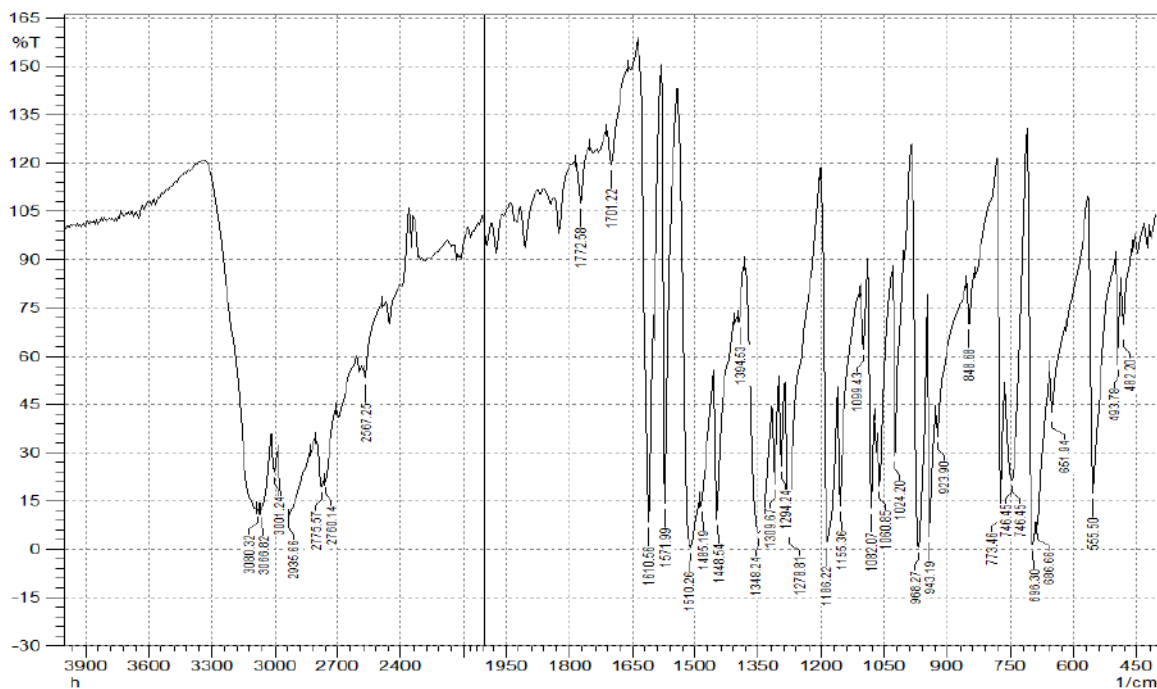


Figure 1: IR spectrum of phozsH ligand

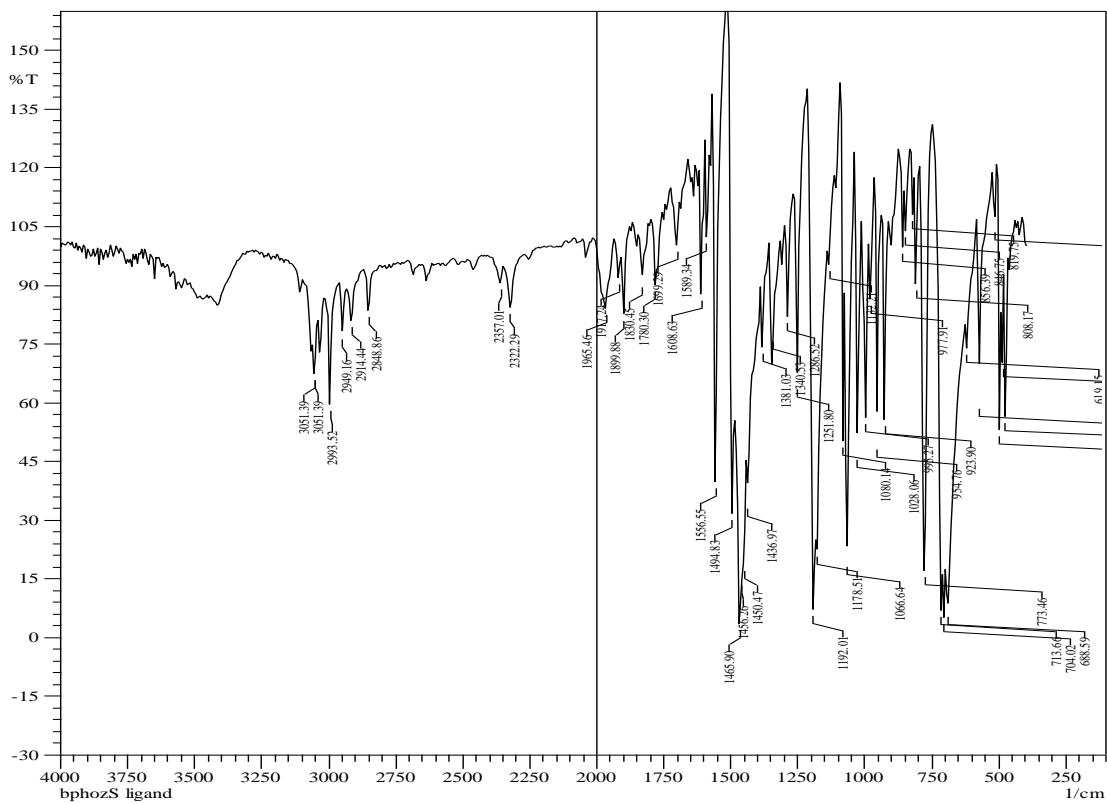


Figure 2: IR spectrum of bpozS ligand

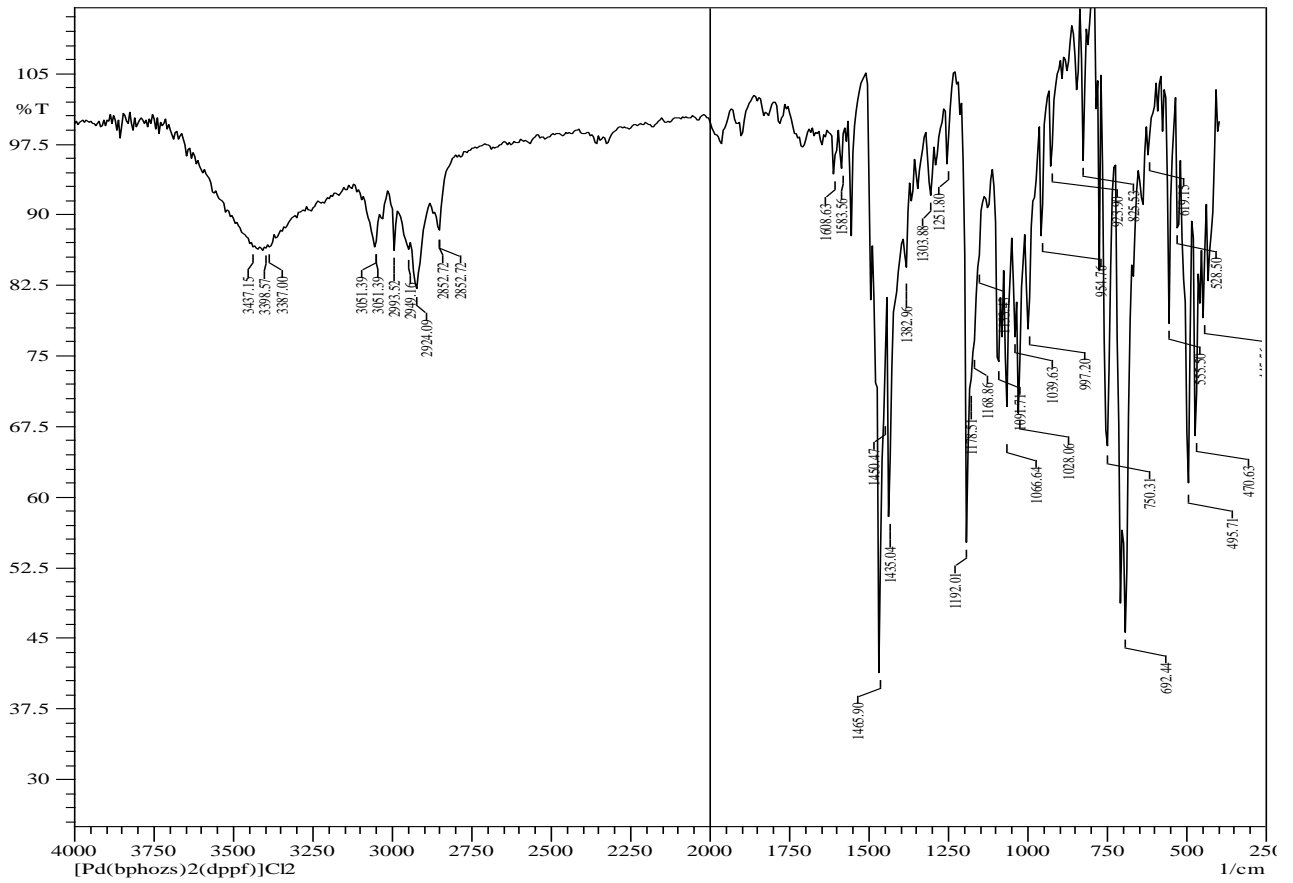


Figure 3: IR spectrum of complex 1

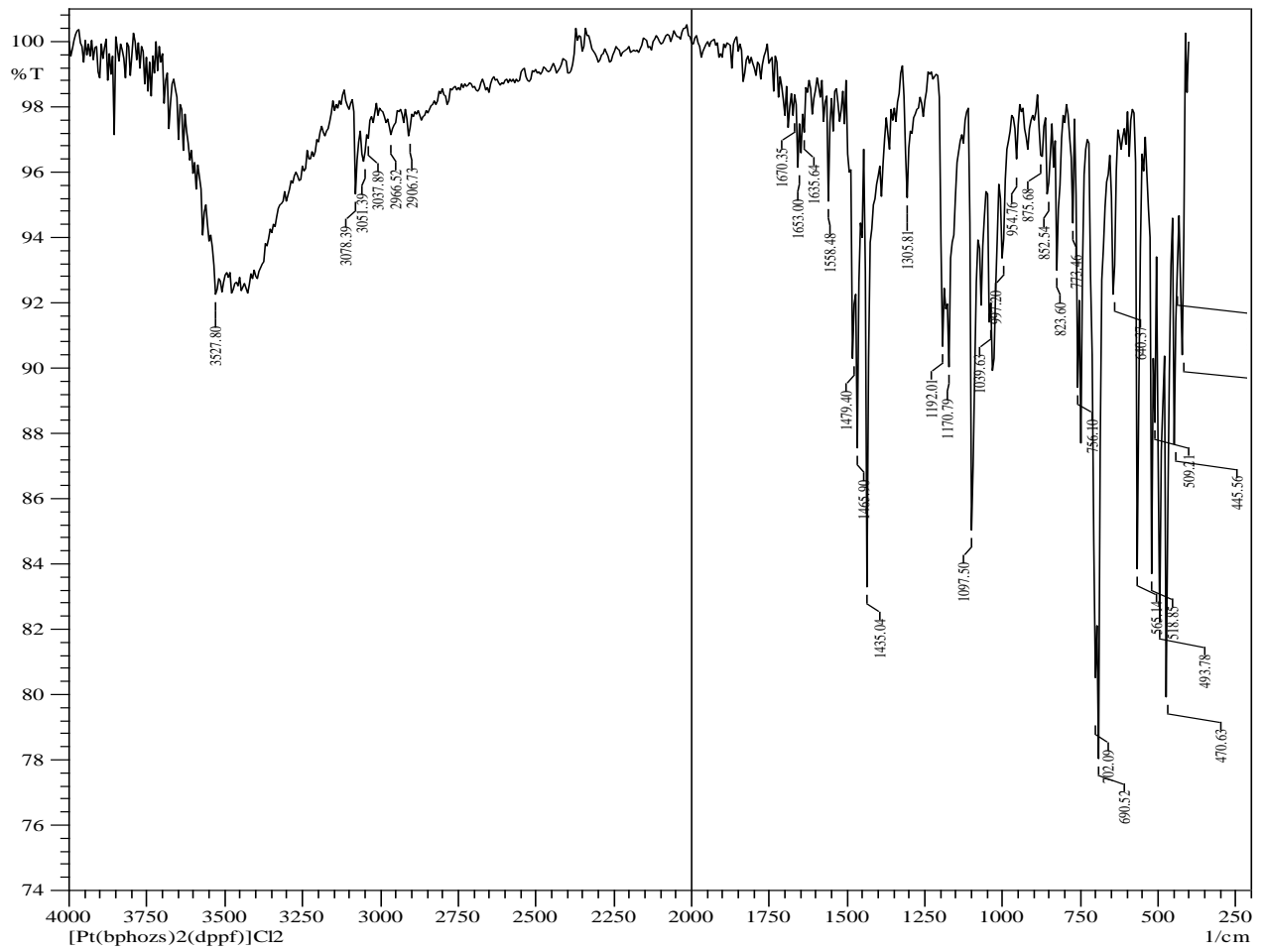
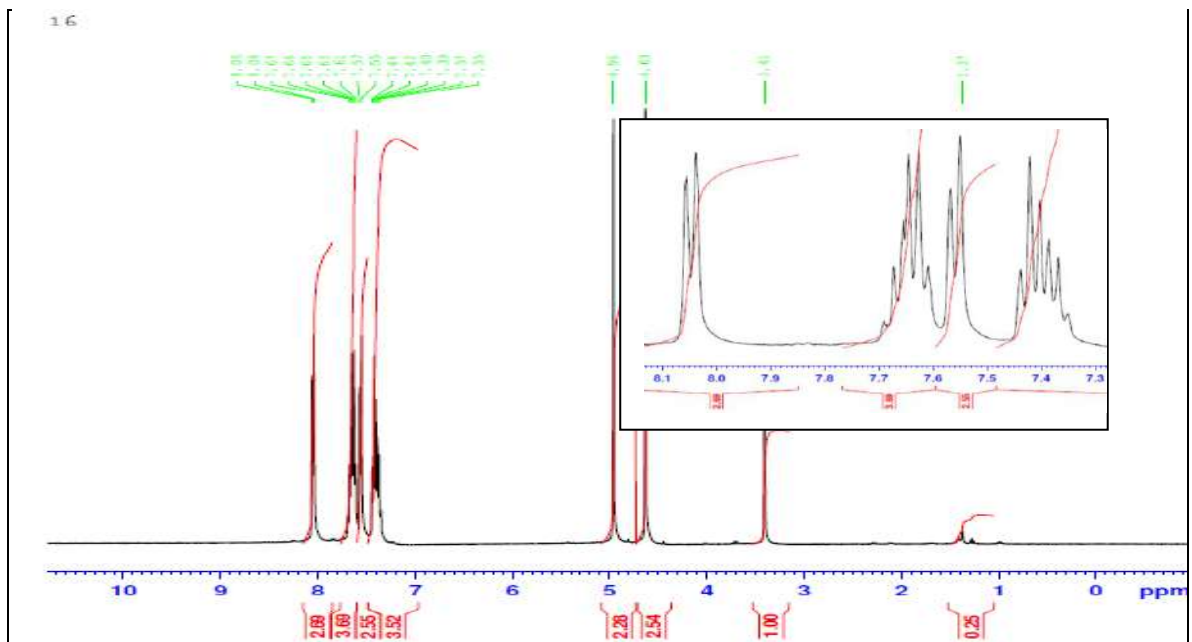


Figure 4: IR spectrum of complex 2

Figure 5: ¹H-NMR spectrum of bpozs ligand

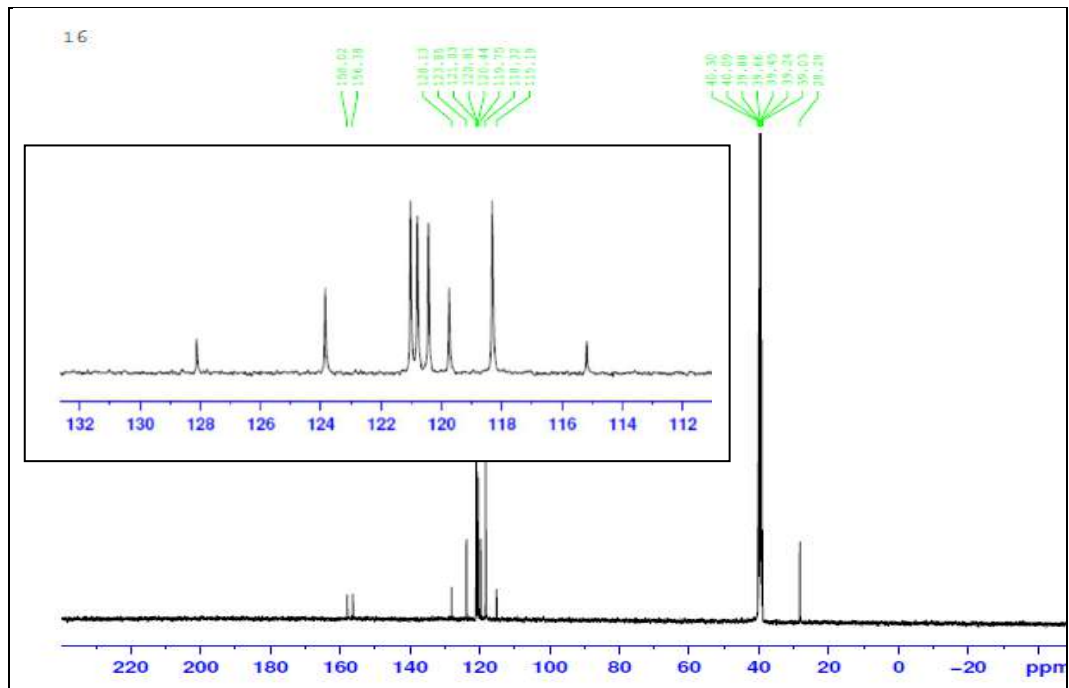


Figure 6: ^{13}C -NMR spectrum of bpozs ligand

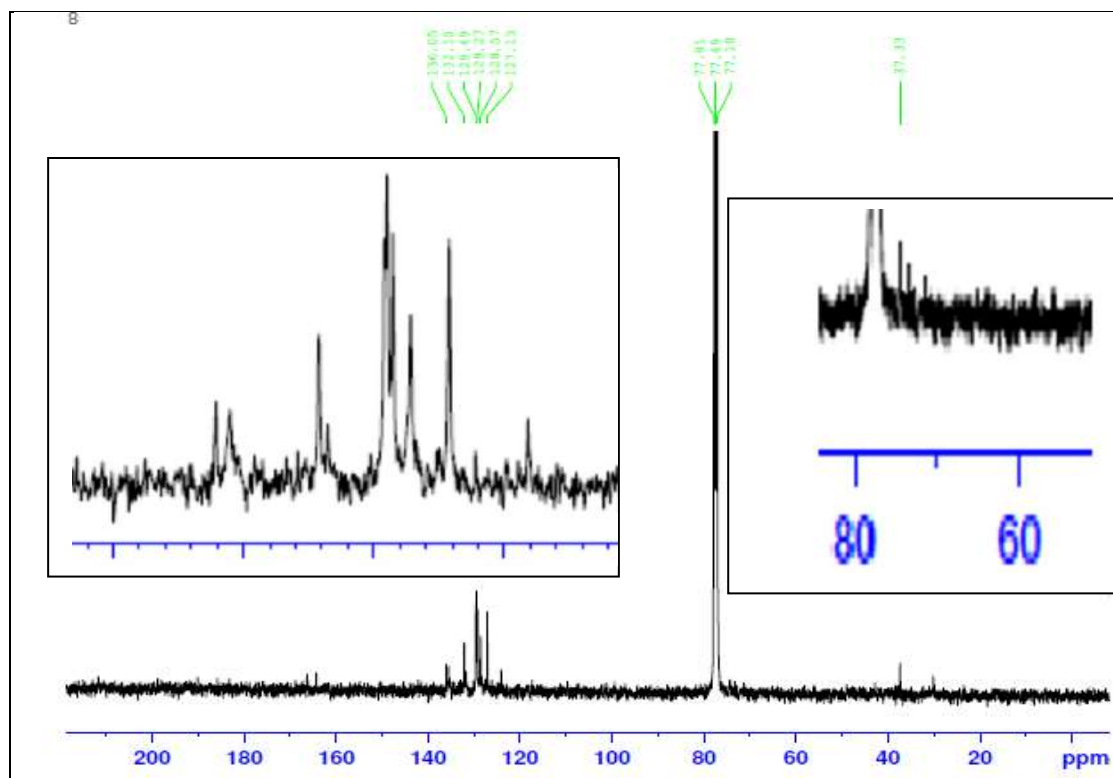


Figure 7: ^{13}C -NMR spectrum of complex 1

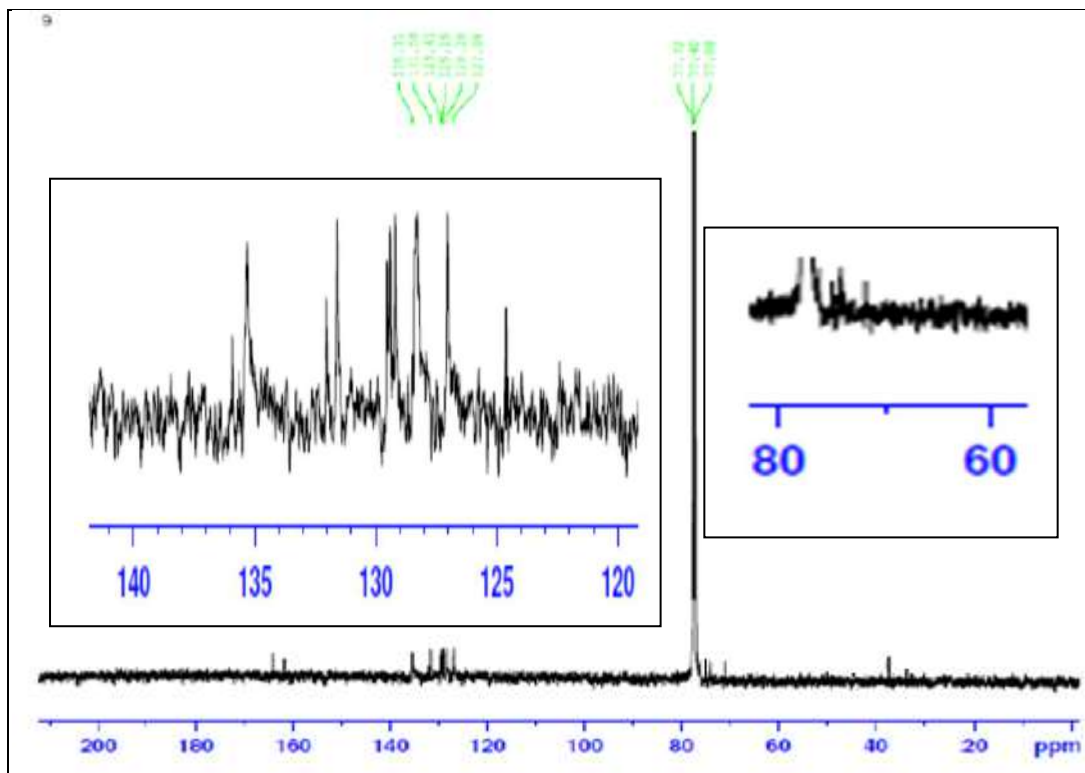


Figure 8: ¹³C-NMR spectrum of complex 2

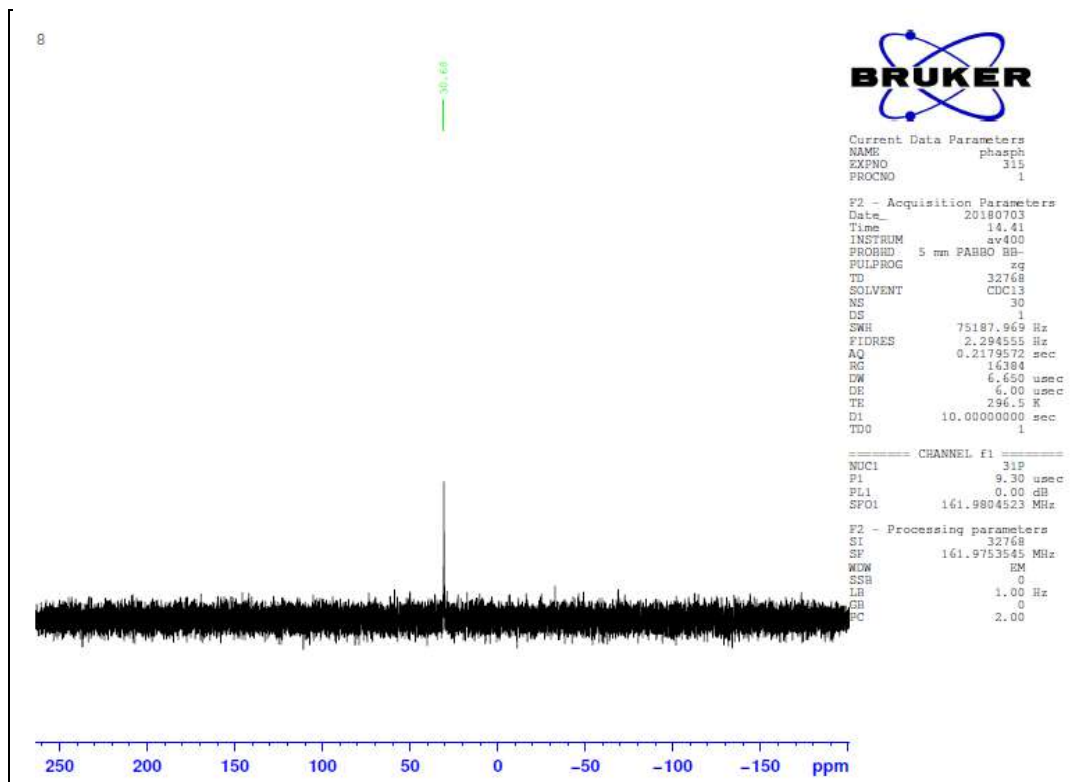


Figure 9: ³¹P-¹H-NMR spectrum of complex 1

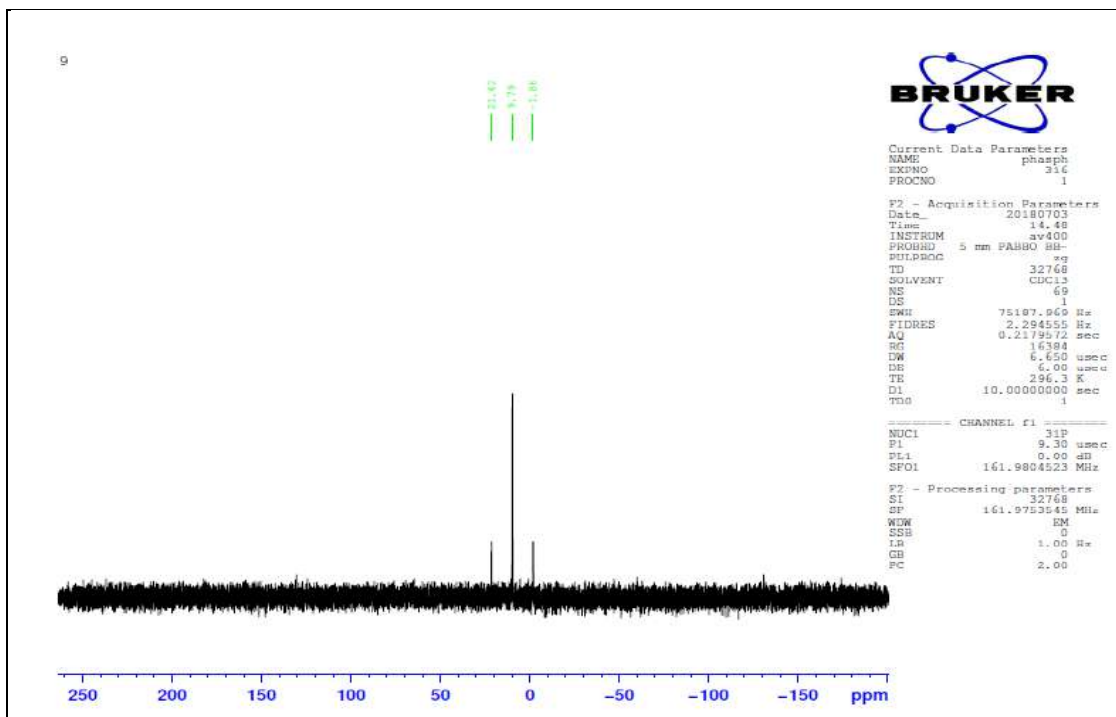
Figure 10: $^{31}\text{P}\{-^1\text{H}\}$ -NMR spectrum of complex 2

Table 1: Colors, molecular weight, melting points and elemental analysis for the synthesized complexes

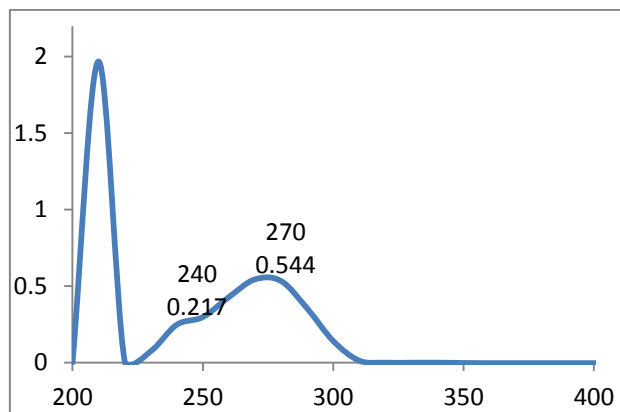
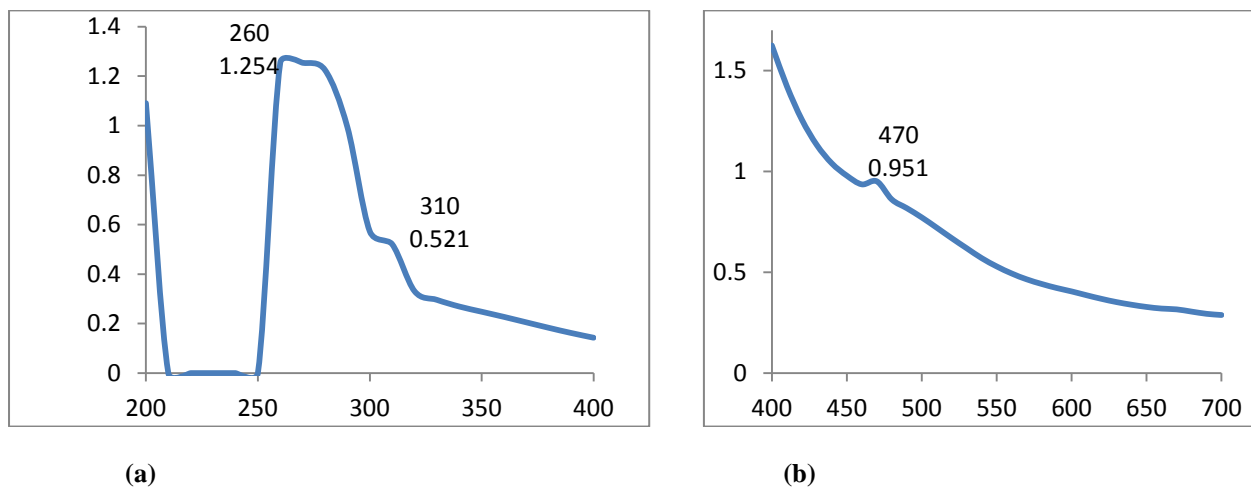
No.	Complexes	Color	M.Wt g/mol	M.P. (°C)	(Calculated) Found %			
					C	H	N	S
	bpoz	White	268.06	95-96
1	$[\text{Pd}(\text{bpoz})_2(\text{dppf})]\text{Cl}_2$	Brown	1267.2	91-92	(60.6) 59.98	(4.10) 4.35	(4.41) 3.62	(5.05) 5.91
2	$[\text{Pt}(\text{bpoz})_2(\text{dppf})]\text{Cl}_2$	Yellow	1355.88	d.p. 253	(56.64) 56.51	(3.83) 4.55	(4.13) 4.26	(4.72) 4.00

Table 2: Electronic spectral bands of the ligand and its metal complexes

Complexes	Absorption band		Assignment Transition
	cm^{-1}	nm	
bpoz	41666	240	$\pi \rightarrow \pi^*$
	37037	270	$n \rightarrow \pi^*$
	38461	260	C.T.
1	32258	310	$^1\text{A}_{1g} \rightarrow ^1\text{E}_g$
	21276	470	$^1\text{A}_{1g} \rightarrow ^1\text{B}_{1g}$
	38461	260	C.T.
2	30303	330	$^1\text{A}_{1g} \rightarrow ^1\text{E}_g$
	23255	430	$^1\text{A}_{1g} \rightarrow ^1\text{B}_{1g}$

Table 3: Molar conductivity ($\text{cm}^2 \cdot \text{ohm}^{-1} \cdot \text{mol}^{-1}$) of (10^{-3} M) solution in DMSO for the synthesized complexes

No.	Complexes	Molar conductivity ($\text{cm}^2 \cdot \text{ohm}^{-1} \cdot \text{mol}^{-1}$)
	bpozs	26
1	$[\text{Pd}(\text{bpozs})_2(\text{dppf})]\text{Cl}_2$	72
2	$[\text{Pt}(\text{bpozs})_2(\text{dppf})]\text{Cl}_2$	68

**Figure 11: Uv.-Vis. spectrum of bpozs ligand****Figure 12: Electronic spectrum of $[\text{Pd}(\text{bpozs})_2(\text{dppf})]\text{Cl}_2$ complex: (a) UV. (b) Vis. Region**

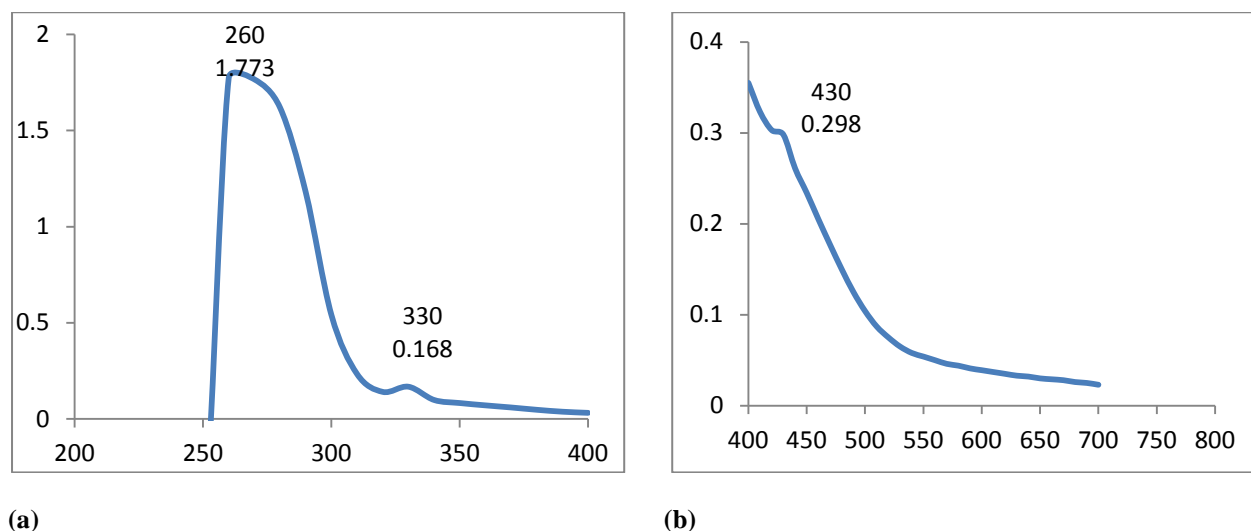


Figure 13: Electronic spectrum of $[Pt(bpozs)_2(dppf)]Cl_2$ complex: (a) UV. (b) Vis. Region

References

- Adil, A. 2017. Synthesis and Spectroscopic Studies of Novel Transition Metal Complexes with 5-Phenyl-2-[2-Hydroxy pyridylacetylhydrazide]-1,3,4-Oxadiazole, *Der. Pharma. Chemica.*, 9(4), 48-52.
- Al-Azzawi, A. and Hamd, A. 2013. Synthesis, characterization and antimicrobial activity evaluation of new cyclic imides 1, 3, 4-thiadiazole and 1, 3, 4-oxadiazole, *Int. J. Res. Pharm. Chem.* 3 (4), 890-897.
- Al-Jibori, S., Afra, S., Modher, Y. and Talal, A. (2007). Mixed ligand palladium(II) and platinum(II) complexes of tertiary diphosphines and benz-1,3-imidazole-2-thione, benz-1,3-oxazoline-2-thione or benz-1,3-thiazoline-2-thione., *Transition Metal Chemistry*, 32, 281–286.
- Al-Jibori, S., Al-Nassiry, A., Hogarth, G. and Salassa, L. 2013. Platinum and palladium bis (diphenylphosphino) ferrocene (dppf) complexes with heterocyclic N-acetamide ligands: Synthesis and molecular structures of $[MCl(sac)(\kappa^2-dppf)]$ ($M = Pt, Pd$, sac = saccharinate), $[PtCl(ata)(\kappa^2-dppf)]$ and $[Pt(ata)_2(\kappa^2-dppf)]$ ($ataH = N$ -(2-thiazolyl) acetamide), *Inorganica Chimica. Acta.*, 398, 46-53.
- Al-Jibori, S., Al-Nassiri, I., Al-Hayaly, L. and Jassim, A. 2002. Mixed ligand transition metal complexes of tertiary phosphines and 5-phenyl-1, 3, 4-oxadiazole-2-thione, *Transition metal chemistry*, 27 (2), 191-195.
- Al-Jibori, S., Birgul, S., Safaa, A., Ahmet, K., Harry S., Christoph W. and Graeme H. 2015. Palladium(II) benzisothiazolate (bit) complexes with amino-, acetylamino-, heterocyclic and phosphine co-ligands. Crystal structure of $[Pd(bit)_2(\kappa^2-dppe)] \cdot 2EtOH$, *Inorganica Chimica Acta.*, 436, 7–15.
- Al-Jibori, S., Khaleel, T., Ahmed, S., Al-Hayaly, L., Merzweiler, K., Wagner, C. and Hogarth, G. 2012. Heteroleptic palladium (II) and platinum (II) complexes of 1, 1-bis (diphenylphosphino) ferrocene (dppf) and heterocyclic thionates: Crystal structures of $[Pt(Phozt)_2(\kappa^2-dppf)]$ ($PhoztH = 5$ -phenyl-1, 3, 4-oxadiazole-2-thione) and $[Pd(bzox)_2(\kappa^2-dppf)]$ ($bzoxH =$ benz-1, 3-oxazoline-2-thione), *Polyhedron*, 41 (1), 20-24.
- Almajan, G., Barbuceanu, S., Saramet, I., Dinu, M., Doicin, C. and Draghici, C. 2008. Synthesis and biological evaluation of various new substituted 1, 3, 4-oxadiazole-2-thiols, *Revista Chim.*, 59 (4), 395-399.
- Aras, N., Hassan, A. 2018, Synthesis and spectroscopic study of 1,2-thiazine system incorporating various ester groups, *ZANCO Journal of Pure and Applied Sciences*, 30 (1); 44-55.
- Bhava, P., Tharmaraj, P., Muthuraj, V. and Umadevi, M. 2013, Synthesis, spectral characterization, biological screening and DNA studies Of 2-(5-mercapto-[1, 3, 4]-oxadiazol-2-yl)phenol transition metal (II) complexes, *International Journal of Engineering and Science*, 2 (12), 16-25.

- Giovanni, S. and Alessio, T. 2019. Metal Complexes of Oxadiazole Ligands: An Overview, *Int J Mol Sci.*, 20(14), 1-17.
- Ivana, V. and Marija, D. (2017) Reactions of platinum(II) complexes with sulfur and nitrogen containing biomolecules: selective intermolecular migration of the thioether-bound platinum(II) complex to the N7 nitrogen atom of guanosine-5'-monophosphate, *Ser. J. Clin Res.*, 1, 1-6
- Jensen, K. and Nielsen, H. 1963. Infrared spectra of some organic compounds of group (VB) elements, *Acta Chem. Scand.*, 17, 1875-1885.
- Joshi, S., More, U., Kulkarni, M., Nelaguddad, K. and Kulkarni, V. 2015. Combined pharmacophore and molecular docking-based in silico study of some pyrrolyl 1, 3, 4-oxadiazole benzothioate derivatives, *Rgush Journal Pharm. Science*, 5 (2), 69-80.
- Kumar, L., Naik, P., Naveen, M., Chandrasekhar, T., Reddy, A., Penchalaiah, N. and Swamy, G. 2014. Synthesis and biological evaluation of some new 2, 5-disubstituted 1, 3, 4-oxadiazoles from 3-(arylsulfonyl) propanehydrazides, *Indian Journal of Chemistry*, 53, 208-211.
- Lobana, T., Verma, R., Hundal, G. and Castineiras, A. 2000. Metal-heterocyclic thione interactions.: 12. Heterocyclic 2-thiolates of platinum (II) and palladium (II): the crystal structures of first examples of cis-[M(η^1 -S-pyridine-2-thiolato)₂ (L-L)]{M = Pt, Pd, L-L = 1,2-bis (diphenylphosphino) ethane; M= Pt, L-L= 1, 2-bis (diphenylphosphino) ethene} complexes, *Polyhedron*, 19 (8), 899-906.
- Nur, R., Fariza, J., Mohd, R., Syahrina, N., Nur, A., Amirrudin, M., Nor, F. and Rozie, S.2018. New Silver Complexes with Mixed Thiazolidine and Phosphine Ligands as Highly Potent Antimalarial and Anticancer Agents, *Hindawi Journal of Chemistry*,1-11.
- Paulo, P., Vitor, S. and Marco, E. 2018. 1,2,4- and 1,3,4-Oxadiazoles as Scaffolds in the Development of Antiparasitic Agents, *J. Braz. Chem. Soc.*, 29 (3), 435-456.
- Pirimova, M., Kadirova, S., Ziyayev, A. and Parpiyev, N. 2020. Synthesis and Research of New Mixed Metal Complexes Co(II), Ni(II), Cu(II) and Mn(II)Based on Ammonium Vanadate and 5-Phenyl-1,3,4-Oxadiazole-2-(3H)-thione, *Journal of Critical Reviews*, 7 (11), 464-471.
- Puxty, G., Bjelosevic, H., Persson, T. And Elmroth, S. 2005. A comparative kinetic study of modified Pt(dppf)Cl₂ complexes and their interactions with L-cys and L-met., *Dalton Transactions*, (18), 3032-3038.
- Rangappa, S., Ashwini, P., Mukunthan, K., Panchangam, M., Gundibasappa, K. and Panchappady, D. 2019. Design, synthesis, and pharmacology of some oxadiazole and hydroxypyrazoline hybrids bearing thiazoyl scaffold: antiproliferative activity, molecular docking and DNA binding studies, *Heliyon 5 Elsevier Ltd.*, 1-30.
- Rezan, A., Hikmat, A., Thomas, I. and Eric, C. 2017. Synthesis and Characterization of Mono and Mixed Ligand, Ni(II), Pd(II) and Pt(II) Complexes of S-5-Phenyl -1, 3, 4-Oxadiazole-2-yl Benzothioate with some Tertiary Diphosphines Ligands, *AIP Conference Proceedings*, 2-22.
- Riyadh, M. 2016. Newmetal complexes of oxadiazole-2-thione-based ligands; Synthesis and structural characterization, *ChemXpress*, 9(2), 178-182.
- Sutton, D. 1968. *Electronic spectra of transition metal complexes: an introductory text.* McGraw-Hill.
- Tank, M. and Acharya, G. 2013. Synthesis and antimicrobial study of some transition metal complexes of novel bidentate heterocyclic ligand: 3-(((8-hydroxyquinolin-5-yl) amino) methyl)-5-phenyl-1, 3, 4-oxadiazole-2 (3H)-thione (HAMPOTe), *Universal Journal of Pharmacy*, 2 (6), 78-82.
- Zainab, M. and Hameedi N. 2020. Synthesis, Characterization, Antimicrobial and Anticorrosion of Studies New 2-(5-(2-(5-hydrazinyl-1,3,4-thiadiazole-2-yl) hydrazinyl)-1,3,4-oxadiazole-2-yl) Phenol With Some Transition Metal Ions, *Sys. Rev. Pharm.*, 11 (3), 840 849.

RESEARCH PAPER

Identification and Quantification of Secondary Metabolites and The Antimicrobial Efficacy of Leaves Extracts of Some Medicinal Plants

Quadri O. Nurudeen, Mansurat B, Falana

¹Department of Biological Sciences, Al-Hikmah University, Ilorin, Nigeria

ABSTRACT:

Azadirachta indica, *Calotropis procera*, *Carica papaya*, and *Vernonia amygdalina* are among the most frequently used plants with proven ethnomedicinal applications in Ilorin, Nigeria. This study investigated the active constituents and antimicrobial efficacy of acetone and aqueous extracts of these plants against *Candida albicans*, *Escherichia coli* ATCC 259220, and *Staphylococcus aureus* ATCC 25923 by the disc diffusion technique. High-Performance Liquid Chromatography (HPLC) fingerprint of the constituents of acetone extracts of *C. papaya*, *A. indica*, and *V. amygdalina* was further investigated. Highest percentage yield (10.20 %) was obtained for acetone extract of *A. indica* while the lowest yield (10.20 %) was obtained for aqueous extract of *C. papaya*. Varying constituents viz. coumarins, glycosides, protein, saponin, anthraquinone, flavonoid, tannin and terpenoid were detected. Different levels of antimicrobial efficacy were exhibited by each of the plants while a synergistic effect was observed at 100 mg/mL concentration of acetone extract of the combination of all the plants. An array of compounds was separated at different peak heights corresponding to concentration of the compounds. Creptolepinone was detected in highest percentage (47.0 %) in acetone extracts of *C. papaya* while phorbol ester was detected in lowest percentage (1.2 %). Myricetin was detected in highest percentage (39.6 %) in acetone extracts of *A. indica* while alpha funebren was detected in lowest percentage (1.5 %). Vernodalinal was detected in highest peak height (48.8 %) in *V. amygdalina* and andrographoside was detected in lowest peak height (0.6 %). This study depicts that the plants may be promising pharmaceutical candidates that can be used in the development of new therapeutic agents.

KEY WORDS: acetone; antimicrobials; azadirachtol; myricetin; vernodalinal; *in vitro*.

DOI: <http://dx.doi.org/10.21271/ZJPAS.33.1.10>

ZJPAS (2021), 33(1);91-106 .

1.INTRODUCTION :

Many antimicrobial agents of natural or semi-synthetic sources are available to fight against infections caused by various pathogens (Rahman *et al.*, 2008). Medicinal plants are significant sources of natural antimicrobials in the development of novel drugs (Perry *et al.*, 1999). Herbal plants are abundant sources of bioactive molecules, which are categorized as aromatic substances and secondary metabolites including phenols or their oxygen-substituted derivatives

(Boligon *et al.*, 2012; Kumar *et al.*, 2010). The biomolecules can be extracted and administered in many forms, the most common of which is as a tisane or a tincture to treat several infections (El-Said and Al-Barak, 2011). Some of these bioactive molecules may also be screened and traded as raw materials for many herbal industries (Paul *et al.*, 2011).

* Corresponding Author:

Quadri O. Nurudeen

E-mail: quadriolaide@yahoo.com

Article History:

Received: 17/02/2020

Accepted: 04/10/2020

Published: 20/02 /2021

Many parts of medicinal plants are consumed as food or for medicinal purposes (Okoko and Ere, 2012; Romasi *et al.*, 2011). *C. papaya* Linn., a commonly cultivated perennial plant with economic importance all over tropical and subtropical countries (Pandey *et al.*, 2016; Reddy *et al.*, 2013), is commonly found in West Africa (Irvine, 1961). It is used traditionally in Nigeria, where it is commonly known as Gwanda, Okwuru-bekee and Ewe ibepe among the Hausa,

Igbo and Yoruba people, to treat various diseases such as cold, fevers, indigestion, diarrhea, eczema, and rheumatism. The leaf extracts, chopped leaves, and latex of *C. procera* have shown great promise as a nematicide in *in vitro* and *in vivo* studies (Khirstova and Tissot, 1995). Also, the roots and leaves of *V. amygdalina* are used therapeutically to treat kidney problems, stomach discomfort and other infections (Banso *et al.*, 1999; Tugume *et al.*, 2006).

Table 1. Medicinal plants tested in this study

Scientific name	Family	Common name	Local names			Traditional Uses
			Hausa	Igbo	Yoruba	
<i>V. amygdalina</i>	Asteraceae	Bitter leaf	Chusar-doki	Onugbu	<i>Ewuro</i>	Treatment of syphilis, gonorrhoea, antidiabetic
<i>C. procera</i>	Apocynaceae/ Asclepeceae	Giant milkweed	Tumfatiya		<i>Bomubomu</i>	peptic ulcer, treats stomach ache, cure skin diseases like measles, jaundice
<i>C. papaya</i>	Caricaceae	Pawpaw leaf	Gwanda	Okwuru-bekee	<i>Ewe ibepe</i>	Treatment of dysentery, diabetes, malaria, convulsion, gonorrhoea, syphilis
<i>A. indica</i>	Meliaceae	Neem	<i>Dogonyaro</i>		<i>Dogonyaro</i>	Treatment of malaria, jaundice, purgative

Despite the available information on these plants, an array of studies has reported variations in active metabolites of plants due to varying climatic condition of different locations of plants. This may consequently affect the qualities of plants and their medicinal potentials. As such, it is necessary to investigate the effect of solvents on the quantity and quality of secondary metabolites of some plants commonly used plants in the study region. Also, to investigate the effectiveness of these plants on common pathogens that are usually associated with infectious diseases.

2. MATERIALS AND METHODS

2.1. MATERIALS

2.1.1 Test Microorganisms and Standardization of Inoculum:

The clinical fungal isolate (*Candida albicans*) and reference bacterial strains (Gram-positive, *Staphylococcus aureus* ATCC 25923 and Gram-negative organism, *Escherichia coli* ATCC 25920) used in this study were obtained on Sabouraud Dextrose Agar slant and nutrient agar slant, respectively, from Microbiology Laboratory of University of Ilorin Teaching Hospital. They were kept at 4 °C and sub-cultured at 37°C for 24 hours on their respective agar before susceptibility testing. While the bacterial plates were incubated overnight at 37°C, the fungal plate was incubated for 48 h at 37°C. The inoculum was standardized by adjusting the McFarland density; the absorbance was adjusted at 580 nm and diluted to 0.5 McFarland turbidity equivalence using a densitometer to achieve the final concentration of 1.5×10^8 cfu/mL of the bacterial strains and 1.0×10^6 spores/mL of the fungal isolate at 530 nm (Ochei and Kolhatkar, 2008). These were used

within 20- 30 minutes of standardization (Wanger, 2007).

2.1.2 Collection of leaves of the medicinal plants

The medicinal plants used in this study were selected based on the frequency of their use and availability in Adeta area of Ilorin. Ilorin is located in the Southern Guinea Savannah of Nigeria with annual rainfall and precipitation of about 1300 mm. Other climatic data of the town is maximum temperature (38 °C), maximum relative humidity (77.50 %) and a 7.1-hour daily photoperiod of 1500 mm (Ejjeji and Adeniran, 2009; Olanrewaju, 2009). The study area, Adeta, was selected based on its topographical

2.2 Extraction of the crude extracts from leaves of the plants

After authentication, extraction was done following preparation of the leaves thus; the leaves were washed, under a running tap and air-dried for five days at room temperature as described by Akerele *et al.* (2008). The dried plant materials were milled separately to a fine powder with an electric miller (Master Chef Blender, Mode MC-BL 1980, China). The powdered material of *A. indica* was weighed (10g) into two separate beakers and was extracted separately by cold percolation method using 100 ml of acetone and aqueous (w/v). The same procedure was followed for *C. procera*, *C. papaya*, and *V. amygdalina* using acetone, and aqueous as the menstruum. The extractions were done for 48 hours with constant shaking at intervals. The homogenate was filtered through Whatman filter paper (Number 1) to yield the crude extract (Nenaah and Ahmed, 2011), which was subsequently evaporated to dryness using a rotary evaporator (Model RE Zhengzhou, Henan China). The crude extracts were weighed, stored in labeled sterile airtight containers and stored at 4 °C for further use. The yield (%) of the extract was determined using the formula:

$$\text{Yield (\%)} = (\text{Dry weight of extract} \div \text{Dry weight of plant material}) \times 100$$

2.3 Sterility testing of the crude extract

This was done using a modified method described by Lalitha (2008). Serial dilution of 1.0 g of each extract was made to reduce the concentration. A quantity (1 g) of the extract was inoculated into 10 mL Mueller Hinton (Hi-Media) broth. Clarity of the broth after incubation at 37 °C

parameters. According to Persson *et al.* (2005), the topographical parameters of a place can be used to delineate its crop management potentials. The area is located in Ilorin West, Nigeria (Latitude: 8.49 North; Longitude: 4.51 East; and Elevation: 339.00m/1112.20ft). Fresh healthy leaves of *A. indica*, *C. procera*, *C. papaya*, and *V. amygdalina* were collected from Adeta area, Ilorin, Nigeria. The taxonomy of each species was established and they were authenticated at Herbarium Unit of the Department of Plant Biology, University of Ilorin, Ilorin Nigeria where voucher specimens were deposited with reference numbers UILH/007/972 for *V. amygdalina*, UILH/001/1001 for *C. procera*, UILH/004/967 for *C. papaya* and UILH/003/860 for *A. indica*.

C for 24 hours indicated the absence of contaminants.

2.4 Preparation of stock solution of the crude extracts

Stock solution of the extract was obtained by dissolving 2.0 g of the extract into sterile test tube containing 20.0 mL of 5.0 % DMSO (95 mL of water added into 5 mL of DMSO). In another test tube a sterile tube containing 20.0 mL of 5.0 % DMSO was combined, 0.5g of each plant, to give 2.0 g of the combination of plants. Subsequently, different concentrations (100.0 mg/mL, 50.0 mg/mL and 25.0 mg/mL) were further prepared from the stock solution by doubling dilution method.

2.5 Preparation of antimicrobial discs containing the crude extracts

Paper discs (6.00 mm) were punched from Whatman filter paper (No. 1). The discs were sterilized in an autoclave for 15 minutes at 15 lbs pressure and allowed to cool. About five sterilized paper discs were aseptically arranged using sterile forceps in sterile Petri-dishes. Petri dishes containing discs were labeled 100 mg/mL, 50 mg/mL and 25 mg/mL, discs in each plate were aseptically impregnated with approximately 20 µl of their respective concentrations of each solvent extract using mechanical pipettes, and they were allowed to dry before storing in labeled airtight containers at 20 °C (Brooks *et al.*, 2004).

2.6 Preparation of antimicrobial discs containing the crude extracts

Paper discs (6.00mm) were punched from Whatman filter paper (No. 1). The discs were sterilized in an autoclave for 15 minutes at 15 lbs pressure and allowed to cool. About five sterilized paper discs were aseptically arranged using sterile forceps in sterile Petri-dishes. Petri dishes containing discs were labeled 100 mg/mL, 50 mg/mL and 25 mg/mL, discs in each plate were aseptically impregnated with approximately 20 μ l of their respective concentrations of each solvent extract using mechanical pipettes, and they were allowed to dry before storing in labeled airtight containers at 20 ° C (Brooks *et al.*, 2004).

2.7 Antibacterial and Antifungal susceptibility testing of the crude extracts

Susceptibility testing of the sterile crude extract was done for all the microbial isolates by the modified Kirby Bauer disc diffusion method (Lalitha, 2008; Parekh and Chanda, 2007). Following the Clinical and Laboratory Standards Institute (CLSI) guideline; 0.1 ml of the respective standardized inoculums of each test organism was uniformly spread onto sterile Mueller Hinton Agar (Hi-Media) plates for the bacterial strains and Sabouraud Dextrose Agar (SDA) for the fungal strains. The plates were allowed to dry, subsequently, discs impregnated with the crude extracts were aseptically placed onto the agar surface and gently pressed with the applicator to ensure contact of the discs with the medium. The crude extracts were allowed to pre-diffuse from the discs into the agar medium for 1 hour on the bench before incubation at 37 °C for 24 hours (for the bacterial strains) and for 48 hours at 30 °C (for the fungal strain). The diameter of clear zones around the discs were measured (mm) with the discs and recorded as the zones of inhibition.

2.8 Preliminary phytochemical

Qualitative phytochemical analyses of the crude extracts were done following the method described by Amadi *et al.* (2004).

2.8.1 Test for Saponins

The extract (1 mL) was diluted with 3 mL of distilled water, this was shaken for 15 min and the formation of a 1 cm layer of foam indicated the presence of saponin.

2.8.2 Test for Flavonoids

The extract (1 mL) was diluted with 1 mL of Sodium hydroxide (NaOH) and hydrochloric

acid (HCL). The development of yellow solution indicated the presence of flavonoids.

2.8.3 Test for Terpenoids

The extract (1 mL) was mixed with 2 mL of chloroform and 2 mL of concentrated sulfuric acid. The formation of a reddish-brown color at the interface indicated the presence of terpenoids.

2.8.4 Test for Coumarins

The extract (1 mL) was mixed with 1 mL of sodium hydroxide (10%). The yellow color indicated the presence of coumarins.

2.8.5 Test for Glycoside

To one mL of the extract was added 20 cm³ of water, heated for 5 minutes on a water bath and filtered through Gem filter paper (12.5 cm). Then 0.2 cm³ of Fehling's solutions A and B was mixed with 5 cm³ of the filtrate until it became alkaline (tested with litmus paper). A brick-red coloration on heating showed a positive

2.8.6 Test for Alkaloids

An equal volume of the extract was mixed with concentrated hydrochloric acid, and a few drops of Mayer's reagent were added. The presence of a green color or white precipitate indicated the presence of alkaloids.

2.8.7 Test for Tannins

The extract (1 mL) was mixed with 2 mL of distilled water followed by a few drops of ferric chloride (10%). A blue or green color indicated a positive result.

2.9 Sample preparation and HPLC analysis

The HPLC fingerprinting of each solvent extract was carried out following thus; powdered dried leaves (1.0 g) was macerated with acetonitrile/water (1:1; v/v, 10.0 mL), then centrifuged for 10 minutes at 3000 rpm and filtered. The crude extract from the filtrate was assayed directly by HPLC-UV; a modular Shimadzu (Nexeramx) LC-10 system comprised of an LC-10AD pump, a CTO-10A column oven, an SPD-10A UV-DAD detector, a CBM-10A interface, and an LC-10 Workstation was used. An LC-18 column (250 mm x 4.6 mm ID x 5 mm) from (Ubondapak, Bellefonte, USA) was employed at 30 °C. Separations were done in the isocratic mode, using acetonitrile: water (40:60; v/v) at a flow rate of 1.0 mL per minute with an injection volume ("loop") of 10 μ L, UV detection was at 254 nm.

2.10 Data Analysis

All the results were obtained in triplicates (n=3), the data were analyzed statistically and presented as mean \pm standard deviation.

3. RESULTS

3.1. Percentage yield after extraction

The percentage yield from 200 g of dry raw leaves of each plant after evaporation of the filtrate to dryness was calculated as powdered to

Table 2. Percentage yield of acetone and aqueous extracts of the plants used in this study

Plant Extract	<i>A. indica</i>		<i>C. procera</i>		<i>C. papaya</i>		<i>V. amygdalina</i>	
	Acetone	Aqueous	Acetone	Aqueous	Acetone	Aqueous	Acetone	Aqueous
Yield from Raw Dry Powder (g)	29.5	23	29.2	21.6	20.9	20.4	28.6	21.6
Percentage Yield (%)	14.75	11.5	14.6	10.8	10.3	10.2	14.3	10.8

3.2. Qualitative phytochemical screening

The phytochemical screening results of aqueous and acetone extracts of the leaves of *A. indica*, *C. papaya*, *V. amygdalina*, and *C. procera* showed the presence of several phytochemical constituents (Table 3). Extracts of *A. indica* leaves showed the presence of varying phytochemical constituents; coumarins, alkaloid, glycosides, protein, saponin were present in the aqueous, and acetone extracts respectively while anthraquinone, flavonoid, and tannin were only present in acetone extract and not in aqueous extract. Terpenoid was present in aqueous extract but absent in acetone extract. The presence of these constituents varied in aqueous and acetone extracts of leaves of *C. papaya* as anthraquinone, alkaloid, flavonoid, glycosides, and saponin were present in aqueous and acetone extracts, respectively. Coumarins and tannin were only present in acetone extract but absent in aqueous extract while protein and terpenoid were only present in aqueous extract and absent in acetone extract. Aqueous and Acetone extracts of leaves of *V. amygdalina* revealed the presence of anthraquinone, alkaloid, coumarin, saponin, tannin, and terpenoid. Flavonoid was present in acetone extract only while glycosides as well as protein were present in aqueous extract only.

yield; 29.50 g (14.75 %) for acetone extract and 23.00 g (11.50 %) for aqueous extract of *A. indica*. *C. procera* was 29.20 g (14.60 %) of acetone extract and 21.60 g (10.80 %) of the aqueous extract. Dry powder of *C. papaya* was 20.90 g (10.30 %) of acetone extract and 20.40 g (10.20 %) for aqueous extract. *V. amygdalina* was 28.60 g (14.30 %) of acetone extract and 21.60 g (10.80 %) for aqueous extract.

Alkaloid, flavonoid, protein, saponin, and terpenoid were present in the aqueous and acetone extracts of *C. procera* leaves. Anthraquinone, coumarin, and glycoside were only present in the aqueous extracts and tannin was only present in the acetone extract.

3.3. In vitro antimicrobial screening

The susceptibility testing of the crude extracts is given in Table 5. Comparatively, among the tested extracts at 100 mg/mL, the highest zone of inhibition (16.06 mm) was given by acetone extract of the combination of the three plants (*C. procera*, *V. amygdalina* and *A. indica*) against *E. coli* while the lowest zone of inhibition (8.00 mm) was given by aqueous extract of *A. indica* against *S. aureus*. At the tested concentration of 50 mg/mL, acetone extracts of *A. indica* and *V. amygdalina* individually gave the highest zones of inhibition (17.00 mm) against *C. albicans* and *E. coli*, respectively. At 25 mg/mL concentration tested, the highest zone of inhibition (21.00 mm) was given by acetone extract of *V. amygdalina* against *E. coli* while aqueous extract of *C. procera* gave the least zone of inhibition (6.00 mm) against *S. aureus*.

Table 3. Phytochemicals in acetone and aqueous extracts of the plants

Constituents	<i>A. indica</i>		<i>C. papaya</i>		<i>V. amygdalina</i>		<i>C. procera</i>	
	Aqueous	Acetone	Aqueous	Acetone	Aqueous	Acetone	Aqueous	Acetone
Anthraquinones	–	+	+	+	+	+	+	–
Coumarins	+	+	–	+	+	+	+	–
Alkaloid	+	+	+	+	+	+	+	+
Flavonoids	–	+	+	+	–	+	+	+
Glycosides	+	+	+	+	+	–	+	–
Protein	+	+	+	–	+	–	+	+
Saponin	+	+	+	+	+	+	+	+
Tannin	–	+	–	+	+	+	–	+
Terpenoid	+	–	+	–	+	+	+	+

+ Presence

– Absence

Table 4. Diameter of zones of inhibition (mm) of the different plant extracts against the test microorganisms at different concentrations

Plants	Solvents	100 mg/mL			50 mg/mL			25 mg/mL		
		<i>E. coli</i>	<i>S. aureus</i>	<i>C. albicans</i>	<i>E. coli</i>	<i>S. aureus</i>	<i>C. albicans</i>	<i>E. coli</i>	<i>S. aureus</i>	<i>C. albicans</i>
<i>A. indica</i>	Acetone	15.00±0.81	16.00±1.18	15.00±0.63	11.00±2.03	12.7±0.63	17.67±0.26	20.00±1.13	11.5±0.53	16.00±2.16
	Aqueous	10.00±0.21	8.00±1.18	10.00±2.10	9.00±0.41	8.41±1.20	8.89±1.30	9.21±1.28	7.36±0.18	7.80±1.22
<i>C. procera</i>	Acetone	16.5±2.13	11.00±2.03	11.00±0.31	15.5±0.63	13.00±0.31	15.00±0.23	15.00±2.63	11.00±0.13	13.5±0.32
	Aqueous	10.20±1.84	8.12±0.84	10.00±1.29	8.23±1.21	8.10±1.34	9.38±0.13	7.42±0.28	6.00±1.02	7.82±0.22
<i>C. papaya</i>	Acetone	15.00±0.23	14.00±1.02	15.00±2.01	10.00±1.13	12.00±1.14	13.00±2.13	11.00±1.92	13.5±2.16	16.00±0.13
	Aqueous	9.10±2.01	10.10±0.18	9.42±1.82	9.00±1.41	8.84±1.20	9.91±0.84	8.01±0.28	8.28±1.14	8.82±0.88
<i>V. amygdalina</i>	Acetone	16.00±1.21	12.75±0.13	16.00±0.14	17.67±1.16	13.67±2.10	17.00±0.12	21.00±2.16	16.00±0.11	20.5±1.01
	Aqueous	12.84±1.26	10.52±1.68	10.02±1.86	10.94±1.48	9.32±0.26	9.92±1.82	9.42±1.87	8.96±1.24	8.38±0.83
Combination of the plants	Acetone	17.06±1.10	15.82±2.31	14.50±1.01	13.00±1.42	13.33±1.22	13.5±0.81	15.33±1.04	14.00±0.82	14.00±1.61
	Aqueous	12.91±1.82	12.13±1.14	11.02±1.86	12.14±0.18	10.12±1.28	10.19±0.14	9.22±1.13	10.10±1.15	9.42±1.36

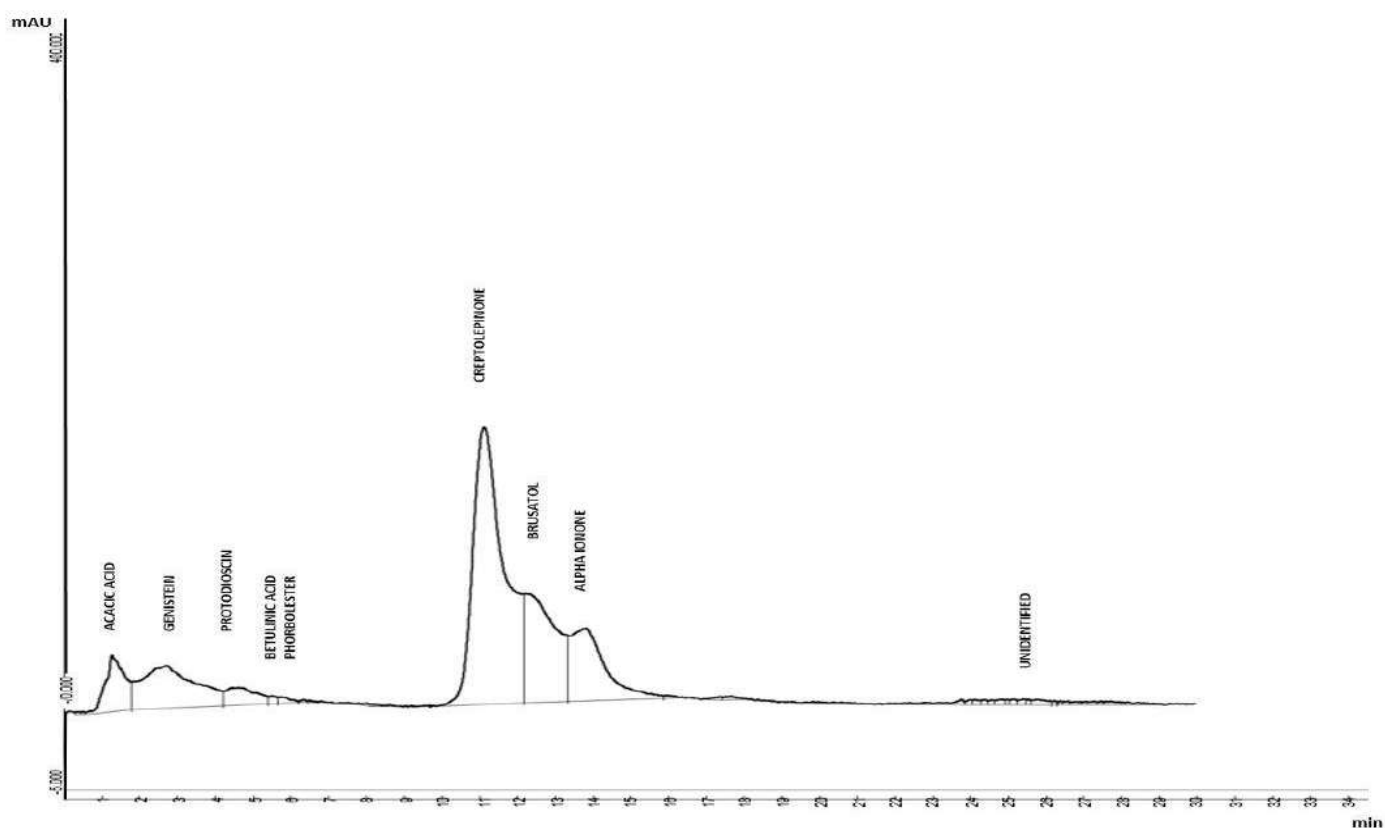
Table 5. Diameter of zones of inhibition (mm) of the control agents

Control	Zone of inhibition (mm)		
	<i>E. coli</i>	<i>S. aureus</i>	<i>C. albicans</i>
Aqueous	7.10±2.00	7.00±0.10	7.02±1.22
5% DMSO	10.10±1.21	11.10±0.22	9.14±0.01

3.4. HPLC analysis of acetone extracts of leaves of *V. amygdalina*, *A. indica*, and *C. papaya*

The concentration of components represented as peak heights, separated in leaves of *C. papaya*, *A. indica*, and *V. amygdalina* sample is shown in the chromatograms profile given in Figures 1, 2 and 3. The percentage of peak heights of compounds detected in *V. amygdalina* is presented in Figure 4; vernodalin (48.8 %) was detected in the highest amount while andrographoside (0.6 %) was the least compound

detected. Out of the seven fractions of compounds (Figure 5) separated in *A. indica*, myricetin (39.6 %), was detected in the highest quantity while alpha funebren (1.5 %) was detected in the least quantity. Out of the compounds detected in *C. papaya* (Figure 6) creptolepinone (47.0 %) was the most abundant while phorbol ester (1.2 %) was the least.

**Figure 1:** Chromatogram profile of Leaves of *C. papaya* by HPLC

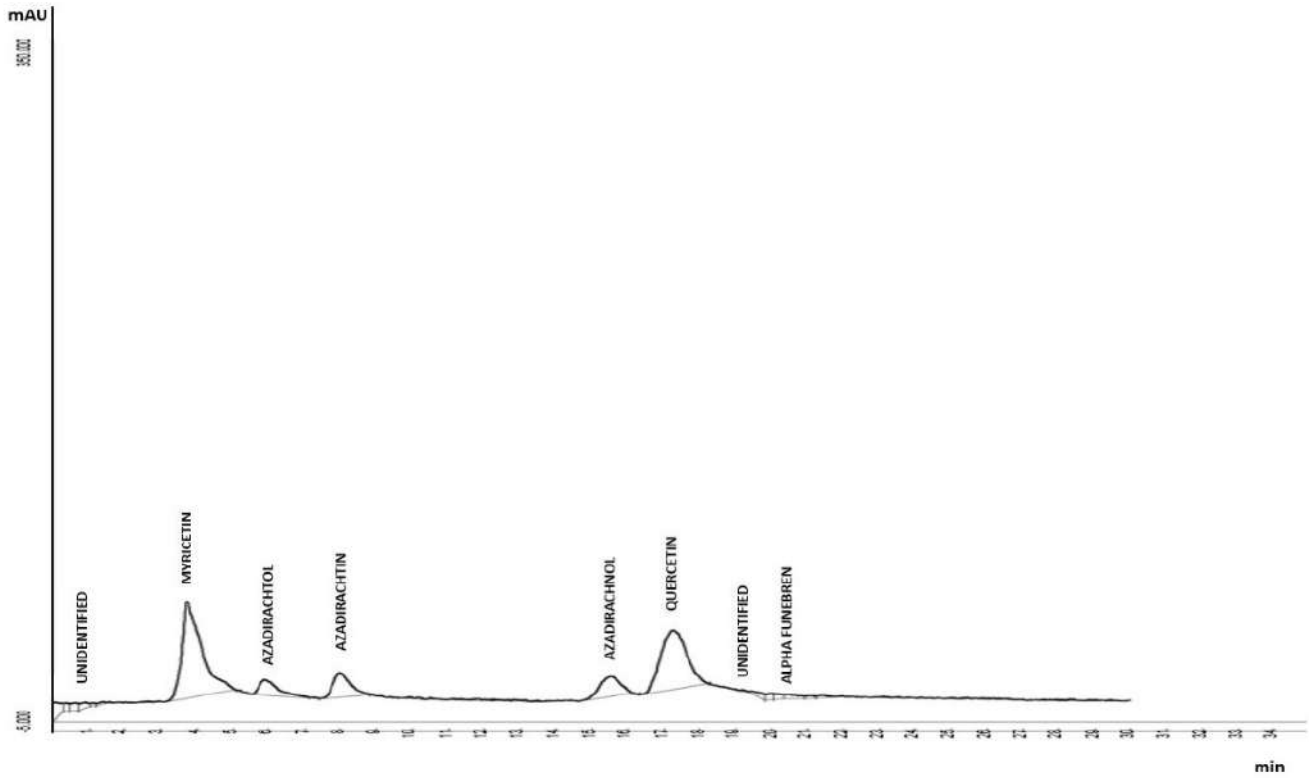


Figure 2: Chromatogram profile of Leaves of *A. indica* by HPLC

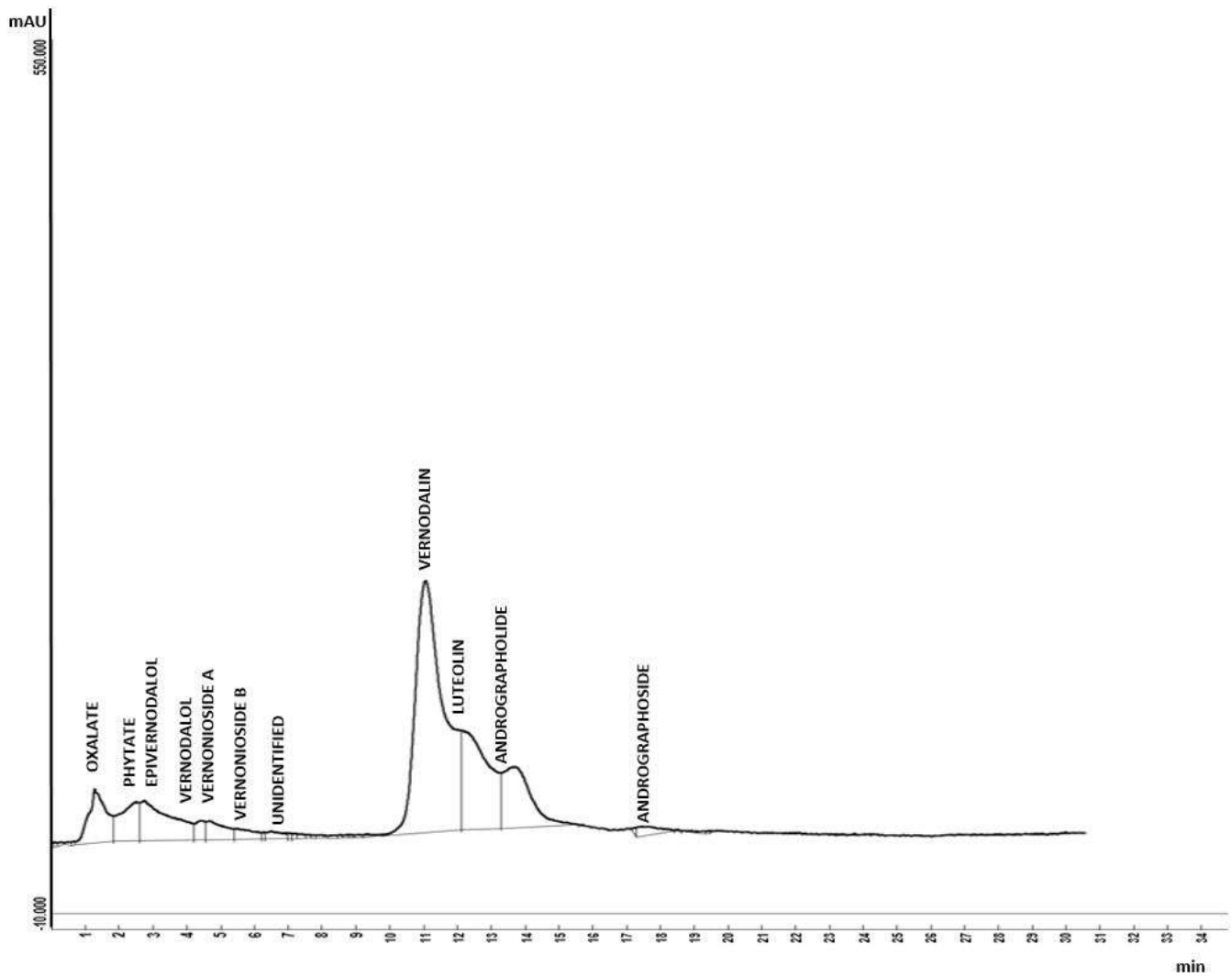


Figure 3: Chromatogram profile of Leaves of *V. amygdalina* by HPLC

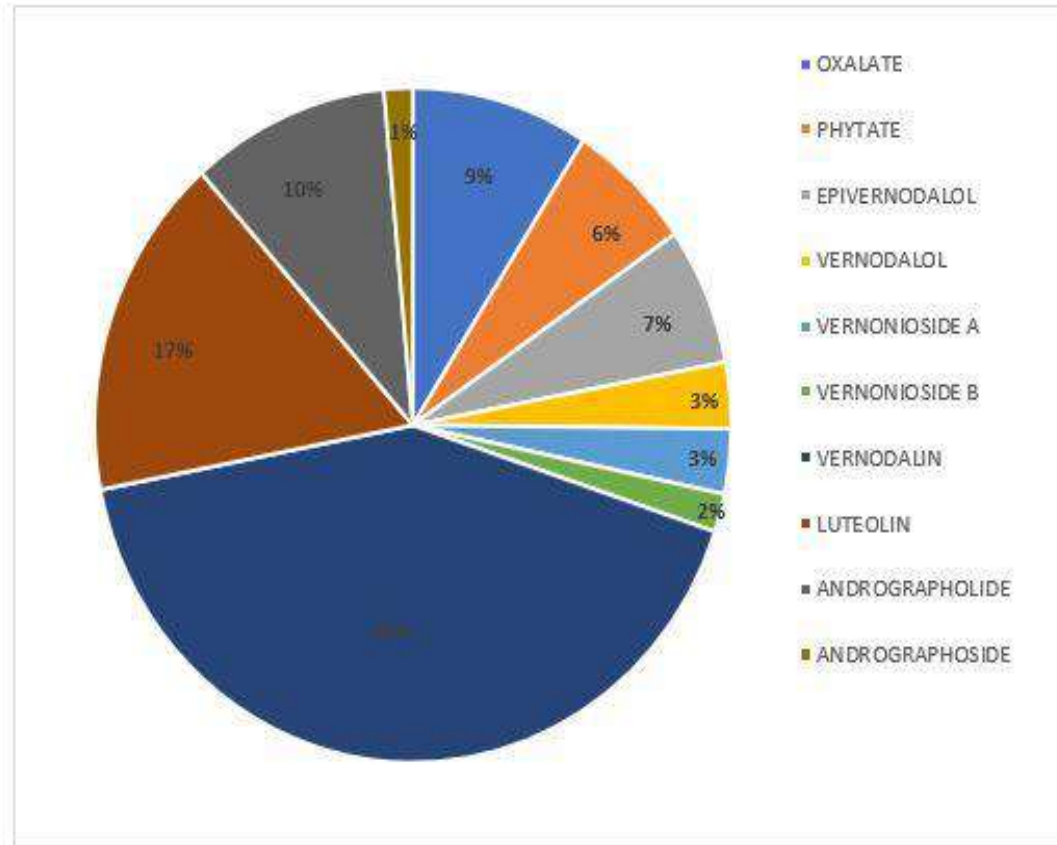


Figure 4: Percentage occurrence of compounds in detected in *V. amygdalina*

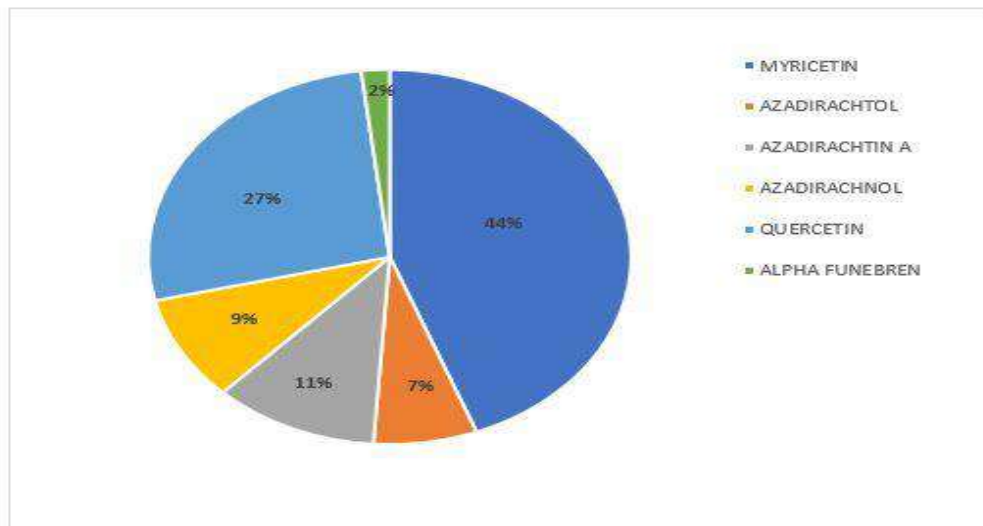


Figure 5: Percentage occurrence of compounds in detected in *A. indica*

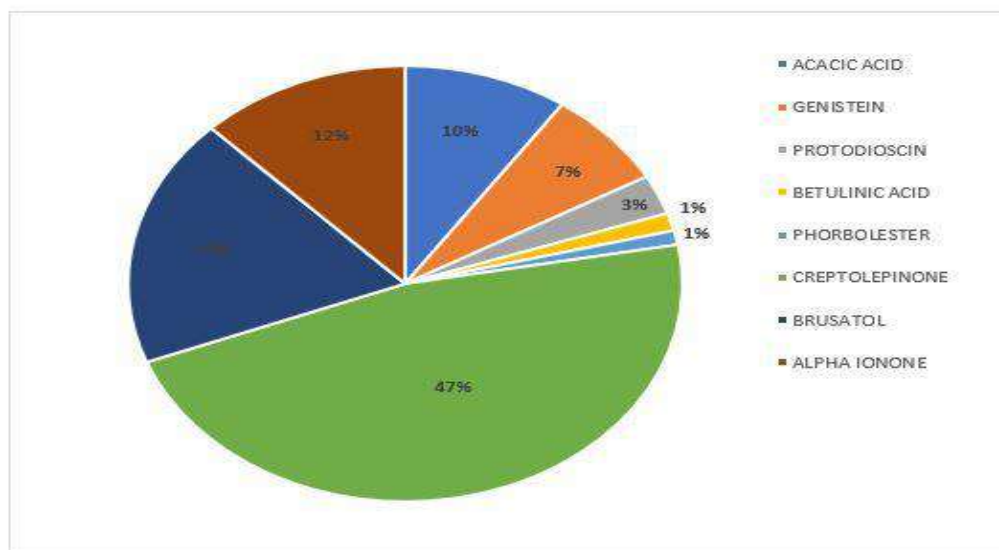


Figure 6: Percentage occurrence of compounds in detected in *C. papaya*

4. DISCUSSION

Medicinal plants are known to harbor inexhaustible compounds known as phytochemicals, which have been reported to be biologically active on the human body (Effraim *et al.*, 2007). Therefore, screening of plants for these phytochemicals has been of great interest to scientists, with the view to detect new drugs against several diseases. In the present study, acetone and aqueous were individually used as a solvent to extract components from *C. papaya*, *A. indica*, *V. amygdalina*, and *C. procera*. This was with the aim of obtaining a variable yield of compounds. As observed in this work, higher yield was obtained for acetone extract of all the plants than aqueous extract. This is in line with the statement that the choice of solvent used in the extraction of plants may affect the yield after extraction (Ncube *et al.*, 2008).

However, this study recorded the presence of secondary metabolites including alkaloid, coumarin, saponin, tannin, anthraquinone and terpenoid in all the plant extracts, but in no particular order. This may be because the solvents used for extraction are both polar solvents and are able to extract similar compounds from the plants. Ajaiyeoba (2002) reported that polar solvents (acetone and aqueous, inclusive) extract more active compounds than non-polar solvents. In another study, it is reported that the extraction of tannins and other phenolics was better in aqueous

acetone than in aqueous methanol (Okunade *et al.*, 2007). In addition, Enyi-Idoh *et al.* (2012) previously reported the presence of compounds such as alkaloid, saponin, tannin, and terpenoid in extracts of *V. amygdalina*. Imaga and Bamigbetan (2013) also reported the presence of flavonoid in extracts of *V. amygdalina*. Andarwulan *et al.* (2012), Sikanda *et al.* (2013) and Nguyen *et al.* (2015) variously reported the presence of flavonoids in *C. papaya* leave extracts, and that agrees with what was reported on *C. papaya* in this work.

The result of phytochemicals of *A. indica* in this study is in accord with former studies that reported the presence of tannins, saponins, flavonoids, alkaloids, glycosides in the ethanolic leaf extract of *A. indica* (Nguyen *et al.*, 2015). Presence of alkaloids, saponins and other phytochemicals in all the plant extracts may be indicative of the presence of broad-spectrum antimicrobial compounds which may be responsible for the antimicrobial properties exhibited by the plants. Previous studies equally showed that secondary metabolites of plants are significant sources of microbicides (Atangwho *et al.*, 2010). Edeoga *et al.* (2005), in his study, reported the physiological and antimicrobial effects of various phytochemicals. In their own study, Ireland and Dziejczak (1986) reported that antimicrobial activities of plants may be attributed to the presence of compounds such as saponins. Another study reported that saponins has antimicrobial activity (Ncube *et al.*, 2008), while

Aliero and Aliero, (2008) and Amaral *et al.* (2009) variously reported the antibacterial activities of alkaloids and flavonoids. Flavonoids have also been confirmed to show antidiarrheal effects (Meite *et al.*, 2009), and this may account for the observed effectiveness of the studied plants against *E. coli*, a known causative agent of gastroenteritis and traveler's diarrhea. Furthermore, tannins have antibacterial properties as they are able to react with proteins to form stable water-soluble compounds that kill bacteria by cell membrane damage (Aliero and Aliero, 2008). Sodipo *et al.* (2000) reported that most phytochemicals are natural antibiotics, as they help the body in fighting infections caused by microorganisms.

In concurrence with the current study on the antimicrobial screening of plant extracts against *E. coli*, *S. aureus* and *C. albicans*, is the antibacterial evaluation of different plants against similar bacterial strains (Khan *et al.*, 2013). Hamadameen (2019) also reported the antibacterial susceptibility of *E. coli* ATCC 25922 while Saeed and Saadullah (2019) reported an antifungal susceptibility of *C. albicans* to some medicinal plants. Similar to our findings are the works of Eja *et al.* (2011), Ogunadare (2011) and Oshodi *et al.* (2004), who variously reported the antimicrobial potentials of *V. amygdalina* on *E. coli* and *S. aureus*. However, the observed variation in the levels of susceptibility of the test organisms to the plant extracts may be attributed to the differences in the cell wall structures of the test organisms. Prescott *et al.* (2001) reported that the potency of an antimicrobial agent varies with target species and Gram-negative outer membrane act as an extra barrier to many environmental substances including antimicrobial agents Tortora *et al.* (2004). In the report of Shittu *et al.* (2004) on *C. procera*, a significant reduction in the total viable microbial counts was observed.

Although all the plant extracts, irrespective of their type and concentration tested, demonstrated varying levels of antimicrobial activities by producing different zones of inhibition (even at the lowest concentration tested) around the test organisms. This may be ascribed to the varying quality of phytochemicals present in them. Iwalokun *et al.* (2004) reported that water could be an ideal solvent for extraction, this is notable in the appreciable levels of antimicrobial

activities exhibited by water extracts of the studied plants. However, the zone of inhibition produced by aqueous extracts was not as high as what was produced by acetone extracts of the plants. This may be justified by higher polarity of acetone than water, and consequently the solubility of more components in acetone. This is in line with the report of Uwah *et al.* (2013) that solubility of compounds occurs at different rates in solvents during extraction.

On an average, *V. amygdalina* displayed highest activity, followed by *A. indica*, *C. procera* and *C. papaya*. However, it was observed that the zones of inhibitions produced by the plant extracts was higher than what was produced when the control agents (aqueous and 5% DMSO) were used individually against the test organisms. This may be attributed to the mixed phytoconstituents in plant extracts compared to the single components of the control agents. Also, when the effects of combination of all the plants were tested at different concentrations against the test organisms, no remarkable effect was observed at 50 mg/mL and 25 mg/mL concentrations but a synergistic effect (an increase in the level of activities) was observed at 100 mg/mL concentration against *E. coli*. This finding concurs with several interesting outcomes that have been reported on the use of a mixture of natural products to treat diseases, most notably the synergistic effects and polypharmacological application of plant extracts reported by Gibbons (2003).

Quantitative analysis is a significant tool to detect the active components in plants (Fraise *et al.*, 2011). HPLC (High-Performance Liquid Chromatography) has emerged as the most popular, powerful and versatile form of chromatography used for the qualitative, semi-qualitative and quantitative phytochemical analysis of herbal drugs. Generally, the majority of these components are responsible for some particular pharmacological effects (Song *et al.*, 2007). The active components of *V. amygdalina* have long been shown to be mainly sesquiterpene lactones like vernodalin and vernoamygdalin and steroid glycosides like vernonioside B1 and vernoniol B. This agrees with our findings in which sesquiterpene lactone (vernodalinol) is among the compounds detected in our study. In various studies, sesquiterpene

lactones have been reported to possess a range of antimicrobial properties (Kupchan *et al.*, 1969; Luo *et al.*, 2011; Amodu *et al.*, 2013). Similar findings have also been reported on components detected in *V. amygdalina* as sesquiterpene lactones, vernolide, vernodalol (Erasto *et al.*, 2007). These support our finding, where Vernodalin was detected in the highest percentage of peak height and that may be attributed to the appreciable antimicrobial effect obtained by *V. amygdalina* extract against the test microorganisms.

Several studies have characterized bioactive compounds from *A. indica* as several types of sesquiterpene lactones (Farombi and Owoeye, 2011). This is in consistence with our study, as six bioactive compounds (Myricetin, quercetin, azadirachtol, azadirachtin A, azadirachnol, and alpha funebren) were detected in *A. indica*, with myricetin and quercetin detected in the highest amount. Sadeghian and Mortazaienezhad (2007) also reported the presence of Azadirachtin in aqueous leaves extracts of *A. indica*. In another study conducted by Soni *et al.* (2012), it was reported that 73.62 % concentration of Azadirachtin was detected in *A. indica*. Cseke *et al.* (1996) reported that Azadirachtin A, with the Empirical formula C₃₅H₄₄O₁₆ is the most abundant biologically active compound in *A. indica*. The antibacterial activities of *A. indica* leave observed in this work may therefore be attributed to the presence of these compounds.

The antimicrobial effect of *C. papaya* extract observed in this study coincides with the eight fractions of compounds (Cryptolepinone, brusatol, Acacic acid, genistein, protodioscin, betulinic acid, phorbol ester) detected by HPLC assay. Genistein has been documented to be present in *C. papaya* (Tan *et al.*, 2012). Sawyer *et al.* (1995) reported that cryptolepine cause severe ultrastructural changes in bacteria and fungi. This finding was further validated by his findings in 2004, which demonstrated the occurrence of lysis in susceptible organisms following exposure to cryptolepine (Sawyer *et al.*, 2004). Acacic acid, a complex glycoside and brusatol (a quassinoid) detected in this work indicate further promising cytotoxic and antimicrobial potentials of *C. papaya*. Brusatol have been reported to have positive impacts on the treatment of various kinds of disease (Beutler, 2009).

5. CONCLUSION

This study has revealed that different solvent extracts of *A. indica*, *C. papaya*, *V. amygdalina*, and *C. procera* harbor varying metabolites and showed different levels of antimicrobial activities against the test pathogens. Therefore, this may serve as baseline information on the quality of plants sourced from Adeta area, Ilorin. It may also provide insightful lead towards the discovery of new bioactive natural products that may be used in the development of new therapeutic drugs against diseases caused by pathogens tested in this study. In line with the findings in this study, it is suggested that further research on the active constituents of plants' extracts should be further isolated, purified and tested individually and in combinations, to ascertain the type of effect (synergistic or antagonistic effects) produced by the constituents.

Acknowledgements

The authors are grateful to Mr. Dele Aiyepetu (University of Ilorin, Ilorin, Nigeria) for the technical assistance provided during this study.

Conflict of Interest (1)

Conflict of Interest Statement

We declare that we have no conflict of interest.

Funding Source

This research did not receive any specific grant from funding agencies in the public, commercial, or not-for-profit sectors.

References

- AJAIYEBOBA, E. 2002. Phytochemical and antibacterial properties of *Parkia biglobosa* and *Parkia bicolor* leaf extracts, *African Journal of Biomedical Research*, 5(1), 125 – 129.
- AKERELE, J.O., OBASUYI, O., EBOMOYI, M.I., OBOH, I.E. AND UWUMARONGIE, O.H. 2008. Antimicrobial activity of ethanol extracts and fractions of the seeds of *Garcinia kola* Hackel (Guttiferae), *African Journal of Biotechnology*, 7(2), 169-172.
- ALIERO, A., ALIERO, B.L. AND BUHARI, U. 2008. Preliminary phytochemical and antibacterial screening of *Scadoxus multiflorus*, *International Journal of Pure & Applied Sciences*, 2(4), 13-17.
- AMADI, B.A., AGOMUO, E.N. AND IBEGBULEM, C.O. 2004. *Phytochemical tests: Research methods in Biochemistry*. Owerri: Supreme Publishers.

- AMARAL, S., MIRA, L., NOGUEIRA, J.MF, DA SILVA, A. P. AND FLORENCIO, M.H. 2009. Plant extracts with anti-inflammatory properties - A new approach for characterization of their bioactive compounds and establishment of structure-antioxidant activity relationships, *Bioorganic & Medicinal Chemistry*, 17(5), 1876-1883.
- AMODU, A., ITODO, S.E. AND MUSA, D.E. 2013. Nigerian Foodstuffs with Tumour Chemosuppressive Polyphenols, *International Journal of Pharmaceutical Science Invention*, 2(1), 12-17.
- ANDARWULAN, N., KURNIASIH, D., APRIADY, R.A., RAHMAT, H., ROTO, A.V. AND BOLLING, B.W. 2012. Polyphenols, carotenoids, and ascorbic acid in underutilized medicinal vegetables, *Journal of Functional Foods*, 4(1), 339- 347.
- ATANGWHO, I.J., EBONG, P.E. EYONG, E.U. AND ETENG, M.U. 2010. Combined administration of extracts of *Vernonia amygdalina* (Del) and *Azadirachta indica* (A. Juss) mimic insulin in time-course body weight and glucose regulation in diabetic and non- diabetic rats, *Nigerian Journal of Biochemistry and Molecular Biology*, 25, 44-49.
- BANSO, A., ADEYEMO, S.O. AND JEREMIAH, P. 1999. Antimicrobial properties of *Vernonia amygdalina* extract, *Journal of Applied Science and Management*, 3, 9 - 11.
- BEUTLER, J. A., KANG, M. I., ROBERT, F., CLEMENT, J. A., PELLETIER, J., COLBURN, N. H., MCKEE, T. C., GONCHAROVA, E., MCMAHON, J. B. AND HENRICH, C. J. 2009. Quassinoid inhibition of AP-1 function does not correlate with cytotoxicity or protein synthesis inhibition. *Journal of Natural Products*, 72(3), 503-6.
- BOLIGON, A.A., BRUM, T.F., FROHLICH, J.K., FROEDER, A.L.F. AND ATHAYDE, M.L. 2012. HPLC/DAD profile and determination of total phenolics, flavonoids, tannins and alkaloids contents of *Scutia buxifolia* Reissek stem bark, *Research Journal of Phytochemistry*, 6(3), 84-91.
- BROOKS, G.F., CARROLL, K.C., BUTEL, J.S., MORSE, S.A. AND MIETZNER, T.A. 2012. *Jawetz, Melnick and Adelberg's. Medical Microbiology*, Twenty Sixth Ed. New York, McGrawHill Publishing Company, Limited
- CALIXTO, J.B. 2000. Efficacy, safety, and quality control, marketing regulatory guidelines for herbals (phytotherapeutic agents), *Brazilian Journal of Medical and Biological Research*, 33(2),179 – 189.
- Cseke, L. J., Kirakosyan, A., Kaufman, P. B., Warber, S. L., Duke, J. and Briemann, H. L. 2006. *Natural Products from Plants*, 2nd edition, Taylor and Francis Group.
- EDEOGA, H.O., OKWU, D.E. AND MBAEBIE, B.O. 2005. Phytochemical constituents of some Nigerian medicinal plants, *African Journal of Biotechnology*, 4(7), 685-688.
- EFFRAIM, I.D., SALAMI, H.A. AND OSEWA, T.S. 2000. The effects of aqueous leaf extract of *Ocimum gratissimum* on haematological and biochemical parameters in rabbits, *African Journal of Biomedical Research*, 3(3), 175-179.
- EJA, M.E., ARIKPO, G.E., ENYI-IDOH, K.H. AND IKPEME, E.M. 2011. An evaluation of the antimicrobial synergy of Garlic (*Allium sativum*) and Utazi (*Gongronema latifolium*) on *Escherichia coli* and *Staphylococcus aureus*, *Malaysian Journal of Microbiology*, 7(1), 49-53.
- EJEJI, C.J. AND KAMORU, A. 2010. Effects of water and fertilizer stress on the yield, fresh and dry matter production of grain Amaranth (*Amaranthus cruentus*). *Australian Journal of Agricultural Engineering*, 1(1), 18-24.
- EL-SAID, S.M. AND AL-BARAK, A.S. 2011. Extraction of insulin like compounds from bitter melon plants, *American Journal of Drug Discovery and Development*, 1(1), 1-7.
- ENYI-IDOH, K.H., UTASALO, S.J., EPOKE, J., ARIKPO, G.E. AND EJA, M.E. 2012. Time-dependent evaluation of the antimicrobial and phytochemical properties of *Vernonia amygdalina* and *Gongronema latifolium*, *The Internet Journal of Herbal and Plant Medicine*, 1(2), 1-7.
- ERASTO, P., GRIERSON, D.S. AND AFOLAYAN, A.J. 2007. Evaluation of antioxidant activity and the fatty acid profile of the leaves of *Vernonia amygdalina* growing in South Africa, *Food Chemistry*, 104(2), 636-642.
- FAROMBI, E.O. AND OWOEYE, O. 2011. Antioxidative and chemopreventive properties of *Vernonia amygdalina* and *Garcinia biflavonoid*, *International Journal of Environmental Research and Public Health*, 8(6), 2533-2555.
- FRAISSE, D., FELGINES, C., TEXIER, O. AND LAMAISON, J.L. 2011. Caffeoyl Derivatives: Major antioxidant compounds of some wild herbs of the Asteraceae family, *Food and Nutrition Sciences*, 2(3), 181-192.
- GIBBONS, S. 2003. An overview of plant extracts as potential therapeutics, *Expert Opinion on Therapeutic Patents*, 13(4), 489-497.
- HAMADAMEEN, B.M. AND HAMAD AMEEN, D. M. 2019. Synthesis, characterization, and antibacterial activity of Novel Mutual Non-Steroidal Anti-inflammatory prodrugs, *ZANCO Journal of Pure and Applied Science*, 31(6);61-74.
- IMAGA, N.O.A. AND BAMIGBETAN, D.O. 2013. *In vivo* Biochemical Assessment of Aqueous Extracts of *Vernonia amygdalina* (Bitter leaf), *International Journal of Nutrition and Metabolism*, 5 (2), 22-27.

- IRELAND, P.A. AND DZIEDZIC, S.Z. 1986. Effect of hydrolysis on sapogenin release in Soya, *Journal of Agricultural and Food Chemistry*, 34(6), 1037-1041.
- IRVINE, F.R. 1961. *Woody plants of Ghana*. London: Oxford University Press
- IWALOKUN, B.A., BAMIRO, S.B. AND DUROJAIYE, O.O. 2004. An antimicrobial evaluation of *Vernonia amygdalina* (Compositae) against gram-positive and gram-negative bacteria from Lagos, Nigeria, *West African Journal of Pharmacology and Drug Research*, 19, 9-15
- KHAN UA, RAHMAN H, NIAZ Z, QASIM M, KHAN J, TAYYABA AND REHMAN, B. 2013. Antibacterial activity of some medicinal plants against selected human pathogenic bacteria, *European Journal of Microbiology & Immunology*, 3(4), 272-274.
- KHIRSTOVA, P. AND TISSOT, M. 1995. Soda-anthroquinone pulping of *Hibiscus sabdariffa* (Karkadeh) and *Calotropis procera* from Sudan, *Bioresource Technology*, 53(1), 67-72.
- KUMAR, S., JENNA, P.K., SABNAM, S., KUMARI, M., TRIPATHY, P.K. 2010. Antibacteria activity of the flowers of *Woodfordia fruticosa* on different microorganism, *International Journal of Pharmaceutical Sciences and Research*, 4, 3225-3228.
- KUPCHAN, S.M., HEMINGWAY, R.J., KARIM, A. AND WERNER, D. 1969. Tumor inhibitors. XLVII. Vernodalinal and vernomygdin, two new cytotoxic sesquiterpene lactones from *Vernonia amygdalina* Del, *Journal of Organic Chemistry*, 34(12), 3908–3911.
- LALITHA, M.K. 2008. Manual on the Antimicrobial susceptibility testing. Published by the Indian Association of Medical Microbiologists. Available from https://www.google.com/url?sa=t&rct=j&q=&esrc=s&source=web&cd=1&cad=rja&uact=8&ved=2ahUKEwjK1cetttbmAhWWSHUIHXucDJYQFjAAegQIAxAC&url=http%3A%2F%2Fwww.ijmm.org%2Fdocuments%2FAntimicrobial.doc&usg=AOvVaw1DL7w_wctLZW7ixpYhCOuMI. Retrieved on the 13th February, 2020.
- LUO, X., JIANG, Y., FRONCZEK, F.R., LIN, C., IZEBVIGIE, E.B. AND LEE, K.S. 2011. Isolation and structure determination of a sesquiterpene lactone (vernodalinal) from *Vernonia amygdalina* extracts, *Pharmaceutical Biology*, 49(5), 464-470.
- Meite, S., N'guessan, J.D., Bahi, C., Yapi, H.F., Djaman, A.J. and Guina, F.G. 2009. Antidiarrheal activity of the ethyl acetate extract of *Morinda morindoides* in rats, *Tropical Journal of Pharmaceutical Research*, 8(3), 201-207.
- NCUBE, N. S., AFOLAYAN, J.A. AND OKOH, A.I. 2008. Assessment techniques of antimicrobial properties of natural compounds of plant origin: current methods and future trends, *African Journal of Biotechnology*, 17(12), 1797-1806.
- NENAAH, E.G. AND AHMED, M.E. 2011. Antimicrobial Activity of Extracts and Latex of *Calotropis procera* (Ait.) and Synergistic Effect with Reference Antimicrobials, *Research Journal of Medicinal Plants*, 5(6),706-716.
- NGUYEN, T.T., PARAT, M.O., HODSON, M.P., PAN, J., SHAW, P.N. AND HEWAVITHARANA, A.K. 2015. Chemical characterization and *in vitro* cytotoxicity on squamous cell carcinoma cells of *Carica papaya* leaf extracts, *Toxins*, 8(1), 1-11.
- OCHEI, J.O., KOLHATKAR, A.A. 2008. *Medical Laboratory Science: Theory and Practice*. New York: McGrawHill Publishing Company, Limited
- OGUNDARE, A.O. 2011. Antibacterial properties of the leaf extracts of *Vernonia amygdalina*, *Ocimum gratissimum* *Corchoroils olitorius* and *Manihot palmate*. *Journal of Microbiology and Antimicrobials*, 3(4): 77-86.
- OKOKO, T. AND ERE, D. 2012. Reduction of hydrogen peroxide-induced erythrocyte damage by *Carica papaya* leaf extract, *Asian Pacific Journal of Tropical Biomedicine*, 2(6), 449–453.
- OKUNADE, M.B., ADEJUMOBI, J.A., OGUNDIYA, M.O. AND KOLAPO, A.L. 2007. Chemical, Phytochemical compositions and antimicrobial activities of some local chewing sticks used in South Western Nigeria, *Journal of Phytopharmacotherapy and Natural Product*, 1(1), 49-52
- OLANREWAJU, R. M., 2009. Climate and the Growth Cycle of Yam Plant in the Guinea Savannah Ecological Zone of Kwara State, Nigeria. *Journal of Meteorological and Climate Science*, 7: 43-48.
- OSHODI, A.A., AMOO, I.A. ELEYINMI, A.F. 2004. Antimicrobial activity of aqueous extracts of *Vernonia amygdalina*, *Garcinia kola* and *Gongronema latifolium* and their blends on some beer spoilage organisms, *Technical Quaterly*, 41(4), 398–402.
- PANDEY, S., CABOT, P.J., SHAW, P.N. AND HEWAVITHARANA, A.K. 2016. Anti-inflammatory and immunomodulatory properties of *Carica Papaya*, *Journal of Immunotoxicology*, 13(4), 590-602.
- PAREKH, J. AND CHANDA, S.V. 2007. *In vitro* antimicrobial activity and phytochemical analysis of some Indian medicinal plants, *Turkish Journal of Biology*, 31(1), 53-58.
- PAUL, R.K., IRUDAVARAJ, V., JOHNSON, M. AND PATRIC, R.D. 2011. Phytochemical and anti-bacterial activity of epidermal glands extract of *Christella parasitica* (L.) H. Lev, *Asian Pacific Journal of Tropical Biomedicine*, 1(1), 8-11.
- PERRY, E.K., PICKERING, A.T., WANG, W.W., HOUGHTON, P.J. AND PERRY, N.S. 1999. Medicinal plants and Alzheimer's disease: from

- ethnobotany to phytotherapy, *Journal of Pharmacy and Pharmacology*, 51(5), 527-534.
- PERSSON, A. PILESJO, P. AND EKLUNDH, L. 2005. Spatial Influence of Topographical Factors on Yield of Potato (*Solanum tuberosum* L.) in Central Sweden. *Precision Agriculture*, 6(4), 341-357.
- PHILIP, K., MALEK, S.N.A., SANI, W., SHIN, S.K., KUMAR S, LAI, H.S., LEE, G. AND SYARIFAH-NUR, S.A. 2009. Antimicrobial activity of some medicinal plants from Malaysia, *American Journal of Applied Sciences*, 6(8), 1613-1617.
- PRESCOTT, L.M., HARLEY, J.P. AND KLEIN, D.A. 2001. *Microbiology*. Fifth Ed. New York: McGrawHill Publishing Company, Limited.
- RAHMAN, M.M., GRAY, A.I., KHONDKAR, P., SARKER, S.D. 2008. Antibacterial and antifungal activities of the constituents of *Flemingia paniculate*, *Pharmaceutical Biology*, 46(5), 356-359.
- REDDY, C.L., KUPPAST, I.J., VEERASHEKAR, T. AND VALLI-KANAGARIA, N.S.S.A. 2013. A review on pharmacological activities of *carica papaya*, *International Journal of Universal Pharmacy and Bio Sciences*, 2(1), 299-307.
- ROMASI, E.F., KARINA, J.K. AND PARHUSIP, A.J.N. 2011. Antibacterial activity of papaya leaf extracts against pathogenic bacteria, *MAKARA Journal of Technology*, 15(2), 173-177.
- SADEGHIAN, M. M. AND MORTAZAIENEZHAD, F. 2007. Investigation of Compounds from *Azadirachta indica* (Neem). *Asian Journal of Plant Sciences*, 6: 444-445.
- SAEED, A.S. AND SAADULLAH, A.A.M. 2019. Isolation, Identification and Antifungal Susceptibility Testing of *Candida* Species from Dermatologic Specimens in Duhok Province, *Zanco Journal of Pure and Applied Sciences*, 31(4), 1-8
- SANCHES, N.R., CORTEZ, D.A.G., SCHIAVINI, M.S., NAKAMURA, C.V. AND FILHO, B.P.D. 2005. An evaluation of antibacterial activities of *Psidium guajava* (L.), *Brazilian Archives of Biology and Technol*, 48(3), 429-436.
- SAWER, I.K. , BERRY, , M.I. AND FORD, J.L. 2004. The killing effect of cryptolepine on *Staphylococcus aureus*. *Letters in Applied Microbiology*, 40, 24-29.
- SAWER, I.K. 1995. Antimicrobial activity of *Cryptolepis sanguinalata*, and mechanisms of action of cryptolepine. PhD thesis. Liverpool John Moores University, UK.
- SHITTU. B.O., POPOOLA, T.O.S. AND TAIWO, O. 2004. Potentials of *Calotropis procera* leaves for Wastewater treatment. Proceedings of the International Conference on Science and National Development held at University of Agriculture, Abeokuta, pp.97.
- SIKANDAR, K. S., TASVEER, Z. B., KANWAL, N., SYED, A. G. AND SHAHAMA, U. K. 2013. Qualitative phytochemical screening and antifungal activity of *Carica papaya* leaf extract against human and plant pathogenic fungi. *International Research Journal of Pharmarmacy*, 4 (7), 83-86.
- SODIPO, O. A. AKINIYI, J. A. AND OGUNBANO, U. S. 2000. Studies on certain characteristics of extracts of bark of *Pausinystalia johimbe* and *Pausinystalia macroceras* (K.Schum.) Pierre ex Beille. *Global Journal of Pure and Applied Sciences*, 6 (1), 83-87.
- SONG, N., XU, W., GUAN, H., LIU, G., WANG, Y. AND NIE, X. 2007. Several flavonoids from *Capsella bursa-pastoris* (L.) medic, *Asian Journal of Traditional Medicine*, 2, 218-222
- SONI, H., MISHRA, K., SHARMA, S. AND SINGHAI, A.K. 2012. Characterization of Azadirachtin from ethanolic extract of leaves of *Azadirachta indica*. *Journal of Pharmacy Research*, 5 (1): 199-201
- SUNDARM, K. M. S., SLOANE, L. AND CURRY, J. 1995. Kinetic of Azadirachtin hydrolysis in model aquatic systems by high liquid chromatography, *Journal of Liquid Chromatography*, 18, 22-24.
- TAN, S., RAMOS, S., MARTIN, M.A., MATEOS, R., HARVEY, M., RAMANATHAN, S., NAJIMUDIN, N., ALAM, M., BRAVO, L. AND GOYA, L. 2012. Protective effects of papaya extracts on tertbutyl hydroperoxide mediated oxidative injury to human liver cells (an *in-vitro* study), *Free Radicals and Antioxidants*, 2(3), 10-19.
- TORTORA, G.J., FUNKE, B.R., CASE, C.L. 2004. *Microbiology: An introduction*. Eighth Ed. San Francisco: Pearson Benjamin Cummings.
- TUGUME,P., KAKUDIDI,E.K., BUYINZA, M., NAMAA LWA,J., KAMATENESI,M., MUCUNGUZI, P. AND KALEMA, J. 2016. Ethnobotanical survey of medicinal plant species used by communities around Mabira Central Forest Reserve, Uganda, *Journal of Ethnobiology and Ethnomedicine*, 12(5).
- UWAH, A. F., OTITOJU, O., NDEM, J. I. AND PETER, A. I. 2013. Chemical composition and antimicrobial activities of adventitious root sap of *Musanga cecropioides*. *Der Pharmacia Lettre*, 5 (2):13-16.
- WANGER, A. 2007. Disk Diffusion Test and Gradient Methodologies. In: Schwalbe R, Steele-Moore L, Goodwin AC, editors. *Antimicrobial Susceptibility Testing Protocols*. Boca Raton: CRC Press. pp. 53-74.

RESEARCH PAPER

Association between some serum oxidative stress biomarkers and lipid profile in type 2 diabetic patients in Erbil City

Hemn Jameel Majeed¹, Gulzar Ismael Ibrahim², Pshtiwan Abdullah Yousif³, Saman Muhsin Abdulkareem⁴

^{1,2,3} Department of Chemistry, College of Education, Salahaddin University-Erbil, Kurdistan-Region, Iraq

⁴ Department of Biology, College of Education, Salahaddin University-Erbil, Kurdistan-Region, Iraq

ABSTRACT:

Increased oxidative stress appears to be a negative factor leading to insulin resistance, dyslipidemia, β -cell dysfunction, impaired glucose tolerance, and ultimately leading to type 2 diabetes mellitus. The aim of the study is to investigate some serum oxidative biomarkers, lipids, and their association with hyperglycemia in patients with type 2 diabetes. The 100 participants (50 patients with type 2 diabetes mellitus and 50 healthy individuals) were enrolled in the present study. Anthropometric measures, serum fasting blood sugar, glycated hemoglobin, oxidative biomarkers, and serum lipid profiles were evaluated. The results showed that the level of malondialdehyde, fasting blood sugar, glycated hemoglobin and lipid profile in patients with type 2 diabetes is higher than those in the control group, while nitric oxide was lower in diabetic than those in the control group. There are also insignificant changes in fasting blood sugar and glycated hemoglobin between baseline and after 3 months follow up. The results showed no linear relationship between oxidative damage and abnormal lipid profiles in patients with type 2 diabetes. It can be concluded that the serum level of malondialdehyde and nitric oxide, along with lipid parameters in patients with type 2 diabetes, can be a useful tool for monitoring of type 2 diabetes.

KEY WORDS: Type 2 Diabetes, Oxidative Stress, Fasting Blood Sugar, Lipid Profile.

DOI: <http://dx.doi.org/10.21271/ZJPAS.33.1.11>

ZJPAS (2021), 33(1);107-112 .

INTRODUCTION:

Diabetes mellitus and its complications are among the most important health problems with very high prevalence, morbidity, and mortality (Deshpande et al., 2008). Type 1 and type 2 diabetes are caused by impaired insulin secretion or its function in the target cell, respectively. Insulin allows glucose from the blood to enter the liver, fat, and skeletal muscle cells and regulates carbohydrates, lipids, and protein metabolism. If these actions are not performed well as a result of impaired insulin secretion or function, plasma glucose levels increased (hyperglycemia) and lead to complications of diabetes and threaten the health of a person with diabetes (American Diabetes, 2009, Ibrahim, 2018).

Type 2 diabetes is linked with some diseases like high blood pressure and dyslipidemia, which are known as risk factors for cardiovascular disease and premature death (Halpern et al., 2010). Microvascular (retinopathy, neuropathy, and nephropathy) and macrovascular disorders, including peripheral vascular disease, ischemic heart disease, and stroke, are the most anatomical derangements and impairments in carbohydrates, fats, and proteins metabolisms and are the main biochemical consequences (Cade, 2008, Abdoulrahman, 2017). Experimental and clinical studies have displayed that oxidative stress and its consequences play a crucial role in the pathogenesis of diabetes and its problems (Oguntibeju, 2019, Matough et al., 2012).

Oxidative stress is defined as an imbalance between the productions of reactive oxygen

* Corresponding Author:

Hemn Jameel Majeed1

E-mail: hemn.majeed@su.edu.krd

Article History:

Received: 16/09/2020

Accepted: 17/10/2020

Published: 20/02 /2021

species (free radicals) and antioxidant defense systems (Pizzino et al., 2017). Reactive oxygen species (ROS), which includes oxygen radicals and its peroxides, are often generated in low levels by cellular organelles such as mitochondria and normal cell reactions. Under these conditions, they participate in several cellular signaling pathways that mediate cellular proliferation and differentiation; however, overproduction of them induce oxidative damage (Nita and Grzybowski, 2016). Oxygen-free radicals by cellular stress-sensitive pathways has been related to insulin resistance and reduced insulin secretion (Karunakaran and Park, 2013). Free radicals induced damage to macromolecules such as lipids, proteins, and DNA and have been identified as a risk factor in various diseases such as cardiovascular disease, neurodegenerative disorders, and cancer (Nita and Grzybowski, 2016). ROS are also linked to induced the expression of proinflammatory cytokines and decreased nitric oxide release that, in turn, cause endothelial dysfunction (Steven et al., 2019, Marchio et al., 2019). Living organisms, from cell to tissue, have extensive and complex strategies to counter oxidant and free radicals. Enzymatic defenses that include enzymes superoxide dismutases, glutathione peroxidases, catalase and paraoxonase, and non-enzymatic defenses like vitamins C and E, beta carotene, and reduced glutathione (GSH) are the most mechanisms to combat free radicals to reduce their oxidative damage (Jelodar et al., 2018, Ngissah, 2013, Abdulkareem and Nanakali, 2019). ROS overproduction is also linked to the oxidation of low-density lipoprotein cholesterol (LDL-C) and lipid peroxidation, which refers to the oxidation of membrane polyunsaturated fatty acids such as arachidonic acid or linoleic acid by free radical. It can alter the structure and the function of biological membranes. Malondialdehyde (MDA) can be used to monitor the degree of oxidative damage in many diseases like diabetes, atherosclerosis, and chronic inflammation (Bigagli and Lodovici, 2019, Ito et al., 2019). Therefore, this study aimed to assess the serum levels of oxidative stress biomarkers and levels of lipid profile in T2DM patients and healthy controls, and their correlation with HbA1c.

Materials and methods

Subjects

In this study, 50 T2DM patients were compared with 50 healthy adults in terms of serum fasting blood sugar (FBS), HbA1c, lipid profile, and oxidative biomarkers levels. This was conducted in Razgari hospital, Erbil. T2DM patients between the age group of 40-70 years of either sex with 5 years history of diabetes were recruited from the outpatient department of medicine. Healthy individuals between the age group of 40-70 years of either sex were enrolled as a control group. In this study, we excluded patients suffering from inflammation and chronic infection, gestational diabetes, type 1 diabetes, renal disease, liver disease, and thalassemia, as well as those treated with diuretics, antioxidants, and steroids or consumed alcohol or cigarettes.

Estimation of different biochemical parameters

Fasting blood sugar, HbA1c, serum nitric oxide levels, serum malondialdehyde (MDA) level, and lipid profile were measured in all the participants. The glucose oxidase method was used to measure FBS (Saifer and Gerstenfeld, 1958). Serum content of lipid profile includes total cholesterol (TC), total triglyceride (TG), low-density lipoprotein (LDL), and high-density lipoprotein (HDL) were estimated by Roche Cobas 400 integral analyzer. Serum NO was estimated by Cortas and Wakid method (Cortas and Wakid, 1990). The serum MDA level as a marker for lipid peroxidation was measured by Bhutia et al. (2011). The serum glycated hemoglobin (HbA1c) was determined by the resin binding method (Weykamp et al., 2009).

Statistical Analysis

The data were expressed as mean \pm SD. An independent *t*-test was used to compare the patient group with the control group. A comparison of baseline and after three months' follow-up was performed by paired *t*-test for the same groups of participants. Significant differences between the patient group (or comparison of mean values) and the control group were denoted by superscript asterisk symbol *, representing significance at $P < 0.05$.

Results and Discussion

The results showed that FBS (male: 198 ± 52.1 ; female: 201 ± 12.3) and HbA1c (male: 8.82 ± 0.91 ; female: 8.91 ± 0.22) significantly were higher in persons with diabetes than a healthy individual (FBS; male: 100.2 ± 7.4 ; female: 95 ± 31.2) and (HbA1c; male: 5.31 ± 0.51 ; female:

5.21±0.51). Also, results showed that the baseline level of these factors and three months of follow up were greater in the patient subjects than in the control subjects (Table 1). There is no significant difference in serum FBS and HbA1c after 3

months of follow-up in diabetic and control groups compared to their baseline levels. There was no significant change in FBS and HbA1c between men and women with diabetes.

Table 1: Age, BMI, FBS, and HbA1c in diabetic and healthy subjects

Subject		Male control	DM (Male)	Female control	DM (Female)
Number of participants		25	25	25	25
Age (year)		52±6.3	54±5.4	53±5.6	54±6.5
Body mass index (Kg/m ²)		23.3±2.3	32.3±3.1***	25.1±2.6	31±4.41**
FBS	Baseline	100.2 ± 7.4	198 ± 52.1***	95 ± 31.2	201 ± 12.3***
	3 Months of follow up	98.45 ± 3.5	196 ± 31.3***	96.5 ± 6.7	204 ± 43.7***
HbA1c	Baseline	5.31 ± 0.51	8.82 ± 0.91*	5.21 ± 0.51	8.91 ± 0.22*
	3 Months of follow up	4.89 ± 0.63	9.14 ± 0.34*	5.04 ± 0.42	9.36 ± 0.75*

*Significant ($P<0.05$), **highly significant ($P<0.01$), ***very highly significant ($P<0.001$).

Well-known complications related to hyperglycemia, such as increased production of the extracellular matrix, cell damage, and impaired vascular function, are involved in the pathogenicity of vascular disease in type 1 and 2 of diabetes (Dalle-Donne et al., 2006). In this study, HbA1c as an index of metabolic control used to evaluate and monitor patients with diabetes. The results showed that HbA1c in the diabetic group is significantly greater than the control group, which is one of the causes of Aamadori reaction (Shinde et al., 2011). The recent increase in the knowledge of free radicals in biology is generating a medicinal revolution that promises a new era of health and disease controlling. Oxygen and nitrogen-free radicals that known as oxidants are highly unstable molecules, which are produced during normal cellular metabolism. Oxygen-free radicals are well known for playing a double role as both detrimental and beneficial species as they can be either dangerous or beneficial to living systems. At physiological level (low or moderate) exerts beneficial effects such as induction of a mitogenic response, defense against infectious agents and the maturation

process of cellular structures; at the high level can react with lipids, DNA and proteins and disrupt the normal function of the cells (Akbari et al., 2016, Bigagli and Lodovici, 2019, Matough et al., 2012, Oguntibeju, 2019).

The mean values of serum MDA and NO levels are shown in Table 2. The results stated that the concentration of MDA in patients with diabetes (male: 3.49±0.92; female: 4.11±0.36) was meaningfully higher than the healthy subjects (male: 1.95±0.75; female: 2.65±0.12); the results also showed that the level of MDA did not change considerably after three months of follow-up in the patient group compared to baseline. The level of NO in patients with diabetes (male: 17.41±8.71; female: 19.51±7.30) was significantly less than the control group (male: 39.21±3.17; female: 45.67±3.41); also, after three months of follow-up, this factor did not change significantly in baseline in the patient group and in the healthy subjects. There was an insignificant difference in serum MDA and NO levels between men and women with diabetes.

Table (2): The mean value of serum MDA and NO of control and diabetic groups

Subject		Male control	DM (Male)	Female control	DM (Female)
MDA (nmol/ml)	Baseline	1.95 ± 0.75	3.49 ± 0.92*	2.65 ± 0.12	4.11 ± 0.36*
	3 Months of follow up	1.87 ± 0.91	4.36 ± 1.11*	2.43 ± 0.33	4.63 ± 0.41*
NO	Baseline	39.21 ± 3.17	17.41 ± 8.71*	45.67 ± 3.41	19.51 ± 7.30*

($\mu\text{mole/L}$)	3 Months of follow up	38.79 \pm 3.65	16.97 \pm 7.32*	47.34 \pm 3.96	18.97 \pm 5.24*
------------------------	------------------------------	------------------	-------------------	------------------	-------------------

*Significant ($P<0.05$), **highly significant ($P<0.01$), ***very highly significant ($P<0.001$).

In our study, MDA's level in persons with T2DM is markedly higher than that in control subjects. As already noted, MDA is a stable byproduct in lipid peroxidation; on the other hand, evidence suggested that oxidation of lipids in lipoproteins (oxidized LDL) and the plasma cell membrane is linked to the incidence of vascular disease in persons with diabetes (Mahreen et al., 2010, Kaefer et al., 2012). The elevated MDA can lead to adverse physiological consequences such as alteration in the membrane's structure and function, inactivate proteins bound to the membrane such as enzymes and receptors that regulate cellular signaling pathways (Mahreen et al., 2010). The elevated MDA can also be involved in oxidizing LDL, which led to atherosclerosis. Our results also indicated that NO level is significantly less in persons with T2DM than that in control. NO is released by endothelial nitric oxide synthase (eNOS) in endothelial cells of vessels.

It was reported that endothelial dysfunction in diabetes largely decreased NO production and its bioavailability (Takahashi and Harris, 2014). It is clear that a decrease in NO concentration causes vascular stiffness and high blood pressure. In agreement with our results, studies have shown

that hyperglycemia induces oxidative damage, and it has a positive correlates with the development of T2DM and its complications (Bigagli and Lodovici, 2019, Matough et al., 2012, Oguntibeju, 2019). In healthy subjects, the levels of oxidative parameters during the three-month follow-up showed no significant change, which could be due to the normal activity of antioxidant systems and normal levels of vitamins such as vitamins C and E.

The mean values (\pm SD) of the serum lipid profile are presented in Table 3. The outcomes showed that the level of TC, TG, and LDL-C in subjects with diabetes (male: 238.68 \pm 41.48, 254.17 \pm 38.60, 143.35 \pm 32.63, respectively; female: 201.86 \pm 30.52, 267.82 \pm 0.29, 111.72 \pm 12.49, respectively) was significantly higher than the control subjects (male: 174.82 \pm 20.24, 156.76 \pm 23.19, 88.70 \pm 8.88, respectively; female: 161.37 \pm 24.27, 127.08 \pm 35.24, 86.27 \pm 15.16, respectively), while the level of HDL-C in patients with diabetes (male: 23.35 \pm 4.30; female: 36.62 \pm 4.68) was significantly less than the control group (male: 37.94 \pm 4.24; female: 46.62 \pm 5.49).

Table 3: The mean values (\pm SD) of serum lipid profile between control and diabetic group after 3 months of follow up

Groups		Male control	DM (Male)	Female control	DM (Female)
TC (mg/dl)	Baseline	174.82 \pm 20.24	238.68 \pm 41.48**	161.37 \pm 24.27	201.86 \pm 30.52***
	3 Months of follow up	168.34 \pm 17.85	241.15 \pm 37.64**	158.43 \pm 21.32	208.54 \pm 29.35***
TG (mg/dl)	Baseline	156.76 \pm 23.19	254.17 \pm 38.60***	127.08 \pm 35.24	267.82 \pm 0.29***
	3 Months of follow up	159.68 \pm 26.76	250.47 \pm 37.64***	126.14 \pm 41.65	256.36 \pm 23.54***
HDL (mg/dl)	Baseline	37.94 \pm 4.24	23.35 \pm 4.30***	46.62 \pm 5.49	36.62 \pm 4.68**
	3 Months of follow up	34.68 \pm 3.68	21.34 \pm 3.64***	49.67 \pm 4.34	34.65 \pm 4.65**
LDL (mg/dl)	Baseline	88.70 \pm 8.88	143.35 \pm 32.63***	86.27 \pm 15.16	111.72 \pm 12.49***
	3 Months of follow up	92.34 \pm 7.68	148.64 \pm 32.4***	83.64 \pm 12.67	114.34 \pm 13.64***

*Significant ($P<0.05$), **highly significant ($P<0.01$), ***very highly significant ($P<0.001$).

Our results showed that high values of TC, TG, and LDL-C, along with a low level of HDL-C observed in a person with T2DM. Like previous

studies, our results showed that T2DM is associated with dyslipidemia (Bhowmik et al., 2018). Various mechanisms, including insulin actions on the regulation of lipoprotein lipase and cholesteryl ester transfer protein (CETP), hepatic production of the apoprotein, and peripheral its actions on muscle and adipose cells are involved in diabetic dyslipidemia (Bhowmik et al., 2018).

In this study, elevated lipid profile (TC, TG, and LDL-C) and oxidative stress biomarkers were observed in T2DM cases. As previously reported (Rao and Kiran, 2011), our results showed that there is no linear relationship between abnormal lipid profile and oxidative parameters (data unshown), and these are two independent risk factors in the DM and its complications. One of this study's limitations was not assessed as confounding factors such as dietary behaviors, physical activity level, and medications that affect lipid profile concentrations. Though, this type of study can well identify important relationships that can be explored in future studies. Therefore, the findings of the present study help provide a basis for subsequent studies in our population to investigate the relations between fat disorders, oxidative damage, and the risk of DM.

Conclusion:

The present study results suggest that the serum level of MDA and NO along with lipid biomarkers (especially TC, TG, and HDL-C) in patients with T2DM can be a useful tool for monitoring of T2DM.

Reference

- ABDOULRAHMAN, K. K. 2017. Lipid profile, oxidative stress and homocysteine in CRF patients pre-and post-hemodialysis in Erbil city. *ZANCO Journal of Pure and Applied Sciences*, 29, 65-73.
- ABDULKAREEM, S. & NANAKALI, N. 2019. QUERCETIN REDUCES OXIDATIVE STRESS DAMAGE TO REPRODUCTIVE PROFILE INDUCED BY 2, 3, 7, 8-TETRACHLORODIBENZO-P-DIOXIN IN MALE ALBINO RATS (*RATTUS NORVEGICUS L.*). *APPLIED ECOLOGY AND ENVIRONMENTAL RESEARCH*, 17, 13185-13197.
- AKBARI, A., JELODAR, G. & NAZIFI, S. 2016. The proposed mechanisms of radio frequency waves (RFWs) on nervous system functions impairment. *Comparative Clinical Pathology*, 25, 1289-1301.
- AMERICAN DIABETES, A. 2009. Diagnosis and classification of diabetes mellitus. *Diabetes care*, 32 Suppl 1, S62-S67.
- BHOWMIK, B., SIDDIQUEE, T., MUJUMDER, A., AFSANA, F., AHMED, T., MDALA, I. A., DO V MOREIRA, N. C., KHAN, A. K. A., HUSSAIN, A., HOLMBOE-OTTESEN, G. & OMSLAND, T. K. 2018. Serum Lipid Profile and Its Association with Diabetes and Prediabetes in a Rural Bangladeshi Population. *International journal of environmental research and public health*, 15, 1944.
- BHUTIA, Y., GHOSH, A., SHERPA, M. L., PAL, R. & MOHANTA, P. K. 2011. Serum malondialdehyde level: Surrogate stress marker in the Sikkimese diabetics. *Journal of natural science, biology, and medicine*, 2, 107.
- BIGAGLI, E. & LODOVICI, M. 2019. Circulating Oxidative Stress Biomarkers in Clinical Studies on Type 2 Diabetes and Its Complications. *Oxidative Medicine and Cellular Longevity*, 2019.
- CADE, W. T. 2008. Diabetes-related microvascular and macrovascular diseases in the physical therapy setting. *Physical therapy*, 88, 1322-1335.
- CORTAS, N. K. & WAKID, N. W. 1990. Determination of inorganic nitrate in serum and urine by a kinetic cadmium-reduction method. *Clin Chem*, 36, 1440-3.
- DALLE-DONNE, I., ROSSI, R., COLOMBO, R., GIUSTARINI, D. & MILZANI, A. 2006. Biomarkers of oxidative damage in human disease. *Clin Chem*, 52, 601-23.
- DESHPANDE, A. D., HARRIS-HAYES, M. & SCHOOTMAN, M. 2008. Epidemiology of diabetes and diabetes-related complications. *Physical therapy*, 88, 1254-1264.
- HALPERN, A., MANCINI, M. C., MAGALHÃES, M. E. C., FISBERG, M., RADOMINSKI, R., BERTOLAMI, M. C., BERTOLAMI, A., DE MELO, M. E., ZANELLA, M. T., QUEIROZ, M. S. & NERY, M. 2010. Metabolic syndrome, dyslipidemia, hypertension and type 2 diabetes in youth: from diagnosis to treatment. *Diabetology & metabolic syndrome*, 2, 55-55.
- IBRAHIM, M. A. 2018. Metformin ameliorates diabetes mellitus in Kurds patients by attenuation of serum cortisol and copper levels. *Zanco Journal of Pure and Applied Sciences*, 30, 48-56.
- ITO, F., SONO, Y. & ITO, T. 2019. Measurement and Clinical Significance of Lipid Peroxidation as a Biomarker of Oxidative Stress: Oxidative Stress in Diabetes, Atherosclerosis, and Chronic Inflammation. *Antioxidants (Basel, Switzerland)*, 8, 72.
- JELODAR, G., AKBARI, A., PARVAEEI, P. & NAZIFI, S. 2018. Vitamin E protects rat testis, eye and erythrocyte from oxidative stress during exposure to radiofrequency wave generated by a BTS antenna model. *International Journal of Radiation Research*, 16, 217-224.

- KAEFER, M., DE CARVALHO, J. A., PIVA, S. J., DA SILVA, D. B., BECKER, A. M., SANGOI, M. B., ALMEIDA, T. C., HERMES, C. L., COELHO, A. C., TONELLO, R., MOREIRA, A. P., GARCIA, S. C., MORETTO, M. B. & MORESCO, R. N. 2012. Plasma malondialdehyde levels and risk factors for the development of chronic complications in type 2 diabetic patients on insulin therapy. *Clin Lab*, 58, 973-8.
- KARUNAKARAN, U. & PARK, K.-G. 2013. A systematic review of oxidative stress and safety of antioxidants in diabetes: focus on islets and their defense. *Diabetes & metabolism journal*, 37, 106-112.
- MAHREEN, R., MOHSIN, M., NASREEN, Z., SIRAJ, M. & ISHAQ, M. 2010. Significantly increased levels of serum malonaldehyde in type 2 diabetics with myocardial infarction. *International journal of diabetes in developing countries*, 30, 49-51.
- MARCHIO, P., GUERRA-OJEDA, S., VILA, J. M., ALDASORO, M., VICTOR, V. M. & MAURICIO, M. D. 2019. Targeting Early Atherosclerosis: A Focus on Oxidative Stress and Inflammation. *Oxidative medicine and cellular longevity*, 2019, 8563845-8563845.
- MATOUGH, F. A., BUDIN, S. B., HAMID, Z. A., ALWAHAIBI, N. & MOHAMED, J. 2012. The role of oxidative stress and antioxidants in diabetic complications. *Sultan Qaboos University medical journal*, 12, 5-18.
- NGISSAH, P. 2013. Lipid Peroxidation and Antioxidant Status in Type 2 Diabetes Mellitus in Ghana.
- NITA, M. & GRZYBOWSKI, A. 2016. The Role of the Reactive Oxygen Species and Oxidative Stress in the Pathomechanism of the Age-Related Ocular Diseases and Other Pathologies of the Anterior and Posterior Eye Segments in Adults. *Oxidative medicine and cellular longevity*, 2016, 3164734-3164734.
- OGUNTIBEJU, O. O. 2019. Type 2 diabetes mellitus, oxidative stress and inflammation: examining the links. *International journal of physiology, pathophysiology and pharmacology*, 11, 45-63.
- PIZZINO, G., IRRERA, N., CUCINOTTA, M., PALLIO, G., MANNINO, F., ARCORACI, V., SQUADRITO, F., ALTAVILLA, D. & BITTO, A. 2017. Oxidative stress: harms and benefits for human health. *Oxidative medicine and cellular longevity*, 2017.
- RAO, V. & KIRAN, R. 2011. Evaluation of correlation between oxidative stress and abnormal lipid profile in coronary artery disease. *J Cardiovasc Dis Res*, 2, 57-60.
- SAIFER, A. & GERSTENFELD, S. 1958. The photometric microdetermination of blood glucose with glucose oxidase. *The Journal of laboratory and clinical medicine*, 51, 448-460.
- SHINDE, S. N., DHADKE, V. N. & SURYAKAR, A. N. 2011. Evaluation of Oxidative Stress in Type 2 Diabetes Mellitus and Follow-up Along with Vitamin E Supplementation. *Indian journal of clinical biochemistry : IJCB*, 26, 74-77.
- STEVEN, S., FRENIS, K., OELZE, M., KALINOVIC, S., KUNTIC, M., BAYO JIMENEZ, M. T., VUJACIC-MIRSKI, K., HELMSTÄDTER, J., KRÖLLER-SCHÖN, S., MÜNDEL, T. & DAIBER, A. 2019. Vascular Inflammation and Oxidative Stress: Major Triggers for Cardiovascular Disease. *Oxidative medicine and cellular longevity*, 2019, 7092151-7092151.
- TAKAHASHI, T. & HARRIS, R. C. 2014. Role of endothelial nitric oxide synthase in diabetic nephropathy: lessons from diabetic eNOS knockout mice. *Journal of diabetes research*, 2014, 590541-590541.
- WEYKAMP, C., JOHN, W. G. & MOSCA, A. 2009. A review of the challenge in measuring hemoglobin A1c. *Journal of diabetes science and technology*, 3, 439-445.

RESEARCH PAPER

Prevalence of obesity-associated with health issues among Koya Technical Institutes Staff in Kurdistan Region, Iraq

Saman R. Abdullah¹, Kochar Kh. Saleh^{1&3}, Karwan M. Khudhir¹, Kochar A. Mahmood², Bahra R. Hamarashid³

¹Department of Community Health, Koya Technical Institute, Erbil Polytechnic University, Erbil, Kurdistan Region, Iraq

²School of Medicine, Koya University, Koya, Kurdistan Region, Iraq

³Department of Biology, Faculty of Science, Firat University, Elazig, Turkey

ABSTRACT:

The obesity rate and its prevalence are increasing with many complications in the population. Obesity is a condition in which the bodyweight gain extended to the point where it causes obstacles to health. Usually, this extended body weight comes from excessive fat which consequences of the imbalance between calories expended and calories consumed. Pre-test questionnaire by utilizing validation of self-administration as a cross-sectional investigation was carried out to diagnose the overview of obesity and health issue risks among Koya technical staff. The height of the staff was calculated by supporting a measuring tape (Seca 206 body meter) and the mass of the body (kg) was measured by providing weighing scale TANTA. Overall, according to the findings of this study, we conclude that body overweight (54.7%) and obesity (18%) are clear among academics and administrate staff of Koya Technical Institute at Erbil Polytechnic University. While normal body weights are (25.3%) and underweight approximately (2%). Analyses of data showed that obesity is a significant difference between married and unmarried of participants, besides, there are many factors appear to have a great role and association with health situation and body overweight such as (age, gender, and level of education, type of work, income and physical activity). Physical activities and lifestyle have a strong relation with obesity, especially its reveal among administrates rather than academics, because of fewer activities and lack of regular exercise.

KEY WORDS: Prevalence, Obesity, Risk factors, Health issues.

DOI: <http://dx.doi.org/10.21271/ZJPAS.33.1.12>

ZJPAS (2021) , 33(1);113-119 .

1.INTRODUCTION:

Obesity has reached a contagious portion of the two sites in advanced and advancing countries. Over the world, an estimated for further one billion ripe being obese and 350 cases are appear effected (Yach *et al.*, 2006). Obesity and overweight are conditions everywhere a main stock of energy is stored in tissue, which leads to a problem or many complication issues related to health, one of the dominant civil well-being problems among industrialized civilization, especially in the USA.

Currently, an obesity well-being problem arises with unindustrialized communities and regions. Fatness is related to half of the most common reasonable death among the population, for instance, blood pressure, cardiovascular disorders, stroke, and diabetes, populations are globally enduring with overweighting and each year increases closely to threefold. Approximately 300,000 people are perishing concerning body overweight, this number of dying by obesity above died vehicle airline accidents (Price *et al.*, 2000). According to (WHO, 2006) obesity in the past was an issue related to a wealthy family and rich nations, however, it's not specific, nowadays there is a health problem of low and middle-

* Corresponding Author:

Saman R. Abdullah

E-mail: saman.abdullah@epu.edu.iq or samanrafeeq715@gmail.com

Article History:

Received: 15/12/2019

Accepted: 12/01/2020

Published: 20/02/2021

income families and nations. Particularly urban one's locations. One of the main risk factors of an expansion incidence and overweight among the public community due to increased consumption of wholly compensate for the energy density of the food's high fat or sugar. Nutritional transformation is this dietary switch (Bourne *et al.*, 2002). In contrast to the food shift, obesity is also due to reduced physical exercise, as many modes of employment and change in travel and urbanization become gradually sedentary (Flegal *et al.*, 1998).

WHO has classified obesity and body overweight by using special measurements a standard overworld which is Body Mass Index, thus $25 \text{ Kg/M}^2 - 29.9 \text{ kg/m}^2$ normal while above is considered as overweight. Globally, many kinds research approved to find detection the body ailment the comorbidities to obesity and have fundamental roles in blindness among many aging patients in consequence diabetic retinopathy, furthermore obesity have a strong association with hormonal abnormality especially in women (Wsoo M. A., 2017, Mohammed and Yousif, 2019). However, in Iraq, which is considered a lower-middle-income country according to the world bank, very little data is available on the extent of the problem of obesity in the academic staffs and some other factors such as disease and low back pain lead to decreased activity and increase the chance to obesity (Khudhir *et al.*, 2018, Khudhir *et al.*, 2017a). The Aim and objectives of the study were to survey the complication of body fat with associated to many factors among the staff of Koya technical institute.

2. MATERIALS AND METHODS

This research was conducted among academics and administrates staff of Koya technical institute at Erbil Polytechnic University between the 20th of January 2018 and the 1st of February 2018. The Ethical Committees of the community health department approved the study; until being used for the analysis, that participant received informed consent in writing. The required sample size was calculated from the Raosoft calculator. A list of all the institute staff was obtained around 160 staff taking part in the study participants. Permanent staff was engaged in this study beside there is no

disabled or sick with chronic illness. 160 of selected to self-character administered questions among technical staffs, 150 of them about 93% had a response, 5 workers leavings the participation, so five workers did not participate in anthropometric measurement.

2.1. Plan and Data Collection:

Data collection: Self-administrative questionnaire was carried out using a standardized questionnaire. A structured questionnaire designed to obtain information regarding age, gender, living place, marital status, level of education, type of job, income), individual factors (physical activity, smoking, alcohol consumption). Age was calculated from the information on birth date and date of the interview. For anthropometric measurement height of staff were admeasurement by utilizing tape meters from (1cm – 2m), participants need to take off their shoes, to prevent the effect of shoes of admeasurement. In addition, the respondent's body weight calculated by digital scale weighting TANITA starts around 1 kg. Participants require to remove any heavy mass to prevent imbalance decrease and increase in body mass (Pengelly and Morris, 2009). The WHO diagnostic criteria were used in classifying the subjects as overweight and obese.

2.1.1. Statistics

Statistical Methods: SPSS was used in the analysis of data; both parameters are classified and measured normally. Descriptive properties interquartile, percentage, frequency, and median of the survey participants were calculated. The relation between obesity and socio-demographic factors was calculated by means of a chi-square study. Statistically significant was considered a p-value < 0.05 . The findings of bivariate analyzes have acted as a framework for multivariate logistic regression research to classify the modified likelihood ratios of variables linked to obesity.

2.1.2. Ethical assessment

permission of morality was received in August 2015 by the Koya Institutes Committee for Morality (Ref: KTI 12512). Each respondent also received informed consent prior to the collection of data. The report told the participants and that it was free to take part in this survey. In addition, participants were guaranteed which all data were considered confidential and would not be used

outside this survey, and were informed regarding the right to refuse it.

3. RESULTS AND DISCUSSION

3.1. RESULTS

There was a total of 150 (response rate = 93%) subjects participated in the study. Non-respondents were those who were refusing to participate in this study and those who did not give approval for measurement of height or weight. [Table 1](#) illustrates the details of the analytics value of individual information who had responded.

Table 1. Socio-Demographics and Individual profile of respondents

Factors	Frequency	Percent age	Median (IQR)
Age groups (years)			36 (16.25)
≤36	76	50.7	
>36	74	49.3	
Gender			
Male	54	36.0	
Female	96	64.0	
Marital Status			
Single	47	31.3	
Married	103	68.7	
Level of education			
Secondary School	4	2.7	
College diploma or equivalent	65	43.3	
Bachelor degree	48	32.0	
Postgraduate degree	33	22.0	
Type of job			
Academic staff	38	25.3	
Administrative staff	112	74.7	
Income			625000(380000)
IQD <500000	65	43.3	
IQD 500000-1000000	80	53.3	
IQD >1000000	5	3.3	

>1000000			
Smoking			
Yes	53	35.5	
No	97	64.7	
Physical activity			
Infrequent (<3 times/week)	93	62.0	
Frequent (≥3 times/week)	57	38.0	
Alcohol Consumption			
Yes	16	10.7	
No	134	89.3	

Age-old and youth of staff between 24 to 56 years, 54.8% younger class (≤34years) while 45.2% older class (>34), the median age 36 years. More than half of them were female (64%), and (36%) were male. The majority were married (68.7%), had postgraduate education level (22%), administrative staff (74.7%), their income was between IQD 500000-1000000 per month (53.3%). The median of income was IQD 625000 per month (interquartile range (IQR) = IQD 380000). As for individual factors, approximately 35.5% of the respondents were smoking and the majority of them (62%) carry out the infrequent physical activity (<3 times/ week). However, only 10.7 % of them were consuming alcohol.

The predominance of body overweight among respondents [Table 2](#) presents and illustrates obesity in KTI staff was 54.7 % and that of obesity was 18.0 %. The distribution of BMI in the study population was as follows: 2.0 % were underweight, 25.3 % had normal BMI, 54.7 % were overweight and 18.0% were obese. Body overweight and obesity aspects.

Table 2. Distribution of body mass index in the population study

Body Mass Index	Frequency	Percentage (%)
Underweight (<18.5 kg/m ²)	3	2.0
Normal (18.5 – 24.99 kg/m ²)	38	25.3

Overweight (≥ 25 - 29.99 kg/m ²)	82	54.7
Obese (≥ 30 kg/m ²)	27	18.0
Total	150	100

The inferential analysis in [Table 3.1](#) illustrates information on individual profiles.

Table 3.1. Risk factors associated with overweight and obesity

Variables	B	S.E	Sig.	Adjusted OR	95% CI
Age				1	
≤36	-	-	-	1	-
>36	0.895	0.606	0.139	2.448	0.747, 8.020
Gender				1	
Male	-	-	-	1	-
Female	2.620	0.772	0.001	0.073	0.016, 0.331
Marital status				1	
Single	-	-	-	1	-
Married	1.367	0.573	0.017	0.225	0.083, 0.784
Level of education				1	
Secondary school	-	-	-	1	-
College diploma or equivalent	21.90	1813	0.999	1	-
Bachelor's degree	19.74	1813	0.999	1	-
Master degree	20.72	1813	0.999	1	-
Type of job				1	
Academic staff	-	-	-	1	-
Administrative staff	0.021	0.873	0.981	1.021	0.153, 50.714
Income				1	
IQD <500000	1.025	1.480	0.489	2782	0.153, 50.714
IQD 500000 - 1000000	1.494	0	0.228	4.454	4
IQD > 1000000	-	1.238	-	1	0.393, 50.423
Physical activity				1	
Infrequent (< 3 times/week)	2.958	0.638	<0.001	19.268	5.519, 67.274
Frequent (≥ 3)	21.330	18139	0.001	0.999	4

times/week					
Constant					

Inferential statistics there is significant ($p=0.015$) differences between younger groups vs. older groups. Also, BMI significantly varies by sex ($p<0.001$), married status ($p<0.002$), level of education ($p<0.001$), type of job ($p<0.001$), income ($p=0.039$), smoking ($p=0.030$), and physical activity ($p<0.001$). However, no significant differences as ($p=0.576$) of respondents who live in urban and rural areas and BMI with respondents who consumed alcohol or not ($P=0.832$).

3.1.1. Risk factors of obesity

Data analyses determine many complications of obesity as shown in [Table 3.2](#).

Table 3.2. Multiple logistic regressions of predictors of musculoskeletal disorders

Factors	Underweight	Normal weight	Overweight	Obese	P value	
Age	n	%	n	n	n	0.015
Younger group (≤ 36)	0	0	24	44	8	
Older group > 36	3	100	63	53.6	30	
			14	38	19	
Gender						< 0.001
Male	3	100	33	53	7	
Female	0	0	86.8	64.6	26	
Living area						0.641
Urban	3	100	38	80	27	
Rural	0	0	100	97.5	100	
Marital status						< 0.001
Single	2	66.7	23	22	0	
Married	1	33.3	15	60	27	

Level of education	0	0	0	0	4	< 0.001
	2		0	0	14.8	
Secondary school	66.7		27	31	5	
			71	37.8	18.5	
College diploma or equivalent	0	0				
	1		5	30	13	
Bachelor's degree	33.3		13	36.5	48.2	
			6	21	5	
Master degree			16	25.7	18.5	
Type of job	0	0	7	25	6	< 0.001
	3		18.4	30.4	22	
Academic staff	100		31	27	21	
			81.6	69.6	78	
Administrative staff						
Income						0.039
IQD <500000	2		24	30	9	
	66.7		73.5	36.6	33.3	
IQD 500000 - 1000000	1		12	51	16	
	33.3		31.5	62.2	59.3	
IQD > 1000000	0		2	1	2	
	0		5	1.2	7.4	
Smoking						0.030
Yes	1		14	35	3	
	33.3		36.8	42.6	11	
No	2		24	47	24	
	66.7		63.2	57.4	89	
Physical activity	1		9	64	19	< 0.001
	33.3		23.7	78	70.3	
Infrequent (< 3times/week)	2		29	18	8	
	66.7		76.3	22	29.7	
Frequent (≥ 3 times/week)						
Alcohol Consumption	0	0	3	10	3	0.832
	3		8	12	12	
Yes	100		35	72	24	
No			92	88	88	

As a daily activity, the economic state of the family all of this method was finally achieved with the significant variables among participants. The result showed 0.073 times as respondents who were female compared to male (OR= 0.073, 95%CI=0.016, 0.331), being obese were 0.255 times higher in respondents who were married as compared to single respondents (OR= 0.255, 95% CI = 0.083, 0.784). In addition, differences of overweight 19.268 in highest level respondents

who were not having a regular exercise (<3 times/week) compared to other respondents who have a regular exercise (≥3 times/week) (OR= 19.268, 95% CI = 5.519, 67.274). The model was a good one and about 62% of differences of obesity were described by way (Nagelkerke R square = 0.615). The Hosmer -Lemeshow test also showed that the model fits well (2=8.823, df=8, p= 0.357).

3.2. DISCUSSION

This study raises and demonstrates the argument of body overweight and some diseases associated with obesity and position of working amongst staffs, around 54.7% to 18% is higher than other academic staffs such as the previous investigation among Malaysia university staffs, who reported the total rate of body fat and obesity was 31.1% to 11.8% respective (Rampal *et al.*, 2007, Khudhir *et al.*, 2017b). Overweight prevalence has been reported in southern China was 25.8% and 7.9% respectively. In Ghana, the obesity of bank workers about 17.8 % and 37.8 % respectively (Addo *et al.*, 2015).

This study manifested that obesity was significant among the older staff than younger staff (77 % vs. 68 % respectively). A similar study conducted and support this result as clear in researches about an adult female in Malaysia, Selangor (Lim *et al.*, 2000, Sidik and Rampal, 2009). There is a significant association between obesity with gender (p < 0.01). Body overweight showed significantly value in woman staff (74%) while the man staff (26%). Similar finding observed in the study of Case and Menendez (2009), that mentioned female staffs had significantly higher BMI than male staffs (Case and Menendez, 2009). Another important association between obesity and marital status found in this research, approximately overweight (p=0.001) who responder is married and overweight and obesity (58.4 % vs. 26.2 %) compared to those who were still unmarried (26.8% vs. 0 % respectively), because of many physiological changes occur after human get married and alter lifestyle, Jeffery (2002) supports this finding in this investigation (Jeffery and Rick, 2002).

The current data of BMI with the type of job in administrative staffs about (69.6% vs. 78% respectively) was higher than academic staff (30.4% vs 22% respectively). In addition,

overweight and fatness have strong concerns with salary and income, whose income more (>1000000 IQD) shows greater body overweight than low salary staff. This result is counterparts with the study of Ziraba and colleagues (Ziraba *et al.*, 2009). It was also noted that non-smoking staff had significantly higher BMI than staff who were smoke ($p < 0.001$).

Inactivity has a great significant risk factor body and creates obesity besides of food source and disorder of homeostasis (Saleh *et al.*, 2019). The prevalence of overweight and obesity between staffs who have infrequent physical activity (<3 times/ week) was (69 % vs 20% respectively) which was higher than obesity between the staffs who have frequent physical activity (≥ 3 times/ week) (31.6 % vs. 14% respectively). This in line with the many study findings, which showed that the level of physical activity decreased the percentage of obesity. They have shown an opposite relationship between obesity, psychological and physical activity, as it's common among other staff in nurse and lecturer in hospital (Staiano *et al.*, 2016, Khudhir *et al.*, 2018). In this study, living area and alcohol consumption have no association with BMI ($p > 0.05$). Multiple logistic regression showed that the female staffs are 0.073 times (OR= 0.073, 95% CI = 0.016, 0.331). The staff who were married 0.255 times more likely to have obesity as compared to the staff who were single (OR= 0.255, 95% CI = 0.083, 0.784). In addition, staff who were not having a regular exercise (<3 times/week) 19.268 chance to have obesity in contrast to staff who have a regular exercise (≥ 3 times/week) (OR= 19.268, 95% CI = 5.519, 67.274).

4. CONCLUSIONS

This investigation found an immense prevalence of obesity and overweight among Koya Technical Institute staff. Socio-demographic and individual factors for instance lifestyle, body physiology related to sex, stage of education, family habits, position in the workplace, income, mode, and physical activity were significantly related to body overweight and obesity. Obesity and body overweight was only estimated by body mass index. The obstacles of this investigation were self-character-reporting questionnaires, in this way the consequences of bias cannot be limited.

This study recommends that high risks of overweight among staff for targeted intervention that induces increased exercise and improves some good habits which lead to reduced body overweight and control the complications of obesity and use superfood instead of energy-dense food.

Acknowledgments

We would like to thank the Dean of Koya Technical Institutes and All participants, for giving us permission to conduct this research.

Conflict of Interest

The authors stated that there was no potential interest in conflict with regard to this article.

REFERENCES

- ADDO, P. N., NYARKO, K. M., SACEY, S. O., AKWEONGO, P. & SARFO, B. 2015. Prevalence of obesity and overweight and associated factors among financial institution workers in Accra Metropolis, Ghana: a cross sectional study. *BMC research notes*, 8, 599.
- BOURNE, L. T., LAMBERT, E. V. & STEYN, K. 2002. Where does the black population of South Africa stand on the nutrition transition? *Public health nutrition*, 5, 157-162.
- CASE, A. & MENENDEZ, A. 2009. Sex differences in obesity rates in poor countries: evidence from South Africa. *Economics & Human Biology*, 7, 271-282.
- FLEGAL, K. M., CARROLL, M. D., KUCZMARSKI, R. J. & JOHNSON, C. L. 1998. Overweight and obesity in the United States: prevalence and trends, 1960–1994. *International journal of obesity*, 22, 39-47.
- JEFFERY, R. W. & RICK, A. M. 2002. Cross-sectional and longitudinal associations between body mass index and marriage-related factors. *Obesity Research*, 10, 809-815.
- KHUDHIR, K. M., MAHMOOD, K. A., SALEH, K. K. & ADULAH, S. R. Psychosocial factors in relation to musculoskeletal disorders among nursing professionals in Raparin Administration. 2018 International Conference on Pure and Applied Science, 2018.
- KHUDHIR, K. M., MAHMOOD, K. A., SALEH, K. K. & HOSSAIN, M. 2017a. A cross sectional study to determine the prevalence and risk factors of low back pain among public technical institute staff in Kurdistan Region, Iraq. *F1000Research*, 6, 182.
- KHUDHIR, K. M., SALEH, K. K., QADIR, M. S., MAHMOOD, K. A. & ARIFFIN, A. A. 2017b.

- Association between work-relate musculoskeletal disorder and ergonomic risk factors among nursing professionals in ranya and qaladiza districts. *Kurdistan journal of applied research*, 2, 65-70.
- LIM, T. O., DING, L., ZAKI, M., SULEIMAN, A., FATIMAH, S., SITI, S., TAHIR, A. & MAIMUNAH, A. 2000. Distribution of body weight, height and body mass index in a national sample of Malaysian adults. *Medical Journal of Malaysia*, 55, 108-128.
- MOHAMMED, B. N. S. & YOUSIF, R. Z. 2019. Intelligent System for Screening Diabetic Retinopathy by Using Neutrosophic and Statistical Fundus Image Features. *ZANCO Journal of Pure and Applied Sciences*, 31, 30-39.
- PENGELLY, C. D. & MORRIS, J. 2009. Body mass index and weight distribution. *Scott Med J*, 54, 17-21.
- PRICE, R. A., REED, D. R. & GUIDO, N. J. 2000. Resemblance for body mass index in families of obese African American and European American women. *Obesity Research*, 8, 360-366.
- RAMPAL, L., RAMPAL, S., KHOR, G. L., ZAIN, A. M., OYUB, S. B., RAHMAT, R. B., GHANI, S. N. & KRISHNAN, J. 2007. A national study on the prevalence of obesity among 16,127 Malaysians. *Asia Pacific journal of clinical nutrition*, 16.
- SALEH, K. K., ABDULLAH, S. R. & MEKHA, R. E. 2019. Estimation of Serum Homeostasis Model Assessment-Insulin Resistance and Lipid Profile in Beta-thalassemia Major Patients and their Correlation with Iron Overload in Koya City. *POLYTECHNIC JOURNAL*, 9, 125-132.
- SIDIK, S. M. & RAMPAL, L. 2009. The prevalence and factors associated with obesity among adult women in Selangor, Malaysia. *Asia Pacific family medicine*, 8, 2.
- STAIANO, A. E., MARKER, A. M., MARTIN, C. K. & KATZMARZYK, P. T. 2016. Physical activity, mental health, and weight gain in a longitudinal observational cohort of nonobese young adults. *Obesity*, 24, 1969-1975.
- WSOO M. A. , R. K. H. 2017. - Correlation between thyroid hormones and body weight in hypothyroid females in Erbil city. *Zanco journal of pure and applied sciences*, 29, 1-9.
- YACH, D., STUCKLER, D. & BROWNELL, K. D. 2006. Epidemiologic and economic consequences of the global epidemics of obesity and diabetes. *Nature medicine*, 12, 62-66.
- ZIRABA, A. K., FOTSO, J. C. & OCHAKO, R. 2009. Overweight and obesity in urban Africa: a problem of the rich or the poor? *BMC public health*, 9, 465.

RESEARCH PAPER

Response of two Chickpea genotypes to different fertilizers composition and different application forms

Kamil Mohamed saleem*, Kawa Abdulkareem Ali**

* General Directorate of planning and follow up, Ministry of agriculture and water resources, Erbil

**College of Agricultural Engineering Sciences, Salahaddin University- Erbil , Kurdistan-Region, Iraq.

ABSTRACT:

A field study was conducted at Grdarashe experimental field (Latitude: 36° 4' N and Longitude: 44° 2' E- elevation 415 m above Sea level), college of Agricultural engineering sciences, Salahaddin University, Erbil Iraqi Kurdistan Region, to investigate the effect of different fertilizers on growth and yield component of two Kabuli Chickpea (*Cicer arietinum* L.) genotypes, Sham and Mexican; the fertilizers composed of five treatments Bio- fertilizer, Foliar applied fertilizer, Urea as a source of nitrogen, di-ammonium phosphate (DAP), and No fertilizer as a control. The experiment designed in completely randomized block. The results showed a significant increase in plant height when treated with foliar fertilizer compared to the control treatment. Di-ammonium phosphate (DAP) treatment was recorded the largest number of primary and secondary branches per plant compared to control treatment. The Number of pods, seed.plant⁻¹ and pods.plant⁻¹, seeds weight (g.plant⁻¹), 100 seeds weight (g) ,biological and economical yield(ton.ha⁻¹),harvest index, protein and fiber ratio increased with Bio-fertilizer treatment, which recorded the highest value compared to the others treatments.

KEY WORDS: Chickpea, Bio fertilizers, productivity parameters

DOI: <http://dx.doi.org/10.21271/ZJPAS.33.1.13>

ZJPAS (2021) , 33(1);120-130 .

INTRODUCTION:

Chickpea (*Cicer arietinum* L.) from fabaceae family is one of the most important edible seed crop in Iraqi Kurdistan and throughout the world because of its high protein (Singh et al., 2018). (Ali, 2017) indicates that chickpea contains 13 to 33% protein, 40 to 55% carbohydrates, and 4 to 10% oil. While different compounds secreted from leaves, stems and pods such content as Malic and oxalic acids have medicinal purposes for bronchitis, catarrh, constipation, diarrhea, catamenia, cholera, digestive conditions and snake bite. These acids are known to lower blood cholesterol level. In Kurdistan region cultivated area of chickpea ranged from 8000 to 9000 hectare in 2017 and 2018, while yield per hectare range from 1 to 0.9 ton (MOAWR, 2019).

Nutritional imbalance and poor nodulation appears to be the main obstacle in a single crop season (Tagore et al., 2013). Farmers distort that chickpea as a legume crop, does not need any fertilizers and usually they grow it without applying any fertilizer, this seems to be the main reason of its low yield in many countries. (Patel and Patel, 1991) observed that some progressive farmers apply a little amount of nitrogenous and phosphorus fertilizer as a starter dose (Ali et al., 2004) . An adequate supply of chemical fertilizers is closely associated with growth and development of plant as the most important inputs in crop production (Kumar et al., 2014) . (Erman et al., 2011) reported that macronutrients such as nitrogen (N), phosphorus (P) and potassium (K) are essential and important for plant growth and yield. While excessive use of chemical fertilizers can pose environmental problems which can cause potential risk for sustainability of agricultural systems (Vance, 1997).

* Corresponding Author:

Kamil Mohamed saleem

E-mail: kamil.abdulrahman@su.edu.krd

Article History:

Received: 23/05/2020

Accepted: 27/08/2020

Published: 20/02 /2021

Nitrogen is a vital basic of chlorophyll, protoplasm, protein and nucleic acid. It is related with high photosynthetic activity, the green colour of stem and leaves, branching, leaf generation and size enlargement, vigorous growth. It improves the quality of foods and protein contents of nourishment grains (Ali et al., 2010).

The use of phosphorus in leguminous crops significantly improves the yield of seeds (Hussain et al., 1981). Meanwhile, with Rhizobium and phosphorus combined applications, the yield of chickpea was significantly increased (Raut and Kohire, 1991).

(Muhammad et al., 2010a) Stated that phosphorus is important for healthy crop growth with an efficient root system and an abundance of nodules. K is essential for nitrogen and carbohydrate metabolism, activation of various enzymes and adjustment of stomata apparatus and water relations (Boyer and Stout, 1959).

Using environmentally safe fertilizers is one of the main components of sustainable agriculture methods. Bio-fertilizers are substances that contain living microorganisms and promotes growth by increasing the availability of primary nutrients, reduces environmental contamination and maximizes crop growth also they are the most

Table (1): Some physical and chemical properties of the soil used in the Grdarashe field experiment

Soil properties	Average Value
Clay	397.60 g.kg ⁻¹
Silt	546.20 g.kg ⁻¹
Sand	56.20 g.kg ⁻¹
Soil texture	SICL (silty clay loam)
Total (N)	1000 mg.kg ⁻¹
Available (P)	4.10 mg.kg ⁻¹
Available (K)	13.65 mg.kg ⁻¹
pH	7.71
EC	0.517 dSm ⁻¹
CEC	22.79 Cmolc.kg ⁻¹
Calcium carbonate	340 g.kg ⁻¹
Organic matter (Walkly and Black method)	9.6 g.kg ⁻¹

* The Soil properties were analyzed in Agriculture Research Centre - Ainkawa /Erbil.

needed techniques in crop yield that increases plant growth and yield (Namvar et al., 2011). although the chemical fertilizers application increased in developing countries, the farmers still believe that there is no need for fertilizers in chickpea fields and this is the main constrain the chickpea production.

This study was conducted to evaluate and compare the use of different fertilizer types and application forms on growth, yield and yield component of two of chickpea genotypes (Sham and Mexican).

2. MATERIALS &METHODS

2.1 Study Site: The experiment was conducted in Grdarashe field (Latitude: 36° 4' N and Longitude: 44° 2' E- elevation 415 m above Sea level) of Agriculture engineering sciences college, Salahaddin University, Erbil Kurdistan Region, during 2019 agriculture season. Some soil physiochemical properties -clay, silt, sand, soil texture (hydrometer method), total nitrogen (kjeldahl method), available phosphor (spectrophotometer), available potassium (flame photometer method), PH (PH meter), EC (electrical conductivity), CEC, calcium carbonate, organic matter, are indicated in table (1).

2.2. Meteorological data was recorded by the automated meteorological station in the field of table (2) (MOAWR, 2019).

2.3. Experimental design: The study involved three fertilization forms soil application of Urea $\text{CO}(\text{NH}_2)_2$ (N 46%) ; DAP $(\text{NH}_4)_2\text{HPO}_4$ (18:46:0) ,seed treatment with bio-fertilizer (Corabac G ,TRM) and foliar application of (Volijob), with no

fertilizer applied treatment which was considered as control . The tested plants were two chickpea genotypes (Sham and Mexican) (table 3), plots were laid out in a (Randomize Complete block design) with three replication and plot size was (1.5*2.1 m) each consisting of 6 rows (each row consisted 15 plants keeping 30 cm apart between rows and 15 cm within plants).

Table (2): Meteorological data for season 2018-2019

Months	Maximum Temp. °C	Minimum. Temp. °C	Average. Temp. °C	Average RH%	Rain precipitation mm
October	38.70	11.35	25.31	35.34	22.61
November	28.24	6.30	15.62	65.83	113.55
December	21.69	13.81	17.70	35.19	18.29
January	19.22	-2.91	8.15	72.88	96.27
February	18.43	-0.02	9.21	71.92	42.42
March	21.54	0.48	11.01	72.25	215.91
April	26.62	3.51	15.06	69.57	125.74
May	39.33	9.25	24.29	41.03	5.84
Jun	44.33	16.67	32.53	19.63	0.00
Total					640.63

* Ministry of Agriculture and Water resources (M.O.AWR 2019)

Table (3): Fertilizer types and their nutrient at percentage components

No.	Fertilizer types	Components	percentage%
1	Corabac (Bio) Microorganism	(Azotobacter, Bacillus megaterium) Gardened cultured Riolete granules	1.0 2.0 97.0
2	Voligop (foliar)	Nitrogen (carbamide) phosphor (Phosphate) potassium (hydroxide) molybdenum (molbidade) Boron (borate)	17.2 4.9 6.3 0.046 0.036
3	Urea	Nitrogen	46
4	Di-Ammonium phosphate (DAP)	Nitrogen, phosphate	18:46:0
5	control	No Fertilizers	—

2.4. Agronomical practices: Experimental plots were prepared by two dry ploughing, land levelling by rotavator, then rows were established by chisel plough after that it was hand seeded with two chickpea genotypes (Sham and Mexican) on 24th of January 2019 with the rate of (60 kg.ha⁻¹) keeping 30 cm (between rows) and 15 cm within plants ,fertilizers were used as Bio (Corabac G) with (20 kg.ha⁻¹), Urea fertilizer with the rate (40 kg.ha⁻¹), DAP (Di-ammonium phosphate) with (60 kg.ha⁻¹) which were soil applied with the sowing process, while foliar fertilizer (VOLIGOP NPK,17.2:4.9:6.3) with rate 50 ml /10 L water (20L/ha) was sprayed after 45 days from sowing.

$$\text{Biological yield} = \text{pod's weight} + \text{seed's wt.} + \text{dry shoot's wt.} \text{ --- (1)}$$

$$\text{Economical yield(t/ha)} = \frac{\text{seed's weight (g/plant)} * 2500}{\text{area plant(m}^2\text{)} * 10000} * 4 \text{ --- (2)}$$

$$\% \text{Harvest index} = \frac{\text{economical yield}}{\text{biological yield}} * 100 \text{ (Dobermann, 2007)----- (3)}$$

2.5.3. Chemical characteristics:

The chickpea seed contents (Nitrogen, Phosphorus, Potassium, Protein, carbohydrate, Oil content, Fibre and Starch) were determined in laboratories of Salahaddin and Duhok universities.

Dried seeds or shoot plant were grinded separately by an electrical blender; crushed

***Total nitrogen:**

Was determined from digested samples by kjeldahl method (Sáez-Plaza et al., 2013)

$$\% \text{ N} = \frac{(T - B) * N * 1.401}{G} \text{ --- (4)}$$

T= ml of sample titrated.

B= ml of Blank titrated.

N= acid normality (0.01N).

G= weight of powder.

***Total phosphor:**

the total phosphorous was estimated from digested samples by spectrophotometer at 410 nm as described by (Schuffelen et al., 1961).

*** Total potassium:**

Flame photometer was used for determination of potassium from plant extract according to (Allen et al., 1974).

*** Total protein:**

It was calculated by multiplying the values of total nitrogen content by 6.25 by following equation according to (Khanizadeh et al., 1995).

$$\% \text{ protein} = \% \text{ Nitrogen} * 6.25 \text{ --- (5)}$$

*** Soluble carbohydrate:**

$$\% \text{ Soluble carbohydrate} = \frac{C(\text{mg}) * \text{extract volume}(\text{ml})}{10 * \text{aliquot}(\text{ml}) * \text{sample wt}(\text{g})} \text{ --- (6)}$$

C=mg glucose obtained from the using graph

2.5. Recorded Data - parameters which have been recorded in this study were:

2.5.1. Growth characteristics

Plant height (cm), number of primary and secondary branches, pods per plant, Grains per plant, Nodules per plant, weights of 100-grains that were recorded after harvesting experimental units.

2.5.2. Yield and yield components

The data that were recorded under this category were biological yield, economical yield and harvest index (HI) according to these equations:

samples were kept in closed plastic tubes, using (0.5 g) powdered of seed and shoot mixed with (10 ml H₂SO₄) sulpheric acid and (2 ml) HClO₄ then Heating them till the color changes from black to white, make Filtration and Complete the Volume to 100 ml by distilled water as described by (Horwitz, 2010) to determine the following:

*** Oil * Fibre * Starch content (Cunniff and Washington, 1997).**

2.6. Statistical analysis: The recorded data means were compared using Duncan multiple range test with a probability of 0.05 using SPSS version 22 and computer analysis (Bah, 2001)

3. RESULTS & DISCUSSION

3.1. The effect of genotypes on some growth and yield characteristics of two chickpea genotypes

3.1.1. Vegetative parameters

As shown in the table (4) the vegetative parameters affected significantly at $P \leq 0.05$ by genotypes. The plant height (cm), number of pods per plant, number of seeds per plant, pods weight (g .per plant), seeds weight (g. per plant), and 100 seed weight (g), were (50.73, 15.00, 13.48, 7.16, 5.99 and 51.85) respectively recorded higher in

Table (4): Effect of genotypes on chickpea vegetative parameters

Genotypes	Plant. Height (cm)	No. primary branch	No. Secondary branch	No. pods (plant ⁻¹)	No. seeds (plant ⁻¹)	pods weight (g. plant ⁻¹)	No. nodules (plant ⁻¹)	seeds weight (g. plant ⁻¹)	100 seed weight (g)
Sham	46.75 b	7.89 a	46.71 a	12.63 b	10.58 b	6.39 b	23.21 a	5.14 b	42.80 b
Mexican	50.73 a	7.20 a	46.04 a	15.00 a	13.48 a	7.16 a	22.50 a	5.99 a	51.85 a

3.1.2. The effect of genotypes on yield and yield components

The results in table (5) refers that the yield parameters affected significantly by genotypes, the higher values (6.82, 1.71 and 24.86) of biological, economical yield (t.ha⁻¹) and Harvest index respectively were recorded by Mexican in comparing with Sham genotype This means that

Table (5): Effects of genotypes on chickpea yield parameters

Genotypes	biological yield (t. ha ⁻¹)	Economical yield (t. ha ⁻¹)	Harvest index%
Sham	6.04 b	1.47 b	23.78 b
Mexican	6.82 a	1.71 a	24.86 a

3.1.3. The effect of genotypes on chemical characteristics

Table (6) clarified that the chemical contents of seeds seed significantly was affected by chickpea genotypes. The percentage of Fibre, nitrogen, and protein were (6.73, 3.07 and 19.20) respectively

Mexican than sham genotype, with exception of numbers of primary and secondary branches per plant in both genotypes there were no differences that may be due to genetic variation. Moreover, no significant variances were noticed between the means of genotypes in number of nodules per plant nodules coexist. Nitrogen and Phosphorus have basic role in plant body, nitrogen being an important part of nucleic acids and proteins which are very essential in promoting the growth. Similarly at early stage phosphorus helped on encouraging root growth and better crop establishment (Dalal and Nandkar, 2010).

the highest yielding genotype (Mexican) had higher ability of producing and transporting primary metabolites that created from the vegetative organs to developing seeds than that in (sham) genotype. Which maybe refer to genetic variability between the two studied chickpea genotypes (Aliu et al., 2016) and (Alam et al., 2017).

recorded by the Sham compared to the Mexican (6.06, 2.88 and 18.01) respectively. These variations may be due to metabolites translocation or dry matter accumulation ,according to (Xu et al., 2013) and (Sharma et al., 2013).

Table (6): Chemical components of genotypes chickpea seeds

Genotype	Starch %	Carbohydrate %	Fibre %	Oil %	N %	P %	K %	Protein %
Sham	51.66 a	58.33 a	6.73 a	5.66 a	3.07 a	1.81 a	0.88 b	19.20 a
Mexican	52.17 a	58.17 a	6.06 b	5.93 a	2.88 b	1.85 a	0.97 a	18.01 b

3.2. The effect of fertilizers type on some growth and yield characteristics of two chickpea genotypes

3.2.1. The effect of fertilizers type on vegetative parameters

According to table (7) the highest plant value (52.24 cm) was recorded in treatments that received foliar applied fertilizer compared to control treatment which was (44.07 cm). Significant effect was observed on secondary branches per plant, the maximum numbers were (58.14) in chickpea plots that treated with Di-ammonium phosphate comparing with control treatment (42.57). These results are agreed with (Ahmed et al., 2010). The greatest number of pods per plant was recorded in plots that treated with Bio-fertilizer 42.17% higher pods per plant than non- treated or control plot, similar results reported by (Togay et al., 2008) and (Kumar et al., 2015). Number of grains per plant (15.18)

significantly increased when treated with Bio-fertilizer about 65.18% grains per plant higher than the control (non-fertilized) plots, as it was referred by (Alam and Seth, 2014). Pods weight g/plant, Grains weight g/plant, 100 seed weight were significantly influenced in Bio-fertilizer plots, they recorded greatest magnitude (8.58, 7.47 and 48.58g) respectively while the lowest were (5.03g) with foliar fertilizer and (4.17 and 45.15g) with control respectively, the impacts of fertilizer were significant on the number of nodules, the greatest numbers (30.19) was recorded with Bio-fertilizer which increased by 65.97% while the chemical added 20.73% more number of nodules per plant compared with control, these data explained the increase of nitrogen percentage in the above situations which lead to stronger plant growth, the results are in accordance with the finding of (Kumar et al., 2015) and (Dutta and Bandyopadhyay, 2009).

Table (7): Effects of fertilizer types on chickpea vegetative parameters

Fertilizers	Plant Height (cm)	No. primary branch	No. Secondary branch	No. pods (plant ⁻¹)	No. seeds (plant ⁻¹)	Pods weight (g. plant ⁻¹)	No. nodules (plant ⁻¹)	Seeds weight (plant ⁻¹)	100 seed weight(g)
Bio	47.82 b	7.88 a b	51.61 a b	17.80 a	15.18 a	8.58 a	30.19 a	7.47 a	48.58 a
Foliar	52.24 a	7.17 a b	43.61 a b	11.97 b	10.60 b	5.03 c	21.44 b c	4.45 b	48.10 ab
Urea	48.55 b	6.91 b	35.93 b	13.04 b	10.67 b	6.54 b	20.92 c	5.17 b	47.07 ab
DAP	51.01 a	9.00 a	58.14 a	13.75 b	14.50 a	7.53 a b	23.53 b	6.56 a	47.73 ab
Control	44.07 c	6.79 b	42.57 a b	12.52 b	9.19 b	6.22 b c	18.19 d	4.17 b	45.15 b

3.2.2. The effect of fertilizers type on yield and yield components

Table (8) indicated the significant effect of fertilizers on Biological yield, Economical yield and Harvest index, the highest value (7.53, 2.13 t.ha⁻¹ and 28.31) respectively by Bio-fertilizer comparing with the non-fertilizer which recorded the lowest value (5.61, 1.19 ton per hectare and

21.08) respectively, The bio fertilizers increase the yield components percentage (34.22%, 79% and 34.30%) for (Biological, Economical yield and Harvest index) over the control. The obvious progress in these treatments may be due to the application of bio-fertilizer and its content of useful bacteria, nitrogen fixing bacteria NFB, phosphate solubilizing bacteria PSB and

Potassium mobilizing bacteria KMB as well as some beneficial fungus, i.e., yeast and Trichoderma. Such bacteria affected plant growth and productivity through their ability to release some supporter's plant growth regulators such as indole acetic acid, ethylene, gibberellins acid and cytokinins as well as increase essential nutrients

supply nitrogen, phosphorus and potassium for plant growth (Dutta and Bandyopadhyay, 2009).

Table (8): Effects of fertilizers on yield parameters

Fertilizers	biological Yield (t. ha ⁻¹)	economical yield (t. ha ⁻¹)	Harvest index%
Bio	7.53 a	2.13 a	28.31 a
Foliar	5.79 b	1.27 b	21.67 b c
Urea	5.99 b	1.48 b	24.70 a b c
DAP	7.24 a	1.87 a	25.86 a b
Control	5.61 b	1.19 b	21.08 b c

3.2.3. The effect of fertilizers type on chemical characteristics

The fertilizers application significantly influenced nutrients and chemical contents of chickpea seeds except on the phosphor and potassium content (table9).The maximum percentage values (7.89, 6.31, 3.25, 0.98 and 20.31) were recorded by the (Fibre, Oil, Nitrogen, Potassium and Protein) in response to the application of bio-fertilizer comparing with the other treatments. Significant effects of bio-fertilizer on the percentage of N,P,K content of chickpea seeds was mentioned by (Kumar et al., 2014) .The protein is the main goal in chickpea which increased by (8.73% and 21.70%) compared to chemical and non-fertilization

treatments respectively. (Mohammadi et al., 2010) indicated that chickpea with bio-fertilizers have significantly higher protein grain, this is also clarified by(Seleiman and Abdelaal, 2018).The starch and carbohydrate recorded highest percentage (54.04 and 59.66)with no fertilizers applied and the lowest(48.62 and 56.52) recorded by bio-fertilizer usage respectively (table 9), these results are in agreement with those obtained by (Jutur and Reddy, 2007).The application of macronutrients (N, P and K) and Bio-fertilizer to chickpea plants illustrated the increase of essential yield components. Macro elements as well as bio and organic fertilizers may cause increase mineral uptake by plant and seed content (Goud et al., 2014).

Table (9): Effect of different fertilizers types on chickpea seed component

Fertilizers	Starch %	Carbohydrate %	Fibre %	Oil %	N %	P %	K %	Protein %
Bio	48.62 b	56.52 b	7.89 a	6.31 a	3.25 a	1.82 a	0.98 a	20.31 a
Foliar	51.54 ab	57.66 ab	6.12 bc	5.80 bc	2.84 c	1.84 a	0.87 a	17.75 c
Urea	52.80 a	58.95 a	6.24 b	5.50 c	3.02 b	1.86 a	0.90 a	18.87 b
DAP	52.59 a	58.45 ab	6.10 bc	6.00 ab	3.10 ab	1.78 a	0.90 a	19.41 ab
control	54.04 a	59.66 a	5.63 c	5.35 c	2.67 c	1.85a	0.95 a	16.69 c

3.3. Combination effect of genotypes and fertilization on some growth and yield parameters of chickpea

3.3.1. Combination effect of genotypes and fertilization on vegetative parameters

Table (10) clarified that interaction of chickpea genotypes and fertilizers application affected significantly on all vegetative parameters, whereas

the highest plant value was (56.57cm) observed by Mexican genotype treated with foliar fertilization compared to control treatment which recorded lowest value (43.19 cm). The greatest numbers of primary and secondary branches per plant were (10.61 and 64.51) respectively recorded by Sham genotype that received Di-ammonium phosphate fertilizer. The highest number of pods per plant (20.92) was obtained with Mexican chickpea using Bio-fertilizer, it increased by (63.82%) compared with control treatment (12.77). Number of grains per plant was (17.09) for Mexican chickpea when treated by Di-ammonium phosphate. The results in the table

(10) shows that Bio-fertilizer application on Mexican genotype obtained maximum Pods and Grains weight per plant (9.66 and 7.70 g) and increased by (60.73% and 66.67%) than control which were (6.01 and 4.62g) respectively, number of nodules per plant was (33.55) recorded the maximum value with Bio-fertilizer application which increased by (83.53%) nodules per plant compared to control treatment (18.28) nodules per plant. The maximum 100 seed weight was (53.37 g) recorded by Mexican types with foliar fertilization impacts comparing to non-fertilized treatment (48.57).

Table (10): Combination effects of genotypes and type of fertilizers on vegetative parameters of chickpea

Genotype	Fertilizer	Height (cm)	primary branch	Secondary branch	no. pods (plants ⁻¹)	no. seeds (plant ⁻¹)	pods wt. (g. plant ⁻¹)	No. nodules (plant ⁻¹)	seeds weight (plant ⁻¹)	100 seed weight (g)
SHAM	Bio	45.81 cd	7.38 b	48.71 abc	14.68 b	14.02 a b	7.49 b	33.55 a	7.24 a b	44.27 b c
	Foliar	47.91 b c	7.71 b	45.16 abc	10.17 b	8.95 cd	4.49 c	21.00 cde	3.60 e	42.83 c
	Urea	47.33 bcd	6.91 b	30.52 c	12.00 b	9.95 cd	5.80 b c	19.67 d e	5.09 c d e	42.83 c
	DAP	47.73 b c	10.61a	64.51 a	14.03 b	11.90 b c	7.76 a b	23.55 c	6.05 abcd	42.33 c
	Control	44.95 de	6.86 b	44.62 a bc	12.27 b	8.05 d	6.42 b c	18.28 e	3.71 e	41.73 c
MEXICAN	Bio	49.83 b	8.38 ab	54.51 a b	20.92 a	16.33 a	9.66 a	26.83 b	7.70 a	52.90 a
	Foliar	56.57 a	6.62 b	42.05 a bc	13.76 bc	12.24 b c	5.56 b c	21.89 c d	5.30 bcde	53.37 a
	Urea	49.76 b	6.92 b	41.33 abc	14.07 b	11.38 b cd	7.28 b	22.17 c d	5.24 c de	51.30 a
	DAP	54.29 a	7.38 b	51.76 a bc	13.47 b	17.09 a	7.31 b	23.50 c	7.06 a bc	53.13 a
	Control	43.19 de	6.71 b	40.52 b c	12.77 b	10.33 cd	6.01 b c	18.11 e	4.62 d e	48.57 a b

3.3.2. Combination effect of genotypes and fertilization on yield and yield components

The results in the table (11) shows that chickpea genotypes interaction with fertilizer treatments had significant impacts on yield parameters, whereas the table explained that biological and economical yield (8.11 and 2.20 t.ha⁻¹) respectively due to Mexican chickpea treatment

with bio-fertilizer. Harvest index recorded highest data (29.45) in Sham genotype plots that treated with bio-fertilizer, due to microorganisms activity in fixing atmospheric nitrogen and release auxins to the root zone to promotes growth, moreover bio-fertilizer enhances bacterial response to nitrogen fixation and soil fertility ([Rees et al., 2005](#)).

Table (11) Combination effects of genotypes and fertilization on yield parameters of chickpea

Genotype	Fertilizer	Biological yield (ton. ha ⁻¹)	Economical yield (ton. ha ⁻¹)	Harvest index
SHAM	Bio	6.95 bcd	2.07 ab	29.45 a
	Foliar	5.15 e	1.03 e	20.02 c
	Urea	5.93 de	1.45 cde	24.48 abc
	DAP	7.07 be	1.73 abcd	24.42 abc
	Control	5.11 e	1.06 e	20.53 c
MAXICAN	Bio	8.11 a	2.20 a	27.16 ab
	Foliar	6.44 bcd	1.51 bcde	23.32 abc
	Urea	6.05 cde	1.50 cde	24.91 abc
	DAP	7.41 ab	2.02 abc	27.3 ab
	Control	6.1 cde	1.32 de	21.6 bc

3.3.3. Combination effect of genotypes and fertilization on chemical characteristics

Table (12) clarified that the (Fibre, Oil, Nitrogen, Protein) had significantly affected by the interaction of chickpea genotype and fertilizer application, the mentioned parameters recorded

the greatest percentage (8.56, 6.69, 3.32 and 20.75) with Sham chickpea treated by Bio-fertilizer, this may be due to the increase in the mineral uptake by plants (Mohammadi et al., 2011).

Table (12): Combination effects of genotypes and type of fertilizers on chickpea seed components

Genotype	Fertilizer	Starch %	Carbohydrate%	Fibre %	Oil %	N %	P %	K %	Protein %
SHAM	Bio	46.64 b	55.22 c	8.56 a	6.69 a	3.32 a	1.81 a	1.03 a	20.75 a
	Foliar	53.2 a	59.26 ab	6.02 cd	5.8 bc	2.88 cd	1.78 a	0.82 a	18.00 cd
	Urea	52.37 a	59.04 ab	6.67 bc	5.08 c	3.16 ab	1.86 a	0.86 a	19.75 ab
	DAP	52.72 a	58.76 ab	6.37 cd	5.38 bc	3.28 a	1.72 a	0.84 a	20.52 a
	Control	53.33 a	59.37 ab	6.05 cd	5.35 bc	2.72 cd	1.88 a	0.83 a	17.00 cd
MAXICAN	Bio	50.60 ab	57.82 abc	7.23 b	5.94 b	3.18 a b	1.84 a	0.94 a	19.87 ab
	Foliar	49.82 ab	56.06 bc	6.23 cd	5.80 bc	2.8 cd	1.91 a	0.92 a	17.50 cd
	Urea	53.24 a	58.87 ab	5.82 de	5.92 b	2.88 cd	1.87 a	0.95 a	18.00 cd
	DAP	52.47 a	58.14 abc	5.84 de	6.63 a	2.93 bc	1.85 a	0.97 a	18.31 bc
	Control	54.76 a	59.96 a	5.22 e	5.36 bc	2.62 d	1.82 a	1.07 a	16.38 d

4. CONCLUSIONS

Fertilization is important for improving chickpea production and bio-fertilizer is the most vital for increasing vegetative growth, yield and chemical characteristics of chickpea seeds, due to its environmentally safe prospective. The Mexican genotype was superior to Sham genotype in this study.

ACKNOWLEDGEMENTS

Authors are thankful to Erbil Agricultural research directorate and their station research managers and staffs for providing equipment's and other facilities during the implementation the experiment

REFERENCES

- AHMED, A. G., AHMED, M., HASSANEIN, M. & ZAKI, N. M. 2010. Effect of organic and bio-fertilization on growth and yield of two chickpea cultivars in newly cultivated land. *Journal of Applied Sciences Research*, 2000-2009.

- ALAM, M., ALI, K. & HOQUE, A. 2017. Yield and yield component of chickpea as affected by boron application. *Journal of Experimental Agriculture International*, 1-9.
- ALAM, S. & SETH, R. K. 2014. Comparative study on Effect of Chemical and Bio-fertilizer on Growth, Development and Yield Production of Paddy crop (*Oryza sativa*). *International Journal of Science and Research*, 3, 411-414.
- ALI, A., ALI, Z., IQBAL, J., NADEEM, M. A., AKHTAR, N., AKRAM, H. & SATTAR, A. 2010. Impact of nitrogen and phosphorus on seed yield of chickpea. *J. Agric. Res*, 48, 335-343.
- ALI, H., KHAN, M. A. & RANDHAWA, S. A. 2004. Interactive effect of seed inoculation and phosphorus application on growth and yield of chickpea (*Cicer arietinum* L.). *International journal of Agriculture and Biology*, 6, 110-112.
- ALI, M. 2017. Response of Chickpea Varieties to Different Irrigation Regimes. *Asian Journal of Advances in Agricultural Research*, 1-7.
- ALIU, S., KAUL, H., RUSINOVCI, I., SHALAMAYRHOFER, V., FETAHU, S. & ZEKA, D. 2016. Genetic diversity for some nutritive traits of chickpea (*Cicer arietinum* L.) from different regions in Kosova. *Turkish Journal of Field Crops*, 21, 155-160.
- ALLEN, S. E., GRIMSHAW, H. M., PARKINSON, J. A. & QUARMBY, C. 1974. *Chemical analysis of ecological materials*, Blackwell Scientific Publications.
- BAH, S. 2001. *Discovering Statistics Using SPSS for Windows: Advanced Techniques for Beginners*. JSTOR.
- BOYER, T. & STOUT, P. 1959. The Micro nutrients elements. *Ann. Rev. Plant Physiol*, 10, 277.
- CUNNIFF, P. & WASHINGTON, D. 1997. Official methods of analysis of aoac international. *Journal of AOAC International*, 80, 127A.
- DALAL, L. & NANDKAR, P. 2010. Effect of NPK and biofertilizers on pigeon pea (*Cajanus cajan* L. Mill Sp.). *The Bioscan*, 5, 171-172.
- DOBERMANN, A. 2007. Nutrient use efficiency—measurement and management. *Fertilizer best management practices*, 1.
- DUTTA, D. & BANDYOPADHYAY, P. 2009. Performance of chickpea (*Cicer arietinum* L.) to application of phosphorus and bio-fertilizer in laterite soil. *Archives of Agronomy and Soil Science*, 55, 147-155.
- ERMAN, M., DEMIR, S., OCAK, E., TÜFENKÇİ, Ş., OĞUZ, F. & AKKÖPRÜ, A. 2011. Effects of Rhizobium, arbuscular mycorrhiza and whey applications on some properties in chickpea (*Cicer arietinum* L.) under irrigated and rainfed conditions 1—Yield, yield components, nodulation and AMF colonization. *Field Crops Research*, 122, 14-24.
- GOUD, V., KONDE, N., MOHOD, P. & KHARCHE, V. 2014. Response of chickpea to potassium fertilization on yield, quality, soil fertility and economic in vertisols. *Legume Research-An International Journal*, 37, 311-315.
- HORWITZ, W. 2010. *Official methods of analysis of AOAC International. Volume I, agricultural chemicals, contaminants, drugs/edited by William Horwitz*, Gaithersburg (Maryland): AOAC International, 1997.
- HUSSAIN, A., ALI, S. & ARSHAD, M. Isolation and identification of effective root nodule bacteria for important grain legumes of Pakistan. Agriculture Research Conference, Islamabad (Pakistan), 23-26 Feb 1980, 1981. PARC.
- JUTUR, P. P. & REDDY, A. R. 2007. Isolation, purification and properties of new restriction endonucleases from *Bacillus badius* and *Bacillus lentus*. *Microbiological research*, 162, 378-383.
- KHANIZADEH, S., BUSZARD, D. & ZARKADAS, C. G. 1995. Misuse of the Kjeldahl method for estimating protein content in plant tissue. *HortScience*, 30, 1341-1342.
- KUMAR, D., ARVADIYA, L., DESAI, K., USADADIYA, V. & PATEL, A. 2015. Growth and yield of chickpea (*Cicer arietinum* L.) as influenced by graded levels of fertilizers and biofertilizers. *The Bioscan*, 10, 335-338.
- KUMAR, D., ARVADIYA, L., KUMAWAT, A., DESAI, K. & PATEL, T. 2014. Yield, protein content, nutrient content and uptake of chickpea (*Cicer arietinum* L.) as influenced by graded levels of fertilizers and bio-fertilizers. *Res. J. Chem. Environ. Sci*, 2, 60-64.
- MOAWR 2019. meteorological data.
- MOHAMMADI, K., GHALAVAND, A. & AGHAALIKHANI, M. 2010. Effect of organic matter and biofertilizers on chickpea quality and biological nitrogen fixation. *World Academy of Science, Engineering and Technology*, 44, 1154-1159.
- MOHAMMADI, K., GHALAVAND, A., AGHAALIKHANI, M., HEIDARI, G. & SOHRABI, Y. 2011. Introducing a sustainable soil fertility system for chickpea (*Cicer arietinum* L.). *African Journal of Biotechnology*, 10, 6011-6020.
- MUHAMMAD, A., AHMAD, H., MUHAMMAD, A., EJAZ, A., SAGOO, A., INAYAT, U., AMIR, H. & MUHAMMAD, M. 2010a. Nodulation, grain yield and grain protein contents as affected by rhizobium inoculation and fertilizer placement in chickpea cultivar bittle-98. *Sarhad Journal of Agriculture*, 26, 467-474.
- MUHAMMAD, A., AHMAD, H., MUHAMMAD, A., EJAZ, A., SAGOO, A. G., INAYAT, U., AMIR, H. & MUHAMMAD, M. 2010b. Nodulation, grain yield and grain protein contents as affected by rhizobium inoculation and fertilizer placement in chickpea cultivar bittle-98. *Sarhad Journal of Agriculture*, 26, 467-474.
- NAMVAR, A., SHARIFI, R. S., SEDGHI, M., ZAKARIA, R. A., KHANDAN, T. & ESKANDARPOUR, B. 2011. Study on the effects of organic and inorganic nitrogen fertilizer on yield, yield components, and nodulation state of Chickpea (*Cicer arietinum* L.). *Communications in Soil Science and Plant Analysis*, 42, 1097-1109.

- PATEL, R. & PATEL, Z. 1991. Effect of farmyard manure, nitrogen, phosphorus and Rhizobium inoculation on the growth and yield of gram (*Cicer arietinum* L.). *Ann. Agri. Res*, 12, 200-02.
- RAUT, R. & KOHIRE, O. 1991. Phosphorus response in chickpea (*Cicer arietinum* L.) with Rhizobium inoculation. *Legume Res*, 14, 78-82.
- REES, D. C., AKIF TEZCAN, F., HAYNES, C. A., WALTON, M. Y., ANDRADE, S., EINSLE, O. & HOWARD, J. B. 2005. Structural basis of biological nitrogen fixation. *Philosophical Transactions of the Royal Society A: Mathematical, Physical and Engineering Sciences*, 363, 971-984.
- SÁEZ-PLAZA, P., NAVAS, M. J., WYBRANIEC, S., MICHAŁOWSKI, T. & ASUERO, A. G. 2013. An overview of the Kjeldahl method of nitrogen determination. Part II. Sample preparation, working scale, instrumental finish, and quality control. *Critical Reviews in Analytical Chemistry*, 43, 224-272.
- SCHUFFELEN, A., MULLER, A. & VAN SCHOUWENBURG, J. C. 1961. Quick-tests for soil and plant analysis used by small laboratories. *NJAS wageningen journal of life sciences*, 9, 2-16.
- SELEIMAN, M. F. & ABDELAAL, M. S. 2018. Effect of Organic, Inorganic and Bio-fertilization on Growth, Yield and Quality Traits of Some Chickpea (*Cicer arietinum* L.) Varieties. *Egyptian Journal of Agronomy*, 40, 105-117.
- SHARMA, S., YADAV, N., SINGH, A. & KUMAR, R. 2013. Nutritional and antinutritional profile of newly developed chickpea (*Cicer arietinum* L.) varieties. *International Food Research Journal*, 20, 805.
- SINGH, R., PRATAP, T., SINGH, D., SINGH, G. & SINGH, A. K. 2018. Effect of phosphorus, Sulphur and biofertilizers on growth attributes and yield of chickpea (*Cicer arietinum* L.). *J Pharmacognosy Phytochemistry*, 7, 3871-3875.
- TAGORE, G., NAMDEO, S., SHARMA, S. & KUMAR, N. 2013. Effect of Rhizobium and phosphate solubilizing bacterial inoculants on symbiotic traits, nodule leghemoglobin, and yield of chickpea genotypes. *International Journal of Agronomy*, 2013.
- TOGAY, N., TOGAY, Y., CIMRIN, K. M. & TURAN, M. 2008. Effects of Rhizobium inoculation, sulfur and phosphorus applications on yield, yield components and nutrient uptakes in chickpea (*Cicer arietinum* L.). *African Journal of Biotechnology*, 7.
- VANCE, C. P. 1997. Enhanced agricultural sustainability through biological nitrogen fixation. *Biological fixation of nitrogen for ecology and sustainable agriculture*. Springer.
- XU, Y., SISIMOUR, E. N., NARINA, S. S., DEAN, D., BHARDWAJ, H. L. & LI, Z. 2013. Composition and properties of starches from Virginia-grown kabuli chickpea (*Cicer arietinum* L.) cultivars. *International Journal of Food Science & Technology*, 48, 539-547.

RESEARCH PAPER

Some Diagnostic and Anatomical Characteristics of Five Taxa from Boraginaceae Juss. Family Erbil, Sulemania and Duhok -Iraq.

Narmin A. Saeed¹ and Jawhar F. Saeed²

¹Department of Field crops, College of Agricultural engineering Sciences, Salahaddin University- Erbil, Kurdistan Region, Iraq

²Department of Biology, College of Education, Salahaddin University- Erbil, Kurdistan Region, Iraq

ABSTRACT:

Some anatomical characteristics of five taxa belong to Boraginaceae family (*Asperugo procumbens* L. Boiss, *Buglossoides arvensis* L. Boiss, *B. tenuiflorum* L. (fil) Boiss, *B. incrassatum* Guss Boiss and *Symphytum kurdicum* Boiss. et Haussk). The study was performed in the mountain region at the north of Iraq where the field trips have been done during the year 2019. Some parts of specimens were anatomically examined by paraffin method, the diagnostic characters of stems, leaves and leaf petioles were identified. Glandular and non-glandular hairs of each species have been determined, the different trichomes in adaxial and abaxial of both leaf surfaces and stems were present. The shapes of stem in cross sections were different between the species, lysigenous canals were present in the stem of *B. tenuiflorum* and *S. kurdicum* and the druses were present only in stem of *B. incrassatum*. The main vascular bundle found in the midrib, the leaf margin shapes were different between species.

KEY WORDS: Anatomy of Boraginaceae, Leaf anatomy of *Symphytum*, Glandular hairs of leaf *Asperugo*, Stem anatomy of *Buglossoides*.

DOI: <http://dx.doi.org/10.21271/ZJPAS.33.1.14>

ZJPAS (2021) , 33(1);131-137 .

1. INTRODUCTION:

There is a remarkable revolution in the investigation of vascular plant anatomy and its use in classification in the last 60 years, the anatomical characters are as valuable as morphological ones and must not be neglected. In taxonomy, every anatomical aspect of plant has been studied without insisting on some and ignoring others, therefore, the quality of information combined are enormous (Stace, 1980). Radford *et al.* (1974) stated that anatomical characters have been employed for systematic purposes well over a hundred years and its results included that anatomical data tend to be most useful at the genus level

and at higher taxonomic categories and the anatomical characters are no more or less reliable than characters from other investigation parts of the plants, also the similarities in structural specialization do not necessarily imply close relationships but may be the result of parallel and convergent evolution and also when anatomical information are coupled with evidences from other investigation parts of the plant will a natural classification be attained.

Metcalf and Chalk (1950; 1965) mentioned that the practical applications alone provide sufficient cause to justify the use of anatomical methods in taxonomic investigations. It may be pointed out that a complete anatomical survey is necessary as a preliminary to the interpretation of Palaeobotanical remains. Furthermore, mentioned adscription for vegetative anatomical characters for many of dicotyledon families including Boraginaceae family with

* Corresponding Author:

Narmin Azeez Saeed

E-mail: narminaziz.99@gmail.com

Article History:

Received: 05/08/2020

Accepted: 08/09/2020

Published: 20/02/2021

identification of some important anatomical characteristics which are considered the merit feature of the family. Cronquist, (1981) hinted to some of the anatomical characteristics of the Boraginaceae through the family description as well.

There is no anatomical study in Iraq pertaining with the understudied taxa of the family Boraginaceae, so this study was the first study according to available literature. The terms in this study depended on the terminologies that come from (Metcalf and Chalk, 1950), (Esau, 1965) and (Radford *et al.*, 1974).

2. MATERIALS AND METHODS

The plant parts as stem, leaf and petiole were obtained from collected samples of Boraginaceae taxa (*Asperugo procumbens*, *Buglossoides arvensis*, *B. tenuiflorum*, *B. incrassatum* and *Symphytum kurdicum*) that existed in different districts from mountain region Kurdistan region of Iraq. The following steps are conducted for preparation the permanent slides of cross sections of the leaves parts and stems; a small parts of the samples were taken in size 0.5-1 cm, then placed in a small vial contain F.A.A. solution for 24 hour at room temperature (Saeed, 2003).

The samples placed in series of ascending concentration of Ethanol 95% for one hour and 100% for three to four hours twice in each concentration. Then the samples were placed in solution of absolute xylene for 3-4 hours twice, then placed in mixture of melted paraffin and xylene 1:1 for half (0.5) hours in an oven at 60 °C. Finally the sample placed in melted pure paraffin only for overnight in an oven at 60 °C. For paraffin wax templates preparation poured with melted paraffin previously covered by thin film of glycerol to prevent adhesion of the paraffin to the metal, as adopted by (Najmaddin and Mahmood, 2016). Sectioning was done by using Rotary Microtome and the samples were cut with 8µm thickness, The slides were dried by putting on hot plate at 45°C and left at room temperature for overnight for completing affixing process (Johansen, 1941). The sections were stained by using Safranin and light green. The sectioning done according to the procedure that modified by (Al-Khazrajy and Aziz, 1990). The sections were examined and the photographs were taken by light microscope Olympus with digital camera system.

3. RESULTS:

1. Cross section of lamina:

The epidermis of the leaf was covered by continuous of waxy layer (cuticle), the cuticle thickness is vary among the taxa, it is thick in most taxa, but appears thin in another such as *A. procumbens* and *B. tenuiflorum* (fig. 3 and 4)

In cross section, the epidermal cells as in species of Boraginaceae were arranged in single irregularly layer, the lumen of cells were appear in spherical, semi-spherical, polygonal, oblong, narrowly oblong, semi quadrate and ovate, which have different size in the same layer of single blade. The external cell walls were convex and thick, the other sides of the cell walls were concave, convex or straight and thin (fig. 3 and 4).

All studied species of the family were dorsiventral and possess heterogeneous mesophyll. The vascular bundles were collateral closed system. The palisade cells were oblong in shape with obvious intercellular spaces, were arranged in (1) layer as in *A. procumbens* and *S. kurdicum*; (2-3) layers as in *B. tenuiflorum*, *B. arvensis* and *B. incrassatum*. The spongy cells have different irregular shapes with ovoid to ovoid oblong, quadrate and rectangular with obvious intercellular spaces, were arranged in (4-7) layers depended on the location and lamina thicknesses, most mesophyll cells were containing tannin also. (fig. 3 and 4)

The trichomes play a role in plant taxonomy, especially for delimitation among morphologically similar taxa in a single genus. In all studied taxa the trichomes occur in peculiar forms and size in different positions and parts of the plants and there were non- glandular trichomes were unicellular in all studied species but they were various shapes and size (fig. 1), conical bristle, they found in leaves of *A. procumbens*. The dimensions of hairs were (24.4-79)×(4-67)µm. Conical falcate, they were presence in the leaves of *B. tenuiflorum*. The dimensions of hairs were (12.2-118)×(6.9-88.2)µm. While cylindrical filiform of pilose, this types present on the leaves of the most studied taxa, as in *S. kurdicum* and *B. incrassatum*. The dimensions of hairs were (370.1-11.3)×(4-59.7)µm and (120.3-16.4)×(6.536.3)µm respectively. The Glandular hairs, they were presence in all studied species, there were unicellular and multicellular hairs; which were various shapes and size (fig. 2), they were sessile glandular hairs consist of multicellular globoid head (trichomes consisting

of small bulbous bases bearing long, hypha-like terminal portions), such as found in the leaves of *A. procumbens*, and *B. incrassatum*; the dimensions of head were $(3.7-79.7) \times (2.2-67.6) \mu\text{m}$. the sessile capitate unicellular hairs, they present in the leaves of *B. arvensis*, *B. tenuiflorum*, and *S. kurdicum*; the dimensions of head were $(6.2-105) \times (4.6-71.8) \mu\text{m}$.

2. Leaves tip and margin:

The leaves margin outline were varying in Boraginaceae member. The margin was straight rounded tip as in *S. kurdicum*, while rounded downward tip as in *B. arvensis* and *B. tenuiflorum*, when rounded slightly downward tip in *A. procumbens* and *B. incrassatum*. The unicellular glandular trichomes found in *B. incrassatum* and *B. tenuiflorum* and the unicellular non-glandular trichomes presence in *S. kurdicum*, while *A. procumbens* *B. arvensis* do not have trichomes (fig. 5).

3. Petiol:

The current anatomical study reveals, that the leaves petiole of high signification taxonomic character, it is owing to; among all studied taxa only two species were petiolate such as *A. procumbens* and *S. kurdicum*, the other studied species was sessile, each of these two species have their particular shape and vascular strand. The petiole has only one large vascular bundle in center; the abaxial was V shape and the adaxial was concave with two lateral projection, each lateral projection contains small vascular bundle of lateral veins (fig. 6).

4. Midrib:

The midribs outline of the studied species were various in shapes, the midrib outline was V-shaped in the abaxial and concave in adaxial as in *A. procumbens*, while the abaxial was rounded and concave in adaxial such as *B. arvensis*, *B. incrassatum* and *B. tenuiflorum*, whereas the midrib is rounded in abaxial surface and adaxial surface in *S. kurdicum*.

The midrib vascular strand was collateral closed arrangement type, relatively larger than other lamina vascular strands, approximately similar in shape in all species, they appear in gibbous or crescent shape, consist of (8-13) xylem straps arrange perpendicularly above phloem tissue. In all species the vascular strand surrounded by (2-3) parenchymatous layers (bundle sheath). Also the species of this family have lacunar collenchyma in adaxial and abaxial

layer. The unicellular trichomes found in *Buglossoides arvensis*; *B. incrassatum* and *B. tenuiflorum*, while *A. procumbens* and *S. kurdicum* do not have trichomes (fig. 7).

5. General Anatomical Description of Stem:

The cross sections outline of stems were varying in shapes in studied taxa of the family, the outline was irregular, with three small projection in *A. procumbens*, circular to semi-circular with four projection (two small and two larger) in *B. arvensis*, circular to semi-circular with one small projection in *B. incrassatum*, circular to semi-circular with one small projection in *B. tenuiflorum*, and irregular with one small projection in *S. kurdicum* (fig. 8).

Non-glandular trichomes were unicellular, Cylindrical bristle like obtuse tip, there were found only in the stem of *B. arvensis*, the dimensions of hairs were $(16.1-) \times (50.8) \mu\text{m}$. Conical falcate presence in the stem of *B. tenuiflorum*, $(12.2-118) \times (6.9-88.2) \mu\text{m}$. Cylindrical filiform of pilose, in the stem of *S. kurdicum* and *B. incrassatum*, $(370.1-11.3) \times (4-59.7) \mu\text{m}$ and $(120.3-16.4) \times (6.536.3) \mu\text{m}$ respectively. Sessile glandular hairs consist of multicellular globoid head, they were found in the stem of *B. incrassatum*, $(3.7-79.7) \times (2.2-67.6) \mu\text{m}$ and Sessile capitate unicellular hairs, they present in the stems of *B. arvensis*, *B. tenuiflorum*, and *S. kurdicum*. The dimensions of head were $(6.2-105) \times (4.6-71.8) \mu\text{m}$. Hypoderms in studied taxa contain lysigenous ducts in *B. tenuiflorum* and *S. kurdicum*, while *B. incrassatum* contains druses (fig. 9). The vascular strands in all studied taxa were continuous circular ring except in *S. kurdicum* which the vascular strands were arranged in interrupted circular ring-like (fig. 10-13).

4. DISCUSSION:

The anatomical study of different parts of Boraginaceae taxa, there were many significant anatomical characteristic are obtained to be taken account of separating the under the genera and species levels, as Al-dabbagh and Saeed, (2019) believed that

the dissimilarity in epidermal tissue, type of trichomes, stem outline, leaf margin, and midrib outline have great roles in separating species especially among closed species within a single genus.

In this study, the microscopic investigation of micromorphology showed various types of trichomes, about five types of both glandular and

non-glandular hairs have been observed in studied taxa.

The epidermal of all Boraginaceae species were contained different types of trichomes in different part of the plant body. This differences are evidence of high taxonomic value of segregation genera and species as mentioned by Najmaddin (2016). (Stace, 1980) believed that the trichomes have significance value at all levels in plant classification, from family to even varieties.

The epidermal cells of the stem, there are single layer according to number of epidermal layers.

The mesophyll layer has limited role in identifying the species; generally it is dorsiventral for example composed of the palisade and spongy parenchyma layers as mentioned by Najmaddin (2016).

The midrib and the margin outline, with their contents have the taxonomic value of the genera and species levels, especially the midrib outlines have particular shape of each genus and species as mentioned by (Al-dabbagh and Saeed, 2020).

The anatomical characters of petioles were best feature of difference between *A. procumbens* and *S. kurdicum*, while another species are sessile.

The outline of the stem clearly showed important variation in the shape. In all species the stem epidermis was single layers. Hypoderms in studied taxa have different pattern in tissue contain, *A. procumbens* composed large parenchymatous cells with very thin walls, while in *B. arvensis*, *B. incrassatum*, *B. tenuiflorum* and *S. kurdicum* composed 3-8 layer of lacunar collenchymatous tissue, with 2-3 layers of parenchymatous tissue toward the pith, the cortex in *B. tenuiflorum* and *S. kurdicum* contain lysigenous, whereas *B. incrassatum* contains druses, these results are matches with what cited by (Metcalfe and Chalk, 1950; 1965). The Boraginaceae taxa contain tannin.

5. CONCLUSION:

The current study demonstrated that the anatomical characteristics have a great role in taxonomic value among studied genera and species of Boraginaceae family, and it has shown approximately some anatomical differences between the studied species especially in morphologically closed taxa within single genus.

Acknowledgements

The Authors acknowledge with many thanks to the botanists Dr. Chnar Najmaddin (College of Science, Salahaddin University-Erbil/Iraq) and Dr. Serwan Taha Al-dabbagh (College of Agricultural engineering Sciences, Salahaddin University-Erbil/Iraq) to help us facilitate the performance of the anatomical processes.

Conflict of Interest (1)

No conflict of Interest

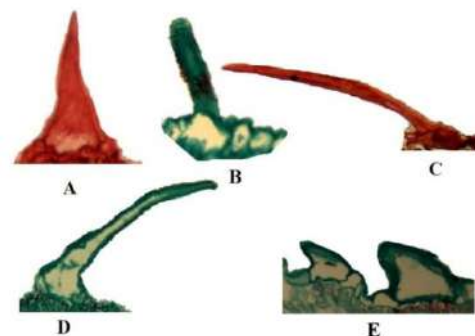


Figure 1: Non-glandular hair types in studied taxa of Boraginaceae:

A- conical bristle; B- Cylindrical bristle-like obtuse tip; C and D- cylindrical filiform of pilose; E- Conical falcate, 40X

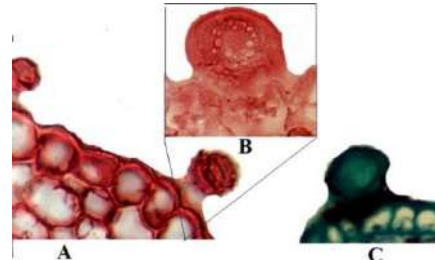


Figure 2: Glandular hair types in studied taxa of Boraginaceae:

A and B- Sessile glandular hairs consist of multicellular globoid head 40X; B- magnified portion 100X; C- Sessile capitate unicellular hairs 40X.

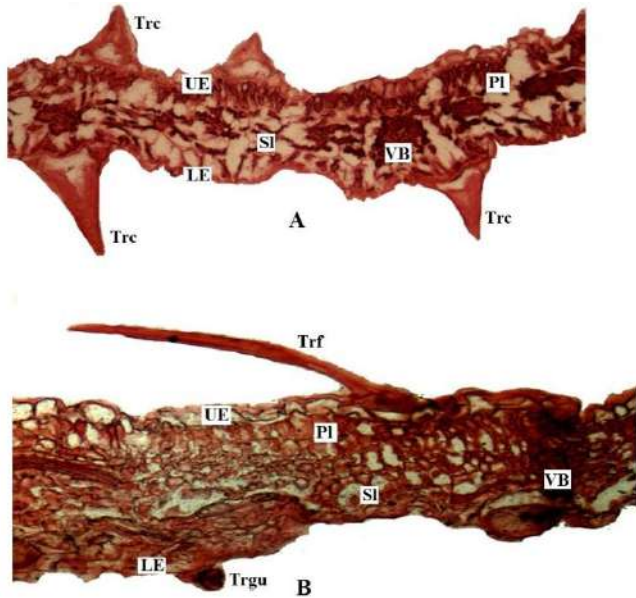


Figure 3: Cross sections of leaf of the studied species of Boraginaceae:
 A- *A. procumbens*; B- *B. incrassatum*; C- *B. arvensis*.
 UE- upper epidermis; LE- lower epidermis; VB- vascular bundle; PI- palisade layer; SI- spongy layer; Trc- Conical bristle; Trf- cylindrical filiform of pilose; Trgu- Unicellular glandular hair and Trgm- Multicellular glandular hair.(40x).

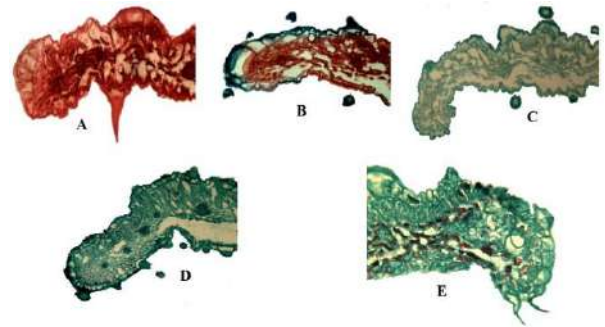


Figure 5: Leaf blade tip and margin outlines in studied taxa of Boraginaceae:
 A- *A. procumbens*; B- *B. incrassatum*; C- *B. arvensis*; D- *B. tenuiflorum*; E- *S. kurdicum*.

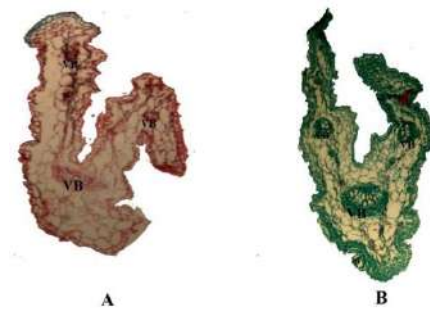


Figure 6: Cross sections of petioles of studied Boraginaceae species. A- *A. procumbens*; B- *S. kurdicum*. (10x).

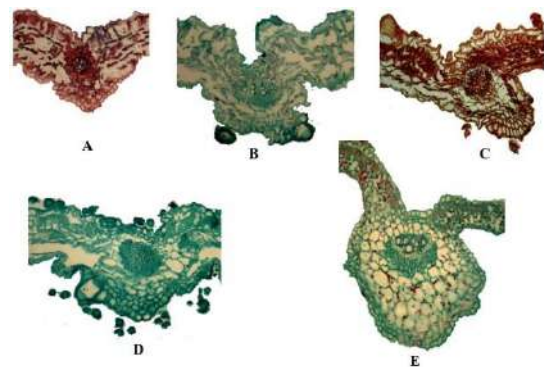


Figure 7: Leaves midrib outline in studied taxa of Boraginaceae:
 A- *A. procumbens*; B- *B. arvensis*; C- *B. incrassatum*; D- *B. tenuiflorum*; E- *S. kurdicum*. (40x).

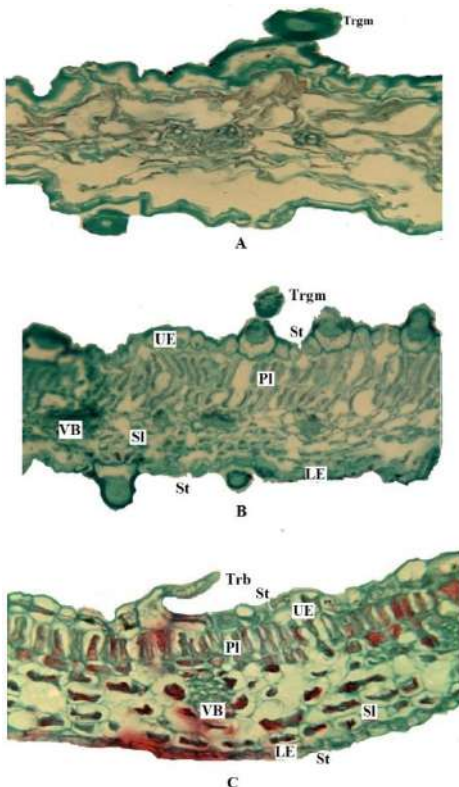


Figure 4: Cross sections of leaf of the studied species of Boraginaceae:
 A- *B. arvensis*; B- *B. tenuiflorum*; C- *S. kurdicum*.
 UE- upper epidermis; LE- lower epidermis; VB- vascular bundle; PI- palisade layer; SI- spongy layer; Trc- Conical bristle; Trf- cylindrical filiform of pilose; Trgm- Multicellular glandular hair and St- stomata.(40x).

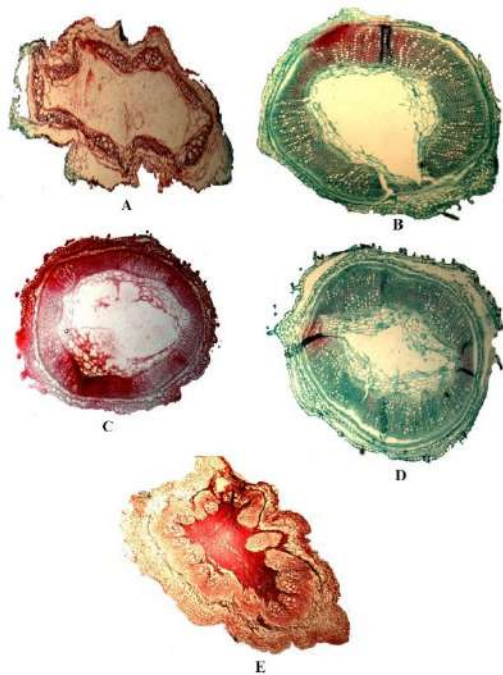


Figure 8: Cross sections of stem outlines of the studied taxa of Boraginaceae: A- *A. procumbens*; B- *B. arvensis* ; C- *B. incrassatum*; D- *B. tenuiflorum* and E- *S. kurdicum*. (10x).

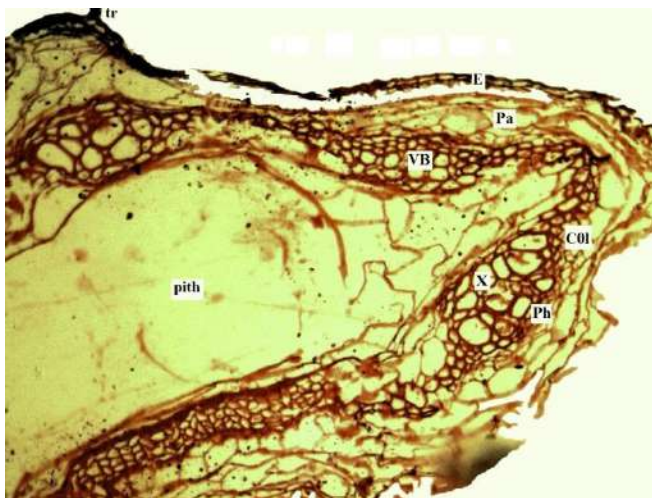


Figure 9: Portions of cross section of the studied *A. procumbens* species stem.

E= Epidermis; tr= trichome Pa= Parenchyma; VB= Vascular bundle; Col=Collenchyma; X= Xylem and Ph= Phloem, (Magnified 40x).

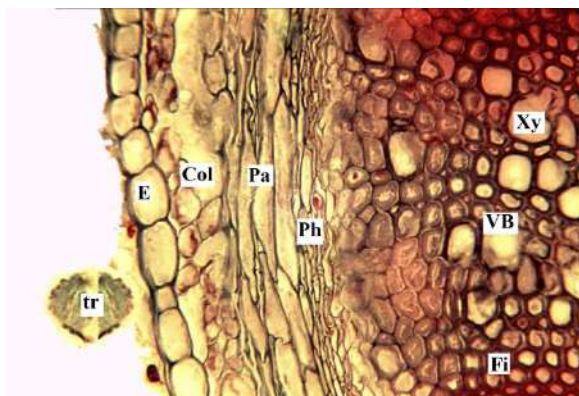


Figure 10: Portions of cross section of the studied *B. arvensis* species stem.

E= Epidermis; tr= trichome Pa= Parenchyma; VB= Vascular bundle; Col=Collenchyma; Xy= Xylem; Fi= Fiber and Ph= Phloem, (Magnified 40x).

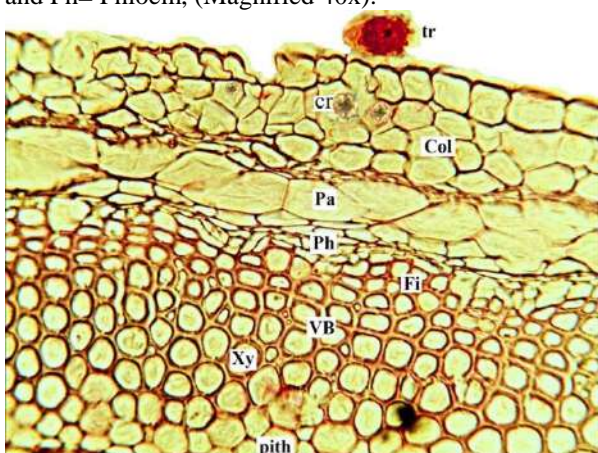


Figure 11: Portions of cross section of the studied *B. incrassatum* species stem.

cr= crystal; tr= trichome Pa= Parenchyma; VB= Vascular bundle; Col=Collenchyma; Xy= Xylem; Fi= Fiber and Ph= Phloem, (Magnified 40x).

References:

- Al-dabbagh, S.T. and Saeed, J.F. 2020. Morphological and Anatomical Variations of Fruits in Some Taxa of Valerianaceae Batsch Family. Iraqi J. Agric. Sci. 51, 101–115.
- Al-dabbagh, S. T. and Saeed, J.F. 2019. The Phenetic Study of Distributed Species of Valerianaceae Batsch Family in Kurdistan Region-Iraq. ZANCO Journal of Pure and Applied Sciences, 31(3); 23-31.
- Al-Khazrajy, T.M. and Aziz, F.M. 1990. Practical in Plant Anatomy and Micro Techniques. Min of higher education and science research, Salahaddin Univ, (in Arabic), Erbil, Iraq, pp.239-246.
- Cronquist, A. 1981. An Integrated System of Classification of Flowering Plants. Columbia University Press, New York, USA, pp.864-894.
- Esau, K. 1965. Plant anatomy of seed plants, Second edi. ed. John Wiley & Sons, Inc., New York. Sydney, pp.767.

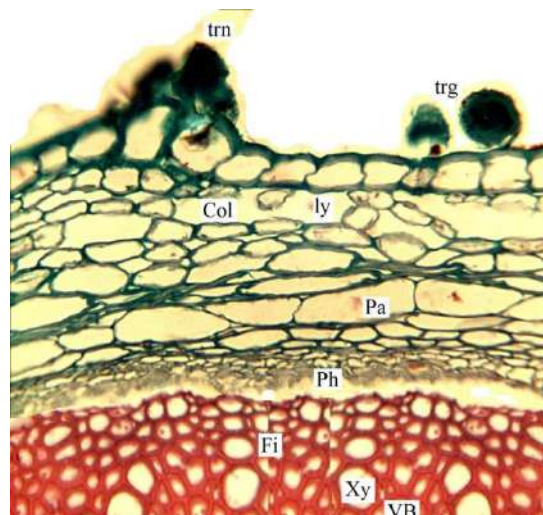


Figure 12: Portions of cross section of the studied *B. tenuiflora* species stem.

trn= non-glandular hair; trg= glandular hair; ly= lysigenous; Pa= Parenchyma; VB= Vascular bundle; Col=Collenchyma; Xy= Xylem; Fi= Fiber and Ph= Phloem, (Magnified 40x).

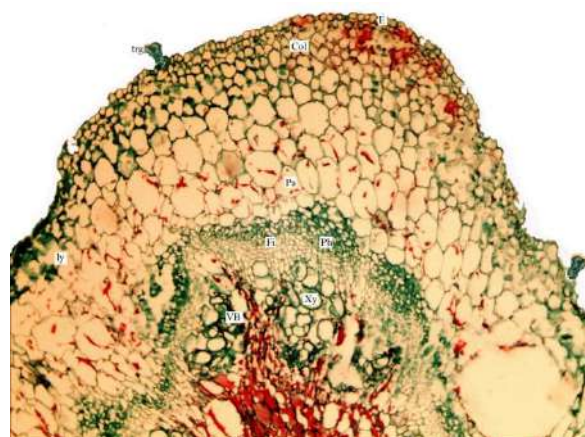


Figure 13: Portions of cross section of the studied *S. kurdicum*.species stem.

trg= glandular hair; ly= lysigenous; Pa= Parenchyma; VB= Vascular bundle; Col=Collenchyma; Xy= Xylem; Fi= Fiber and Ph= Phloem, (Magnified 40x).

- Johansen, D.A. 1941. Plant Microtechnique, Nature. McGraw-Hill Book Company, New York and London. <https://doi.org/10.1038/147222b0>
- Metcalf, C.R. and Chalk, L. 1965. Anatomy of the Dicotyledons, Vol. II. ed. Clarendon press. Oxford, London, Great Britain, pp.446..
- Metcalf, C.R. and Chalk, L. 1950. Anatomy of the Dicotyledons, Vol.I. ed. Oxford University Press, London, UK, pp.80-87..
- Najmaddin, C. and Mahmood, B.J. 2016. Anatomically And Palynologically Studies Of Some Carthamus tinctorius Genotypes. Int. J. Biol. Sci. Vol. 03, 1–13. <https://doi.org/10.7150>
- Radford, A.E., Dickson, W.C., Massey, J.R. and Bell, C.R. 1974. Vascular Plant Systematics. Harper and Row, New York, pp.891.
- Saeed, J.F. 2003. Systematic Study of the genus Campanula L. (Campanulaceae) in Iraq. PhD thesis, Education College, Salahaddin University-Erbil, Erbil, Iraq.
- Stace, C.A., 1980. Plant Taxonomy and Biosystematics. Pitman Press, Bath, Great Britain, pp.279.

RESEARCH PAPER

Optimizing Electro-oxidation, Electrocoagulation and Electro-Fenton processes for Treating Model Pesticide Wastewater containing Bromuconazole

Yusuf Yavuz ^{a,*}, Mohammed Azeez OTHMAN ^b

^a Anadolu University, Dept. of Environmental Engineering, Turkey

^b Anadolu University, Graduate School of Applied Sciences, Dept. of Environmental Engineering, Turkey

ABSTRACT:

In this work the removal efficiency of Bromuconazole and chemical oxygen demand (COD) from aqueous solution using different electrochemical processes (electro-oxidation process (EOP), electrocoagulation process (ECP) and electro-Fenton process (EFP) were investigated. All experiments were achieved at the natural pH of solution. The effects of some parameters such as current density and H₂O₂ concentration on COD and pesticide removal efficiency have been carried out at an initial pH of 8.45, current density 5,10,15,20 mA/cm², an initial pesticide concentration of 300 mg/L, 5mM Na₂SO₄ support electrolyte and temperature of 30°C. The COD decrease at the end of 80 minutes of treatment from 1200 to 167.52 mg/L by EOP, to 248.26 mg/L by ECP, and to 237.94 mg/L by EFP. Results showed that a high COD reduction was obtained by EOP (85.59%), followed by EFP (80.48%) and electrocoagulation at (79.51 %) with a constant current density of 20, 20, 15 mA/cm² respectively. The removal of bromuconazole pesticide exhibited a pseudo-second-order reaction with rate constant 0.0009 mg⁻¹Lmin⁻¹. Moreover, energy consumption, the cost of degradation and sludge formation were also determined.

KEY WORDS:

DOI: <http://dx.doi.org/10.21271/ZJPAS.33.1.15>

ZJPAS (2021) , 33(1);138-145. .

INTRODUCTION:

During the last years, an increasing concentration on environmental protection and sustainability led to more firm laws that aim to minimizing rate and levels of outflow pollution. On the other hand, research and development has grown into more functional alternative technologies to enhance wastewater treatment processes, without making additional damage to environmental. Industrial wastewater is complex and always consists of inorganic and organic compounds, that make a process of treatments difficult due to the lack of a comprehensive treatment strategy. The water polluted with organic compounds, a best economically feasible alternative process is biological oxidation treatment, although some of toxic molecules do not degrade adequately by such treatment process. (Panizza and Cerisola, 2009).

Electrochemical methods represent an environmentally and economically applicable alternative, in which major reagent is electron, that is efficient, versatile, clean and productive in relation to its cost. (Kapalka, et al., 2010 and Andrade et al.,2007). The electrochemical treatment processes have been greatly used for treatment of wastewater contaminated with pesticides, pharmaceuticals and dyes (Rajeshwar et al.,1994, Silva et al., 2011 and Ciríaco et al., 2009). It has been focused and concentrated on pesticides compounds due to its harmful effect on the human health and the environment (Zaleska and Hupka, 1999 & Wang et al.,2007). Pesticide compounds toxic and harmful to non-target living organisms including humans in which inter the body within the food chain (Chiron *et al.*, 2000). Large number of pesticide compounds are non-

* Corresponding Author:

Yusuf Yavuz

E-mail: mohammed.othman@su.edu.krd

Article History:

Received: 19/01/2020

Accepted: 13/09/2020

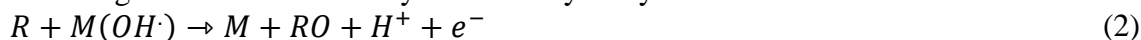
Published: 20/02 /2021

biodegradable due to its molecular structure that have stable strong bonds. Natural water pollution with pesticide has become a widespread issue. Wastewater originates from pesticide producing industries during cleaning actions after batch operation of the synthesis operation. It usually includes toxic pesticide residues and organics which threatens the quality of ground and surface water (Wang et al.,2007). Wastewater from pesticide manufacturing plants and agricultural industries were evaluated to have pesticide contamination scales of 500 mg/L (Menegola et al., 2005). Among this such class of contaminants, Bromuconazole pesticide take our attention due to their high photochemical stability; its resist to photolysis and hydrolysis is not predicable to be a considerable process in the breakdown of pesticide bromuconazole in aquatic systems.

Bromuconazole compound belongs to the set of triazole fungicides. It is applied as a broad-spectrum fungicide, with curative and preventative action, in order to control the diseases caused by deuteromycetes, basidiomycetes, and ascomycetes (EPA, 2002). Its registered toxicity data include the acute oral LD₅₀ in rats (365mg/kg) with data

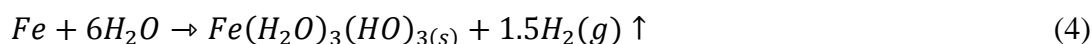
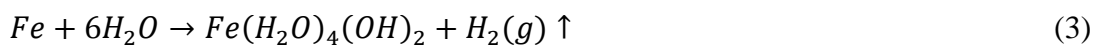


After that organic matter oxidize by absorbed hydroxyl radicals



In which RO indicate oxidizing organic matter and may be further oxidizing by the hydroxyl radicals ($\cdot OH$) formed from water electrolysis.

1.2 Theory of EC Process



1.3 Theory of EF Process

In EFP, pollutants are break down by the presence of Fenton's reagent in the media together with anodic oxidation at surface of anode



showing that rat's exposure to Bromuconazole produced lesions in all parenchymatous organs including hepatoma and later increase in liver weight (Shchepetkin *et al.*, 2003). Toxicity caused by bromuconazole can be enhance the production of reactive oxygen species in addition to enhancing lipid peroxidation endogenous and antioxidants depression (Cheng et al., 2007).

The using of electrochemical treatment methods for removal of pesticides are of concern. ECP, EOP and EFP are the excellent ways to solve environmental issue produced by the outflow of these effluents. The present work involves removal of Bromuconazole from solutions prepared from the commercially available pesticide by ECP, EOP and EFP. The removal of pesticides by such methods was evaluated with impact of initial pH.

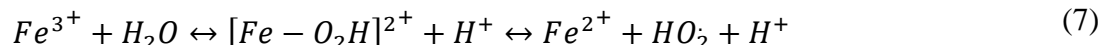
1.1 Theory of EO Process

The toxic pollutants are break down by oxidant such as O₃, ClO₂, OH, Cl₂, O, ClOH, H₂O₂ etc., which are formed from anodic oxidation within the electrolysis (Babuponnusami and Muthukumar., 2012).

ECP is based on in-situ production of coagulants, together, there is a production of hydrogen on a cathode that allows removal of pollutant by sedimentation or floatation. Overall chemical reactions are:

(Greenberg and Clesceri,1992). hydroxyl radical is then generated in the media by a traditional Fenton's reaction between ferrous ion and hydrogen peroxide (Eq. 5):

Renovation of Fe^{2+} may also be done by the oxidation of the organics with H_2O_2 or by reaction with hydroperoxyl radical (HO_2^\cdot) as shown in reaction below:



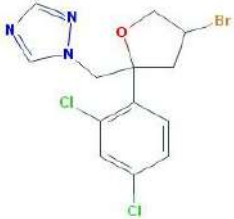
2. Materials and methods

2.1 Chemicals

Pesticide used in present work was Bromuconazole. Bromuconazole solutions were prepared from the commercially found pesticide solution having a Bromuconazole concentration of 480 g/L. This concentration is similar to that applied by farmers. The property of a

Bromuconazole is shown at Table 1. All solutions were prepared by distilled water. Potassium dichromate ($K_2Cr_2O_7$) Standard solutions, sulfuric acid (H_2SO_4) reagent with silver sulphate (Ag_2SO_4), has been prepared in order to measure the COD. The COD was determined by a closed reflux colorimetric technique (Chen et al., 2000). All chemicals used were reagent grade.

Table 1. Structure of pesticide present in sample

Name	Structure
Bromuconazole $C_{13}H_{12}BrCl_2N_3O$	
Molecular weight (g/mol)	377.063

2.2 Equipment's and Procedures

The electrochemical cell consists of a 600 mL glass reactor. Experiments were conducted with 400 mL of the sample and 5 mM of Na_2SO_4 was used as supporting electrolyte. Electrodes were connected to a digital DC power supply Statron 3262.3 model (0-4 A and 0-300 V). The stable stirring speed of 300 rpm with magnetic stirrer was applied along the experiment process. The electrochemical treatment was applied at room temperature and atmospheric pressure. Duration of electrolysis was 80 min. the samples has been drawn at regular intervals of time in order to evaluate the reduction efficiency in COD. All

experiments were repeated duplicate. A constant current density of 5, 10 15, and 20 mA/cm^2 has been applied in all the three electrode systems for comparison.

2.3 Boron doped diamond electrodes

electrode set up

Electrolysis was performed with DC power supplies using two BDD electrodes (one anode and one cathode) with the length of 5 cm and width of 3.7 cm and the distance between two electrodes of 0.5cm. The supporting electrolyte (Na_2SO_4) of 5mM and 10mM was added. The samples were withdrawn at a regular time interval of 20 min for 80 min. laboratory scale electrochemical reactor shown in Figure (1).

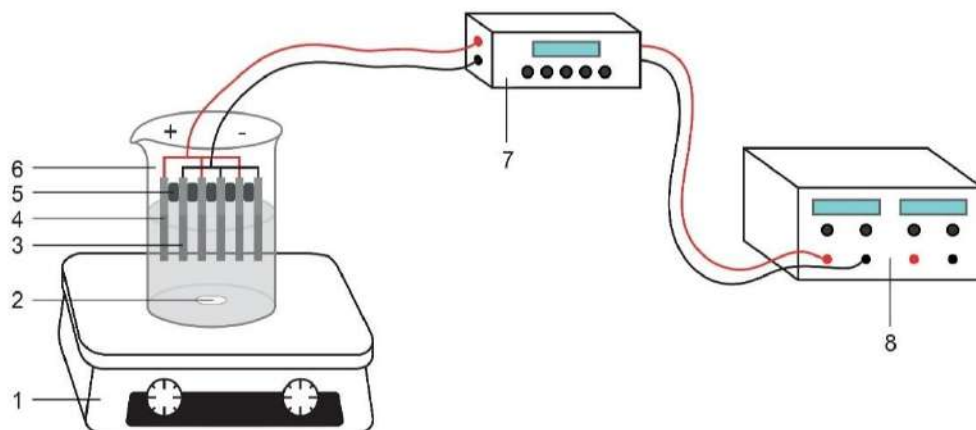


Figure 1 Schematic of experimental electrocoagulation system (1. thermostatic magnetic stirrer, 2. magnet, 3. cathode, 4. anode, 5. Rubber Insulator, 6. beaker, 7. polarity changer, 8. DC power supply)

2.4 Analytical techniques

During experiments, samples were collected and instantly measured without using any filter. Chemical oxygen demand data were obtained with a procedure shown by TS2789 standard (water

quality-Determination of COD). The samples were titrated with ferric acid ammonium sulphate (FAS) which was previously standardized to determine the amount of potassium dichromate consumed (Yavuz, 2007).

COD removal percentages of obtained samples were calculated as follows:

$$\text{COD removal \%} = \frac{(\text{COD}_o - \text{COD}_t)}{\text{COD}_o} * 100$$

**(Error!
No text of
specified
style in
document..1)**

Where COD_o (initial) and COD_t (any time) of the pesticide treatment samples and calculated in mg/L.

Remaining pollutants of bromuconazole pesticide were evaluated with the UV-visible spectrophotometer at $\lambda_{\text{max}} = 230$.

3. Results and Discussion

Despite the used electrochemical processes have their disadvantages and advantages, existing paper aims to understand the extent of pesticide removal in wastewater. Comparison of the methods (EFP, EOP, and ECP) at certain conditions of a current density and time duration aids the identify a point at which best removal of pesticide could be done.

3.1 COD removal capacity

It has been noticed that an initial pH of wastewater solution is remarkable operating factor effecting the electrochemical treatment performance (Emanjomeh and Sivakuma, 2009). In order to evaluate its effect during the treatment process, the sample pH was kept at its normal range.

In the case of Electrocoagulation, the higher COD reduction efficiency noted at the end of 80 min was 79.51 %. The current density was 20 mA/cm^2 and pH 7.79. This is may be due to the fact that the $\text{Fe}(\text{aq})$ ions formation and then their oxidation to $\text{Fe}^{3+}(\text{aq})$ led to precipitation of $\text{Fe}(\text{OH})_3$; At higher pH the oxidation by oxygen became higher. During EOP, the generated hydroxide reacts with organic pollutants found in the samples (Yavuz, 2007). At the end of 80 min of

experiment, higher COD removal was 85.59% with a current density of 15 mA/cm² and pH 5.32

It may be summarized that at an acidic pH, chlorine is found in the form of a Hypochlorous acid (HOCl) which demonstrate the oxidation process. During EFP, the removal efficiency of COD was 80.48% at the end of 80 min. current density was 15 mA/cm² and pH 7.84. When the applied current density is high, COD removal is directly proportional to the

Hydrogen peroxide concentration (Yavuz, 2007). low COD removal was seen during other conditions for all of studied methods.

Although, an optimal pH obtained during treatment process was 7.84 because of organics compound or its intermediate products reactions that might interact with iron species that led to the formation of iron complexes which assist catalytic cycles of iron. The highest COD removal efficiency was determined as shown in the (Fig. 1).

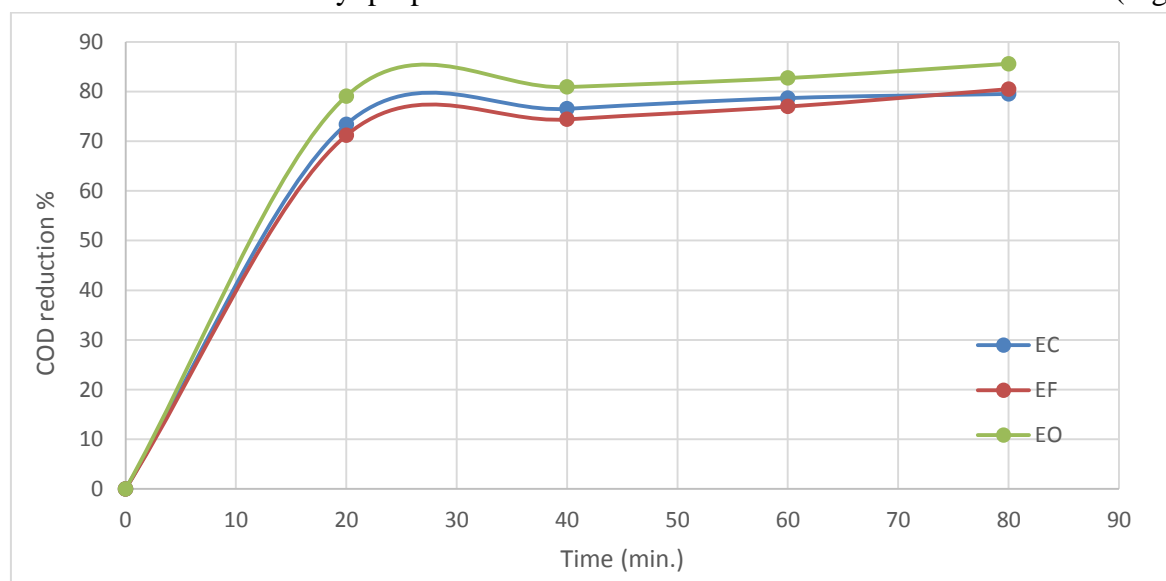


Fig.1. Variation of COD removal efficiency for electrochemical processes (Co=300mg/l, 5mM Na₂SO₄, natural pH, i=20mA/cm² for EC and 15 mA/cm² for EF, EO).

3.2 Energy consumption

During electrochemical treatment process, an important economic parameter is energy

$$\text{Energy Consumption (E)} = \frac{I \cdot V \cdot t}{\text{Vol} \cdot 1000} \quad (9)$$

then I, V and t stand for electrical current intensity (A), average voltage of the EC system (v), and reaction time (h), respectively.

From the data of ECP, higher COD reduction percentage of about 79.51% was observed with an energy consumption of about 170.12 kWh/m³ while, in the EFP and EOP case, the higher COD reduction was 80.48 and 85.59 % with the energy consumption of 96.73 and 54.09 kWh/m³ respectively. EOP energy consumption is lower than that of the EFP. EFP

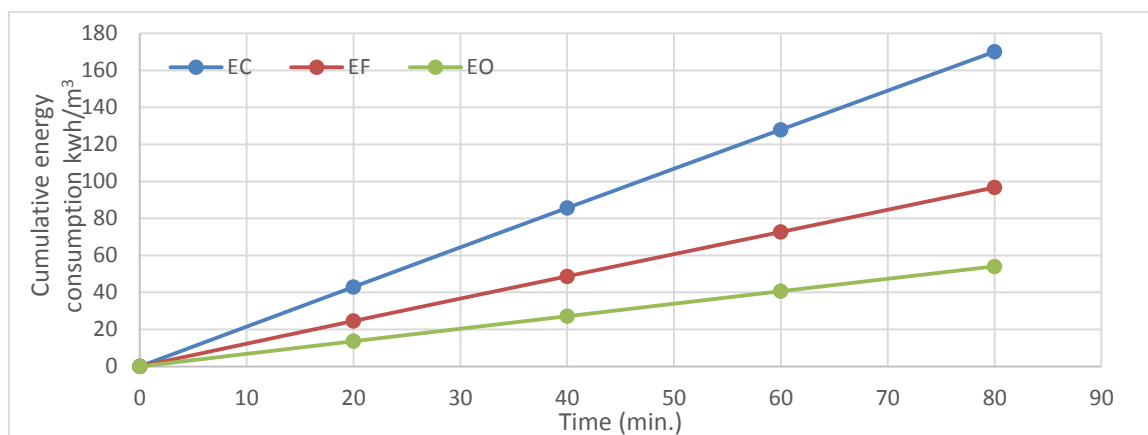
consumption (kWh/m³) (Eslami *et al.*, 2013). This parameter is calculated from the bellow equation:

has slightly lower percentage of COD removal (Fig.2) because of higher removal efficiency of BDD.

An experimental result showed that among the used treatment processes, EOP is the best due to high percentage of COD removal and also low energy consumption. Energy consumptions and COD removal efficiency are shown in Table 2.

Table 2. Selected results obtained for degradation of pesticide samples using three different processes

Process	Applied current (mA/cm ²)	Electrolysis Time (min)	COD removal (%)	Energy Consumption (KWh/m ³)
Electrooxidation	15	80	85.59	54.09
Electrocoagulation	20	80	79.51	170.12
Electro-Fenton	15	80	80.48	96.73

Fig.2.Variation in energy consumption of different electrochemical processes. (Co=300mg/l, 5mM Na₂SO₄, natural pH, i= 20mA/cm² for EC and 15 mA/cm² for EF, EO)

3.3 Energy Cost

The cost of energy (dollar/m³) for pesticide removal of each treatment process was

calculated by the following below equation:

$$\text{cumulative energy consumption} \frac{\text{KWh}}{\text{m}^3} * \text{Unit price} \left(\frac{\text{dollar}}{\text{KWh}} \right) \quad (10)$$

Table 3 summarizes energy costs of the pesticide's degradation by different electrochemical treatment processes. within EF, 80.48% COD reduction was carried out with an energy cost of 7.22 dollar/m³ at 80 min. The EO

has less energy cost, 3.72 dollars/m³, and a maximum COD reduction efficiency of 85.59 %. Among these used three treatment processes, ECP has the maximum energy cost (11.71 dollars/m³) with reduction efficiency (79.51%).

Table 3. Degradation cost of pesticide for different electrochemical processes

Process	Applied current (A)	Potential different (V)	Cumulative energy consumption KWh / m ³	Unit price (dollar/kWh)	Energy cost (dollar /m ³)
EO	1.24	13.0	54.09	0.07	3.72
EC	1.66	30.5	170.12	0.07	11.71
EF	1.24	23.3	96.73	0.07	7.22

3.4 Sludge formation

In the ECP and EFP, dissolved ions of ferrous formed at the anode change to ferric ions. there is a fact that ferric ions (Fe^{3+}) are a coagulation material and produce $\text{Fe}(\text{OH})_3$ contained sludge.

In EC, amount of sludge increased from 2.25 to 2.94 g per 400 ml bromuconazole wastewater by rising the current density from $5\text{mA}/\text{cm}^2$ to $20\text{mA}/\text{cm}^2$ within 5mM supporting electrolyte. Flock formations in EC processes became visible after the 3 min. It was investigated that the amount of sludge settled increased directly with the increased of applied electrical power and reaction duration. So, the colour of the sludge was green. This is because of Fe(II) ions settling as $\text{Fe}(\text{OH})_2$. In EFP the amount of sludge at the end of 20min of experiments for best removal efficiency is 2.94 g per 400 ml wastewater by increasing the current density in the same manner as EC within 5mM supporting electrolyte. The colour of the settled sludge was brown. In EFP the mineralization of some carbons to carbon dioxide occur, so finally less sludge formed in compare to that formed by ECP. there is a considerable advantage of EOP in terms of sludge, this process does not produce sludge since the hydroxyl radicals formed on anode's surface (Yavuz, 2007).

4. Conclusion

The feasibility of electrochemical processes for Bromuconazole pre-treatment are shown, which include EOP, ECP, EFP processes. The effects of parameters such as current density, electrolyte type, and H_2O_2 concentration were investigated on COD reduction and removal efficiency of bromuconazole pesticide.

It was seen that these variables remarkably affected Bromuconazole removal efficiency. The obtained Results in the EOP treatment at pH 5.32, indicates a noticeable decrease in COD from 1192.74 to 167.52 mg/L. The EFP treatment gives noticeable removal percentages of COD. Up to 80.48 %, COD lowering was occurred at pH 7.84 with average energy consumption ($96.73\text{ kWh}/\text{m}^3$) and moderate energy cost ($7.22\text{ dollar}/\text{m}^3$). within ECP, the highest COD removal efficiency of 79.51 % was noticed at pH 7.79 with high energy consumption of ($170.12\text{ kWh}/\text{m}^3$) and high energy cost ($11.71\text{ dollars}/\text{m}^3$).

Overall EFP and EOP showed best COD removal efficiency. So EOP is suggested for the treatment of wastewater polluted with pesticide in terms of COD reduction, cost of energy, and energy consumption. The treatment processes must be directly followed by a biological treatment process in order to make it cost-effective and to promote the performance.

References

- Andrade, L. S., Ruotolo, L. A. M., Rocha-Filho, R. C., Bocchi, N., Biaggio, S. R., Iniesta, J., ... & Montiel, V. (2007). On the performance of Fe and Fe, F doped Ti-Pt/PbO 2 electrodes in the electrooxidation of the Blue Reactive 19 dye in simulated textile wastewater. *Chemosphere*, 66(11), 2035-2043.
- Babuponnusami, A., & Muthukumar, K. (2012). Advanced oxidation of phenol: a comparison between Fenton, electro-Fenton, sono-electro-Fenton and photo-electro-Fenton processes. *Chemical Engineering Journal*, 183, 1-9.
- Chen, X., Chen, G., & Yue, P. L. (2000). Separation of pollutants from restaurant wastewater by electrocoagulation. *Separation and purification technology*, 19(1), 65-76.
- Cheng, H., Xu, W., Liu, J., Wang, H., He, Y., & Chen, G. (2007). Pretreatment of wastewater from triazine manufacturing by coagulation, electrolysis, and internal microelectrolysis. *Journal of Hazardous Materials*, 146(1), 385-392.
- Chiron, S., Fernandez-Alba, A., Rodriguez, A., & Garcia-Calvo, E. (2000). Pesticide chemical oxidation: state-of-the-art. *Water Research*, 34(2), 366-377.
- Ciríaco, L., Anjo, C., Correia, J., Pacheco, M. J., & Lopes, A. (2009). Electrochemical degradation of ibuprofen on Ti/Pt/PbO 2 and Si/BDD electrodes. *Electrochimica Acta*, 54(5), 1464-1472.
- Emamjomeh, M. M., & Sivakumar, M. (2009). Review of pollutants removed by electrocoagulation and electrocoagulation/flotation processes. *Journal of environmental management*, 90(5), 1663-1679.
- EPA (2002). Bromuconazole. Pesticide Fact Sheet, Environmental Protection Agency Office of Pesticide Programs Registration Division, Fungicide Branch, 1200 Pennsylvania, Avenue NW, Washington.
- Eslami, A., Moradi, M., Ghanbari, F., & Mehdipour, F. (2013). Decolorization and COD removal from real textile wastewater by chemical and electrochemical Fenton processes: a comparative study. *Journal of Environmental Health Science and Engineering*, 11(1), 31.
- Greenberg, A. E., & Clesceri, L. S. (1992). EATON; AD Standard methods for the examination of water and wastewater. *Washington, American Public Health Association*.
- Kapalka, A., Fóti, G., & Comninellis, C. (2010). Basic principles of the electrochemical mineralization of organic pollutants for wastewater treatment.

- In *Electrochemistry for the Environment* (pp. 1-23). Springer New York.
- Menegola, E., Broccia, M. L., Di Renzo, F., Massa, V., & Giavini, E. (2005). Study on the common teratogenic pathway elicited by the fungicides triazole-derivatives. *Toxicology in vitro*, 19(6), 737-748.
- Panizza, M., & Cerisola, G. (2009). Direct and mediated anodic oxidation of organic pollutants. *Chemical reviews*, 109(12), 6541-6569.
- Rajeshwar, K. I. J. G., Ibanez, J. G., & Swain, G. M. (1994). Electrochemistry and the environment. *Journal of applied electrochemistry*, 24(11), 1077-1091.
- Shchepetkin, I. A., Cherdyntseva, N. V., & Kagiia, V. T. (2003). Effect of sanazole and metronidazole on the production of reactive oxygen species by macrophages. *Antibiotiki i khimioterapiia= Antibiotics and chemotherapy [sic]/Ministerstvo meditsinskoi i mikrobiologicheskoi promyshlennosti SSSR*, 48(3), 7-10
- Silva, R. G. D., Aquino Neto, S., & Andrade, A. R. D. (2011). Electrochemical degradation of reactive dyes at different DSA® compositions. *Journal of the Brazilian Chemical Society*, 22(1), 126-133.
- Wang, J., Sun, W., Zhang, Z., Zhang, X., Li, R., Ma, T., ... & Li, Y. (2007). Sonocatalytic degradation of methyl parathion in the presence of micron-sized and nano-sized rutile titanium dioxide catalysts and comparison of their sonocatalytic abilities. *Journal of Molecular Catalysis A: Chemical*, 272(1), 84-90.
- Yavuz, Y. (2007). EC and EF processes for the treatment of alcohol distillery wastewater. *Separation and purification technology*, 53(1), 135-140.
- Zaleska, A., & Hupka, J. (1999). Problem of disposal of unwanted pesticides deposited in concrete tombs. *Waste Management and Research*, 17(3), 220-227.

RESEARCH PAPER

Assessment of phenology and toxicity of *Prangos platychna* Boiss. in Halgurd mountain of Iraqi Kurdistan

¹Jwan Khidhr Rahman *, ²Dara Muhamed Ameen Jaff

¹ Department of Environmental Sciences, College of Science, Salahaddin University-Erbil, Kurdistan Region, Iraq.

²Department of Biology, College of Education, Salahaddin University-Erbil, Kurdistan Region, Iraq

ABSTRACT:

Prangos platychna Boiss, a wild plant belongs to the Apiaceae family, it is a native plant of Kurdistan Region-Iraq. Root, leaves, stem and flowers of the plant were collected from Halgurd mountain Iraqi Kurdistan region. Its initial growth begin in May, flowering at the beginning of June and reaches fruit formation by the end of June until the last week of July, while the seed formation and dispersal were begun by the end of July until the end of August. Ethanol extract of different parts of the *P. platychna* has significant cytotoxicity potential on the human liver carcinoma cell and the activities of cytotoxicity can be classified as root > stem > flowers > leaves. Toxicity of water extract assayed against *Triticum aestivum* L.(wheat) and *Hordium vulgare* L(barley) and *Lolium rigidum* Gaud, results were indicated that the germination percentage and the root elongation decreased gradually with increasing the concentration of extraction until complete inhibition. *T. aestivum* shows higher tolerance ability to root, leaf, stem and flower extracts. As well as there was inhibition of *Lolium rigidum* due to all parts extract. Thus *P. platychna* Boiss can be used as a herbicide.

KEY WORDS: cytotoxicity; liver carcinoma; wheat, barley; Lolium.

DOI: <http://dx.doi.org/10.21271/ZJPAS.33.1.16>

ZJPAS (2021) , 33(1);146-156 .

1.INTRODUCTION:

In the Iraq especially Kurdistan region is well known for its flora and the abundance of wild plants and their natural products that its people have long used as traditional medicine, food and other uses (Hamad et al., 2017). The family *Apiaceae* is regarded as one of the important families for its chemical contents. The genus of *Prangos* belongs to the family of *Apiaceae*, under the order of *apiales*, having thirty species distributed from the Mediterranean to central Asia, fourteen of them found in Turkey (Ahmed et al., 2011). While, seven of them found in the different areas of Kurdistan region of Iraq, which are *P.platychna* Boiss., *P.ferulacea* L, *P. uloptera* DC., *P.asperula* Boiss., *P.pabularia* Lindl., *P.peucedanifolia* Fenz, and *P.carymbosa* Boiss. The *P.*

platychna Boiss is a perennial plant, length can reach up to (1-1.5m), naturally growing in the high mountains in the Kurdistan region of Iraq, on rocky slopes at the altitude of 2200-2800m above sea level. Their species were distributed more in the Halgurd mountain (Ghazanfar and Edmondson, 2013).

The phenomenon of phenology is a biological process that involves a series of cyclical steps such as vegetative growth, flowering, fruit formation and seed formation and dispersal (Valdez-Hernández, 2015). Toxicity assay is an important aspect in the investigating processes of neighboring plant's inhibition growth and studies of cytotoxicity. Such processes were encouraged by natural plant products that have an effect on certain plants. Part of this study was concerned about the extracts from the roots, leaves, stems and flowers of *P. platychna* Boiss with regard to their cytotoxicity on human liver carcinoma

* Corresponding Author:

Jwan Khidhr Rahman

E-mail: jwanbio9@gmail.com

Article History:

Received: 31/12/2019

Accepted: 14/10/2020

Published: 20/02 /2021

cells and toxicities toward other plants. Our survey on the availability of the literature on a plant, as yet, no study covered the scientific information about the phenology and toxicity of this plant species.

2. MATERIALS AND METHODS

2.1 Description of studied location

Halgurd mountain in Kurdistan region well-known for its various flora species. It is located in

the north east of Erbil city. The studied area in the mountain is of altitude; 36:42.30758N, longitude; 44:52.29358E and about 96 km distant from Erbil city. Location and topography map of the area was measured by using the global positional system (GARMIN/GPS 72), (Figure 1).

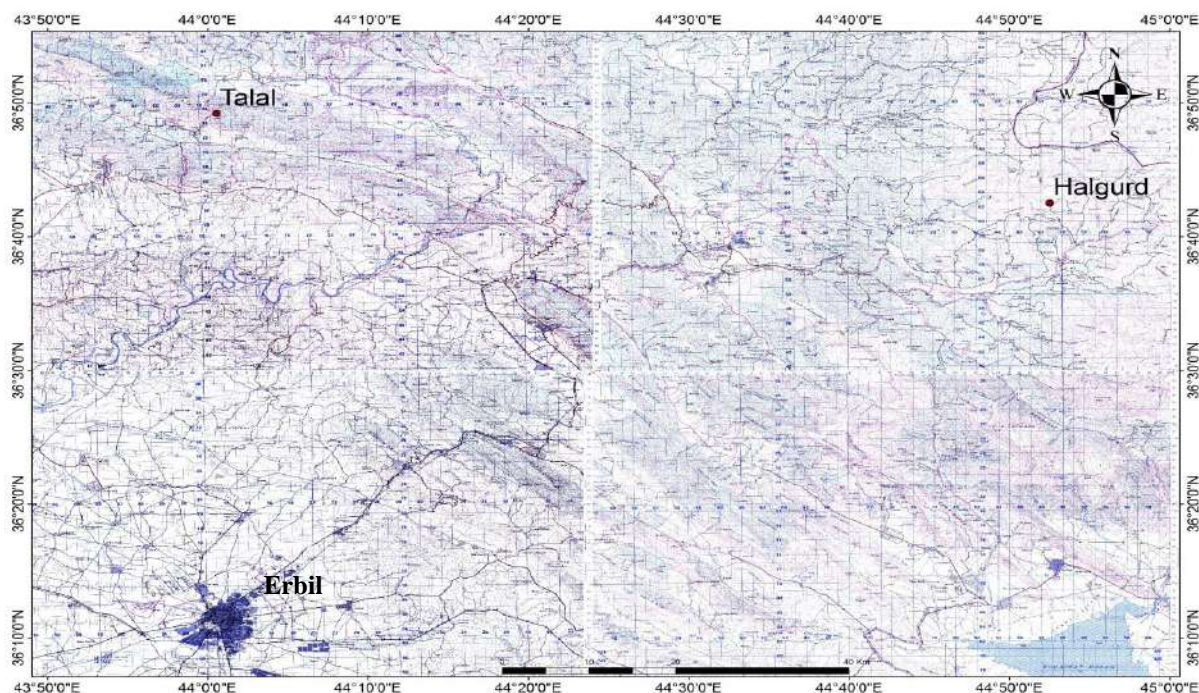


Figure 1: Location and topography map of Halgurd mountain.

2.2 plant material collection and treatment

Different plant parts of *P. platychna* Boiss were collected during May to July of 2017 from the Halgurd mountain in Kurdistan region of Iraq, at the altitude of 2170m. The different plant parts root, leaves, stem and flowers of the *P. platychna* Boiss were collected, cleaned and shed dried at the room temperature near 38-40°C till the constant weight obtained. The dried parts grinded slowly sieved to obtain a fine powder and preserved in tight closed bottles according to (Yeo et al., 2014).

2.3 Extraction method

Dry powder of each plant part (10.0g) mixed with petroleum ether (40-60%), ethanol (99.9%) and distilled water, for three days at room temperature (30-40 °C) and repeated for three

times with stirring a regular interval. The extracts solution was filtered through double layer of muslin cloth and Whatman NO.1 filter paper and concentrated using a rotary evaporator to obtain the crude of plant extracts (Yeo et al., 2014).

2.4 Assessment of life cycle and Phenological stage of *Prangos platychna* Boiss plant

Regular visits were arranged every week during 2017-2018 to monitor the life cycle of *P. platychna* Boiss in Halgurd mountain and follow the phenological stages during the life cycle; vegetative growth, flowering, fruit formation and seed formation and dispersal stage (Mirinejad, 2015).

2.5 Cytotoxicity of *P. platychna* Boiss against human liver carcinoma cells

The cytotoxicity of *P. platychna* was evaluated by the determination of their IC₅₀ using

the MTT (3-(4,5-Dimethylthiazol-2-yl)-2,5-diphenyltetrazolium) test, a colorimetric method for monitoring cell survival in vitro assay. The basic of this test is change the yellow color of Tetrazolium salt to the violet crystals in the culture medium. The liver cell line (HepG2) was collected from the Pasteur Institute of Iran. The ninety six well plates were used, and 1×10^4 cells/well were incubated with 90 μ l of Dulbecco's Modified Eagle's Medium (DMEM) supplemented with 10% Fetal Bovine Serum (FBS) containing different concentrations of ethanol extracts that ranging from 1 to 500 μ g/ml, and incubated over night at 37 °C in a CO2 incubator (5%). Then, 10 μ l of MTT solution (5mg/ml) was transferred into each well and the mixture was incubated for 4h at 37 °C. After incubation time, 100 μ l of Dimethyl Sulfoxide (DMSO) was added into each well to dissolve the formazan from the MTT and incubated at 37 °C for 24h. ELISA reader (BioTech, USA) used for measuring the absorbance at a wavelength of 570nm. Untreated cell (<1%DMSO) was used as control (Chanda and Nagani, 2013), the percentage of the reduction of viability was calculated as follow:

$$\text{Viability \%} = \text{OD}_e / \text{OD}_c * 100 \dots (1)$$

Where: OD_e: is the mean value of the measured optical density of the extract of the sample, OD_c: is mean value of the measured optical density of the control. For each concentration tested, five replicated wells were used and 50% inhibition of cell growth (IC₅₀) used as an analysis parameter. The lower value of viability % was indicated the sample has a higher potential of cytotoxicity. The sample was considered cytotoxicity if the percentage viability was <70% and non cytotoxicity if the value of percentage viability was > 70% (Cannella et al., 2019).

2.6 Assessment of toxicity of *P. platychnaena* Boiss on seed germination and root elongation of some plants

2.6.1 Choose the plant seeds

The decision to choose the crop *Triticum aestivum* L. (wheat), *Hordium vulgare* L (barley) and wild plant *Lolium rigidum* Gaud seeds for this assay depends on the availability of the weed and uses of the crops in our area which plays an important role in the economics of the region. Seeds of all of them were obtained from the Directorate of Research Center of plants in Erbil. In this experiment we choose *Triticum aestivum*

L., *Hordium vulgare* L. and *Lolium rigidum* Gaud. seeds to evaluated the effect of *P.platychnaena* Boiss parts extracts on their germination and root growth.

2.6.2 Preparation of plant stock solution and bioassay

The effect of plant extract on the germination and root elongation of tested plants were studied in the laboratory. The obtain of a stock solution (w/v) , weight (1gm) of extracted plant parts such root, leaves, stem and flowers were dissolved in distilled water, 2.5 % DMSO and 2 % DMSO, respectively. The stock solution of each extract (10mg/ml) were further diluted with the distilled water, 2.5%DMSO and 2%DMSO, respectively, to different concentration (0.5, 1.5, 2.5, 3.5, 4.5 and 5.5 mg/ml). From each treatment taken 10 seeds were placed in a petri dish of 9.0cm in diameter, lined with Whatman No.1 filter paper, moistened with 7ml of each extract at different concentrations. All petri dishes were incubated in the growth chamber at 22±2^o C. Germination % (G %) and root elongation, were measured after 7 days and statistically analyzed (Javaid et al., 2006, Kapur and Govil, 2000). Germination % was calculated according to (Kanimarani, 2018), with the following equations.

$$\text{Germination \%} = (\text{Total no. of germinated seeds} / \text{Total no. of tested seeds}) * 100 \dots (2)$$

The seed inhibition percentage of the *P.platychnaena* against the *T. aestivum* L., *H. vulgare* L. and *L. rigidum* Gaud were calculated as per the formula described by (Hoque et al., 2003), and used in the IC₅₀ calculation. The value of IC₅₀ was determined on the bases of the equation used by (Ali and Taha, 2016).

$$\text{I} = \text{C} - \text{T} * 100 / \text{C} \dots (3)$$

Where: I = seed inhibition percentage, C= Response of control plant, T= Response of treated plant

2.7 Statistical analysis

The cytotoxic activities, germination rate and root elongation of the *P. platychnaena* Boiss were statistically analyzed using ANOVA table, by Dunnett's multiple comparison tests, by Graph Pad-Prism version 7. All results arranged as mean ± standard error for each data and *P* value less than 0.05 considered as statistically significant differences among them.

3. RESULTS AND DISCUSSION

3.1 Assesment of the phenology of *P. platychnaena* Boiss in Halgurd mountain

The results in Figure 2 showed the stage of growth and development of *P. platychna* Boiss started from the 1st week of May, then 2nd stage the vegetative growth which initiated in the 2nd week of May, and continued until the end of May, while the flowering stage started from the beginning of June and continues until the end of June. Also, the fruit formation is initiated at the

end of June and continues until the last week of July. On the other hand, some plants started with seed formation and dispersal after the month of July and continue until the last week of August. Finally, the degradation of the vegetative growth gradually occurs and the plant died, by the end of September (Castro-Diez et al., 2003).

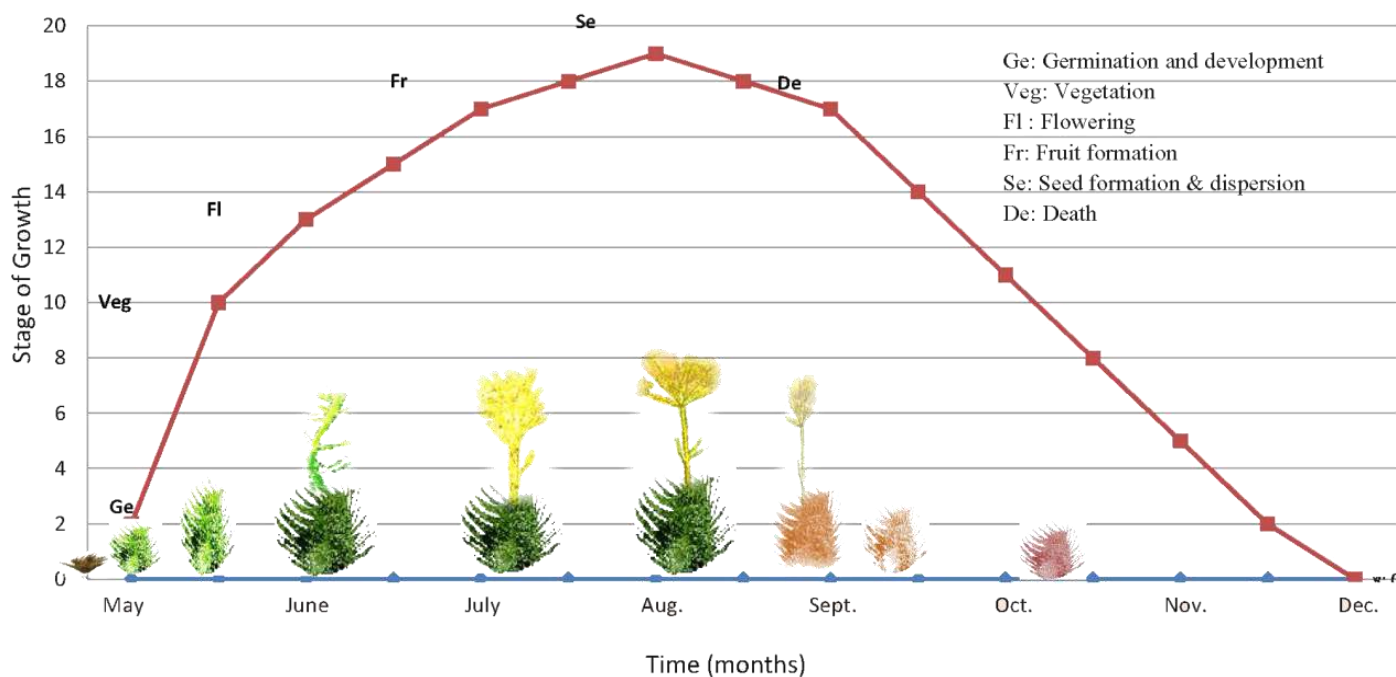


Figure 2: Growth and phenological stages of *Prangos platychna* Boiss from May to September.

3.2 Assessment of cytotoxicity of *P. platychna* Boiss against human liver carcinoma cells

In order to determine the rate of inhibition of the cell growth, the cytotoxicity of *P. platychna* Boiss extracts were carried out against liver carcinoma cell line (HepG2) at different concentrations. Statistical analysis showed that the plant extracts have a potential inhibitor effect on the growth of liver carcinoma. The concentration of the extracted of plant parts as root, leaves, stem and flowers have significantly affected against the growth of liver carcinoma cells were 50,100,10 and 10 μ g/ml respectively. The results showed the cell viability percentage decrease with an increase in the concentration of plant extracts (Table 1). While, the IC₅₀ values of the of the root, leaves, stem and flowers extracts were 94.0, 299.0,108.0 and 208.0 μ g/ml, respectively (figure 3). The activities of extraction

of the plant parts against liver carcinoma cells can be classified as root > stem > flowers > leaves. This finding indicated that the root part has higher cytotoxicity potential than the other parts due to containing the chemical compounds may have more potential activities against the growth of liver carcinoma cells. In comparison the cytotoxicity of *P. platychna* Boiss with other *Prangos* species, that partial agreement with results showed by (Shokoohinia et al., 2014), root extract by acetone of *P. ferulacea* L. showed the cytotoxicity effect on the human ovarian carcinoma. According to (Farooq et al., 2014), the phytochemical analysis of methanol:dichloromethane (1:1) for root extract of *P. pabularia* led to isolation of osthol compound, which have potential of cytotoxicity against epidermoid carcinoma (A431), lung (NCI-H322), prostate (PC-3) and colon (HCT-116) cell lines.

Generally, natural chemical compounds found in the plant such as phenolic acid, tannins,

coumarins, flavonoids, terpenes, ..etc, have a major role in the prevention and treatment of cancer. The bioactivities of these compounds were responsible for their anti-inflammatory effects, anti-carcinogenic, inhibition proliferation and

contribute to their apoptosis by stopping the cell cycle (Huang et al., 2010, Booth and Bohlmann, 2019).

Table 1: Effect of *P. platychna* Boiss root, leaf, stem and flower extract concentrations on human liver carcinoma cell viability.

Concentration of extracts & their control	Cell viability (%)			
	Root	Leaf	Stem	Flower
Control	100±7.4	100±7.4	100±7.4	100±7.4
1.0 µg/ml	91.5±5.8	92.9±2.82	90.9±2.89	87.1±7.8
10.0µg/ml	87.2±5.23	89.2±4.2	79.1±6.8*	81.1±2.4*
50.0µg/ml	73.9±5.3*	90.4±1.67	74.6±4.7	67.6±3.6*
100.0µg/ml	57.2±5.3*	68.6±2.7*	36.69±6.2*	55.2±3.0*
200.0µg/ml	21.0±3.49*	59.0±2.4*	27.78±3.9*	51.8±3.7*
500.0µg/ml	25.3±3.7*	38.6±1.46*	20.3±3.5*	39.3±2.8*

Values was mean ± standard error, Symbol * refer to the significant differences among treated cell and control cell line

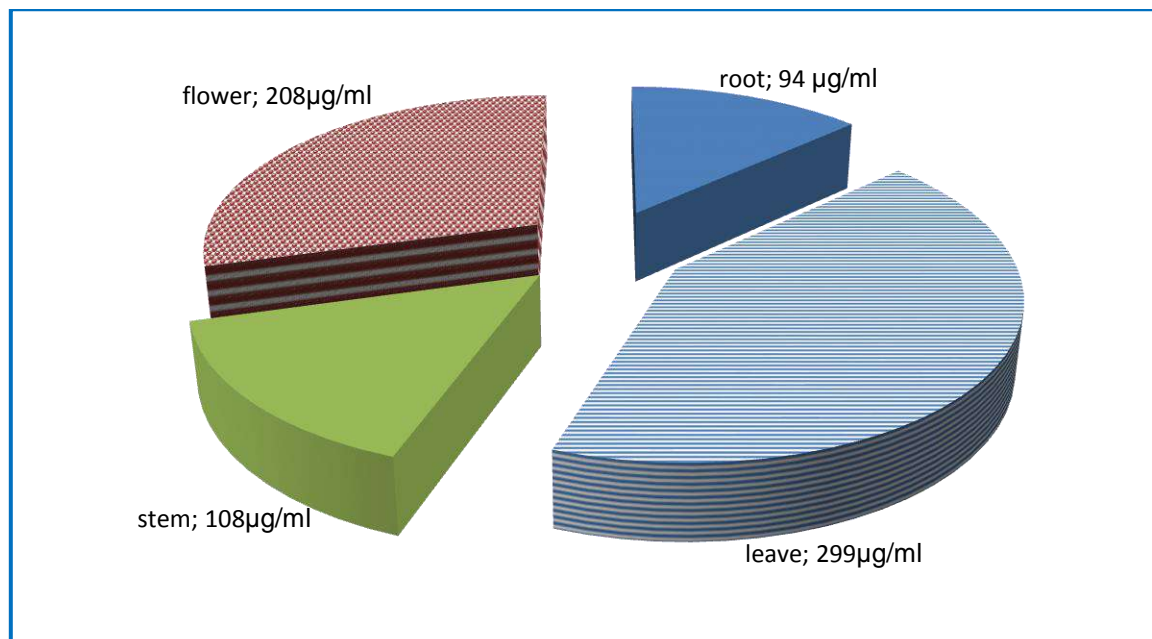


Figure 3: The values of IC₅₀ of *P. platychna* Boiss root, leaf, stem and flower extracts on liver carcinoma cell line growth

3.3 Assessment the toxicity of *P. platychna* Boiss on seed germination and root elongation

Seed germination and root elongation (radicals) of *Triticum aestivum*, *Hordium vulgare* and *Lolium rigidum* seeds, during the 7 days of treatment with different plant parts extraction of *P. platychna* Boiss, depends on the type of treated seeds and the phytochemical compounds in a part of the *P. platychna* Boiss plant used. The results revealed that the minimum percentage of germination rate for *T. aestivum*, *H. vulgare* and *rigidum* seeds were 27±3.3, 7±3.3 and 13±3.3% respectively, found in the water root extracts at 4.5, 2.5 and 2.5 mg/ml respectively, while the leaves water extracts showed an adverse effect on the percentage germination rates of *T. aestivum*, *H. vulgare* and *L. rigidum* seeds, in which the minimum value were 10±0.0, 10±0.0 and 10±5.7% respectively, which obtained by using 3.5, 2.5 and 2.5 mg/ml of extract, respectively. On the other hand, the minimum value of the germination percentage of all three plant seeds against stem water extract was 20±5.7, 10±0.0 and 7±3.3%, respectively, by concentrations the amount of 4.5, 2.5 and 2.5 mg/ml respectively. Finally, the water extraction of the *P. platychna* Boiss flowers showed the minimum percentage of germination rate which

recorded 10±0, 7±3.3 and 7±3.3% against *T. aestivum* L., *H. vulgare* and *L. rigidum*, respectively, found at the level of 2.5 mg/ml respectively. The statistical analysis showed significant differences ($P < 0.05$) among the treatment data at different concentrations with control data. While the germination percentage rate of each of *T. aestivum*, *H. vulgare* and *L. rigidum* were don't detected when ethanol and petroleum ether extract were used, those results were shown in Table 2.

The results in Figure (4, 5,6 and 7) indicated that the minimum value of root elongation for *T. aestivum* L., *H. vulgare* and *L. rigidum* seeds when treated with water root extract at 4.5, 2.5 and 2.5 mg/ml, were 3.83±0.44, 4.3±0.33 and 1.1±0.1 cm/plant, respectively. On the other hand, water extracts of leaves showed an adverse effect on the root elongation of *T. aestivum* L., *H. vulgare* and *L. rigidum* seeds, in which the lowest value was 1.33±0.06, 1.33±0.33 and 1.6±0.16 cm/plant, respectively, which obtained by concentrations 3.5, 2.5 and 2.5 mg/ml of extract, respectively. While, the minimum value of root elongation of all three plant seeds against stem water extract was 4.5±0.28, 5.3±0.33 and 1.3 ±0.15 cm/plant respectively, by using the amount of 4.5, 2.5 and 2.5 mg/ml respectively. Finally, the water extraction of the *P. platychna* Boiss flowers showed the minimum

value of root elongation which recorded 1.66 ± 0.33 , 2.43 ± 0.29 and 1.16 ± 0.08 cm/plant against *T. aestivum* L., *H. vulgare* and *L. rigidum*, respectively, recorded at the level of 2.5mg/ml, respectively. The statistical analysis of data revealed the significant differences ($P < 0.05$) among the treatments compare with control data at different concentrations of plant extraction. As well as, root elongations of each of *T. aestivum* L., *H. vulgare* and *L. rigidum* were don't detected when ethanol and petroleum ether extract were used.

In general, seed germination and root elongation were wide and rapidly used toxicity tests because of sensitivity and suitability for unstable chemical compounds (Lin and Xing, 2007). The results indicated that the germination percentage and the root elongation development decreased gradually with increasing the concentration of extraction until complete inhibition will occur due to increasing the accumulation of the phytochemical compounds which showed adverse effects on the growth of a seed. The data revealed the *T. aestivum* plant seedling was more resistance toward the extracts of root, leaf, stem and flowers of the *P.*

platychlaena Boiss plant than that of *H. vulgare* and *L. rigidum* seedling, this may be related with the chemical compounds and physiological structure of their seeds and their genetically performance (Lin and Xing, 2007). This phenomenon allows *T. aestivum* to grow in the areas covered with the *P. platychlaena* Boiss plant. While the toxicity of ethanol and petroleum ether extracts don't detect because the extracts by both solvents don't soluble in water and it requires to add DMSO to increase solubility, thus the later solution prevented seeds germination (Hung et al., 1992).

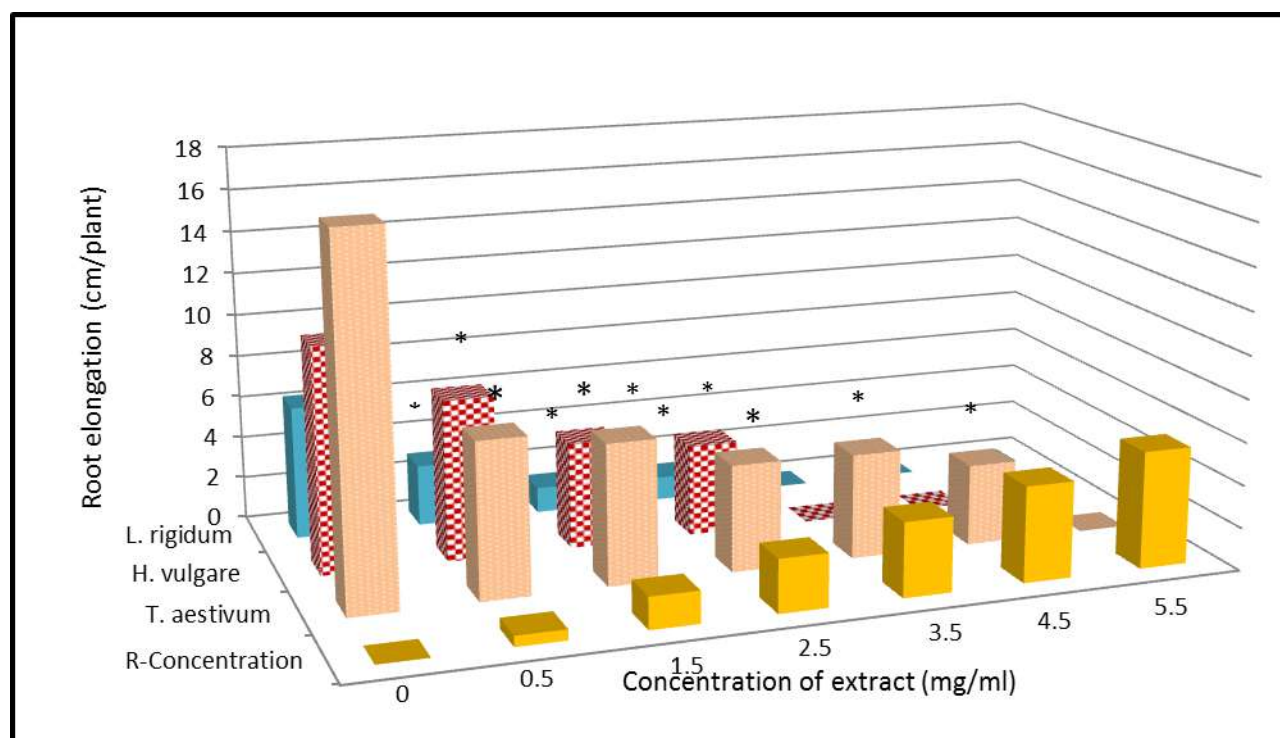
The results showed that the range of variation in the IC_{50} values of the water extracts of root, leaves, stem and flowers of *P. platychlaena* Boiss was 0.48- 2.62mg/ml, Figure 8. This finding showed that the part of the flower of this plant has a lower value of IC_{50} and higher toxicity potential, the other parts. Therefore, toxicity level can be arranged as: flowers > leaves > stem > roots, this may be due to the proportion of the amount and type of phytochemicals produced in the flowers of this plant.

Table 2: Germination percentage of seeds incubated with different extracts from different plant parts of *P. platychlaena* Boiss.

Extracts	Plant parts	Concentration (mg/ml)	Germination rate (%)		
			<i>T. aestivum</i>	<i>H. vulgare</i>	<i>L. rigidum</i>
Water	Root	Control	90±0.0	92±1.66	97±1.6
		0.5	83±8.8	60±5.7*	80±5.7
		1.5	60±5.77*	22±1.6*	40±5.7*
		2.5	33±3.3*	7±3.3*	13±3.3*
		3.5	30±0.0*	0.0±0.	0.0±0.
		4.5	27±3.3*	0±0.	0±0.
		5.5	0.0±0.0	0.0±0.0	0±0.0
	Leaf	Control	93±3.3	90.0±0.0	93±3.3
		0.5	55±2.8*	50±0.0*	47±3.3*
		1.5	30±0.0*	30±5.7*	37±8.8*
		2.5	20±5.7*	10±0.0*	10±5.7*
		3.5	10±0.0*	0.0±0.0	0.0±0.0
		4.5	0.0±0.0	0.0±0.0	0.0±0.
		5.5	0.0±0.0	0.0±0.0	0.0±0.0
	Control	93±3.3	92±1.6	93±3.3	
	0.5	90±5.7	60±5.7	63±3.3	

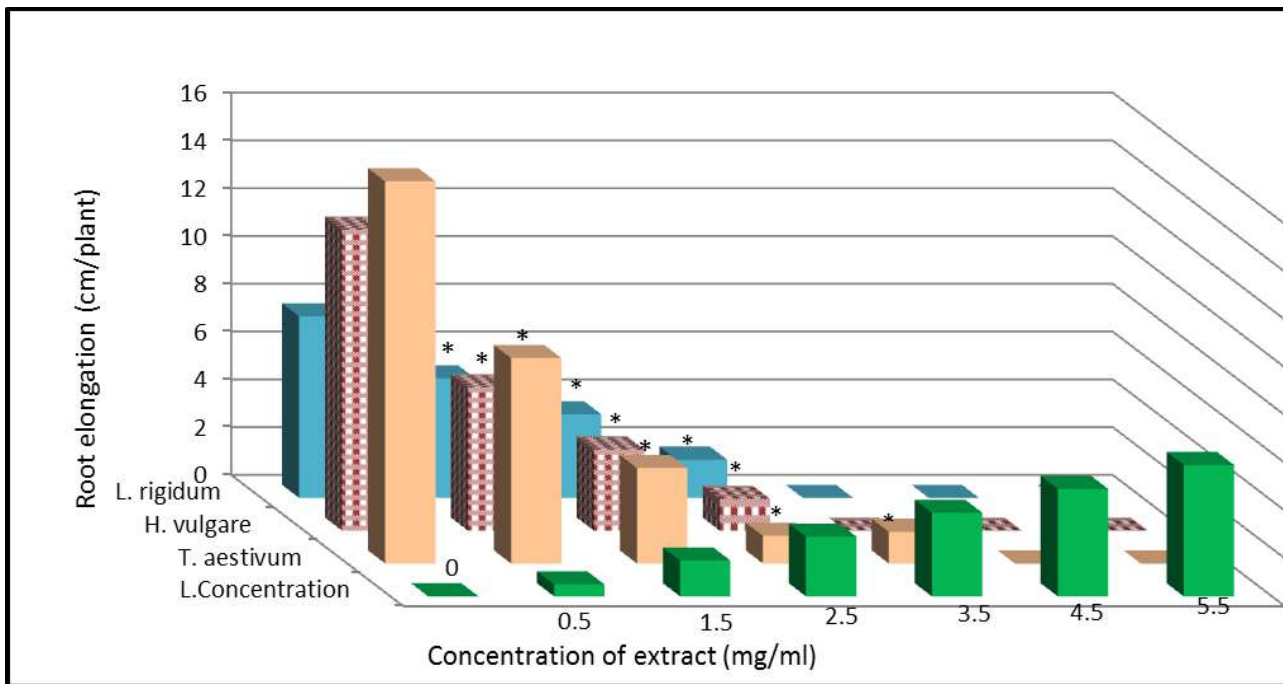
	Stem	1.5	50±5.7*	17±3.3*	30±0.0*
		2.5	27±3.3*	10±0.0*	7±3.3*
		3.5	23±6.6*	0±0.0	0.0±0.0
		4.5	20±5.7*	0.0±0.0	0.0±0.0
		5.5	0.0±0.0	0.0±0.0	0±0.0
	Flower	Control	97±3.3	91.0±1.6	91±0.5
		0.5	53±3.3*	45±2.8*	48±1.6*
		1.5	23±3.3*	30±5.7*	25±2.8*
		2.5	10±0.0*	7±3.3*	7±3.3*
		3.5	0.0±0.0	0.0±0.0	0.0±0.0
		4.5	0.0±0.0	0.0±0.0	0.0±0.0
Ethanol	All parts	Control	N.D.	N.D.	N.D.
		all concentration	N.D.	N.D.	N.D.
Petroleum ether	All parts	Control	N.D.	N.D.	N.D.
		all concentration	N.D.	N.D.	N.D.

The symbol * significantly treated data with control data at ($P < 0.05$), Values are expressed as mean \pm standard error, N.D.: Not Detect



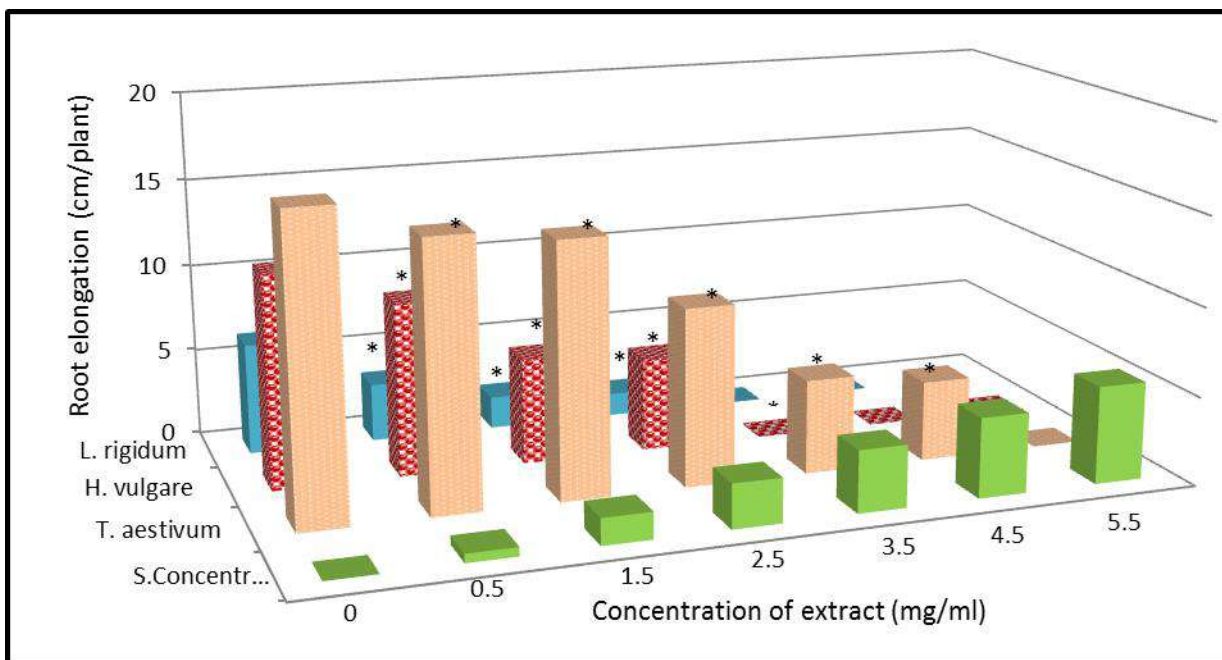
Values are mean, Symbol *: it means significantly among treatment and control data

Figure 4: Effect of *P. platyclaena* Boiss root extract concentration on root length (cm)



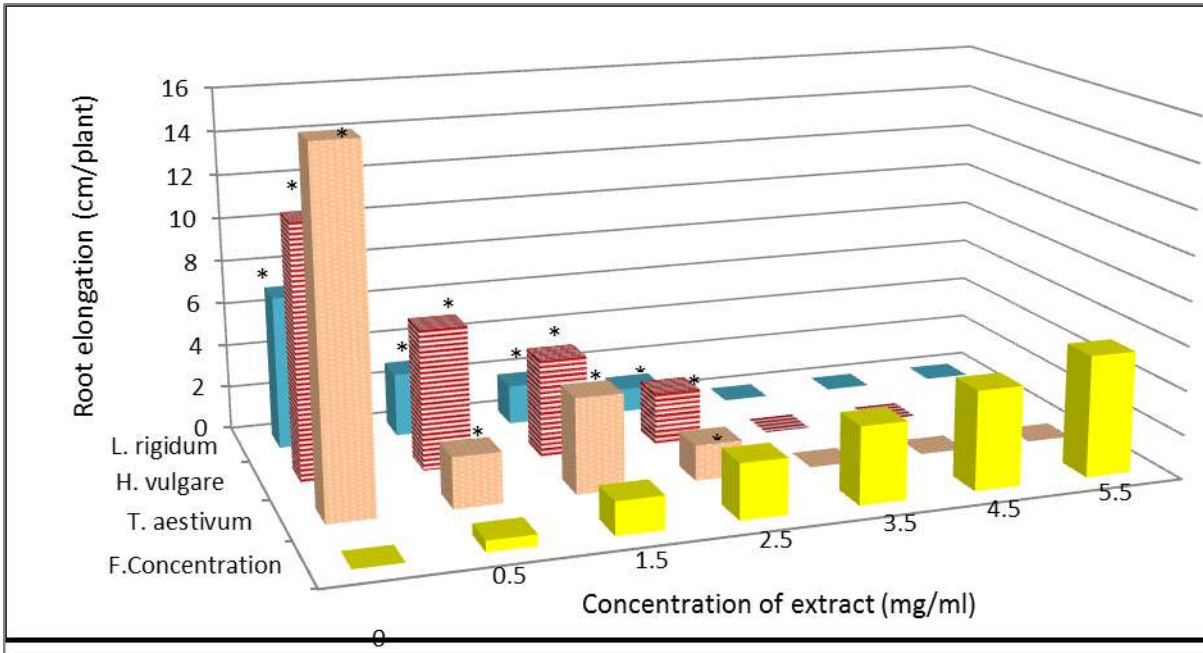
Values are mean, Symbol *: it means significantly among treatment and control data

Figure 5: Effect of *P. platychlaena* Boiss leaf extract concentration on root length (cm)



Values are mean, Symbol *: it means significantly among treatment and control data

Figure 6: Effect of *P. platychlaena* Boiss stem extract concentration on root length (cm)



Values are mean, Symbol *: it means significantly among treatment and control data

Figure 7: Effect of *P. platyclaena* Boiss flower extract concentration on root length (cm)

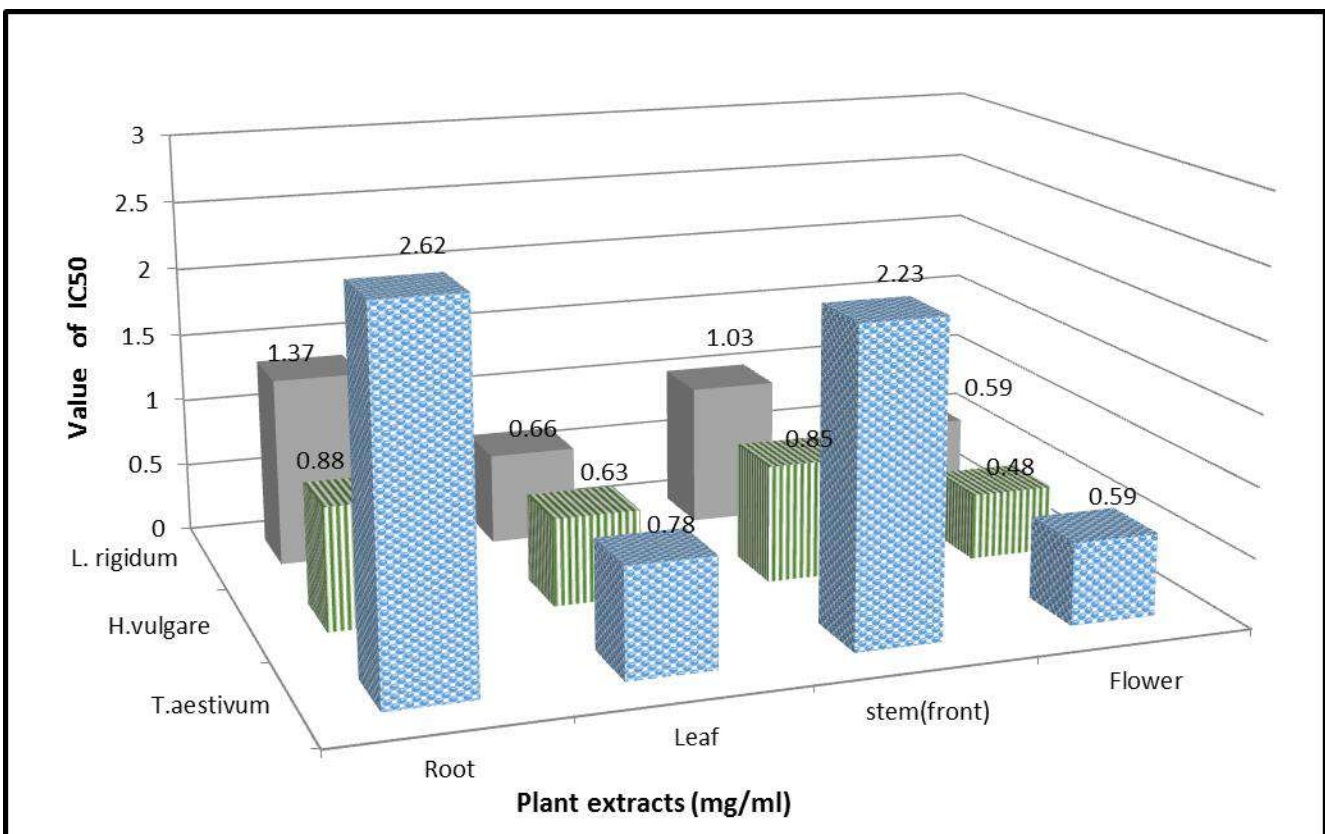


Figure 8: Value of IC₅₀ of *P. platyclaena* Boiss root, leaf, stem and flower extracts against *Triticum aestivum* L, *Hordium vulgare* L and *Lolium rigidum* Gaud .

4. CONCLUSIONS

Summary of the results showed that the phenological characters of *Prangos platycheana* Boiss started from June to August. Root, stem, leaf and flower extracts showed significant cytotoxic potential on human liver carcinoma cell. As well as flower water extract have more effects to inhibit both germination percentage and root elongation of *Triticum aestivum* L., *Hordium vulgare* L and *Lolium rigidum* Gaud.

Acknowledgments

Great thanks to Dr. Abdullah shukur from the Biology department, College of Education, University of Salahadden, for helping in identifying the species.

Conflicts of Interest

The authors declare no conflict of interest.

References

- AHMED, J., GUVENC, A., KUCUKBOYACI, N., BALDEMIR, A. & COSKUN, M. 2011. Total phenolic contents and antioxidant activities of *Prangos* Lindl. (Umbelliferae) species growing in Konya province (Turkey). *Turkish Journal of Biology*, 35, 353-360.
- ALI, H. H. & TAHA, K. K. 2016. Effect of three plant extracts on controlling of Tomato damping-off disease. *ZANCO Journal of Pure and Applied Sciences*, 28, 1-6.
- BOOTH, J. K. & BOHLMANN, J. 2019. Terpenes in *Cannabis sativa* - from plant genome to humans. *Plant Science*, 284, 67-72.
- CANNELLA, V., ALTOMARE, R., CHIARAMONTE, G., DI BELLA, S., MIRA, F., RUSSOTTO, L., PISANO, P. & GUERCIO, A. 2019. Cytotoxicity evaluation of endodontic Pins on L929 cell line. *BioMed Research International*, 2019, 1-5.
- CHANDA, S. & NAGANI, K. 2013. In vitro and in vivo methods for anticancer activity evaluation and some Indian medicinal plants possessing anticancer properties: An overview. *Journal of Pharmacognosy and Phytochemistry*, 2, 140-152.
- FAROOQ, S., SHAKEEL U, R., DANGROO, N. A., PRIYA, D., BANDAY, J. A., SANGWAN, P. L., QURISHI, M. A., KOUL, S. & SAXENA, A. K. 2014. Isolation, cytotoxicity evaluation and HPLC-quantification of the chemical constituents from *Prangos pabularia*. *PLoS One*, 9, 1-9.
- GHAZANFAR, S. A. & EDMONDSON, J. R. 2013. Flora of Iraq. *National Herbarium of Iraq of the Ministry of Agriculture, Baghdad*, 5, 109-220.
- CASTRO-DIEZ, P., MILLA-GUTIERREZ, R. & MONTSERRAT-MARTI, G. 2003. Comparison of methods to study plant phenological patterns. The case of *Halimium atriplicifolium* (Cistaceae). *Phyton*, 43, 59-78.
- HAMAD, R., BALZTER, H. & KOLO, K. 2017. Multi-criteria assessment of land cover dynamic changes in Halgurd Sakran national park (HSNP), Kurdistan region of Iraq, using remote sensing and GIS. *Land*, 6, 1-17.
- HOQUE, A. T. M. R., AHMED, R., UDDIN, M. B. & HOSSAIN, M. K. 2003. Allelopathic effect of different concentration of water extracts of *Acacia auriculiformis* leaf on some initial growth parameters of five common agricultural crops. *Pakistan Journal of Agronomy*, 2, 92-100.
- HUANG, W.-Y., CAI, Y.-Z. & ZHANG, Y. 2010. Natural phenolic compounds from medicinal herbs and dietary plants: potential use for cancer prevention. *Nutrition and Cancer*, 62, 1-20.
- HUNG, P. E., FRITZ, V. A. & WATERS, L. 1992. Infusion of shrunken-2 Sweet Corn seed with organic solvents: Effects on germination and Vigor. *HortScience*, 27(5), 467-470.
- JAVAID, A., SHAFIQUE, S., BAJWA, R. & SHAFIQUE, S. 2006. Effect of aqueous extracts of allelopathic crops on germination and growth of *Parthenium hysterophorus* L. *South African Journal of Botany*, 72, 609-612.
- KANIMARANI, S. M. S. A. 2018. Effect of seed exposure to direct Electrical current on germination and seedlings growth of three cowpeas (*Vigna unguiculata* L.) Cultivars. *Zanco Journal of Pure and Applied Sciences*, 30, 168-179.
- KAPUR, P. & GOVIL, S. R. 2000. Experimental Plant Ecology. *Daryaganj, New Delhi, India*, pp105.
- LIN, D. & XING, B. 2007. Phytotoxicity of nanoparticles: inhibition of seed germination and root growth. *Environmental Pollution*, 150, 243-250.
- MIRINEJAD, S. 2015. Autecology of endemic plant "*Prangos haussknechtii* Boiss" in Kohgiluyeh-va-Boyerahmad province, Iran. *Biological Forum – An International Journal*, 7, 300-303.
- SHOKOOHINIA, Y., SAJJADI, S. E., GHOLAMZADEH, S., FATTAHI, A. & BEHBAHANI, M. 2014. Antiviral and cytotoxic evaluation of coumarins from *Prangos ferulacea*. *Pharmaceutical Biology*, 52, 1543–1549.
- VALDEZ-HERNÁNDEZ, M. 2015. Vegetative and reproductive plant phenology. *Biodiversity and Conservation of the Yucatán Peninsula*.
- YEO, Y. L., CHIA, Y. Y., LEE, C. H., SOW, H. S. & YAP, W. S. 2014. Effectiveness of maceration periods with different extraction solvents on in-vitro antimicrobial activity from fruit of *Momordica charantia* L. *Journal of Applied Pharmaceutical Science*, 4, 16-23.

RESEARCH PAPER

Improving VoIP Transmission for IEEE 802.11n 5GHz MANET

Ghassan A. QasMarrogy

Department of Communication and Computer Engineering, College of Engineering, Cihan University-Erbil, Kurdistan Region, Iraq

ABSTRACT:

In catastrophic scenarios, rescue teams need to communicate with each other without any fixed infrastructure while moving, such as search and rescue, firefighter, police, and tactical networks i.e. MANET. In these scenarios Mobile Ad hoc Networks (MANETs) can support immediately Voice Over Internet Protocol (VoIP) service to be used, with fast deployment, low cost, and flexibility during movement. Recently the new mobile devices support the new frequency of IEEE 802.11n 5GHz that gives better performance requirements to MANET, with enhanced Quality of Service (QoS) and bandwidth (B.W). This paper will calculate and improve VoIP service in MANET that operates under IEEE 802.11n 5GHz frequency, with comparing two main routing protocols AODV and OLSR, and analyzing some QoS requirement such as end-to-end delay, throughput, and retransmission attempts using Network Simulator (NS2).

KEY WORDS: VoIP; Buffer Size; MANET Routing Protocols; IEEE802.11n 5GHz; Max Receive Lifetime.

DOI: <http://dx.doi.org/10.21271/ZJPAS.33.1.17>

ZJPAS (2021) , 33(1);157-162 .

1. INTRODUCTION :

In these days, the technology plays very important role in government initiatives to set up and build a new important communication through the years to support new services to the technology sectors (Mohammed, B. and Maulod, S., 2016).

Technology allows mobile devices to exchange voice messages and calls over an internet connection, it depends on different types of codec used, which converts and compress analog to a digital signal to be transmitted, and each coding gives different frame rate (bps) that affect the voice quality in MANET [Abou Haibeh, L, Hakem, N & Safia, 2017].

MANET is a group of mobile devices connected wirelessly with adapter called Wireless Network Interface Card (WNIC) while moving without any fixed infrastructure, it continuously changes its topology all the time, therefore it used by tactical networks like search and rescue, firefighter, and the police [Afaqui, MS, Garcia-Villegas, E & Lopez-Aguilera, 2016]. To transfer data in MANET, routing protocols must be applied guiding the packets from the source to the final destination [Alqaysi, H & QasMarrogy, GA 2015]. Recently WNICs works with the frequency of IEEE802.11n 5GHz, which provides larger bandwidth from the old IEEE802.11a, b, g, that gives data rate of 11Mbps up to 54Mbps that considered very inefficient for high-quality VoIP transmission [AlShahwan, F, Alshamrani, M & Amer, AA 2018]. VoIP quality in MANET can depend on many factors such as WNIC characteristics, buffer size, transmission power, data rate, max receiving lifetime, and the large

* Corresponding Author:

Ghassan A. QasMarrogy

E-mail: <mailto:ghassan.qasmarrogy@cihanuniversity.edu.iq>

Article History:

Received: 07/07/2020

Accepted: 10/09/2020

Published: 20/02 /2021

packet processing [Aman, AHM, Hashim, A-HA, Abdullah, A, Ramli, H & Islam, S 2017].

This paper will focus on calculating, modulating and enhancing the buffer size and max receive lifetime in IEEE 802.11n 5GHz WNIC parameters for VoIP transmission over MANET, with using Network Simulator 2 (NS2) and analyzing and comparing two famous routing protocols AODV and OLSR regarding end to end delay, throughput, and packet loss to ensure highest QoS result.

The rest of the paper will be structured as follows. Section II shows the proposed calculations of IEEE 802.11n 5GHz parameters and VoIP transmission techniques. while section III presents the experimental results, analysis, and comparison. And finally, section IV provides a conclusion and direction for the future work of the paper.

2. LITERATURE SURVEY

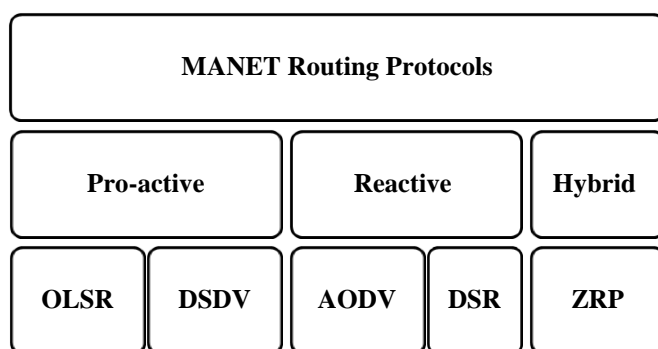
Many researchers tried to enhance and optimize VoIP service in MANET, in [Patel, N.K., Saxena, P., Singh, R. and Kumar, S] the reasercher tryes a novel method of signaling for broadcast voice is proposed for multi-hop broadcast voice communication in tactical Mobile Ad-hoc Network (MANET) with Time Division Multiple Access (TDMA) as underlying MAC scheme, the results show better and enhanced quality with lower delay and higher throghput. in [Antwi-Boasiako, E, Kuada, E & Boakye-Boateng, K 2016] a new approach implemented to improve the SIP voice signaling system in OLSR for MANET by modifying the routing parameters, the analysis shows an effective reducing in the delay and enhancing signaling performance. While in [Aman, AHM, Hashim, A-HA, Abdullah, A, Ramli, H & Islam, S 2017] proposed multicast protocols were used to decrease the delay of the receiver's processing, the analysis shows more accurate results using the proposed method. In (Mohammad, A.S. and Potrus, M.Y., 2016)

An analysis for TCP was done regarding the throughput during the movement of MANET wireless nodes, it shows a comparison with different types of TCP comparison, the result shows a better performance regarding the metric analyzed. In [Chandel, ST & Sharma, S 2016] an attempt was used to apply fuzzy logic for optimal

routing results to transfer voice data through MANET, the result shows more accuracy, with lower delay. In [Chen, Y-H, Hu, C-C, Wu, EH-K, Chuang, S-M & Chen, G-H 2017] a comparison was made to examine the transmission of VoIP with different types of routing protocols to analyze the best protocol, the result shows that the DYMO protocol is better to be used in an ad hoc network. while, in [Erciyes, K, Dagdeviren, O, Cokuslu, D, Yilmaz, O & Gumus, H 2011] a new approach to control the congestion of the network was used during VoIP transmission, with estimating the queue size for optimal result, the analysis shows that this approach gives better performance from the existing parameters used in transmission. Finally, in [QasMarrogy, GA 2020] a new performance was done for video transmission over 5Ghz flying drones to measure the throughput, delay and transmission attempts using buffer size variation, where it was proven that the variation in buffer size can affect and enhance the transmission of video for UAV's Drones.

3. MANET IEEE 802.11N-5GHZ WNIC PARAMETERS and CALCULATIONS

To direct packets through MANET, routing protocols must be applied to find the best routes available. There are 3 types of routing



protocols namely, proactive, reactive, and hybrid as shown in Figure 1 [Ghosh, T, Tiwari, S & Sahay, J 2017]. Two routing protocols AODV, and OLSR were analyzed for this paper, as they are the best for VoIP as shown in many studies [Hassine, K & Frikha, M 2017] [Jin, C, Wei, DX & Low, SH 2006].

Figure 1: Types of MANET routing protocol [12].

Hoc On-Demand Distance Vector (AODV) is a reactive routing protocol, it uses broadcast discovery mechanism and sequence number to find the best fresh recent routes to the

destination. It starts his discovery phase when a node needs to transmit data to another node, and record his routes in its routing table until the source node finishes transmitting, then the routes will be deleted, and start new path discovery again when needed. Therefore, it causes lower overhead and more delays during transmission [Hassine, K & Frikha, M 2017].

While Optimized Link State Routing (OLSR) is a proactive routing protocol, it uses a group of selected nodes called Multipoint Relays "MPR's to exchange their recent routing information between them, giving a speed to route discovery phase. OLSR broadcast hello messages and store all the fresh routes all the time on a frequent interval, with or without a request from source nodes, therefore when a node needs to transmit, a route will be available immediately. Therefore, it causes less delay and more overhead during transmission [Kumari, N, Gupta, SK, Choudhary, R & Agrwal, SL 2016].

VoIP performance can depend on two factors, the WNIC parameters, and VoIP Codec as shown in table 1.

Table (1) Bandwidth Comparison for VOIP Codecs [1].

Voice Codec	Bandwidth (Kbps)
G.711	64
G.722	64
G.723.1	6.3
G.726	32
G.728	16
G.729	8

Therefore, the required B.W and size for the VoIP codec packet can be calculated from the following equations (1) (2) (3) [Marrogy, GA 2013].:

$$\text{Packet size} = (\text{L2 header}) + (\text{IP/UDP/RTP header}) + (\text{payload voice size}) \quad (1)$$

$$\begin{aligned} \text{Packets Per Second (PPS)} &= (\text{codec bit rate}) \\ &\div (\text{payload voice size}) \quad (2) \end{aligned}$$

$$\text{Bandwidth} = \text{packet total size} * \text{PPS} \quad (3)$$

To calculate a 60 second, VoIP codec 729 will be used, and based on the above equations, B.W and size required will be the following:

$$\begin{aligned} \text{Total Packet Size (bytes)} &= (\text{18 bytes}) + (\text{40 bytes}) \\ &+ (\text{20 bytes}) = \text{78 bytes} * \text{8bit} \\ &= \text{624 bits} \\ \text{Voice Payload Size} &= (\text{20 bytes}) * \text{8 b} = \text{160 bits} \end{aligned}$$

$$\begin{aligned} \text{Packets Per Second PPS} &= (\text{8 Kb/s}) \div (\text{160 bits}) \\ &= \text{50 pps} \\ \text{B.W/Call for 1 second} &= (\text{624 bits voice packet size}) \\ &* \text{50 pps} = \text{31.2 Kb/s} \end{aligned}$$

Therefore for calculating 600 seconds of VoIP B.W Size

$$\text{B.W Call for 600 S} = \text{31.2Kbps} \times \text{600s} = \text{18.82Mbps}$$

Where total packet size is the maximum size of the packet transmitted, voice payload size is the size of which carries the encoded voice data.

WNIC parameters can also affect the VoIP performance, these parameters keep the wireless connections between all network devices up to date. Therefore, using the new frequency of IEEE802.11n 5GHz will offer lower end to end delay, packet loss, with higher data throughput [Mondal, A, Misra, S & Maity, I 2018]. In MANET, these parameters give different results with device movement and size variation, with acceptable packet loss below 5% [QasMarrogy, GA, Alqaysi, HJ & Almashhadani 2017], where more can decrease the network performance.

3.1. WNIC Parameters: Buffer Size

When a frame packet received in the destination device, it gets stored and queued in WNIC buffer until all frames reached, then the WNIC will process the fragmented packet. The variable size of the buffer can enhance the performance of MANET, while the fixed size can decrease the performance [Rautu, D, Dhaou, R & Chaput, E 2017]. The required size of the buffer can be calculated from the following equation (4):

$$\text{WNIC Buffer Size} = (\text{RTT} \times \text{B.W}) \div \sqrt{N} \quad (4)$$

Where RTT is the round-trip time, that takes the message to send and acknowledge received from the destination. B.W is the bandwidth of the link, and N is the connection's number through transmission, where in [Savithri, V & Marimuthu, A 2017] was approved the optimal value is 5 for N. Therefore, the calculated buffer size for this paper will be

$$\text{Size} = (\text{600} \times \text{1024} \times \text{1024} \times \text{0.01}) \div \text{25} \approx \text{256,000bits}$$

To analyze optimal results for IEEE 802.11n 5GHz MANET, four cases will be calculated and simulated (128,000 - 256,000 - 512,000 - 1024,000) bits.

3.2. WNIC Parameters: Max Receive Lifetime

After storing the received frames in buffers with fragmentation technique is on, it remains there for a specific time until all packet frames received to be processed. Otherwise, if all frames weren't received during the specified interval

time, the frames drop for new frames to be stored [Shenoy, SU, Kumari, S & Shenoy, UKK 2017]. Therefore, if the time variate in MANET, it can give a different result. To calculate optimal results for IEEE 802.11n 5GHz MANET, four cases will be calculated and simulated (0.1 - 0.5 - 1 - 1.5) second.

4. RESULTS AND DISCUSSION

Two scenarios were calculated and analyzed, the first scenario calculates the buffer size variations, while the second calculates the variation in Max Receive Lifetime, finally, both scenarios will compare AODV and OLSR for best results.

In this paper, a 1000 m² with 50 moving devices (1.4 m/s human walking speed) were simulated in NS2 simulator, using a frequency of IEEE802.11n 5GHz and 600Mb/s data rate, a VoIP codec 729 sizes of 19Mb were transmitted for 10 minutes over MANET, with two routing protocols AODV and OLSR. 10 repetitions for each scenario were calculated for optimal average results, also the first 100 seconds is the white state to find fresh routes, which may affect the result, therefore no transmission and analysis was done [Singh, P, Sharma, AK & Kamal, T 2016].

The simulations of IEEE802.11n 5GHz buffer size scenario in figure 2, 3, 4 shows the best results calculated for throughput is between 128,000 and 256,000 bits, and it decreases when the buffer size increase, because when the buffer size is increased, it needs more time to process the queued frames, which cause more delay, and decrease the throughput of processed packets, also more delay can cause the incoming packets to be dropped while the queued packet get processed, which increases the retransmission attempts [Yildiz, HU, Tavli, B & Yanikomeroğlu, H 2015].

AODV shows better throughput, but higher delay and retransmission attempts than OLSR. In AODV the source node with low-speed mobility obtains the routes faster while reducing the broadcasts messages to find new routes, which also decrease the requirement for memory and routes duplications, but due to the nature of

reactive protocols, it causes higher delay to find the routes and transmit the data, while OLSR remains stable during all buffer size calculations.

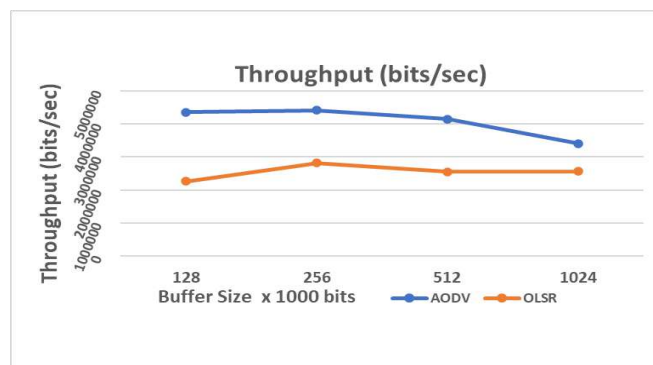


Figure 2: Throughput (b/s) of AODV and OLSR Protocols with Buffer Size Variation

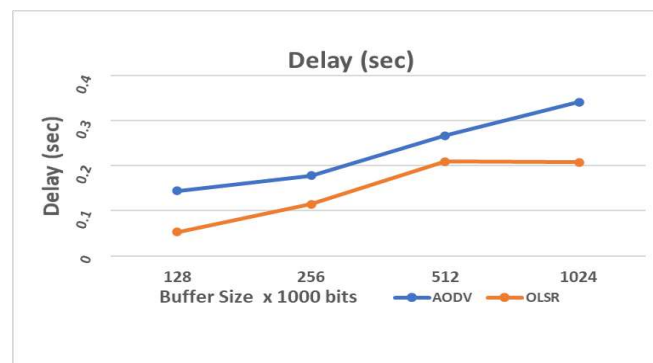


Figure 3: Delay (s) of AODV and OLSR Protocols with Buffer Size Variation

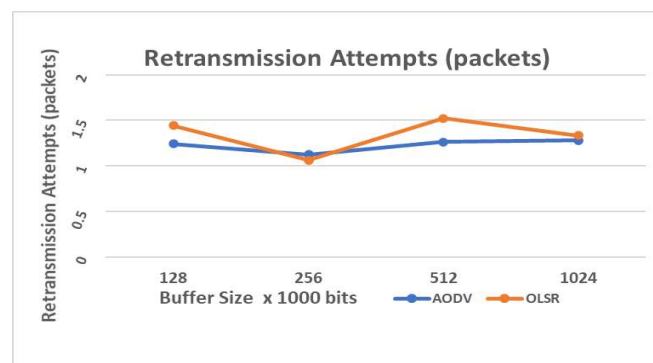


Figure 4: Retransmission Attempts (Packets) of AODV and OLSR Protocols with Buffer Size Variation

The simulations of MAX receive lifetime scenario in figure 5, 6, 7 shows the best results calculated for throughput is 0.1 second. When the time is very low, all IEEE802.11n 5GHz WNIC parameters for all nodes in MANET are synchronized faster, and routes will establish with the lowest delay as possible while increasing the time can cause the WNIC parameters to synchronize slower, thus it needs more time to find fresh better routes to destination.

When time increases AODV remains high for throughput, but it still has a higher delay and retransmission attempts than OLSR. In 0.5 second AODV enhances its performance for the lower delay and retransmission attempts, with higher throughput, which is considered an optimal

parameter enhancement for the AODV routing protocol.

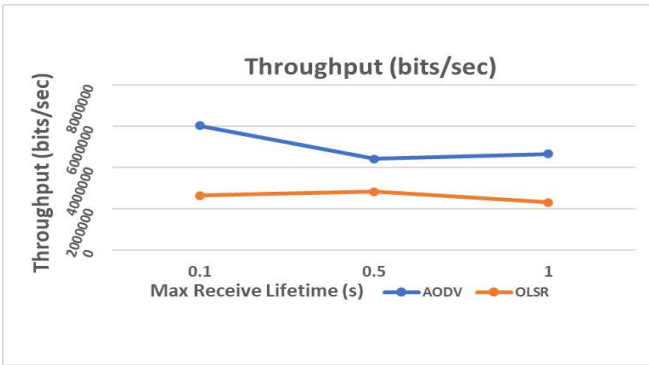


Figure 5: Throughput (b/s) of AODV and OLSR Protocols with MAX Receive Lifetime

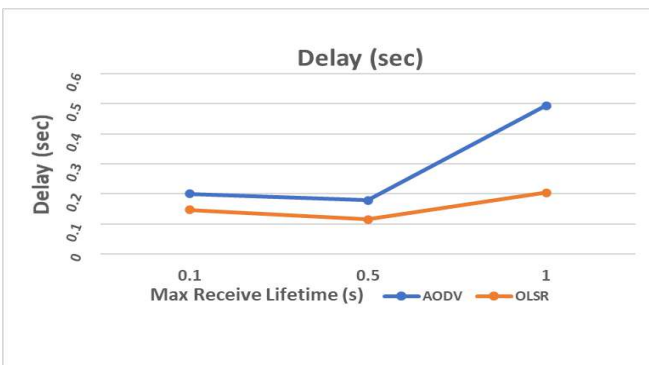


Figure 6: Delay (s) of AODV and OLSR Protocols with MAX Receive Lifetime

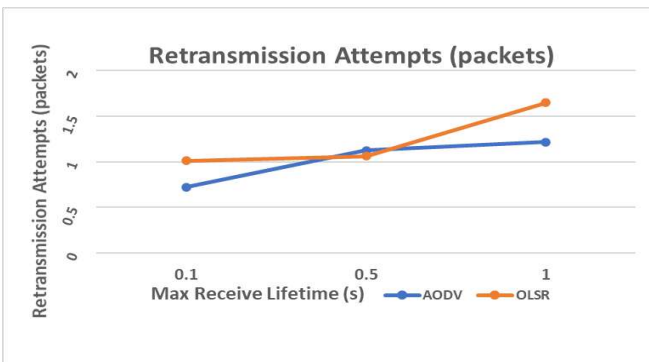


Figure 7: Retransmission Attempts (Packets) of AODV and OLSR Protocols with MAX Receive Lifetime

5. CONCLUSIONS and FUTURE WORK

Nowadays VoIP communication is essential for wireless networks especially tactical networks. In this paper, an improvement for VoIP transmission over MANET was done, by calculating the optimal IEEE802.11n 5GHz WNIC parameter's buffer size and max receive lifetime for mobile devices, with two famous routing protocols AODV and OLSR. The analysis shows the optimal result for buffer size for VoIP was 128,000 and 256,000 bits while the best max

receive lifetime was 0.1 and 0.5 seconds. AODV shows better result than OLSR with throughput, but higher-end to end delay. While OLSR remains stable most of the experiment. AODV also shows enhancement when increasing the MAX receive lifetime to 0.5 with lower delay and higher throughput

For future work, a recommendation is advised to use different types of VoIP codec with more calculations, to ensure more accurate and optimal results to be found for all IEEE802.11n 5GHz WNIC parameters.

References

- About Haibeh, L, Hakem, N & Safia, OA 2017, 'Performance evaluation of VoIP calls over MANET for different voice codecs', IEEE, pp. 1-6.
- Afaqui, MS, Garcia-Villegas, E & Lopez-Aguilera, E 2016, 'IEEE 802.11 ax: Challenges and requirements for future high efficiency WiFi', IEEE Wireless Communications, vol. 24, no. 3, pp. 130-137.
- Alqaysi, H & QasMarrogy, GA 2015, 'Performance Analysis Of Video Streaming Application Over Manets Routing Protocols', International Journal Of Research In Computer Applications And Robotics, vol. 3, pp. 22-28.
- AlShahwan, F, Alshamrani, M & Amer, AA 2018, 'Dynamic Novel Cross-Layer Performance Enhancement Approach for SIP over OLSR', IEEE Access, vol. 6, pp. 71947-71964.
- Aman, AHM, Hashim, A-HA, Abdullah, A, Ramli, H & Islam, S 2017, 'Packet Loss and Packet Delivery Evaluation Using Network Simulator for Multicast Enabled Network Mobility Management', International Journal of Future Generation Communication and Networking, vol. 10, no. 4, pp. 41-50.
- Antwi-Boasiako, E, Kuada, E & Boakye-Boateng, K 2016, 'Role of codec selection on the performance of IPsec secured VoIP', IEEE, pp. 2508-2514.
- Chandel, ST & Sharma, S 2016, 'Experimental analysis of various protocols on VoIP traffic with different CODECS in Wireless LAN', IEEE, pp. 109-113.
- Chen, Y-H, Hu, C-C, Wu, EH-K, Chuang, S-M & Chen, G-H 2017, 'A delay-sensitive multicast protocol for network capacity enhancement in multirate MANETs', IEEE Systems Journal, vol. 12, no. 1, pp. 926-937.
- Erciyes, K, Dagdeviren, O, Cokuslu, D, Yilmaz, O & Gumus, H 2011, 'Modeling and simulation tools for mobile ad hoc networks', Mobile ad hoc networks: Current status and future trends, vol., pp. 37-70.
- Ghosh, T, Tiwari, S & Sahay, J 2017, 'Enhanced rate of wlan using different protocols in

- infrastructure and ad-hoc mode', IEEE, pp. 405-409.
- Hassine, K & Frikha, M 2017, 'A VoIP focused frame aggregation in wireless local area networks: Features and performance characteristics', IEEE, pp. 1375-1382.
- Jin, C, Wei, DX & Low, SH 2006 'FAST TCP: motivation, architecture, algorithms, performance', IEEE, pp. 2490-2501.
- Kumari, N, Gupta, SK, Choudhary, R & Agrwal, SL 2016, 'New performance analysis of AODV, DSDV and OLSR routing protocol for MANET', IEEE, pp. 33-35.
- Marrogy, G.A.Q., 2020. ENHANCING VIDEO STREAMING TRANSMISSION IN 5 GHZ FANET DRONES PARAMETERS. Telecommunications and Radio Engineering, 79(11).
- Marrogy, GA 2013, 'Performance analysis of routing protocols and TCP variants under HTTP and FTP traffic in MANET's', thesis, Eastern Mediterranean University (EMU)-Doğu Akdeniz Üniversitesi (DAÜ).
- Mohammad, A.S. and Potrus, M.Y., 2016. A Method for Compensation of TCP Throughput Degrading During Movement Of Mobile Node. ZANCO Journal of Pure and Applied Sciences, 27(6), pp.59-68.
- Mondal, A, Misra, S & Maity, I 2018, 'Buffer size evaluation of openflow systems in software-defined networks', IEEE Systems Journal, vol. 13, no. 2, pp. 1359-1366.
- Patel, N.K., Saxena, P., Singh, R. and Kumar, S., 2019, July. A novel voice signaling protocol for tactical broadcast voice communication in mobile ad hoc network. In 2019 10th International Conference on Computing, Communication and Networking Technologies (ICCCNT) (pp. 1-4). IEEE.
- QasMarrogy, GA, Alqaysi, HJ & Almashhadani, YS 'Comprehensive Study of Hierarchical Routing Protocols in MANET using Simple Clustering', p. 62.
- Rautu, D, Dhaou, R & Chaput, E 'Maintaining a permanent connectivity between nodes of an air-to-ground communication network', IEEE, pp. 681-686.
- Savithri, V & Marimuthu, A 'Forward linear predictive queuing based window adjustment policy for congestion control in voice over MANET (VoMAN)', IEEE, pp. 1-4.
- Shenoy, SU, Kumari, S & Shenoy, UKK 'Comparative Analysis of TCP Variants for Video Transmission Over Multi-hop Mobile Ad Hoc Networks', Springer, pp. 371-381.
- Singh, P, Sharma, AK & Kamal, T 2016, 'An adaptive neuro-fuzzy inference system modeling for VoIP based IEEE 802.11 g MANET', Optik, vol. 127, no. 1, pp. 122-126.
- Yildiz, HU, Tavli, B & Yanikomeroglu, H 2015, 'Transmission power control for link-level handshaking in wireless sensor networks', IEEE Sensors Journal, vol. 16, no. 2, pp. 561-576.

RESEARCH PAPER

Influences of Environmental Quality and safety & security on the Liveability of Residential Complexes in Erbil City

Maysa Ghazi Thanoon¹, Hamid Turki Haykal ²

^{1&2} Department of Architecture, College of Engineering, Salahadden University, Erbil, Kurdistan Region, Iraq

ABSTRACT:

Liveability is a place based theory that makes the city a great place to live, it seeks to plan our living communities to promote good health, support the social cohesion and create safe and secure environment for the residents. This research seeks to examine the influence of two factors on liveability; the environmental quality and safety & security and their related issues. Five residential complexes implemented by the investment sector and located in different geographic locations in Erbil city are chosen as case study samples. The study employs an interrelated measuring tool by using spatial analysis check list and questionnaire survey with the residents. Results of the statistical analysis showed that significant differences were found between the residents satisfaction about their living environment in term of the studied factors, while non-significant differences were found between the results of both measuring tools used.

KEY WORDS: Liveability; Environmental Quality; Safety and Security; Spatial analysis; Residents' satisfaction.

DOI: <http://dx.doi.org/10.21271/ZJPAS.33.1.18>

ZJPAS (2021) , 33(1);163-177 .

1. INTRODUCTION

Livability is one of the recent vital theories on the level of urban planning, liveability among developing countries' cities is a concerning issue and paid less attention (Beiglu *et. al*, 2019). It is regarded as an indicator of quality of life and urban quality issues in the urbanized areas (Giap *et. al*, 2014). Rapid and often unplanned urbanization has become a global phenomenon that increased the exposure of people and urban assets to higher degrees of attention to liveability (Beiglu *et. al*, 2019).

In Kurdistan region, a rapid growth of urbanization and urban development have been launched as a result of the approval of 175 housing projects in Kurdistan Region during the period from 1/8/2006 till 28/7/2019, which 86 housing projects of them are located in Erbil province (Board of Investment, 2019). As a result the city is facing numbers of challenges in term of environmental degradation, also in adequate shelters and poorly maintained environmental and physical infrastructures (Ibrahim *et.al*, 2015). Moreover, the rapid urbanization as well as the lack of planning regulations affected negatively on residential land use which are more likely to have less open spaces and more load on infrastructure (Shingali and Malaika, 2016; Ibrahim *et.al*, 2015).

1.1 Definition of terms:

Many terminologies and definitions associated with quality of life have been used to define the liveability, Flint in 2013 defined liveability as a part of the community and mentioned that

* Corresponding Author:

Maysa Ghazi Thanoon

E-mail: maysa.danoon@su.edu.krd

Article History:

Received: 20/07/2020

Accepted: 19/09/2020

Published: 20/02 /2021

Community liveability refers to the environmental and social quality of an area as understood by inhabitants, It is the sum of factors that add up to a community's quality of life including the built and natural environments (Flint, 2013). Livability could be result of summation of many factors that add up to a community's quality of life which consist of the built and natural environments, economic prosperity (Partners for Liveable Communities, 2011). To summarize the term 'liveability' refers to the living condition of the place, reflects the people's evaluation about their living environment and the extent to which the place is fit to live or not.

1.2 Dimensions of livability:

The (National Research Council, 2002) of America, classified the liveability dimensions in to three essential groups, namely Social, Economic and Environmental dimensions, in the same context Aguiar and his colleagues in 2018 confirmed that physical social and economic dimensions as the main characteristics of urban liveability (Aguiar et.al, 2018), see figure 1. Heylen in 2006 indicated that Liveability refers to four dimensions: the quality of the dwelling/building included (acoustic isolation, density, comfort/size and maintenance), the quality of physical environment including the level of services and facilities, the quality of the social environment, resident characteristics and finally safety of the neighborhood. Others introduced another dimensions of liveability that are characterizing the urban areas and classified them in to seven groups which are: built and natural environment, economic prosperity, social stability and equity, adequate physical infrastructure, public health, safe streets and finally the educational opportunity (Tomalto and Mallach, 2015). According to Appleyard and his colleagues liveability has two distinctive dimensions that are: performance dimensions and prescriptive dimensions, the former one focuses on both the qualities and measures which are descriptive criteria of liveability while the latter one describes policy interventions and final status of outcomes, in other words performance dimension describes what should be measured whereas prescriptive dimension provides guidance for implementation such as more affordable

housing and wider transportation choices (Appleyard *et.al*, 2014)

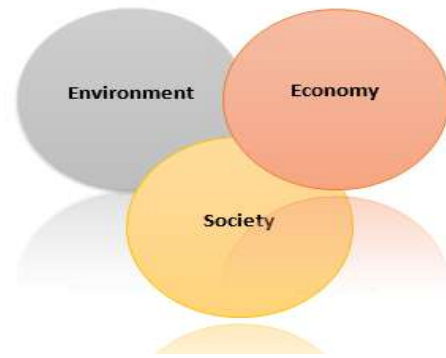


Figure 1 Dimensions of liveability (National Research Council, 2002)

1.3 Spatial scales of Urban Liveability:

Kashef in 2016 conducted an analytical review about urban liveability, he synthesized the dimensions of urban liveability which presents the linkage and relationship among environmental, economic and social dimensions, and he produced a conceptual model based on natural systems and built systems that captures the intellectual building blocks of urban liveability. Urban liveability is categorized in to three spatial scales, the first one is related to the city level whereas liveable city is defined as habitable and fit to live (Ruth and Franklin, 2014), such indexes were created to rank cities in term of liveability like Mercer and Monocle that adopt safety and environmental issues as forefront assessment indicators (Takahashi et.al, 2018). In regarding to the neighborhood level as a second spatial scale of urban liveability. Liveable neighborhoods according to the AARP (American Association of Retired People) and Public Policy Institute liveability seeks to promote creative policies that address residents' desire to live safe & secure, age friendly and healthy neighborhoods and communities, it is considered the first tool to asses and measure liveability at the neighborhood level based on the following seven categories: Housing, Neighborhood, Environment, Health, Transportation, Engagement and Opportunity. Public space level was categorized as the third spatial scale of urban liveability. Nasution & Zahrah in 2014 concluded that the enhancement of the public open space will create a better perception to overall quality of life while

the functional factor was the most significant factor that affects people's satisfaction. Ali and Ali (2018) confirmed that liveliness of the public open spaces is related to the safety of the place. Based on the previous literature urban liveability based on three spatial scales, various indicators have been addressed that impact the liveability of the community and make it a desirable place to live. Figure 2. Summarizes the main dimensions and indicators of liveability according to the previously mentioned studies and literature

1.4 The Scope of the Study:

This study will scope on environmental quality and safety & security factors and its influence on the neighborhood's liveability.

1.4.1 Environmental quality:

The environmental quality is an important indicator for livability studies as it has a direct effect on human activities and opportunities by creating a healthy physical and social environment (Bigio and Dahiya, 2004). According to European Environment Agency a pressure on urban environment and threats on people's well-being and health may be created if the environmental issues are neglected through urban planning process (European Environment Agency, 2015). One of the most environmental problems that are facing the urbanized areas is the air pollution according to the location of pollution source such as the waste collection & management areas and the industrial land use zones, therefore, selecting a suitable location for them has been always unsolved subject for human as the improper place causes water, soil & air contamination, at the local level- in Kurdistan Region no instructions or regulations have been presented regarding to the buffer zone of any pollution source, regarding to the instructions provided by the Department of Environment of Iran land fill (or any waste management zone) must be placed at a distance of 10-15km from the city (Derakhshandeh & Beydokhti, 2014). In addition, environmental problems are matching with hygienic, economic, aesthetic & environmental quality desired by the public (Xue et. al, 2010). In term of pollution sources the current study will focus on the presence of any pollution source within the studied areas as well as the distance between the studied residential areas and the pollution sources in Erbil city (the waste collection zone, northern industrial zone and the southern industrial zone) to be assessed according to the regulations in this

term, moreover, the aesthetic value and cleanliness are based as indicators.

1.4.2 Safety & Security:

In October 2016, the Third United Nations Conference on Housing and Urban Sustainable Development was held, and the "New Urban Agenda" was released, urban safety was considered as one of the most influential factors to evaluate cities in term of urban liveability (Lihu et. al, 2020). Based on Maslow's hierarchy of needs, the aspect of safety indicator is considered as the second most important factor after the physiological needs, this hierarchy indicates that one will not attain life satisfaction if the absence of threats to safety is not guaranteed, accordingly the perception of safety is a critical aspect in achieving quality of life. Crime prevention tactics are suggested for residential environments in urban areas including building fences and walls, creating territorial spaces, increasing outdoor lighting and installing guard booths and surveillance cameras (Sakip et.al, 2013). Figure 3 shows the current research indicators.

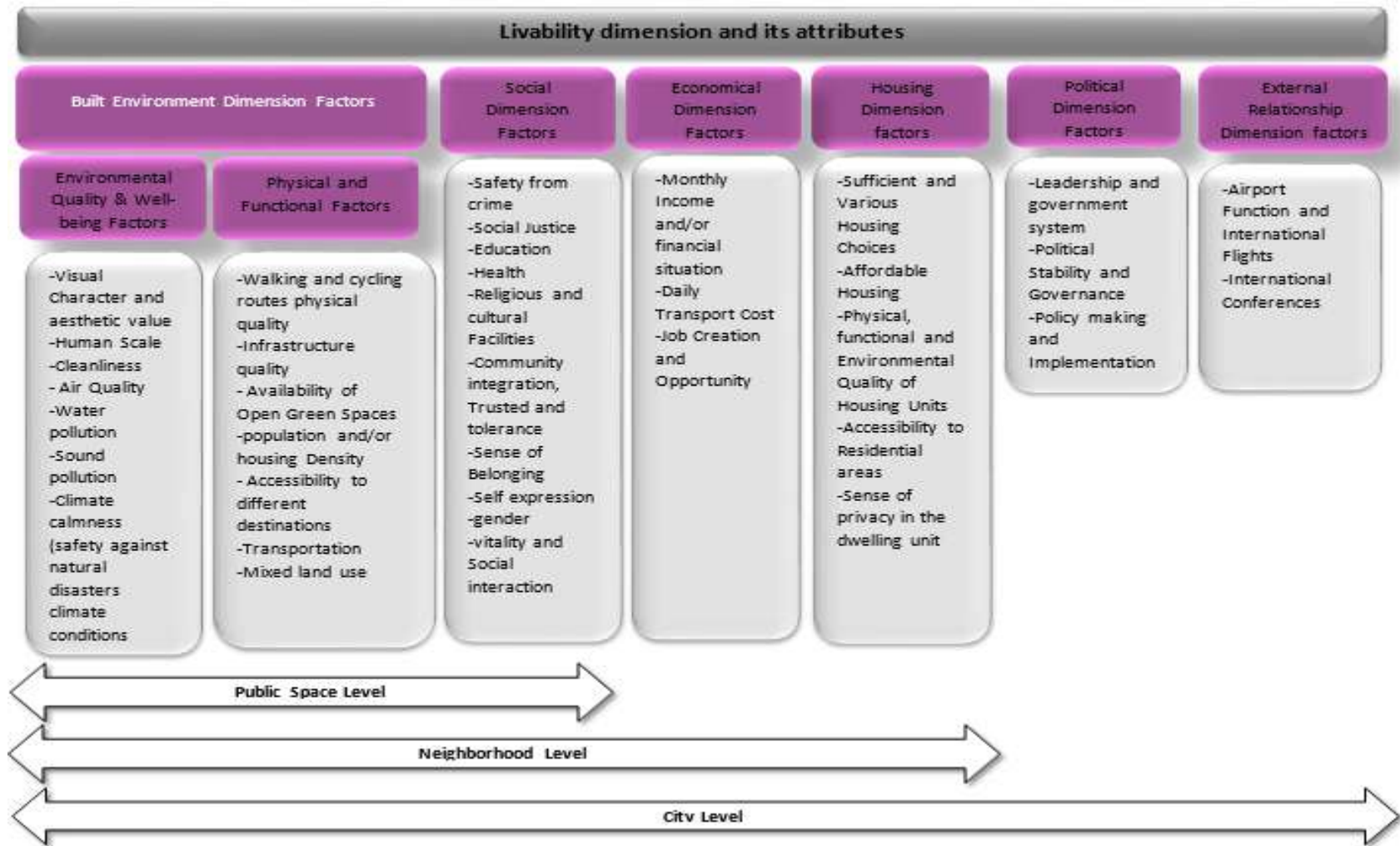


Figure 2 Liveability dimensions and its indicators as conducted from previous studies and literature according to each spatial scale (the researcher)

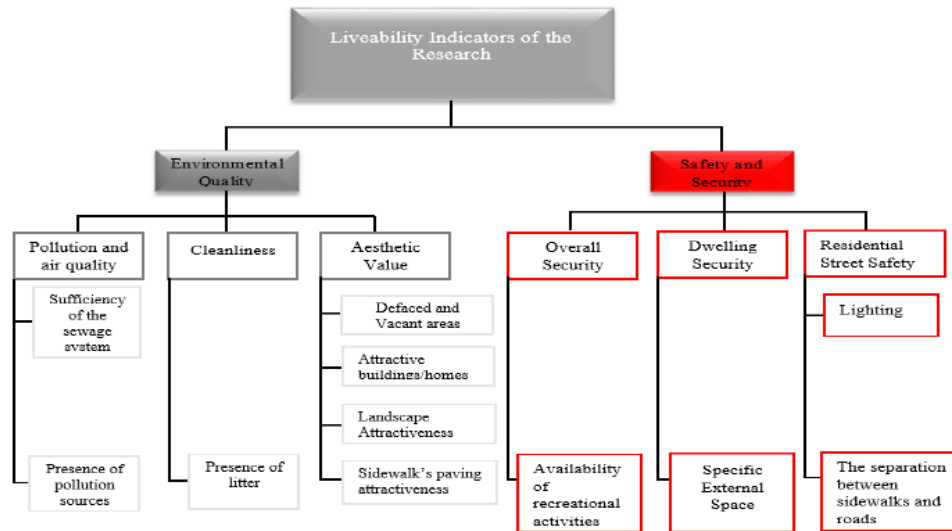


Figure 3 Liveability Indicators of the current research (the researcher)

1.5 Research Problem

The majority of the previous studies have been conducted abroad, more over Beiglu and his colleagues stated that ‘more research is required to see how liveability issues are experienced and assessed in urban neighborhoods in developing countries’ (Beiglu et. al, 2019). Therefore, the liveability issue in Erbil city is uncertain and questionable. (In this regard, there is a lack of considering research and investigations in Erbil city about the influence of environmental quality and safety & security on liveability), therefore, the main objective of this study is to clarify the role of the environmental quality and safety & security on the liveability presence in Erbil city residential complexes. According to the above the research problem is: there is no evidence if the local’s satisfaction about the livability of their residential complexes matches the livability as measured through the spatial analysis when the assessment includes many levels indicators to use both of the measuring tools in evaluating the studied areas that are located in different geographic locations in Erbil city in term of their liveability.

1.5.1 Research Objectives

1. To objectively measure the studied liveability indicators through the spatial analysis check list of the studied residential complexes
2. To compare the satisfaction degrees of residents with the studied liveability indicators using a questionnaire survey in the studied residential complexes

3. To determine if a match exists between the objective spatial analysis results and the subjective questionnaire survey measurement of liveability
4. To specify the highest and lowest level of liveability of the studied residential complexes

1.5.2 Research Questions

1. Are there differences in the actual presence of the environmental quality and safety & security indicators as measured by the spatial analysis checklist amongst the studied residential complexes?
2. Are there differences in the residents’ satisfaction degree about the environmental quality and safety & security indicators amongst the studied residential complexes?
3. Are the results of the spatial analysis matching with the results of the questionnaire survey’s results in term of the studied liveability indicators?

1.5.3 Research Hypothesis

1. Differences are shown in the actual presence of the studied factors of liveability by using the spatial analysis checklist amongst the studied residential complexes
2. The satisfaction of Residents’ about the studied liveability factors amongst the studied residential complexes varies.
3. Matching exists between the results of the spatial analysis and the questionnaire survey.

2. Research Methodology

This research was conducted in five residential complexes in Erbil city, the research was based on two measuring tools that included: spatial analysis checklist as most geographical inquiries on liveability have been based on objective measures (Saitluanga, 2014) and questionnaire survey as it is preferred for planning and policy purpose as it is providing more valuable feedback (Ibrahim and Chung, 2003). In this study the scoring value of the spatial analysis checklist ranges from (1 for highly inefficient and 5 for highly efficient). Visual field survey and ArchGIS software are based as a supportive tool for the spatial analysis and measuring the distance between the studied residential complexes and the pollution sources in

the city to calculate the final scoring values of the studied indicators, see table 1. Regarding to the questionnaire survey as a second measuring tool a Likert scale ranging from ‘1-5’ is used for rating the statements that related to each studied factor denoting ranges from ‘1’ highly dissatisfied to ‘5’ highly satisfied ‘2, 3 and 4’ represent dissatisfied, neutral and satisfied respectively, a pilot test for the questionnaire among small cross section of the population was conducted to refine the final questionnaire form before implementing the formal survey, see table 2.

Table 1. Spatial analysis Checklist’s Results of the Studied Areas

A. Environmental Quality	
1. Availability of toxic fumes &/or pollution source <input type="checkbox"/> 1 <input type="checkbox"/> 2 <input type="checkbox"/> 3 <input type="checkbox"/> 4 <input type="checkbox"/> 5 A1	3.2 Frequency of garbage Collection <input type="checkbox"/> 1 <input type="checkbox"/> 2 <input type="checkbox"/> 3 <input type="checkbox"/> 4 <input type="checkbox"/> 5
2.Sewage system availability and maintenance <input type="checkbox"/> 1 <input type="checkbox"/> 2 <input type="checkbox"/> 3 <input type="checkbox"/> 4 <input type="checkbox"/> 5 A2 The average score of below Mentioned aspects	B. Safety and Security
2.1 Availability of storm water drainage system <input type="checkbox"/> 1 <input type="checkbox"/> 2 <input type="checkbox"/> 3 <input type="checkbox"/> 4 <input type="checkbox"/> 5	4.Controlled entrances by guarding points <input type="checkbox"/> 1 <input type="checkbox"/> 2 <input type="checkbox"/> 3 <input type="checkbox"/> 4 <input type="checkbox"/> 5 B4
2.2 Maintenance condition of storm water pipes <input type="checkbox"/> 1 <input type="checkbox"/> 2 <input type="checkbox"/> 3 <input type="checkbox"/> 4 <input type="checkbox"/> 5	5.The neighborhood is not overlooked on isolated area <input type="checkbox"/> 1 <input type="checkbox"/> 2 <input type="checkbox"/> 3 <input type="checkbox"/> 4 <input type="checkbox"/> 5 B5
2.3 Grey water drainage system <input type="checkbox"/> 1 <input type="checkbox"/> 2 <input type="checkbox"/> 3 <input type="checkbox"/> 4 <input type="checkbox"/> 5	6.The availability of lighting in public Spaces, roads and sidewalks <input type="checkbox"/> 1 <input type="checkbox"/> 2 <input type="checkbox"/> 3 <input type="checkbox"/> 4 <input type="checkbox"/> 5 B6
3.Cleanliness <input type="checkbox"/> 1 <input type="checkbox"/> 2 <input type="checkbox"/> 3 <input type="checkbox"/> 4 <input type="checkbox"/> 5 A3 The average score of below Mentioned aspects	7.Availability of enclosed fence for each dwelling unit <input type="checkbox"/> 1 <input type="checkbox"/> 2 <input type="checkbox"/> 3 <input type="checkbox"/> 4 <input type="checkbox"/> 5 B7
3.1 Availability of Garbage cans <input type="checkbox"/> 1 <input type="checkbox"/> 2 <input type="checkbox"/> 3 <input type="checkbox"/> 4 <input type="checkbox"/> 5	8.Presence of traffic control device (speed bumps, stop signs) <input type="checkbox"/> 1 <input type="checkbox"/> 2 <input type="checkbox"/> 3 <input type="checkbox"/> 4 <input type="checkbox"/> 5 B8

Table 2. Questionnaire form

Questionnaire Form							
Complex Name			Complex location				
HD: Highly Dissatisfied N: Neutral HS: Highly Satisfied D: Dissatisfied S: Satisfied							
NO.	Indicators		Degree of Satisfaction				
1.Environmental Quality			HD 1	D 2	N 3	S 4	HS 5
1	There are no polluted and bilge water puddles						
2	There are no bad smells in the neighborhood						
3	There are barely exhaust fumes while walking in my neighborhood						
4	The neighborhood is absent of litter						
5	There are no incomplete buildings or vacant areas that decreases the attractiveness of the neighborhood						
6	The form of the neighborhood buildings is attractive						
7	The landscaping of the neighborhood is attractive						
8	The sidewalks of the neighborhood have proper paving patterns						
2. Safety and Security							
9	You can walk safely at night in the neighborhood						
10	There are outdoor recreational activities & amenities that makes the residents feel safer during the entire day.						
11	Each dwelling unit has an enclosed external space that increases the sense of safety						
12	There is a sufficient lighting in the neighborhood that increases the sense of safety at nigh						
13	There is a separation between pedestrians and vehicles that increases the safety in busy streets						

2.1 Sample Selection

Investment housing projects were selected in this study as they represent the largest percentage of newly implemented residential projects. The selected residential complexes were characterized as single housing units, completely constructed complexes and the complexes are occupied by the local residents. Total of 250 households were interviewed by distributing 50 form for each residential complex to get a valid feedback about the residents’ satisfaction about their living environment in term of the studied factors, SPSS (Statistical Package for Social Sciences) software was used to analyse and tabulate the data. The selected residential

complexes as shown in Figure 4 were as following.

1. **Dream City** is located in the city centre
2. **Italian 2 City** located on Masif Salahaddin Road;
3. **New Azadi** Project located on Bahrka Road;
4. **Ashti 2** City located on Koya Road;
5. **Altun City** located on Kirkuk-Bansllawa Road.

The selected residential complexes are located in different locations in Erbil city to determine the in equalities between them in term of the studied indicators, the process of assessment (as previously mentioned in sec.2) based on both check list by scoring the sub indicators that related to each studied indicator and the questionnaire survey with the residents.

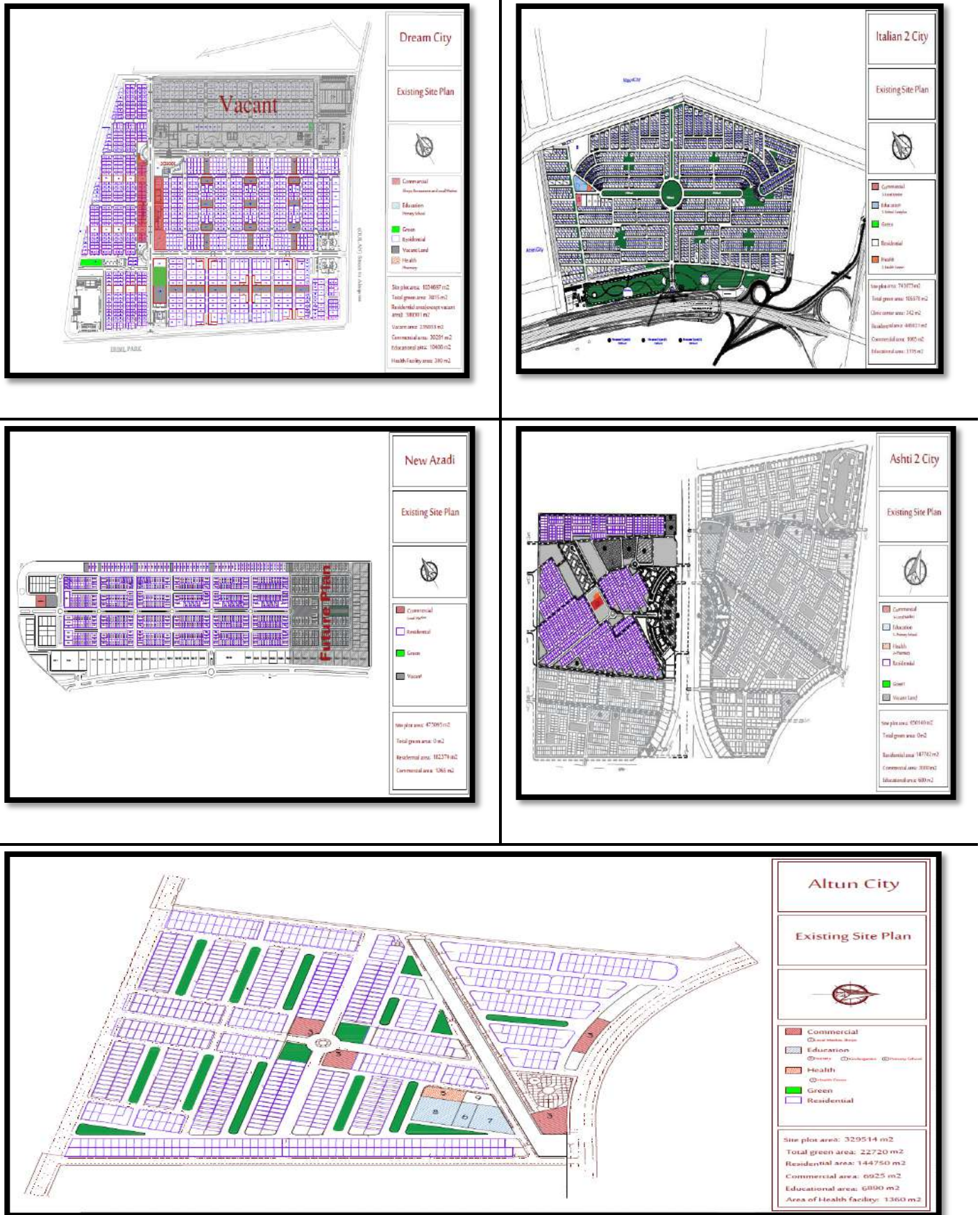


Figure 4: The Selected Residential Complexes

The scoring values of the tested indicators (environmental quality and safety and security) are provided in Table 3.

3. Results and Discussion

3.1 Results and Discussion of the spatial analysis check list

Table 3. Spatial analysis Checklist’s result of the studied areas

Factors	Environmental Quality									Safety and Security					
	A1	A2			Average	A3		Average	Total Average	B4	B5	B6	B7	B8	Total Average
		2.1	2.2	2.3		3.1	3.2								
Altun City	1	2	2	4	3	4	3	4	2.6	1	4	4	4	1	2.8
Dream City	2	4	4	4	4	3	3	3	3	5	5	5	3	4	4.4
Italian 2 City	3	5	5	4	5	5	5	5	4.3	5	2	4	4	5	4
Ashty 2	5	1	3	4	3	4	4	4	4	5	3	1	4	1	2.8
New Azadi	3	4	4	4	4	4	4	4	3.6	5	2	5	1	4	3.4
Total average scoring value of each indicator	Environmental Quality								3.5	Safety and Security					3.48

3.1.1 Analysis and Discussion of Environmental Quality Indicators

To analyse the environmental quality of each complex, the researchers identified the average mean score for the related sub-indicators (A1 to A3) to indicate the final scoring value that represents this indicator for each complex, as shown in Figure 5.

A complex with a higher scoring mean value means that the complex seems to promote health which is enhancing the overall quality of life, while the lowest scoring value is supposed to presence of pollution source within the residential area and poor quality of both sewerage system and the cleanliness. The average scoring values of all the selected complexes were as follows: Italian 2 City, 4.3; Ashti 2, 4; New Azadi, 3.6; Dream City, 3 and Altun City, 2.6

The result confirmed that the highest average scoring value was recorded for Italian 2 City, in term of existence of pollution source “3” scoring value is recorded (as the pollution source is

existing along one of the Italian city borderline from the exterior side, but in term of sewerage system and cleanliness “5” is recorded as the distributed and maintained storm water pipes are covering more than 80% of the complex as well as the efficiency of garbage collection services. The lowest scoring value 2.6 represents the poor environmental quality of Altun city according to the existence of pollution source within the complex and poor sewage which cause an environmental risk for the residents.

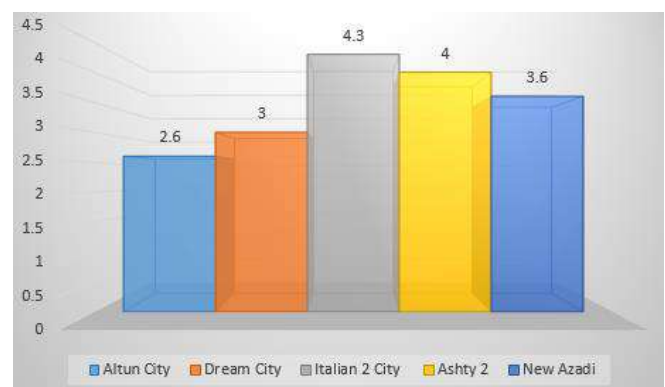


Figure 5 Average scoring values of Environmental Quality indicators for each studied area.

3.1.2 Analysis and Discussion of Safety and Security Indicators

Safety and security indicator is scored based on five sub-indicators (B4-B8) by using various techniques as mentioned before (GIS & field visual survey). The average scoring values for these indicators were calculated for each case study, as shown in Figure 6.

The maximum scoring value was recorded for Dream City with a scoring value of 4.4, according to this result we can say that Dream city is the safest and the most secure one, according to its location in the city center zone, it is surrounded completely by occupied area of residential, commercial & institutional uses, also in term of controlled entrances the complex does not have any through pass traffic or uncontrolled entrances. Moreover the majority of Dream city’s public spaces and residential streets are covered with lighting and traffic control devices which increase the sense of both safety & security, While both of Altun city & Ashti 2 recorded the minimum scoring value (2.8) amongst the studied samples, according to Altun city the entrances are not controlled & there is a lack of traffic control devices (less than 10% of the residential streets are covered), while in Ashti 2 there is a lack of both street lighting & traffic control devices, moreover Ahti 2 is surrounded by isolated area from two sides, all that affected negatively on the overall scoring value. Italian 2 city is rated as the second one as the complex is surrounded by non-occupied area from three sides (not completed & suspended residential projects). New Azadi project recorded 3.4 scoring value, it seems to has a fair level of safety & security as it is surrounded with non-occupied area from three sides, moreover the entrance is controlled by guarding points & camera and about 75% of the streets are covered with lighting & traffic control devices. The scoring values illustrate a clear image that all the selected residential complexes hold between fair and efficient level of safety and security and no one of them scored (1) or (2). As a result, creating more liveable residential environment affected by two main aspects: firstly: the vitality of the surrounded area, secondly: the presence of such a features like the lighting, controlled

entrances and speed control devices. Accordingly, the first research question about the differences in the actual presence of the studied liveability indicators in the selected residential complexes is answered. In terms of Environmental Quality, Italian 2 City recorded the maximum scoring value of 4.3, whereas Altun City recorded the minimum scoring value of 2.6. With regard to safety and security indicator, Dream City achieved the maximum scoring value of 4.4, and the minimum scoring value for both Altun City and Ashti 2 City was 2.8. According to the conducted results the validity of the first research hypothesis is proven.



Figure 6 Average scoring values of Safety and Security indicators for each studied area

3.2 Results and Discussion of the Questionnaire Survey

3.2.1 Analysis and discussion of the degree of residents’ satisfaction about the environmental quality indicators

The statements that were tested the environmental quality indicator in the questionnaire were included pollution source & air quality, cleanliness and aesthetic value. The statistical descriptive results of environmental quality amongst the studied complexes indicate that the total mean score depended on the residents’ view was 3.21 with a standard deviation of 0.84. The maximum value of the respondents’ agreement about environmental quality was recorded in Italian 2 city 3.96 with a standard deviation 0.53, while the minimum mean 2.26 with a standard deviation 0.87 was recorded for New Azadi complex. The means of each Ashti 2 city, Dream city and Altun city were 3.47, 3.32 and 3.03 respectively as shown in Table 4. The ANOVA result was (F = 50.120, p<0.05). Accordingly, a statistically significant difference exists amongst

respondents' satisfaction from the studied areas in regarding to the environmental quality indicator.

Table 4. Descriptive Analysis and One-Way ANOVA of Environmental Quality Indicator

Indicator	Case Study	N	Mean	Standard Deviation	Standard Error	F-test	p-value
Environmental Quality	Altun City	50	3.03	0.80	0.11	50.120	0.000*
	Dream City	50	3.32	0.48	0.07		
	Italian 2 City	50	3.96	0.53	0.07		
	Ashti 2 City	50	3.47	0.24	0.03		
	New Azadi	50	2.26	0.87	0.12		
	Total	250	3.21	0.84	0.05		

* Significant at level (p< 0.05)

3.2.2 Analysis and discussion of the degree of residents' satisfaction about safety and security indicators

The statements that were tested safety and security indicator in the questionnaire were included the availability of recreational activities, dwelling's unit security and residential streets safety. The result indicates that Italian 2 city scored the highest degree of residents' satisfaction about the safety & security indicator. While New Azadi recorded the lowest degree of residents' satisfaction about it. On the other hand the scoring value of Dream city, Ashti 2 city and Altun city were slightly less than the scoring value of Italian 2 city as shown in table 5, this satisfaction is related to the high security level all over Erbil

city. The result of ANOVA test was (F=50.420, P< 0.05). Accordingly, the result illustrate that there were statistical significant differences amongst the respondents from the studied complexes in respect to the safety & security indicator.

From the aforementioned results of the degree of residents' satisfaction with the environmental quality and safety and security indicators, the second research question about the difference in

the degree of residents' satisfaction with the studied liveability indicators amongst the selected residential complexes was answered and the validity of the second research hypothesis is proven. Figure 7 presents the outcomes of both measuring tools amongst the studied areas.

Table 5. Descriptive analysis and one-way ANOVA test of safety and security indicator.

Indicator	Case Study	N	Mean	Standard Deviation	Standard Error	F-test	p-value
Safety and Security	Altun City	50	3.32	0.81	0.11	50.42	0.000*
	Dream City	50	3.44	0.63	0.09		
	Italian 2 City	50	3.98	0.57	0.08		
	Ashti 2 City	50	3.36	0.30	0.04		
	New Azadi	50	2.12	0.92	0.13		
	Total	250	3.25	0.91	0.06		

* Significant at the level 0.05 (p< or=0.05), n=250

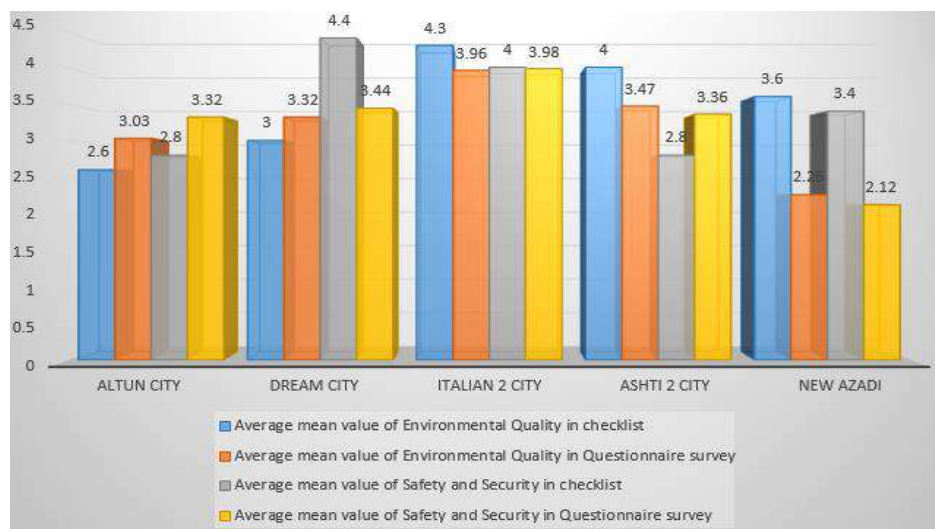


Figure 7 results of both measuring tools amongst the studied complexes

3.3 Comparison of the results of the spatial analysis evaluation and the questionnaire survey evaluation

A paired sample *t*-test was performed to examine the third research question regarding the correspondence between the results of the

checklist and the questionnaire survey. As shown in Table 6 and based on a significance

level of $p < 0.05$, insignificant differences occurred between the results of the checklist and the questionnaire survey in relation to the two selected liveability indicators. The *p* values for both tested pairs (Pairs 1 and 2) were more than 0.05. This result supports the accuracy and reliability of both tools and proves the validity of the third research hypothesis that states (**Matching exists between the results of the spatial analysis and the questionnaire survey**).

Table 6. Comparison of the questionnaire and checklist results

Comparison of the Questionnaire (Q) and Checklist (CH) results		Standard			
		Mean	Deviation	t-value	Significance (p-value)
Pair 1	Environmental Quality (Questionnaire)	3.208	0.628	-0.911	0.414
	Environmental Quality (Checklist)	3.500	0.700		
Pair 2	Safety and Security (Questionnaire)	3.24	0.682	-0.623	0.567
	Safety and Security (Checklist)	3.480	0.716		

* Significant at level (p<0.05)

4. Conclusion

After analyzing and discussing the selected case study samples, the following findings were obtained:

- According to the spatial analysis check list the maximum scoring value is recorded for Italian 2 city in term of environmental quality and for Dream city in term of safety and security factor, while the minimum scoring value for both studied factors is recorded for Altun city.
- The questionnaire survey results showed that the highest mean value of residents’ satisfaction is recorded for Italian 2 city (located on Masif Salahaddin Road) for both studied factors which means this zone is characterized with the majority of best criteria and regulations to achieve the liveability concept, whereas the lowest mean value of residents’ satisfaction is recorded for New Azadi (located on Bahrka Road), therefore, more attention is needed for the complexes located in this zone in term of environmental quality regulations and safety and security measures to promote their level of liveability.
- Regarding to the above mentioned results differences exist in the actual presence of the studied factors amongst the selected cases which prove the validity of the first research hypothesis. Based on this achievements urban planners and designers can get benefits from the results through planning and designing process and follow the guide lines to achieve

the qualitative residential environment in any location in the city.

- ANOVA test results indicate statistical significant differences between the residents’ satisfaction which proves the validity of the second research hypothesis.
- As the results of paired sample t-test confirmed a corresponding between the results of both spatial analysis check list and the questionnaire survey the validity of the results of both tools are proven as well as the third research hypothesis is confirmed. Therefore, the check list can be used by the planners as a tool to evaluate and assess the residential complexes before constructions and implementations stage.
- The results extracted from this research can provide a support and contribution to diagnose the defects and shortcomings for the existing residential complexes which provide a reliable database for the upcoming residential projects to avoid repeating design errors.

5. Recommendations

- In term of Environmental quality the study recommends the following:
 1. Take in to account the environmental quality of the site as an important issue when identifying the residential land use locations in the city.
 2. Determine a buffer zone of urban waste land and industrial land use in the city to avoid the penetration by another land use in case of the future expansion of the city specifically for the residential land use to prevent any hazardous or

harmful conditions which negatively affects health.

- In term of Safety & Security indicator the study recommends the following:

1. Selecting sites for the residential complexes that are surrounded by an occupied area with mixed land use to increase the sense of security.

2. Using a sufficient lighting in the public spaces and streets of the residential complexes to rise the sense of safety.

3. Using a sophisticated technology to control the security situation of the entrances for the residential complexes such as cameras or any other digital tools.

Acknowledgments

Special thanks to the staff of the General Director of Investment of Erbil, and the administration staff of the five studied housing projects to support the authors with the necessary data to carry out this study and thanks to Mapping Info office to provide the authors with the required satellite images and data.

Conflict of Interest

The authors declare that there is no conflict of interest.

References

- AARP (American Association for retired people). 2018. Livable communities: An Evaluation Guide, public policy institute, Washington, USA.
- Aguiar, B., Murias, P. and González, D. 2018. Sustainable Urban Liveability: A Practical Proposal Based on Composite Indicator. *Sustainability*, 11 (86), 1-18.
- Ali, A. and Ali, L. 2018. Evaluating quality of city Square, a practical survey on Neshtiman park / Erbil city. *Zanko journal for pure and applies sciences*, 30 (6), 8-36.
- Appleyard, B., Ferrell, C., Carroll, M. and Taecker, M. 2014. Toward Livability Ethics: A Framework to Guide Planning, Design and Engineering Decisions, *Journal of the Transportation Research Board*, 2403, 62-71.
- Beiglu, F., Ghafari, S. and Taheri, A. 2019. Infill Architecture as a Solution for Livability and Historical Texture Quality Promotion, *Civil Engineering Journal*, 5(1), 165-171.
- Bigio, A. and Dahiya, B. 2004. Urban Environment and Infrastructure *Toward Livable Cities, the International Bank for Reconstruction and Development/THE WORLD BANK*, Washington, DC 20433 USA.
- Board of Investment. 2019. List of Licensed Projects in Kurdistan Region-Approved Licenses by BOI & Governorates DGs, accessed on 8 August 2019, http://boi.gov.krd/licensed_projects.html
- Derakhshandeh, M. and Beydokhti, T. 2014. Management of Landfill Locating of Urban Waste, *European Online Journal of Natural and Social sciences*, 3(3), 32-39.
- EEA European Environmental Agency. 2015 EEA European Environment Agency The European Environment — State and Outlook 2015: Synthesis Report European Environment Agency, Copenhagen 2015.
- Flint, R. W. 2013, *Practices of Sustainable Community Development. A Participatory Framework for Chang*, Springer, Napa, CA, USA.
- Giap, T., Thye, W. and Aw, G. 2014. A new approach to measuring the liveability of cities: The Global Liveable Cities Index, *World Review of Science, Technology and Sust. Development*, 11(2), 176-196.
- Heylen, K. 2006. Liveability in social housing: Three case-studies in Flanders, *ENHR conference "Housing in an expanding Europe: theory, policy, participation and implementation"*, Ljubljana, Slovenia, 2 - 5 July.
- Ibrahim, M., & Chung, W. 2003. Quality of life of residents living near industrial estates in Singapore, *Social Indicators Research*, 61(2), 203–225.
- Ibrahim, R., Mushatat, S. and Abdilmonem, M. 2015. City Profile-Erbil, *Cities/The International Journal of Urban Policy and Planning*/, 49, 14-25.
- Kashef, M. 2016. Urban livability across disciplinary and professional boundaries, *Frontiers of Architectural Research*, 5, 239–253.
- Lihu, P., Xiaowen, L., Shipeng, Q., Yingjun, Z. And Huimin, Y. 2020. A multi-agent model of changes in urban safety livability, *Simulation: Transactions of the Society for Modeling and Simulation International*, 1-17.
- Nasution, A. and Zahrah, W. 2014. Community Perception on Public Open Space and Quality of Life in Medan, Indonesia, *Procedia - Social and Behavioral Sciences*, 153, 585-594.
- National Research Council. 2002. *Community and Quality of Life: Data Needs for Informed Decision Making*, Washington, DC: The National. Academies Press. <http://doi.org/10.17226/10262>
- Partners for Livable Communities. 2011, accessed March, 2019, https://scrc.gmu.edu/finding_aids/plcrecords.html
- Ruth, M. & Franklin, R. 2014. Livability for all? Conceptual limits and practical implications, *Applied Geography Journal*, 49, 18-23.
- Saitluanga, B. 2014. Spatial Pattern of Urban Livability in Himalayan Region: A Case of Aizawl City, India, *an International and Interdisciplinary Journal for Quality-of-Life Measurement*, Springer, 117(2), 541–559.
- Sakip, S., Johari, N. and Salleh, M. 2013. Perception of Safety in Gated and Non-Gated Neighborhoods, *Procedia - Social and Behavioral Sciences*, 85, 383 – 391.
- Shingali, H. and Malaika, M. 2016. Commercializing cities, challenges, and impacts, Duhok city, *Zanko journal for pure and applies sciences*, 28(2), 153-161.

- Takahashi, K., Kudo, S., Tateishi, E., Furukawa, N., Nordqvist, J. and Allasiw, D. 2018. Identifying Context-Specific Categories for Visualizing Livability of Cities—a Case Study of Malmö, *Journal of Challenges in Sustainability*, 6(1), 52-64.
- Tomalto, R. and Mallach, A. 2015. *America's Urban Future: Lessons from North of the Border*, Island Press, Washington.
- Xue, J., Wang, Q., Liu, Sh., Yang, J. and Wui, T. 2010. Removal of heavy metals from municipal solid waste incineration (MSWI) fly ash by traditional and microwave acid extraction, *Journal of Chemical Technology and Biotechnology*, 85(9), 1268-1277.

RESEARCH PAPER

High Harmonic Reduction Using Passive Filters of Mountain Steel Company

Asmahan Y. Husen¹, Kamal H. Younis², Ameen A. Fatah³

¹Department of Electric, College of Engineering, Salahaddin University-Erbil, Kurdistan Region, Iraq

²Department of Electric, College of Engineering, Salahaddin University-Erbil, Kurdistan Region, Iraq

³Institute of Electric, College of Engineering, Salahaddin University-Erbil, Kurdistan Region, Iraq

ABSTRACT:

An increasing amount of power electronics has created an immediate effect on the value of the electrical power source. Both of high control manufacturing loads and national loads explain harmonic in the system voltage. In this paper, characterized by nonlinear loads, are classified into two types of harmonics, current source harmonics, and voltage source harmonics. Harmonic distortion has usually been deleted via the usage of LC passive filter. The proposed technique is to get lower THD as long as possible and high power factor and high efficiency, properties of the passive filter is demonstrated in experiments for harmonic compensation in MOUNTAIN STEEL Company before and after filtering, by taking the voltage THD of a different time in a day.

KEY WORDS: Harmonic Compensation, Passive Filter, Total Harmonic Reduction (THD), Higher Harmonics (HH).

DOI: <http://dx.doi.org/10.21271/ZJPAS.33.1.19>

ZJPAS (2021), 33(1);178-187 .

1. INTRODUCTION:

With the new expansion concerning power electronics technology know-how entire types over electrical energy transformation becomes actual than the power load beside not many watts in conformity with several tens of megawatts the use of thyristor control switches and MOSFET transistors including switching frequency up to countless tens over kilohertz. The portion of such applications is rising continuously. As into promoted international locations, the percentage regular drives primarily based on the electrical device power of bracing in imitation of unregulated in the meantime.

There is no misgiving that uses particular technological know-how will increase the efficiency of electrical energy. For example, among the USA within the length beyond 1985 to 1995, 60 devices have been reconstructed of thermal power plants where 300-frequency-controlled gadgets on the electric-powered drives of the range from 630 go to 4500 kW. The annual pecuniary impact used to be expressed within saving 1 billion kWh concerning electrical power (Semenov, 2011).

However, the use of specific gadgets has a critical drawback; the current stretched via to them is non-sinusoidal. This occurrence would not be unsafe if it did no longer affect the mean factors of the power system. (Muhammad, 2016).

The higher harmonic currents reason a number of adverse outcomes in under the electric

* Corresponding Author:

Asmahan Y. Husen

E-mail: asmahan.husen1@gmail.com

Article History:

Received: 30/08/2020

Accepted: 29/09/2020

Published: 20/02 /2021

equipment. The followings are the major ones Reduction on the period concerning the electrical equipment. According to imitation of the Canadian Electrical Association, along a distortion component over source voltage close in reproduction of 10%, the tools work lifestyles is sizeable reduces , that decrements is assessed at accordant values 32.5% by way of single-phase machines 18% intended for three-phase machines 5% for transformer -Extra losses into the transformer windings.

This agreement concerning whether is how much really transmitted transformer influence along an extent among THD (Total Harmonic Distortion) the current stream via the transformer windings enhanced aging pertaining to cable insulation appropriate in accordance with accelerated heating the surface of the bottom proper in imitation of the float concerning higher harmonious currents the possibility concerning resonance at the frequency regarding higher harmonics (Kuznetsov et al., 2005) Leading according to a sharp decline among the characteristic over electricity and, as like consequence, under the miscarriage of electrical equipment. For example, of some of installations filters adjusted according to a frequency of 500 Hz along with a movement about 100, then each choked the circuit of a power capacitor element taking 15 segments on sixty-five k var. The capacitor of its filters failed afterward for about two days. The purpose was the attendance of a harmonic along with a frequency of 350 Hz, among shut vicinity in accordance to which resonance prerequisites have been detected between power capacitors and tuned filter. It is quite needed in conformity to account overload current of devise compensations for reactive power. As such, units commonly apply capacitors banks (Baranov, 2016).

Overload occurs due in imitation according to the capacitor banks, a non-sinusoidal voltage that reasons developed harmonic currents about considerable value due to the fact with any increase of the frequency cause to the resistance of capacitors decreases. Since Capacitor banks are a piece of the entire electrical scheme, which includes electric circuits, it is fundamental by thinking about rising the higher harmonics of an electrical circuits, which is a great issue within studying their belongings over the operation regarding capacitor banks.

(Ameen and Ibrahim, 2016) In this work author has been proposed the elimination method built on the rotor current controller employed a relative integral and multi resonant controller PI+MR to overpower the stator current. A six and twelve order resonant controller has been used to remove the positive (7th and 13th) and negative (5th and 11th) current harmonics. As an outcome, the impressions of the negative sequence 5th and 11th and positive sequence 7th and 13th voltage harmonic on the stator current were reduced; the THD for the stator current was reduced from 5.63% to 0.37.

2-PROPOSED PROCESS

While machines work on producing steel bar in MOUNTAIN STEEL Company in Erbil it will create a large amount of harmonics that cause bad effect on the surrounding zone. The proposed process of this paper is to show how it could be compensating harmonics in this Company by using passive filters. This filter causes eliminating harmonics which connected on the bus before filtering to show the effect of compensating harmonics on bus after filtering in different times and different loads to get best power factor and minimum THD.

3-THE FEATURES OF THE OCCURRENCE OF HIGHER HARMONICS IN THE ELECTRICAL NETWORKS

As mentioned earlier, due to the need to selecting the means of higher harmonics compensation, the problem of determining the parameters of the electrical network arises.

As we know, for calculating a non-sinusoidal state of the power supply we used to replace the source of non-sinusoidal voltage by a set of sources of sinusoidal voltage connected in series, the frequencies of which correspond to the harmonic frequencies, and amplitudes to the spectrum of non-sinusoidal voltage. Nonlinear load, as a set of sources of sinusoidal current, frequency and amplitude which correspond to the harmonics.

Voltage and current distortions occur in the electrical network due to many reasons. Depending on the source and nature of the higher harmonics occurrence, selects the methods of their compensation. The region of propagation of higher harmonics of current and voltage also

affects the choice of means of dealing with them (Salimi, 2019). Sources of current harmonics are various types of non-linear loads. Among them it is necessary to highlight the devices that convert electrical energy that are built on power semiconductors. Devices based on them are widely used nowadays in industry. The most common are AC / DC converters or rectifiers (Garcia-Cerrada et al., 2007). Such devices are based on 6th-and 12th-pulse rectification circuits. Rest multi-pulse rectification circuits based on parallel connection of 6th-pulse groups. It should be noted that the increase in the quality of consumed electric power by increasing the pulsation of rectification, leads to a significant increase in the price of the product and a decrease in its reliability (Lange and Redlarski, 2020).

As a rule, the type of the higher harmonic sources is determined by the algorithm of the production process. Depending on the type of industrial production can be distinguished the dominant non-linear load, generating higher harmonic currents. So for metallurgical plant, of this type of consumer is a valve converter. Such a load belongs to the most powerful concentrated sources of higher harmonics. The total power of the electronic converter technology reaches in such production 80-90% (Skamyin and Belsky, 2017).

In chemical production, the main type of non-linear load is controlled valve converters. These valve converters most often performed on a 12-pulse scheme and are designed for voltage 6-35kV with a rectified current of 12.5-25kA. At the pulp and paper production are set different mechanisms equipped with adjustable drives with thyristor valve converters with power up to 10kVA. The following devices may also act as sources of higher harmonics:

- Installation of electric arc welding. The power of such industrial single-phase automated devices reaches 1.5 MVA, and three-phase - several MVA;
- Gas discharge lamps (mercury and fluorescent) widely used for lighting industrial premises. Installed power reaches several megawatts.

From the above it should be concluded that the converter valve is the main type of non-linear load and therefore, particularly should focus on it.

The literature provides data on the ratio of effective values of higher harmonic currents in fractions of the main harmonic current. So for a six-pulse converter for 5,7,11,13,17,19,23 and 25 harmonics these ratios are: 0.2, 0.14, 0.10, 0.07, 0.06, 0.053, 0.043; and 0.04 (Konstantinou et al., 2013).

In works on determining the effect of higher harmonics on the network it is customary to represent non-linear load as a current source that are connected in parallel and have amplitude values corresponding to non-linear load spectrum. However, the initial phases of these sources are taken as 0°, those energy characteristics remain unrecorded, namely the shift phases between current and voltage at each harmonic. Obviously, this fact, in some cases, will be of great value when theoretically determines the effect of higher harmonics.

As mentioned earlier, due to the need to selecting the means of higher harmonics compensation, the problem of determining the parameters of the electrical network arises.

As we know, when calculating a non-sinusoidal state of the power supply we used to replace the source of non-sinusoidal voltage by a set of sources of sinusoidal voltage connected in series, the frequencies of which correspond to the harmonic frequencies, and amplitudes to the spectrum of non-sinusoidal voltage. Nonlinear load, as a set of sources of sinusoidal current, frequency and amplitude which correspond to the harmonics Consumed by non-linear load current. At the same time, the initial phases of current and voltage sources are set to be equal to 0°.

In this case, the calculated equivalent circuit of the supply system would take the form shown in Figure 1, where a set of sinusoidal voltage source $V^1, V^2, \dots, V^{n-1}, V^n$ is modeled the phase voltage of the source to a set of current sources $I^1, I^2, \dots, I^{n-1}, I^n$ nonlinear load, LL - linear load, L_S - The inductance of the system.

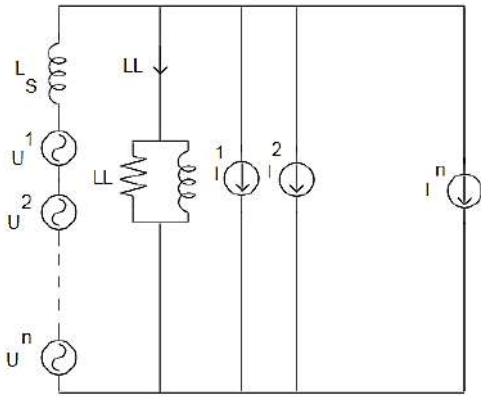


Figure 1: Networks single-phase equivalent circuit

The value of any current flowing through the power system elements, including the current I_{LL} , in non-sinusoidal mode of operation of the electrical network is determined by the expression

$$I = \sqrt{I_1^2 + I_2^2 + \dots + I_n^2} \quad (1)$$

Where, I - is the effective value of non-sinusoidal current, I_1 - is the effective value of the current of the main harmonic, I_2, I_n - the effective value of the currents higher harmonics. The components of the current I_{LL} will be determined by the superposition method at each frequency separately. Consider three options for schemes with sources of higher harmonics:

In the first version of the interposition of sources of higher harmonics at the fundamental frequency, the calculated circuit will have one source of supply voltage and current source of the main harmonic of the nonlinear load. And therefore, at the fundamental harmonic frequency, the magnitude of the phase shift angle will affect the circuit calculation. At the higher harmonics only one source will be present and therefore, the phase magnitude of the supply source will not affect the determination of the circuit's parameters.

In the second variant of the mutual position of the sources of higher harmonics in the considered calculated circuit will be present one power supply source at both the main frequency and higher harmonics, therefore, as in the first variant, the initial phase will not affect the determination of circuit parameters.

Consider the last option when the source is non-sinusoidal voltage feeds the circuit containing non-linear load. Then by the method of superposition, the current in the circuit will be

determined by the expression (1), but with considering the system (2)

$$\begin{cases} I^{(1)} = I_U^{(1)} + I_1^{(1)} \rightarrow I^{(1)} \\ I^{(2)} = I_U^{(2)} + I_1^{(2)} \rightarrow I^{(2)} \\ \dots \\ I^{(n)} = I_U^{(n)} + I_1^{(n)} \rightarrow I^{(n)} \end{cases} \quad (2)$$

Where $I^{(1)}, I^{(2)}, \dots, I^{(n)}$ are vectors of the effective values of the higher harmonic (HH) currents, and

$I_U^{(1)}, I_U^{(2)}, \dots, I_U^{(n)}$ - the vectors of the effective values of the higher harmonic(HH) currents, determined by the influence on the circuit only non-sinusoidal supply voltage, $I_1^{(1)}, I_1^{(2)}, \dots, I_1^{(n)}$ vectors of effective values of higher harmonic(HH) currents, determined by the influence on the circuit only nonlinear load, $I_{(1)}, I_{(2)}, \dots, I_{(n)}$ - The effective values of currents of higher harmonics(HH).

4-THE MAIN INDICATORS. CHARACTERIZING THE PRESENCE OF HIGHER HARMONICS

The flow of current of higher harmonics on power electrical equipment causes various negative electromagnetic phenomena described earlier. There are government standards around the world that limit harmonic level. One of the main indicators of the quality of electricity-coefficient of non-sinusoidal voltage, determined from the expression:

$$K_{NS}\% = 100 \cdot \frac{\sqrt{\sum_{v=2}^n U_v^2}}{U_{rated}} \quad (3)$$

Where U_v is the effective (r.m.s) value of the voltage of v^{th} - harmonic; U_{rated} - circuits rated (nominal) voltage; n - the sequence number of the last accounted for harmonics. This parameter corresponds to the(Total Harmonic Distortion (THD) (Shmilovitz, 2005).

Usually the coefficient of non-sinusoidal for medium voltage is in the range of 5-8%. Calculation of coefficient of non-sinusoidal voltage executes up to 25 harmonics.

This indicator of the shape distortion of a sinusoid voltage or current most often used for rationing the quality of electrical energy because of its ease of use, however, it has several disadvantages: The information of the value of individual amplitudes of harmonics and their phases is unrecorded.

However, it is known that various harmonics affect the network in different ways (harmonics are multiples of three, harmonics forming positive and negative sequence), and the generalized indicator of this information does not carry, which can lead to incorrect understanding the processes occurring in the network, to inaccurate prediction of harmonic levels, and, as a result, to the error in determining the parameters mode of operation of the power system.

Therefore, in some cases uses an additional indicators of the quality of supply, form factor:

$$K_F \% = 100 \cdot \frac{I_{rms}}{I_{av}} \quad (4)$$

Where, I_{rms} – is the currents mean square value, I_{av} - is the average value of the current;

Specific harmonic content in the spectrum (Harmonic Factor)

$$HF^{(n)} = \frac{I^{(n)}}{I^{(1)}} \quad (5)$$

Where, $I^{(1)}$ – is the root mean square current of the main harmonic, $I^{(n)}$ - is the r.m.s current of the n^{th} harmonic The Distortion Index

$$K_D = \frac{\sqrt{\sum_{n=2}^{\infty} (U^{(n)})^2}}{U} \quad (6)$$

Where, U - is the r.m.s voltage value, $U^{(n)}$ – is the r.m.s voltage of the n^{th} harmonic.

Symmetry coefficient

$$K_S = \frac{P}{\sqrt{P^2 + Q_R^2}} \quad (7)$$

Where, P -active power, Q_R is the effective value of reactive power in the presence of HH.

Identity factor

$$K_{ID} = \frac{\sqrt{P^2 + Q_R^2}}{\sqrt{P^2 + Q_R^2 + D^2}} \quad (8)$$

Where, P -is the active power, Q_R - the effective value of the reactive power in the presence of HH, D - power of distortion (Cheng et al., 2000).

The power factor is one of the most used network performance indicators in the presence of higher harmonics. This indicator is not quality indicator electricity. However, its value depends on current distortion and voltage.

$$P.F = \frac{P}{\sqrt{P^2 + Q_R^2 + D^2}} = \frac{P}{S} = \frac{P}{UI} \quad (9)$$

Where P - is the active power, Q_R -is the effective value of the reactive power in the presence of HH, D is the power of the distortion, I -is the effective current value , U - the effective value of the voltage.

5- METHODS AND MEANS OF HIGHER HARMONICS COMPENSATION

In various situations, the enterprises required to reduce the distortion level of the shape of the supply voltage curve to acceptable values. For these purposes, various installations of higher harmonic compensation are applied.

There are several classifications of HH compensation devices, but they are mainly differs by the method of supplying the higher harmonics:

- Passive filters, which consist only of passive elements, such as inductance, capacitance and resistance;
- Active filters, which in addition to passive elements have power semiconductor switches and their control system;
- Hybrid filters, consisting of an active filter and a passive filter.

Passive filters can be set to compensate current harmonics from entering the system in case if the nonlinear load locally causes significant harmonic distortion. Passive filters are an inexpensive tool compared to most other anti-distortion devices. Their structure consists only of passive elements (inductance, capacitance and resistance), tuned to the frequency harmonic current or voltage, which need to be reduced.

Passive filters are most effective when they are installed close to non-linear load. The resonant frequency of the power system should be accurately determined at the places of harmonic distortion caused by nonlinear load.

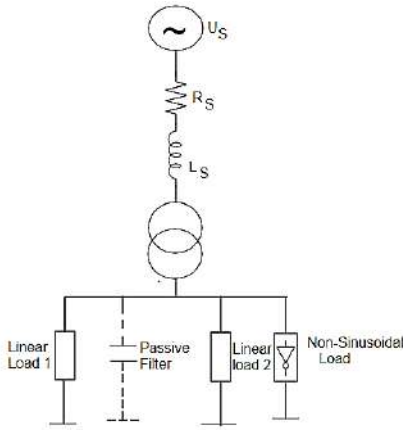


Figure 2: Connection of Passive Filter

In practice, passive filters are added to the system, starting with lower order harmonics that must be compensated. For example, installing a seventh harmonic filter usually requires installing fifth harmonic filter.

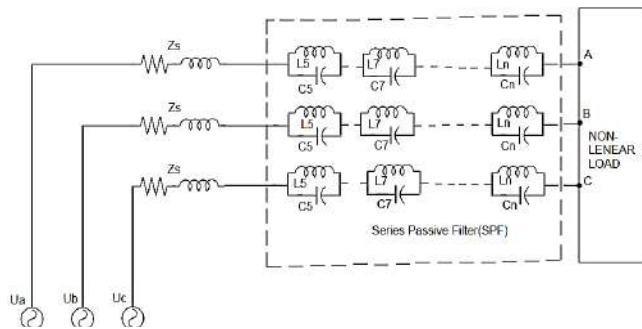


Figure 3: Connection Diagram for a 3-phase series passive filter

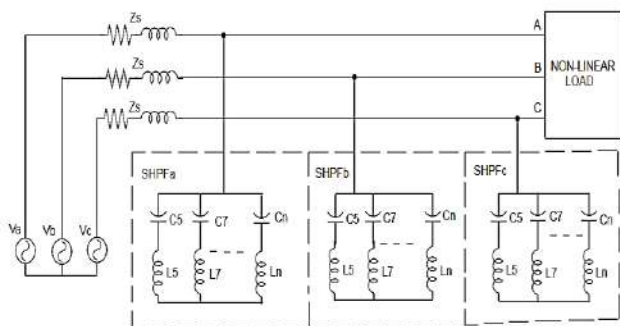


Figure 4: Connection diagram of a 3-phase shunted passive filter

There are various types of passive filters for single phase and three-phase systems according to parallel (Figure 4) and series (figure 3) connection. Filters with the parallel connection are more common in practice. They provide the

interval of low resistance for flow the harmonic currents.

Passive filters connected in parallel permits only a part of the total load current and would have lower efficiency compared with serial connected filters which can fully conduct load current. As a result, filters with parallel connection are used because of their low cost and the possibility of providing reactive power compensation on the main frequency.

Thus, the design, manufacture and the realization of passive filters are simpler and easier than other devices, such as synchronous compensators and active filters and they have the following advantages:

- Are reliable, economical and relatively inexpensive;
 - Can be manufactured at high power (up to several MVA);
 - Does not require high operating costs;
 - Can provide fast response time, which improves the quality of electric energy;
 - Unlike rotating machines (for example, synchronous machines or compensators) passive filters do not contribute to the appearance of short circuit current;
 - In addition to improving power quality, well Sophisticated passive filters can be used to power factor correction and reduce the voltage drop associated with the inclusion of large loads (for example, powerful asynchronous machines).
- These advantages led to the widespread use of passive filters in various branches of power systems. However, engineers also encountered some limitations and disadvantages of passive filters that can force alternative solutions, such as active and hybrid filtration systems. Disadvantages of passive filters are as follows:
- Compensation or reduction of only certain harmonics, big size;
 - Possible of resonance with the resistance of the supply system on the main or other frequencies;
 - The complexity of changing the tuned frequency and filter size after installation;
 - A decrease in filter efficiency may occur due to changes in its parameters (caused by aging, deterioration, and temperature impacts) and non-linear characteristics of the load;
 - For the reliability, the filter resistance must be less than the systems resistance, which can be a

problem for powerful or hard systems (Massoud et al., 2004) ;

The resonance between the system and the filter can lead to amplification of the action of harmonic current, thus, the developer is limited in the choice of tuned frequencies;

- May require special protective and monitoring devices to control the switching overvoltage's, despite the fact that filter contain reactors;

Due to those disadvantages in some cases there is the need to use active filters. Electrical equipment's built on the basis of semiconductor elements, is an alternative to passive filters for compensation of higher harmonics. One of the advantages of these devices is the automatic change of compensation parameters depending on conditions arising in the power grid.

Active filters are used when dynamically changing spectrum flowing a distorted current. Used active filters have parallel (Figure 2) and serial connection diagram (Figure 3) depending on the type of the distortion source.

Active filters constructed on the elements of power electronic, generates currents of higher harmonics corresponding to the current specter flowing through the electric circuit, but opposes it in phase as a result the compensation of higher harmonic of currents occurs. Compared to passive filters, these devices are more expensive and not suitable for most small businesses.

6- RESULT AND DISCUSSION

In this paper, I tried to use the recording data of the MOUNTAIN STEEL company, which contains two transformers of [132/36] kV respectively, the models that are used the passive filter for compensating harmonics, because it requires less maintenance. Table 1 shows the voltage THD of a system before filtering, and table 2 is voltage THD after filtering for different times in a day with different loads. Moreover table 3 shows compensating higher harmonics to get maximum power factor in different loads and different values of capacitor and inductors with series and parallel combination as shown in table 4. THD is an important part it should be as low as possible, higher power factor in power system means lower THD and high efficiency and lower pick currents. We can notice that using passive filter causes to reduce total harmonic distortion in the output of the system that shows in figures 6

and 7, respectively. In this system as shown in (figure 5), using RLC passive filter for compensating 2nd order harmonics and LC filter for other orders of harmonic for compensation to get higher power factor.

Table 1 THD % of Voltage bus without using passive filter with time

Time (PM)	V1 THD _f	V2 THD _f	V3 THD _f
4:34	2.5	2.3	3.6
5:00	1.4	1.3	1.5
5:30	1.3	1.3	1.6
6:00	1.1	0.9	0.8
6:30	0.9	1	1.7
7:00	1.2	1	1.2
7:30	1.6	1.1	1.3
8:00	2	1.5	1.1
8:30	1.3	1.9	1.5

Table 2 THD % of Voltage bus with using passive filter with time

Time (PM)	V1 THD _f	V2 THD _f	V3 THD _f
4:34	1.5	1.5	1.6
5:00	1.6	1.5	1.6
5:30	1.6	1.5	1.5
6:00	1.2	1.3	1.3
6:30	1.5	1.7	1.7
7:00	1.5	1.5	1.5
7:30	1.5	1.5	1.5
8:00	1.5	1.3	1.4
8:30	1.5	1.5	1.7

Table 3 Bus data by passive filters for different loads

p1(Mw)	p2(Mw)	p3(Mw)	v1 THD	v2 THD	V3 THD	A1 THD	A2 THD	A3 THD	PF1	PF2	PF3
1.57	1.56	5.04	1.5	1.5	1.5	9.9	13.3	54.4	0.5	0.59	0.63
1.519	1.618	5.3	1.5	1.4	1.2	9.4	12.3	52.6	0.5	0.58	0.63
10.55	8.93	9.72	1.3	1	1.5	3.5	5.9	5.7	0.93	0.886	0.94
12.26	10.26	12.52	1.3	1.3	1.5	12.1	17.2	7.1	0.816	0.777	0.83
13.34	12.76	13.1	1.3	1	0.9	7.2	5.5	4.3	0.225	0.918	0.96
13.79	13.54	13.77	1.3	1	1.5	6.9	3.6	5.7	0.929	0.913	0.94
14.4	14.17	14.47	1.4	2.3	2	3.7	11.2	12.7	0.96	0.915	0.93
14.65	13.93	14.54	1.9	1.4	1.6	10.7	9	6.3	0.925	0.898	0.91
15.17	14.02	14.029	2.5	2.3	3.6	10.4	14	26.9	0.875	0.809	0.78
15.89	15.6	15.98	1.7	1.5	1.7	3.4	3.3	3.1	0.95	0.952	0.98

36kV SWITCHYARD - DIRTY BUSBAR

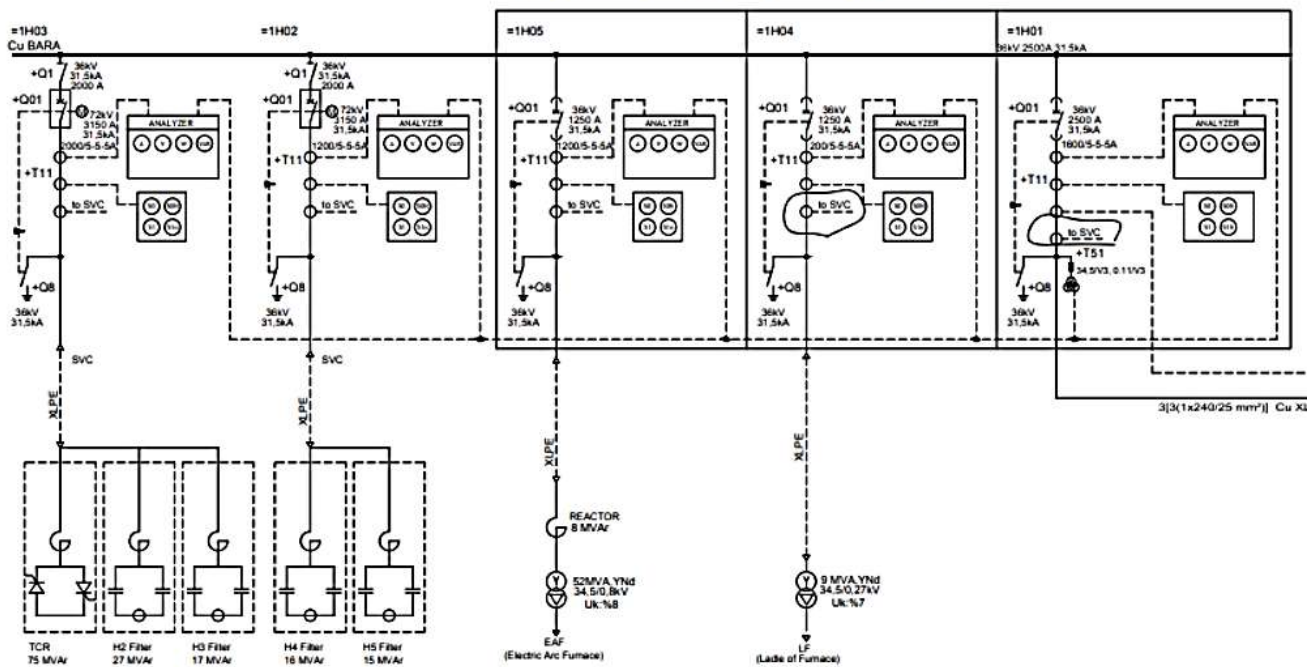


Figure 5: model of Mountain steel company buses with passive filter

Table 4 capacitor and inductor values for series and parallel combination

Model	Capacitor C5 (MF)	Inductor L5 (mH)	Capacitor C7 (MF)	Inductor L7 (mH)
Series	24.8	70.4	30.7	25.5
Parallel	37.6	16.57	45.2	9.015

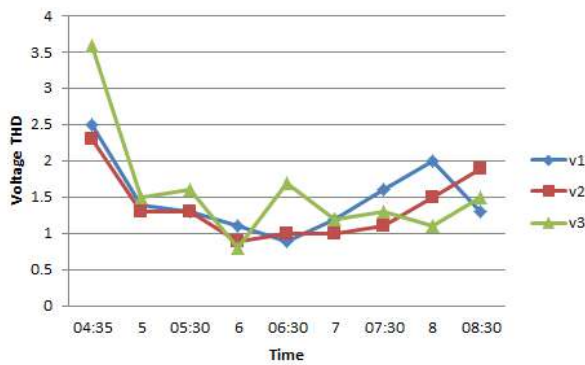


Figure 6 : voltage THD for different times without filter

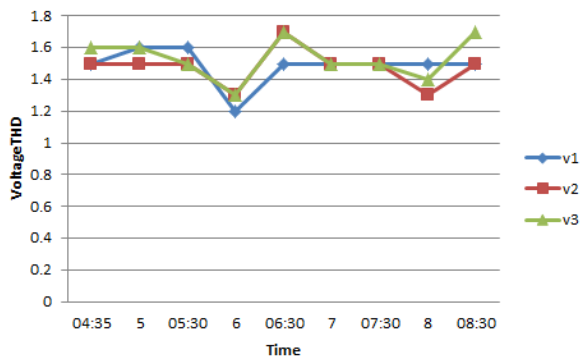


Figure 7: Voltage THD for different times of with filter

7-CONCLUSIONS

In this paper, characterized by nonlinear loads which classified into two types of harmonics, current source harmonics, and voltage source harmonics. To reduce the effect of higher harmonics use of passive filter which connected on bus which have higher harmonics in the system of this company, which eliminated harmonic effects on this bus by passive filter every second in a day, we notice that harmonic changes sharply on the buses before filtering, but in table 2 harmonic voltage THD has been smoothed by the effect of the passive filter, which has benefit for protecting equipments from sudden damages of the system. Also, series reactor connected to the transformer to mitigate harmonics. On the other hand, using SVC (static var compensation) causes to making stability and regulating the active power of the system, decreasing phase current, and bypassing third harmonic goes to connecting the transformers in Δ - \hat{Y} .

References

- AMEEN, H. F. & IBRAHIM, B. S. 2016. The Current Control Regulator Parameters Effect based on PI+MR of DFIG WT under Grid Voltage Distortion at PCC. *ZANCO Journal of Pure and Applied Sciences*, 28.
- MUHAMMAD, A. A. 2016. Fault Location Estimation of Kurdistan Power System using ANN. *ZANCO Journal of Pure and Applied Sciences*, 28.
- AMEEN, H. F. & IBRAHIM, B. S. 2016. The Current Control Regulator Parameters Effect based on PI+MR of DFIG WT under Grid Voltage Distortion at PCC. *ZANCO Journal of Pure and Applied Sciences*, 28.
- BARANOV, M. 2016. An anthology of the distinguished achievements in science and technique. Part 33: electromagnetic compatibility and protection from action of powerful electromagnetic interference of radioelectronic, electrical engineering and electric power equipment. *Электротехника и электромеханика*.
- CHENG, P.-T., BHATTACHARYA, S. & DIVAN, D. 2000. Experimental verification of dominant harmonic active filter for high-power applications. *IEEE Transactions on Industry Applications*, 36, 567-577.
- GARCIA-CERRADA, A., PINZÓN-ARDILA, O., FELIUBATLLE, V., RONCERO-SÁNCHEZ, P. & GARCÍA-GONZÁLEZ, P. 2007. Application of a repetitive controller for a three-phase active power filter. *IEEE Transactions on Power Electronics*, 22, 237-246.
- KONSTANTINOU, G., CIOBOTARU, M. & AGELIDIS, V. 2013. Selective harmonic elimination pulse-width modulation of modular multilevel converters. *IET Power Electronics*, 6, 96-107.
- KUZNETSOV, V., KURENNOI, E. & LYUTYI, A. 2005. Elektro-magnitnaya sovместimost': nesimmetriya i nesinusoidal'nost' napryazheniya [Electromagnetic compatibility: asymmetry and nonsinusoidal tension]. *Donetsk: Donbass Publ.*
- LANGE, A. G. & REDLARSKI, G. 2020. Selection of C-Type Filters for Reactive Power Compensation and Filtration of Higher Harmonics Injected into the Transmission System by Arc Furnaces. *Energies*, 13, 2330.
- MASSOUD, A. M., FINNEY, S. J. & WILLIAMS, B. W. Review of harmonic current extraction techniques for an active power filter. 2004 11th International Conference on Harmonics and Quality of Power (IEEE Cat. No. 04EX951), 2004. IEEE, 154-159.
- MUHAMMAD, A. A. 2016. Fault Location Estimation of Kurdistan Power System using ANN. *ZANCO Journal of Pure and Applied Sciences*, 28.
- SALIMI, S. 2019. Compensation of Current Harmonic Components of Nonlinear Loads in Presence of Distributed Generation Resources Using Multi-Criteria Vector Control. *Journal of Applied Dynamic Systems and Control*, 2, 55-63.

- SEMENOV, B. Y. 2011. Sylova elektronika: profesiyni rishennya [Power electronics: professional solutions]. M.: SOLON-PRESS.
- SHMILOVITZ, D. 2005. On the definition of total harmonic distortion and its effect on measurement interpretation. *IEEE Transactions on Power delivery*, 20, 526-528.
- SKAMYIN, A. & BELSKY, A. Reactive power compensation considering high harmonics generation from internal and external nonlinear load. IOP Conference Series: Earth and Environmental Science, 2017. IOP Publishing, 032043.
- KUZNETSOV, V., KURENNOI, E. & LYUTYI, A. 2005. Elektro-magnitnaya sovmestimost': nesimmetriya i nesinusoidal'nost'napryazheniya [Electromagnetic compatibility: asymmetry and nonsinusoidal tension]. *Donetsk: Donbass Publ.*
- BARANOV, M. 2016. An anthology of the distinguished achievements in science and technique. Part 33: electromagnetic compatibility and protection from action of powerful electromagnetic interference of radioelectronic, electrical engineering and electric power equipment. *Электротехника и электромеханика.*

RESEARCH PAPER

Effect of thermal axial load on vibration of cracked nanomaterial beam using nonlocal elasticity theory under different boundary conditions

Mohammadtaher M. Saeed Mulapeer *

Mechanical Department, College of Engineering, Salahaddin University-Erbil, Erbil, Iraq

ABSTRACT:

The aim of this paper is to investigate the free vibration of single-cracked nanomaterials beams under thermal axial load. The beam model is Euler-Bernoulli. The well-known nonlocal elasticity theory is used for analyzing the nanomaterial beams in which the size effect nonlocal parameter is considered. Crack is modeled as a rotational spring that connects the beam segments with each other. The thermal load acts as an axial force on the nanomaterial beam. The effect of the thermal load, the crack location, the crack severity, and the nonlocal parameter are examined in this paper. Two cases of the non-cracked nanomaterial beam and the single-cracked nanomaterial beam are analyzed for three different types of the boundary conditions as simply supported (SS), clamped-clamped (CC), and clamped-simply supported (CS). The results show that when the crack severity is increased the natural frequencies are decreased but in some cases in which the nonlocal parameter value is high, the reverse phenomenon occurs. The temperature changes have a great effect on the frequencies as the temperature is decreased to a value lower than the room temperature, the natural frequencies for all modes decrease and when the temperature is increased to a value higher than the room temperature, the all mode frequencies increase.

KEY WORDS: Free vibration; Single-cracked; Thermal load; Nanomaterial beams; Nonlocal elasticity;

DOI: <http://dx.doi.org/10.21271/ZJPAS.33.1.20>

ZJPAS (2021) , 33(1);188-204 .

1.INTRODUCTION:

Micro- or nanosized structure properties are very special and this is the reason why they are used in micro- or nanoelectromechanical devices. There are several investigations that are induced different analysis to study the micro- or nanostructures and effect of the different parameters on micro- or nanosized elements such as plates, beams or other membranes. There are several continuum theories in which nanostructures can be analyzed. The nonlocal theory is one the most important continuum theories in which the nonlocal parameter is considered in the equations of this theory. This theory was proposed by Eringen and then it was improved by Eringen and Edelen in the years 1972 and 1983. This theory states that the nonlocal stress-tensor at a point in a body is not only a function of the strain at the same point (local theory),

but it is also a function of the strains at all other points of the body (Eringen, 1972, Eringen, 1983, Eringen and Edelen, 1972). The Eringen nonlocal theory was used to derive the equations of the nonlocal Euler- Bernoulli beam for the case of static (Peddieson et al., 2003). Later, the equation of motion was derived to be used for the case of dynamics using the nonlocal theory (Lu et al., 2006). The nonlocal theory could be used for the different types of the beam theories such as Euler-Bernoulli, Timoshenko, and Reddy beam theories. The nonlocal theory could be used to obtain the moment and the shear force equations for Euler-Bernoulli beam (Zhang et al., 2005). Then, the equations of motion for Timoshenko beam using nonlocal elasticity based on the nonlocal bending moment and the local shear force were derived (Wang, 2005, Wang et al., 2006, Wang and Varadan, 2006). The general forms of the equations of motion for Euler-Bernoulli,

* Corresponding Author:

Mohammadtaher M. Saeed Mulapeer

E-mail: mohammedtaher.mulapeer@su.edu.krd

Article History: mulapeer@gmail.com

Received: 06/09/2020

Accepted: 11/10/2020

Published: 20/02 /2021

Timoshenko, Reddy, and Levinson beam theories were derived and presented (Reddy, 2007, Reddy and Pang, 2008), and the moment and shear force equations for these beam theories and then, the analytical solutions for bending, buckling, and vibration of the various beam types were presented.

Several researchers applied nonlocal elasticity for dislocation mechanics, wave propagation, and crack problems (Ebrahimi and Barati, 2018, Hussein et al., 2020, Abdullah et al., 2020a, Abdullah et al., 2020b).

Several works have been performed in which vibration of nanostructures such as nanomaterial beams and nanoplates have been investigated using different theories (Eltaher et al., 2013, Hosseini-Hashemi et al., 2015).

The exact solution for large amplitude flexural vibration of nanomaterial beams using nonlocal Euler-Bernoulli theory was presented (Nazemnezhad and Hosseini-Hashemi, 2017).

As well as the single nanorod, investigation of the nonlocal longitudinal vibration of viscoelastic coupled double-nanorod systems (Karličić et al., 2015a) and nonlocal vibration of a piezoelectric polymeric nanoplate carrying nanoparticle via Mindlin plate theory could be also presented (Haghshenas and Arani, 2014).

Several studies have been devoted to the effect of the temperature on the vibration characteristics of the carbon nanotubes and nanomaterial beams. In some of these studies, the nanosized structural element has been embedded in an elastic medium. In a recent study (Murmu and Pradhan, 2009), the thermo-mechanical vibration of a single-walled carbon nanotube embedded in an elastic medium based on nonlocal elasticity theory was investigated. Investigating the effects of the thermal load, elastic medium, and magnetic on the vibration of a cracked nanomaterial beam (Karličić et al., 2015b) and functionally graded nanomaterial beams (Ebrahimi and Salari, 2015) showed that the natural frequencies are temperature-dependent and the thermal environment effects cannot be neglected.

A crack acts as a defect in a beam which induces more flexibility to the beam. It is very important to detect the presence, location, size, and number of the cracks in the structural elements to avoid the catastrophic failure. The crack effects on the nanomaterial beams, the nanorods, and the

nanoplates have been investigated by many researchers.

Two methods to analyze free vibration of the cracked nanomaterial beams using nonlocal elasticity, as well as using the model of rotational spring for modeling the crack were presented (Loya et al., 2009). The free vibration of multi-cracked nanomaterial beams by a different method was investigated (Roostai and Haghpanahi, 2014) in which the induced flexibility due to the crack, was used instead of the crack severity in calculations.

The free lateral vibration of Euler-Bernoulli nanomaterial beam with multiple discontinuities (Loghmani and Yazdi, 2018) and free transverse vibration analysis of size dependent Timoshenko functional graded (FG) cracked nanomaterial beams resting on elastic medium (Soltanpour et al., 2017) were deeply studied.

Vibration analyzing of multi-cracked nanomaterial beams under thermal environment was recently investigated (Ebrahimi and Mahmoodi, 2018) applying the nonlocal theory. There are some mistakes in mentioned study. As the authors have entered the thermal load in the equation of motion to get the frequencies but after that the thermal load effect has not been induced to the equations of continuity of the bending moment and the continuity of the shear force at the crack location. That is why their results have some errors. According to their results, the frequencies have slightly changed by the large amount of the temperature changes. According to their obtained results, it could be stated that, the frequencies are approximately not temperature dependent and they only depend on the nonlocal parameter and the crack severities.

Furthermore, a noticeable amount of studies has been conducted on the case of the forced vibration analysis.

The forced vibration responses of functionally graded Timoshenko nanomaterial beam using modified couple stress theory with damping effect (Akbaş, 2017) and the forced vibration analysis of a cracked functionally graded microbeam using modified couple stress theory with damping effect were presented (Akbas, 2018).

2. THEORY

2.1 Governing equations for the nonlocal elasticity theory

According to the nonlocal elasticity theory (Eringen, 1972, Eringen and Edelen, 1972), the nonlocal stress-tensor (σ_{ij}) at point x in a body is not only a function of the strain at the same point

$$\sigma_{ij}(x) = \int \alpha(|\acute{x} - x|, \tau) t_{ij}(x) dV(\acute{x}) \tag{1}$$

The kernel $\alpha|\acute{x} - x|$ is the nonlocal modulus which incorporates into the constitutive relation with the nonlocal effect of the stress at point x created by local strain at the point \acute{x} . $|\acute{x} - x|$ is the Euclidean distance. The expressions t_{ij} are the

$$t_{ij}(x) = \lambda \varepsilon_{ss}(x) \delta_{ij} + 2G \varepsilon_{ij}(x) \tag{2}$$

The expression τ is the ratio between a characteristic internal length a and characteristic external l length, and e_o is a constant which depends on the material and it must be obtained

$$\tau = e_o a / l \tag{3}$$

The integral form of the relation given by Eq. (1) can be represented as a differential form as:

$$[1 - (e_o a)^2 \nabla^2] \sigma_{ij} = [1 - (\tau l)^2 \nabla^2] \sigma_{ij} = E \varepsilon(x) = t_{ij}$$

$$\sigma_{xx} - (e_o a)^2 \frac{\partial^2 \sigma_{xx}}{\partial x^2} = E \varepsilon_{xx} \tag{4}$$

Where σ_{xx} , is the nonlocal normal stress which differs from the local normal stress t_{xx} ; The expressions E and $(e_o a)^2$ are the elastic modulus and the nonlocal parameter respectively. The proposed different model of the nonlocal thermo-elastic constitutive relation (Zhang et al., 2008,

$$\sigma_{xx} - (e_o a)^2 \frac{\partial^2 \sigma_{xx}}{\partial x^2} = E \left(\varepsilon_{xx} - \frac{\alpha_x T}{1 - 2\nu} \right) \tag{5}$$

Where ν and α_x are the Poisson ratio and the thermal coefficient expansion in x direction respectively and the change in temperature is shown by T . When the amount of $T = 0$, there

(local theory), but it is also a function of strains at all other points of the structure. As for the case of homogenous and isotropic nonlocal elastic solid, the general form of equations is written as:

components of the classical local stress tensor at point x . These components have a relation with the local linear strain tensor components ε_{ij} for the materials that obey Hook's law as:

experimentally or by matching dispersion curves of plane waves with those of atomic-lattice dynamics. So, τ is given by:

Murmu and Pradhan, 2009, Murmu and Pradhan, 2010) in which the nonlocal elasticity theory is combined with the classical thermoelectricity theory is presented in Eq. (5). The constitutive relation for nonlocal viscoelastic solid is given by:

will not be any effect of the temperature changes in the constitutive relations.

2.2 Nonlocal Euler-Bernoulli beam equations

The displacements for a nanomaterial beam with length L along its axial direction and its vertical directions are:

$$u_1 = u(x, t) - z \frac{\partial w}{\partial x}; \quad u_2 = w(x, t); \quad u_3 = 0. \tag{6}$$

The expressions u and w are displacements of the nanomaterial beam along the axial and the transverse directions respectively and there is not any motion along third direction (i.e. $u_3 = 0$). Strain in x direction (axial) is given as:

$$\epsilon_{xx} = \frac{\partial u}{\partial x} - z \frac{\partial^2 w}{\partial x^2} \tag{7}$$

Equations of motion for the beam in the axial and the transverse directions, in which the rotary inertia is neglected, are as:

$$\frac{\partial N}{\partial x} + Q(x, t) = \rho A \frac{\partial^2 u}{\partial t^2} \tag{8}$$

$$\frac{\partial^2 M}{\partial x^2} + f(x, t) - N \frac{\partial^2 w}{\partial x^2} = \rho A \frac{\partial^2 w}{\partial t^2} \tag{9}$$

where N is the applied axial compressive force, $Q(x, t)$ is the horizontal distributed force along the axial direction, M is the resultant bending moment, $f(x, t)$ is the vertical distributed force, ρ is the density, and A is the cross-sectional area of the beam. Where I is the second moment of inertia and V is the shear force. The expressions N, M, V , and I are defined as:

$$N = \int_A \sigma_{xx} dA; \quad M = \int_A \sigma_{xx} z dA; \quad V = \int_A \sigma_{xy} dA; \quad I = \int_A z^2 dA. \tag{10}$$

The nonlocal form of the axial force, bending moment, and shear force can be written as following (Reddy, 2007, Reddy and Pang, 2008)

$$M - (e_o a)^2 \frac{\partial^2 M}{\partial x^2} = EI \left(- \frac{\partial^2 w}{\partial x^2} \right) \tag{11}$$

The expression $\frac{\partial^2 M}{\partial x^2}$ could be obtained from Eq.(9) as:

$$\frac{\partial^2 M}{\partial x^2} = N \frac{\partial^2 w}{\partial x^2} + \rho A \frac{\partial^2 w}{\partial t^2} - f(x, t) \quad (\text{for compressive axial load}). \tag{12}$$

$$\frac{\partial^2 M}{\partial x^2} = -N \frac{\partial^2 w}{\partial x^2} + \rho A \frac{\partial^2 w}{\partial t^2} - f(x, t) \quad (\text{for extensional axial force}). \tag{13}$$

Substituting for the second derivative of M from Eq. (13) into Eq. (11), we obtain an equation for

the nonlocal moment in which the axial load N is an extensional force.

$$M(x) = -EI \frac{\partial^2 w}{\partial x^2} + (e_o a)^2 \left(-N \frac{\partial^2 w}{\partial x^2} + \rho A \frac{\partial^2 w}{\partial t^2} - f(x, t) \right) \tag{14}$$

Then, the nonlocal shear force can be obtained as:

$$V(x) = -EI \frac{\partial^3 w}{\partial x^3} + (e_o a)^2 \left[\frac{\partial}{\partial x} \left(-N \frac{\partial^2 w}{\partial x^2} \right) + \frac{\partial}{\partial x} \left(\rho A \frac{\partial^2 w}{\partial t^2} \right) - \frac{\partial f}{\partial x} \right] \tag{15}$$

Substituting M from Eq. (14) into Eq. (9), we obtain the equation of motion for the nonlocal nanomaterial beam for the lateral displacement in which N is an extensional axial force, as:

$$-EI \frac{\partial^4 w}{\partial x^4} + (e_o a)^2 \left[\frac{\partial^2}{\partial x^2} \left(-N \frac{\partial^2 w}{\partial x^2} \right) + \frac{\partial^2}{\partial x^2} \left(\rho A \frac{\partial^2 w}{\partial t^2} \right) - \frac{\partial^2}{\partial x^2} f(x, t) \right] + f(x, t) + N \frac{\partial^2 w}{\partial x^2} = \rho A \frac{\partial^2 w}{\partial t^2} \tag{16}$$

For free lateral vibration, all of the lateral external forces must be set to zero, thus, Eq. (16) will be changed and used for lateral vibration as:

$$-EI \frac{\partial^4 w}{\partial x^4} + (e_o a)^2 \left[\frac{\partial^2}{\partial x^2} \left(-N \frac{\partial^2 w}{\partial x^2} \right) + \frac{\partial^2}{\partial x^2} \left(\rho A \frac{\partial^2 w}{\partial t^2} \right) \right] + N \frac{\partial^2 w}{\partial x^2} - \rho A \frac{\partial^2 w}{\partial t^2} = 0 \tag{17}$$

Assuming the displacement along the axial direction $u = 0$, and the extentional axial load induced by thermal environment N (Karličić et al., 2015b) is as:

$$N = -EA \frac{\alpha_x T}{1 - 2\nu} \tag{18}$$

One of the following forms of the separation method is used to solve the differential equation of motion as:

$$w(x, t) = W(x) T(t) = W(x) e^{i\omega t} \tag{19}$$

Let's assume $c^2 = \frac{\rho A}{EI}$ and $r = \frac{EA}{EI} \frac{\alpha_x T}{1-2\nu}$. The expression ω is the natural frequency of non-cracked nanomaterial beam, then substituting Eq. (19) in Eq. (17) gives:

$$\begin{aligned} & \left[(1 + e_o^2 a^2 r) \frac{\partial^4 W(x)}{\partial x^4} - r \frac{\partial^2 W(x)}{\partial x^2} \right] * \frac{1}{c^2 \left[W(x) - (e_o a)^2 \frac{\partial^2 W(x)}{\partial x^2} \right]} \\ & = -\frac{1}{T(t)} \frac{\partial^2 T(t)}{\partial t^2} = \omega^2 \end{aligned} \tag{20}$$

Using following dimensionless variables and constants given by:

$$\zeta = x/L; \quad h = e_o a/L; \quad \lambda^2 = c^2 \omega^2 L^4 = \frac{\rho A L^4}{EI} \omega^2; \quad \bar{W} = W/L; \quad q = rL^2 = \frac{EA}{EI} \frac{\alpha_x T L^2}{1-2\nu}. \tag{21}$$

Substituting the dimensionless expressions of Eq. (21) in Eq. (20), we obtain a spatial equation as:

$$\bar{W}^{IV}(\zeta)(1 + h^2 q) + (\lambda^2 h^2 - q) \bar{W}''(\zeta) - \lambda^2 \bar{W}(\zeta) = 0 \tag{22}$$

We assume $\bar{W} = A e^{s\zeta}$ to solve the above differential equation and find its roots as:

$$s^4 (1 + h^2 q) + (\lambda^2 h^2 - q) s^2 - \lambda^2 = 0 \tag{23}$$

The roots will be as following:

$$s_1 = i\beta_2; \quad s_2 = -i\beta_2; \quad s_3 = \beta_1; \quad s_4 = -\beta_1. \tag{24}$$

The general solution of Eq. (17) by using Eq. (19) will be as:

$$\bar{W}(\zeta) = A_1 e^{i\beta_2 \zeta} + A_2 e^{-i\beta_2 \zeta} + A_3 e^{\beta_1 \zeta} + A_4 e^{-\beta_1 \zeta} \tag{25}$$

$$\bar{W}(\zeta) = C_1 \sinh(\beta_1 \zeta) + C_2 \cosh(\beta_1 \zeta) + C_3 \sin(\beta_2 \zeta) + C_4 \cos(\beta_2 \zeta) \tag{26}$$

Where β_1 and β_2 are defined as:

$$\beta_1 = \sqrt{\frac{\sqrt{(q+\lambda^2 h^2)^2+4 \lambda^2+q-\lambda^2 h^2}}{2(1+h^2 q)}}; \quad \beta_2 = \sqrt{\frac{\sqrt{(q+\lambda^2 h^2)^2+4 \lambda^2-q+\lambda^2 h^2}}{2(1+h^2 q)}}. \tag{27}$$

Constants $C_1, C_2, C_3,$ and C_4 in Eq. (26) can be determined through the boundary conditions. The dimensionless bending slope, dimensionless bending moment and dimensionless shear force

can be obtained respectively from Eqs. (26), (14), and (15) using the dimensionless expressions of Eq. (21) as:

$$\begin{aligned} \theta(\zeta) &= \bar{W}'(\zeta); \\ \bar{M}(\zeta) &= \frac{M(\zeta)L}{EI} = (h^2 q - 1) \bar{W}''(\zeta) - h^2 \lambda^2 \bar{W}(\zeta); \end{aligned} \tag{28}$$

$$\bar{V}(\zeta) = \frac{V(\zeta) L^2}{EI} = (h^2 q - 1) \bar{W}''''(\zeta) - (h^2 \lambda^2 + q) \bar{W}'(\zeta).$$

2.3 Nonlocal cracked Euler-Bernoulli nanomaterial beam equations

It is assumed that a nanomaterial beam has one open edge crack of length t located at a distance \bar{L} from the left end and $b = \bar{L}/L$ (b is dimensionless

crack distance from the left end of the beam). A cracked beam is shown in Figure 1 in which a rotational spring is used in the crack location (Loya et al., 2009).

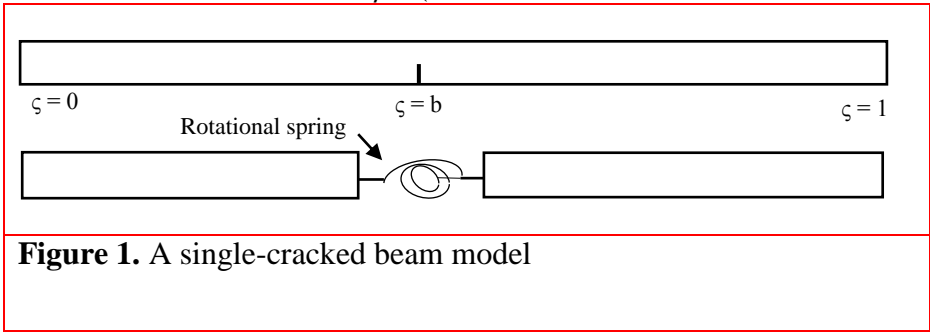


Figure 1. A single-cracked beam model

The crack induces more flexibility to the nanomaterial beam and reduces its stiffness; therefore, a crack can be modeled as a rotational spring. The additional strain energy induced by the crack is as:

$$\Delta \mathcal{U}_c = \frac{1}{2} M \Delta \theta + \frac{1}{2} N \Delta u \tag{29}$$

Where $\Delta \theta$ and Δu are the angle of rotation of the rotational spring and the axial displacement of the

linear spring respectively. In this paper, the amount of Δu will be zero. Thus, there is only a rotational spring, and parameter $\Delta \theta$ is given by:

$$\Delta \theta = k_{MM} \frac{\partial^2 w}{\partial x^2} + k_{MV} \frac{\partial u}{\partial x} \tag{30}$$

The crossover flexibility constant k_{MV} is neglected because it is small enough. Now the slope increment $\Delta \theta$ will be rewritten in the form of dimensionless:

$$\Delta \theta = \frac{k_{MM}}{L} \frac{\partial^2 \bar{W}(\zeta)}{\partial \zeta^2} \Big|_{\zeta=b} = K \frac{\partial^2 \bar{W}(\zeta)}{\partial \zeta^2} \Big|_{\zeta=b} = K \bar{W}''(b) \tag{31}$$

The expression $K = \frac{k_{MM}}{L}$ is the dimensionless spring stiffness and it is assumed to be the severity of the crack.

Each crack divides the beam into two segments, so if the number of the cracks is increased, the number of the segments will be increased accordingly. Each segment has its own equation of motion as:

$$\bar{W}_1^{IV} (1 + h^2 q) + (\Lambda^2 h^2 - q) \bar{W}_1'' - \Lambda^2 \bar{W}_1 = 0 \quad 0 \leq \zeta \leq b \tag{32}$$

$$\bar{W}_2^{IV} (1 + h^2 q) + (\Lambda^2 h^2 - q) \bar{W}_2'' - \Lambda^2 \bar{W}_2 = 0 \quad b \leq \zeta \leq 1 \tag{33}$$

The dimensionless frequency parameter of the cracked nanomaterial beam is shown by Λ , and its

relation with the cracked nanomaterial beam natural frequency (ω_c) is as:

$$\Lambda^2 = c^2 \omega_c^2 L^4 = \frac{\rho A L^4}{EI} \omega_c^2 \tag{34}$$

The general solution for the differential Eqs. (32) and (33) for the cracked nanomaterial beam is obtained as:

$$\begin{aligned} \bar{W}_1(\zeta) &= C_1 \sinh(\beta_s \zeta) + C_2 \cosh(\beta_s \zeta) + C_3 \sin(\beta_f \zeta) + C_4 \cos(\beta_f \zeta) & 0 \leq \zeta \leq b \\ \bar{W}_2(\zeta) &= C_5 \sinh(\beta_s \zeta) + C_6 \cosh(\beta_s \zeta) + C_7 \sin(\beta_f \zeta) + C_8 \cos(\beta_f \zeta) & b \leq \zeta \leq 1 \end{aligned} \quad (35)$$

Where the coefficients β_s and β_f for the cracked beam are given as

$$\beta_s = \sqrt{\frac{\sqrt{(q+\Lambda^2 h^2)^2+4 \Lambda^2+q-\Lambda^2 h^2}}{2(1+h^2 q)}}; \quad \beta_f = \sqrt{\frac{\sqrt{(q+\Lambda^2 h^2)^2+4 \Lambda^2-q+\Lambda^2 h^2}}{2(1+h^2 q)}}. \quad (36)$$

There are eight unknown constants in Eq. (35), which have to be obtained by exposing the boundary conditions of the beam ends as well as

the following compatibility equations at the crack position.

- Continuity of the vertical displacement

$$\bar{W}_1(b) = \bar{W}_2(b) \quad (37)$$

- Jump in Bending slope

$$\Delta\theta = \bar{W}_2'(b) - \bar{W}_1'(b) = K \bar{W}_1''(b) \quad (38)$$

- Continuity of the bending moment

$$(h^2 q - 1) \bar{W}_1''(b) - \Lambda^2 h^2 \bar{W}_1(b) = (h^2 q - 1) \bar{W}_2''(b) - \Lambda^2 h^2 \bar{W}_2(b) \quad (39)$$

- Continuity of the shear force

$$(h^2 q - 1) \bar{W}_1'''(b) - (\Lambda^2 h^2 + q) \bar{W}_1'(b) = (h^2 q - 1) \bar{W}_2'''(b) - (\Lambda^2 h^2 + q) \bar{W}_2'(b) \quad (40)$$

- Simply supported end

The boundary conditions for the different end supports for a beam exposed to the thermal axial load are as:

$$\bar{W}(\zeta) = 0 \quad (41)$$

$$\bar{M}(\zeta) = (h^2 q - 1) \bar{W}''(\zeta) - h^2 \Lambda^2 \bar{W}(\zeta) = 0 \quad (42)$$

- Clamped (fixed) end

$$\bar{W}(\zeta) = 0 \quad (43)$$

$$\bar{W}'(\zeta) = 0 \quad (44)$$

- Free end

$$\bar{M}(\zeta) = (h^2 q - 1) \bar{W}''(\zeta) - h^2 \Lambda^2 \bar{W}(\zeta) = 0 \quad (45)$$

$$\bar{V}(\zeta) = (h^2 q - 1) \bar{W}'''(\zeta) - (h^2 \Lambda^2 + q) \bar{W}'(\zeta) = 0 \quad (46)$$

It is worth of mentioning that the mode shapes of the nanobeams can be obtained through Eq. (19) in which $w(x, t)$ is the mode shape for the beam deformation, and $W(x)$ is mode function. Once, it is needed to find $W(x)$ which is the dimensional mode function or $W(\zeta)$ which is the non-dimensional mode function (see Eq. (22)) and then multiply it by the time function $e^{i\omega t}$ to obtain the dimensional mode shape $w(x, t)$ or the non-dimensional mode shape $w(\zeta, t)$.

1 3. RESULTS AND DISCUSSION

In this paper, the effect of the thermal load as well as the nonlocal parameter, the crack severity, and the crack position is investigated for three different types of the beam supports such as the simply supported, the clamped-clamped, and the

clamped-simply supported. The case study of the research of (Roostai and Haghpanahi, 2014) is considered in this paper but in their work the length of the beams was not considered in calculations. In this paper, the length of the nanobeam is $L = 1 \text{ nm}$ and the height of the beams is $t = 0.1 \text{ nm}$ and the amount of $A/I = 12/t^2$. The amount of the coefficient of thermal expansion is considered as $\alpha_x = -1.6 \times 10^{-6}$ for

temperature change equal to or lower than the room temperature and $\alpha_x = 1.1 \times 10^{-6}$ for temperature change higher than the room temperature. As for this work $\alpha_x = -1.6 \times 10^{-6}$ for $T = 0 \text{ K}, T = 100 \text{ K}$, and $T = 200 \text{ K}$, while $\alpha_x = 1.1 \times 10^{-6}$ for the temperature changes higher than the room temperature such as $T = 400 \text{ K}$ and $T = 600 \text{ K}$ (Yao and Han, 2006). The

cases of non-cracked beams are recalculated and the results are tabulated in Table 1 to verify the accuracy of this study and they well agree to the

indicated reference (Phadikar and Pradhan, 2010, Roostai and Haghpanahi, 2014).

Table 1. Comparison of the frequencies of non-cracked simply supported nanobeam. ($e_0 a = T = 0$).

h	Mode1			Mode2			Mode3		
	Present	(Phadikar and Pradhan, 2010)	(Roostai and Haghpanahi, 2014)	Present	(Phadikar and Pradhan, 2010)	(Roostai and Haghpanahi, 2014)	Present	(Phadikar and Pradhan, 2010)	(Roostai and Haghpanahi, 2014)
0	9.8696	9.8697	9.8700	39.4784	39.4848	39.4780	88.8264	88.8984	88.8260
1	2.9936	2.9936	2.9940	6.2051	6.2061	6.2050	9.3722	9.3796	9.3720

3.1 Simply supported beam (SS)

In this paper, the simply supported (SS) beam is analyzed for the cases of non-cracked and single cracked for the different temperature values. For the case of the single-cracked, the first crack location is $\zeta = 0.3$ and then, the second position for the crack is chosen to be $\zeta = 0.5$. The results of the beam with a crack at $\zeta = 0.5$ are presented Table 2 and they are graphically shown in Figs. 2 and 3. As a crack is introduced to the beam, the natural frequencies decrease and as much as the crack severity increases, the natural frequencies decrease as already reported in several researches (Abdullah et al., 2020a, Hussein et al., 2020). This is because of a reduction in the bending stiffness of the nanomaterial beam due to the presence of the crack. When $T = 0$ K (temperature change), it means that the temperature does not have any effects on the frequencies. As much as the temperature increases the frequencies decrease and when the temperature increases to a temperature value higher than the room temperature, the frequencies increase. It is obvious from the results that the temperature can have great effects on the frequencies specially when the amount of the nonlocal parameter increases.

It is observed that when the effects of the crack and the nonlocal parameter are zero (i.e., $K = 0$ and $h = 0$), the temperature change can affect the natural frequencies, but its effect on the first frequency is very significant comparing to the second and third frequencies. As much as the crack severity increases, the frequencies of all modes decrease as shown in Figs. 2, 3, and 4. The reason is that by increasing the crack severity, amount of the additional flexibility introduced by the crack, increases. The highest range of decrease

in the frequencies occurs when $h = 1$, $K = 0.075$, and $T = 200$, as it is seen the crack severity and the nonlocal parameter are high values while the value of the temperature change is value lower than the room temperature. The frequencies increase when the crack location is near to the fixed end. Comparing the frequencies of two different crack locations of 0.3 and 0.5, it is observed that when the crack distances from the fixed end, the frequencies of all modes decrease. It means that in the case of the crack location of $\zeta = 0.3$, the frequencies are higher than the frequencies of the case in which the crack locates at $\zeta = 0.5$. It is worth mentioning that the second mode is independent of the crack severity value when the crack locates at $\zeta = 0.5$. The reason is for the fact that the crack location is exactly the position of one of the nodes of the second mode, consequently, the second mode is independent of the crack severity change in this case because, the amount of the bending slope at both sides of the point on which the crack locates, will be the same, and there will not be any changes and any jumps in the bending slope. The third mode frequencies are not very sensitive to the crack severity when the amount of the nonlocal parameter is higher than zero as shown in Figs 3 and 4, while the first and the second modes are very sensitive to the crack severity at high temperatures and high nonlocal parameter values. Fig. 5 shows a comparison of the first frequency of the different crack locations, in which the amount of K and h are the highest and it is seen that the frequencies are dependent on the crack location. It is interesting to see that at the temperatures equal to or lower than the room temperature, the frequencies of the case of the crack location of

$\zeta = 0.3$ are higher than the case of the crack location at $\zeta = 0.5$. At the temperature values higher than the room temperature, the frequency

values of the case of the crack location of $\zeta = 0.5$ are higher than the case of the crack location of $\zeta = 0.3$.

Table 2. First three dimensionless frequency parameters for a single-cracked simply supported beam with different nonlocal parameter h and different crack severity K . Crack position $\zeta = 0.5$.

h	T	$K = 0$			$K = 0.0086$			$K = 0.0325$			$K = 0.075$		
		Λ_1	Λ_2	Λ_3	Λ_1	Λ_2	Λ_3	Λ_1	Λ_2	Λ_3	Λ_1	Λ_2	Λ_3
0	0	9.8696	39.4784	88.8264	9.7858	39.4784	88.0824	9.5634	39.4784	86.2059	9.2023	39.4784	83.4368
	100	9.6266	39.2377	88.5861	9.5491	39.2377	87.8483	9.3437	39.2377	85.9880	9.0111	39.2377	83.2448
	200	9.3773	38.9955	88.3451	9.3063	38.9955	87.6134	9.1186	38.9955	85.7694	8.8156	38.9955	83.0523
	400	10.5089	40.1330	89.4840	10.4090	40.1330	88.7233	10.1430	40.1330	86.8023	9.7076	40.1330	83.9622
	600	10.8144	40.4563	89.8110	10.7070	40.4563	89.0420	10.4206	40.4563	87.0989	9.9501	40.4563	84.2234
0.5	0	5.3003	11.9744	18.4390	5.2551	11.9744	18.2819	5.1342	11.9744	17.8632	4.9349	11.9744	17.1943
	100	4.8327	11.1551	17.2441	4.7997	11.1551	17.1279	4.7110	11.1551	16.8167	4.5637	11.1551	16.3101
	200	4.3149	10.2707	15.9600	4.2915	10.2707	15.8755	4.2286	10.2707	15.6482	4.1236	10.2707	15.2732
	400	6.4125	13.9820	21.3833	6.3102	13.9820	21.0269	6.0403	13.9820	20.1066	5.6106	13.9820	18.7881
	600	6.9018	14.8847	22.7128	6.7417	14.8847	22.1529	6.3268	14.8847	20.7660	5.6903	14.8847	19.0097
1	0	2.9936	6.2051	9.3722	2.9681	6.2051	9.2923	2.8996	6.2051	9.0793	2.7861	6.2051	8.7389
	100	2.0553	4.4219	6.7232	2.0487	4.4219	6.7027	2.0307	4.4219	6.6469	1.9996	4.4219	6.5515
	200	0.7771	1.6013	2.3071	0.7771	1.6010	2.3071	0.7771	1.6001	2.3071	0.7771	1.5985	2.3071
	400	4.6893	9.5192	14.3209	4.9808	9.5192	15.2226	5.8963	9.5192	17.0368	7.2657	9.5192	18.0715
	600	5.3389	10.8014	16.2393	5.4728	10.8014	16.6665	5.8712	10.8014	17.8188	6.6411	10.8014	19.2409

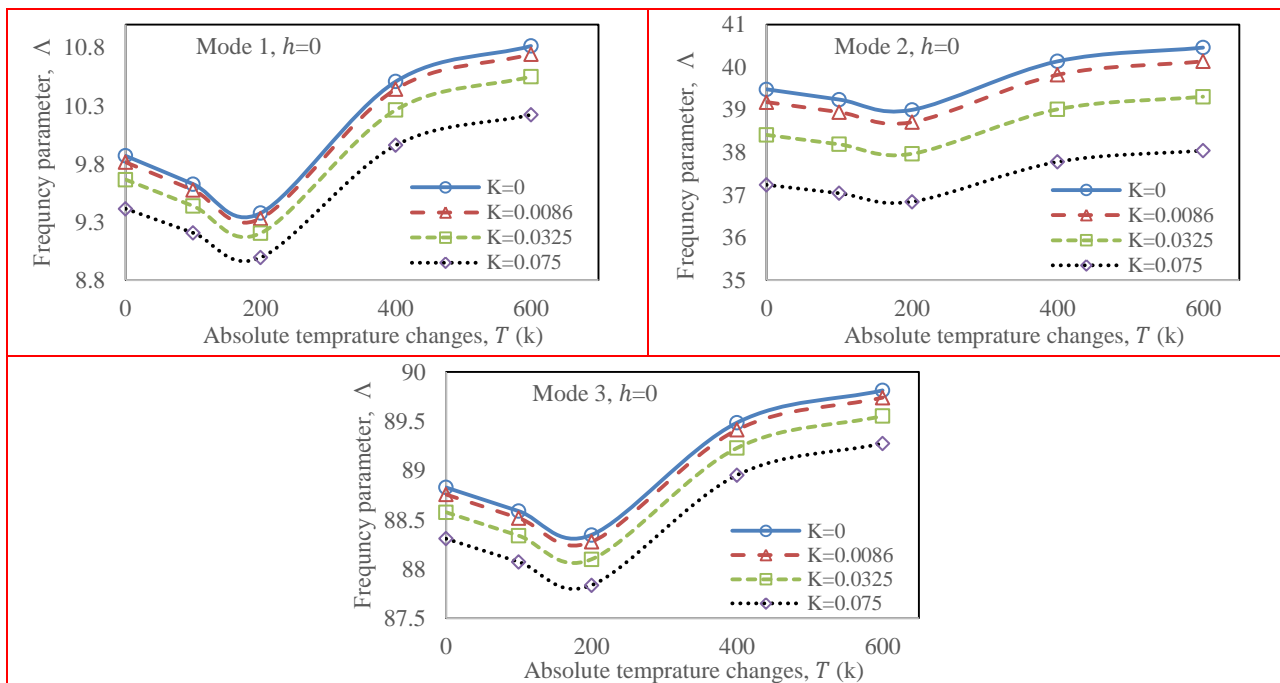


Figure 2. First three frequency parameters for a single-cracked SS beam versus temperature changes. ($\zeta = 0.3$ and $h = 0$).

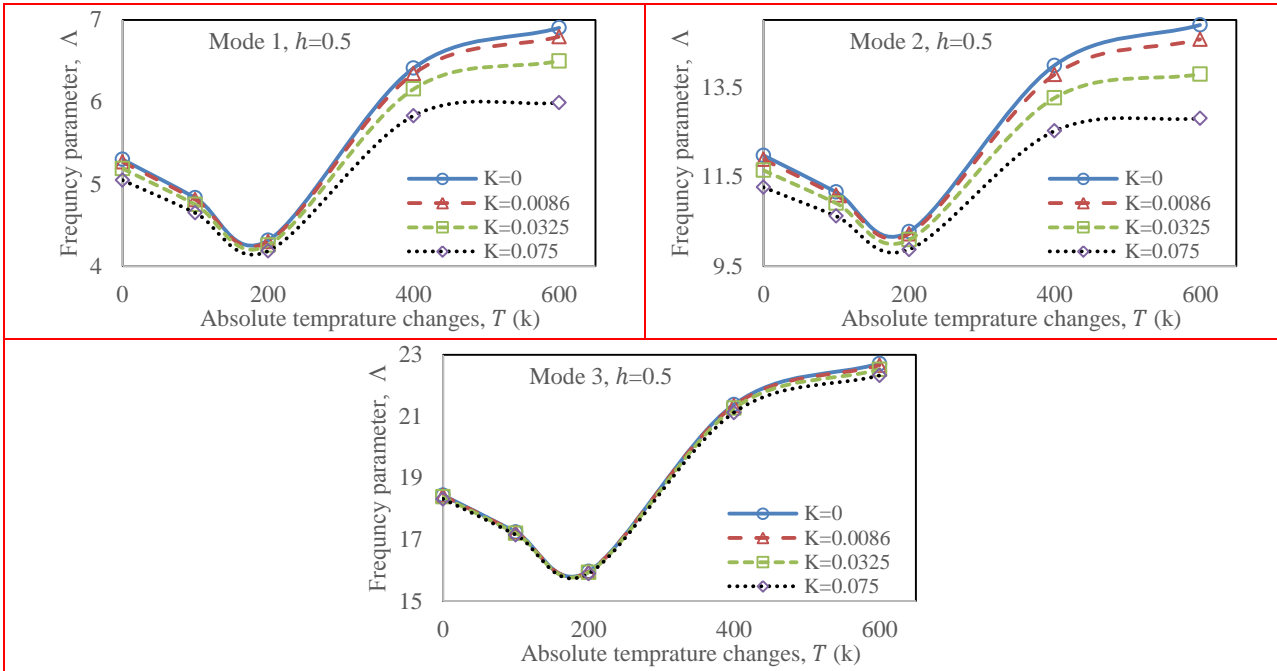


Figure 3. First three frequency parameters for a single-cracked SS beam versus temperature changes. ($\zeta = 0.3$ and $h = 0.5$).

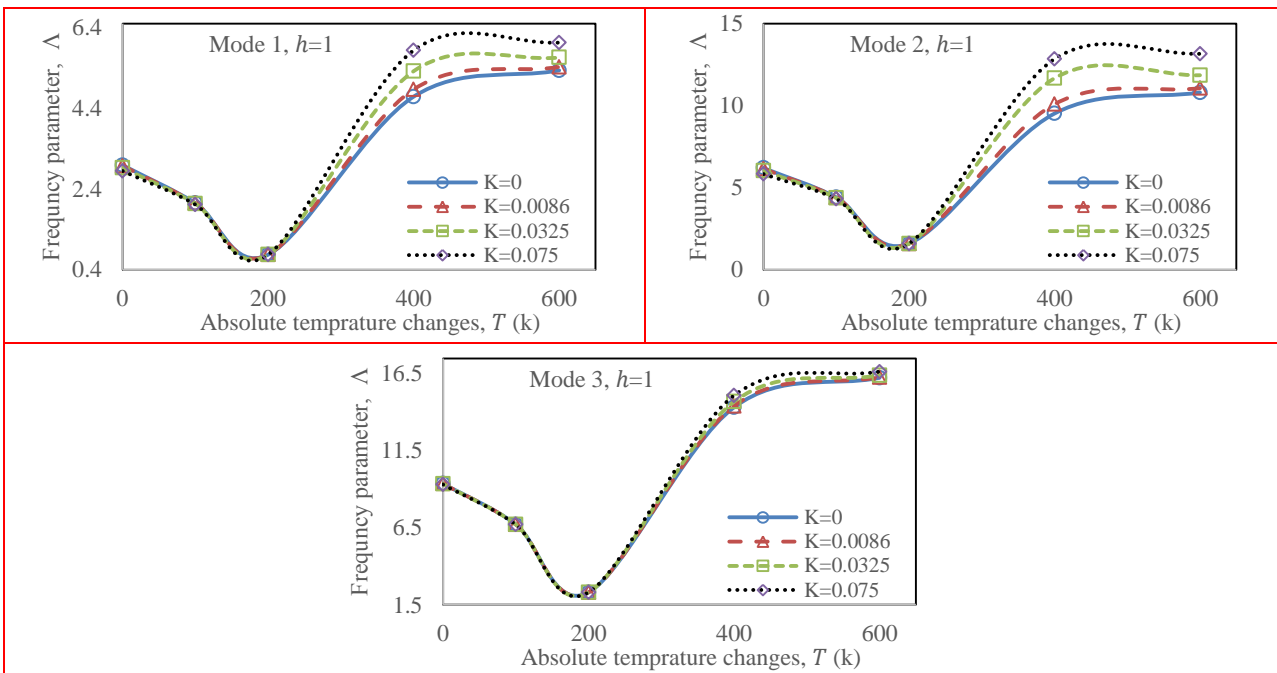


Figure 4. First three frequency parameters for a single-cracked SS beam versus temperature changes. ($\zeta = 0.3$ and $h = 1$).

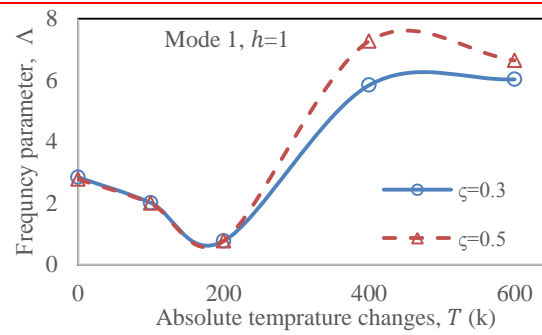


Figure 5. A comparison of the first frequency parameter of a single-cracked SS beam versus temperature changes for two cases of crack positions $\zeta = 0.3$ and $\zeta = 0.5$. ($K = 0.075$ and $h = 1$).

3.2 Clamped-clamped beam (CC)

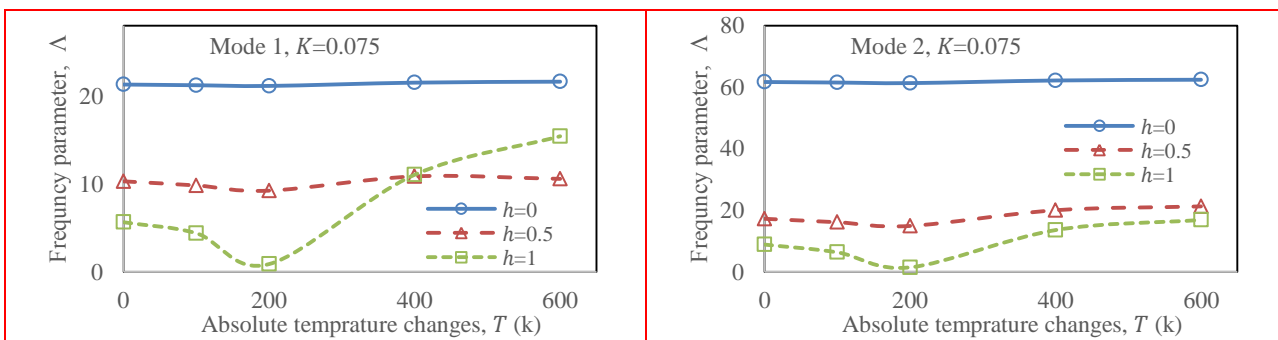
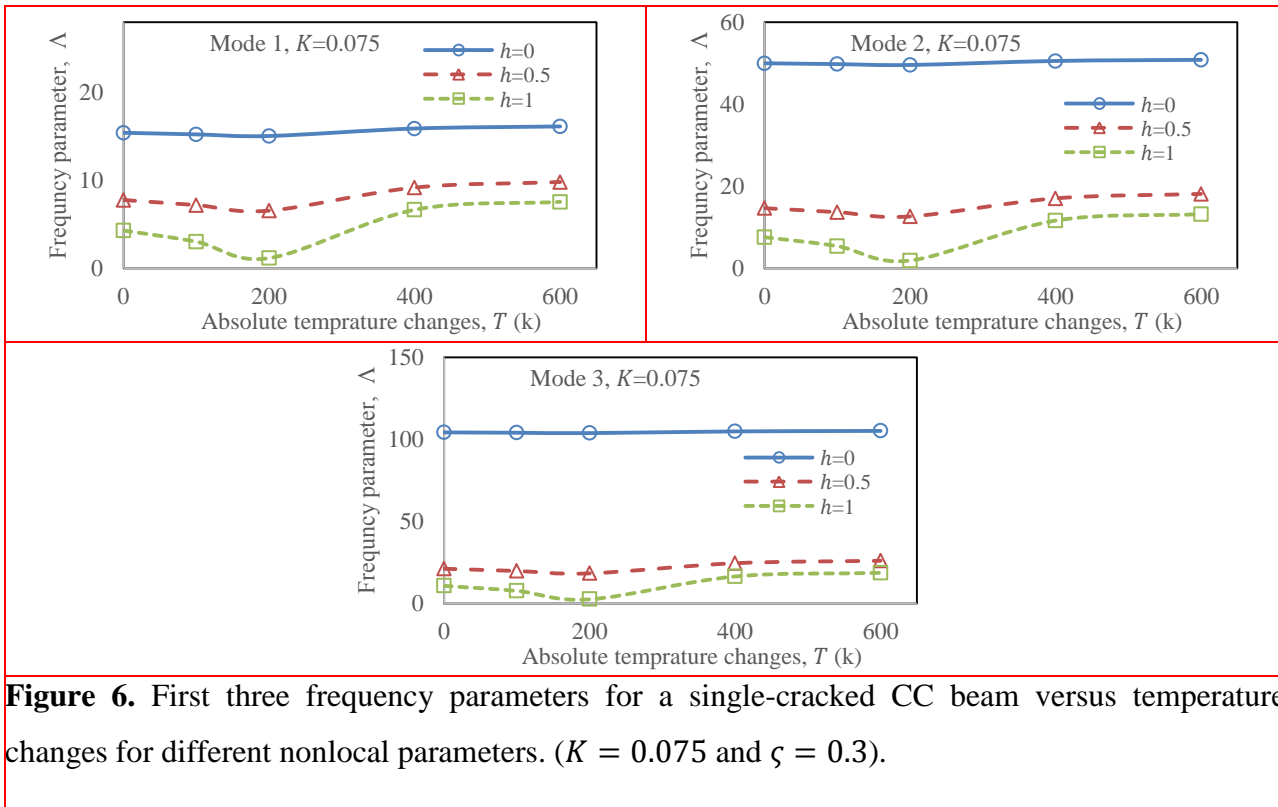
The first three frequency parameters of the clamped-clamped (CC) nanomaterial beams are presented in Table 3 for the crack location of $\zeta = 0.5$. When the crack location is $\zeta = 0.3$, all of the frequency modes decrease by increasing the crack severity, and when the nonlocal scale effect parameter (h) increases, the frequencies of all modes decrease. But, when the crack location is $\zeta = 0.5$, the frequency of the second mode remains constant while the crack severity increases at a certain temperature. The reason is that the point $\zeta = 0.5$ is a node for the second mode. As the nonlocal parameter increases, the frequencies of all modes decrease. The range of the decrease in the frequencies for the crack location of $\zeta = 0.5$ is greater than the case of the crack location of $\zeta = 0.3$ in contrast to non-cracked beam. This is because as the crack location reaches farther from the fixed end, the induced flexibility is increased. However, in some of the cases, especially at higher temperatures, the reverse phenomenon occurs. It is observed that the frequencies are sensitive to the temperature changes. As for the temperatures lower than the room temperature, the frequencies decrease and for the temperatures higher than the room temperature, the frequencies increase. As the crack severity and the nonlocal parameter reach the high values at any temperature, the changes of the frequencies will be significant. The third mode frequency is very sensitive to the temperature changes. The first mode sensitivity to the

temperature changes is not as sensitivity as the second and the third modes as shown in Figs. 6 and 7. For a single crack located at $\zeta = 0.3$, the frequencies of the cases $h = 0.5$ and $h = 1$ approach to each other at the temperatures higher than the room temperature (i.e., $T = 400K$ and $T = 600K$). Thus, it is observed that when the temperature and the crack severity have high values, the effect of the nonzero nonlocal parameter is not significant because the effect of h will be smaller than the effect of the thermal load q in Eqs. (36), (39), and (40). As the amount of the first mode frequency for the higher nonlocal parameter (i.e. $h = 1$) is a higher value in contrast to the lower nonlocal parameter ($h = 0.5$) as shown in Fig. 7. When the temperature is equal to or lower than the room temperature before decreasing to $T = 200K$, the value of the first mode frequency in the case of the crack location of $\zeta = 0.3$ is higher than the case of the crack location of $\zeta = 0.5$, but when the temperature reaches a value higher than the room temperature the frequency of the case of the crack location of $\zeta = 0.5$ is higher than the case of the crack location of $\zeta = 0.3$ but for the second mode the reverse phenomenon occurs as shown in Fig. 8. Thus, when the temperature change effect is taken into account, it is observed that a higher value of the nonlocal parameter does not always cause in decreasing the frequencies, and the location of the crack is not always a tool to predict whether a certain frequency decreases or it increases.

Table 3. First three dimensionless frequency parameters for a single-cracked clamped-clamped beam with different nonlocal parameter h and different crack severity K . Crack position $\zeta = 0.5$.

h	T	$K = 0$			$K = 0.0086$			$K = 0.0325$			$K = 0.075$		
		Λ_1	Λ_2	Λ_3	Λ_1	Λ_2	Λ_3	Λ_1	Λ_2	Λ_3	Λ_1	Λ_2	Λ_3

	0	22.3733	61.6728	120.9034	22.2335	61.6728	119.8822	21.8691	61.6728	117.3354	21.2965	61.6728	113.6559
	100	22.2409	61.4933	120.6405	22.1078	61.4933	119.6917	21.7610	61.4933	117.1609	21.2173	61.4933	113.5064
0	200	22.1076	61.3133	120.5445	21.9812	61.3133	119.5009	21.6524	61.3133	116.9860	21.1379	61.3133	113.3566
	400	22.7330	62.1635	121.4406	22.5755	62.1635	120.4044	22.1634	62.1635	117.8140	21.5124	62.1635	114.0656
	600	22.9106	62.4073	121.7239	22.7444	62.4073	120.6646	22.3091	62.4073	118.0525	21.6195	62.4073	114.2697
	0	10.9914	17.2730	24.3324	10.9047	17.2730	24.1141	10.6738	17.2730	23.5350	10.2985	17.2730	22.6344
	100	10.2395	16.1487	22.7861	10.1892	16.1487	22.5961	10.0540	16.1487	22.0911	9.8296	16.1487	21.2915
0.5	200	9.4279	14.9400	21.1269	9.4049	14.9400	20.9613	9.3428	14.9400	20.5204	9.2380	14.9400	19.8130
	400	12.8338	20.0422	28.1501	12.5643	20.0422	27.8130	11.8758	20.0422	26.9344	10.8613	20.0422	25.6996
	600	13.6622	21.2921	29.8766	13.2035	21.2921	29.4290	12.0827	21.2921	28.2942	10.5783	21.2921	26.8740
	0	6.0566	8.8954	12.4530	6.0061	8.8954	12.3451	5.8712	8.8954	12.0590	5.6509	8.8954	11.6158
	100	4.3161	6.3778	8.9537	4.3256	6.3778	8.8813	4.3520	6.3778	8.6870	4.3994	6.3778	8.3656
1	200	2.2934	3.6257	4.9190	0.7744	1.4915	2.2722	0.8185	1.4915	2.2148	0.8981	1.4915	2.1155
	400	9.2913	13.5968	19.0020	10.5666	13.5968	18.9908	10.8138	13.5968	18.9612	11.0453	13.5968	18.9114
	600	10.5428	15.4189	21.5425	11.1657	15.4189	21.4415	13.1919	15.4189	21.1618	15.4189	16.8933	20.5632



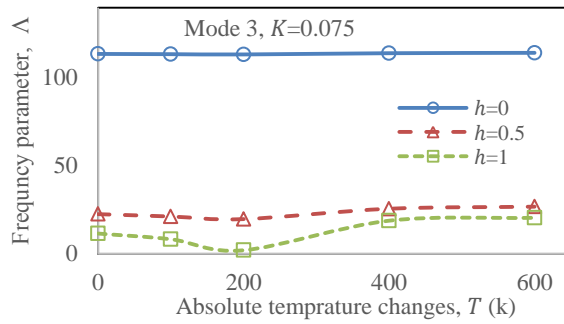


Figure 7. First three frequency parameters for a single-cracked CC beam versus temperature changes for different nonlocal parameters. ($K = 0.075$ and $\zeta = 0.5$).

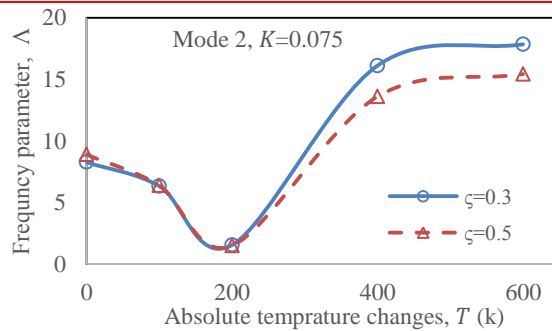
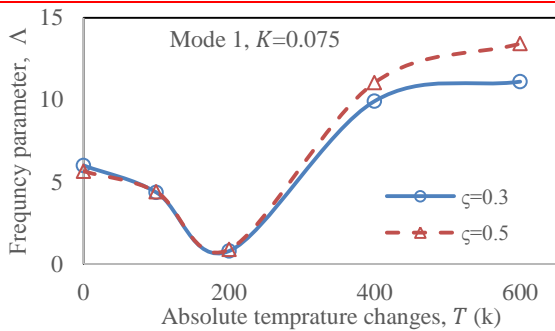


Figure 8. Comparison of first and second frequency parameters of a single-cracked CC beam with temperature changes for two cases of crack positions $\zeta = 0.3$ and $\zeta = 0.5$. ($K = 0.075$ and $h = 1$).

3.3 Clamped-simply supported beam (CS)

The results of the clamped-simply supported (CS) beam are presented in Table 4 for the single crack located at $\zeta = 0.5$. The non-cracked beam results are obtained when the amount of crack severity K is equal to zero. The frequencies of all modes decrease by decreasing the temperature to the values lower than the room temperature and they increase when the temperature increases to the temperature values higher than the room temperature. But when the amount of the nonlocal parameter increases, the changes in the frequencies become more significant as shown in Fig. 9. Modes one and three of the case of the crack location at $\zeta = 0.3$ are higher than the case in which the crack locates at $\zeta = 0.5$, but the second mode of the case of the crack location of

$\zeta = 0.5$ is higher than the case of the crack location of $\zeta = 0.3$. The frequencies of all modes decrease at the temperatures lower than the room temperature and they increase with increasing at the high temperatures. Increasing the nonlocal parameter h results in decreasing the frequencies of all modes as shown in Fig. 10. As the crack severity increases, the frequencies decrease because the flexibility of the beam increases due to the crack; but when the nonlocal parameter h reaches to a very high value (i.e., $h = 1$), the frequencies increase with increasing the crack severity at the temperatures lower and higher than the room temperature but not at the room temperature.

Table 4. First three dimensionless frequency parameters for a single-cracked clamped-simply supported beam with different nonlocal parameter h and different crack severity K . Crack position $\zeta = 0.5$.

h	T	$K = 0$			$K = 0.0086$			$K = 0.0325$			$K = 0.075$		
		Λ_1	Λ_2	Λ_3	Λ_1	Λ_2	Λ_3	Λ_1	Λ_2	Λ_3	Λ_1	Λ_2	Λ_3
	0	15.4182	49.9649	104.2477	15.3288	49.9094	103.4959	15.0935	49.7639	101.6045	14.7167	49.5332	98.8313
	100	15.2379	49.7584	104.0310	15.1544	49.7036	103.2847	14.9350	49.5599	101.4079	14.5847	49.3321	98.6577

0	200	15.0552	49.5510	103.8138	14.9778	49.4969	103.0731	14.7746	49.3550	101.2109	14.4510	49.1304	98.4837
	400	15.9028	50.5283	104.8414	15.7977	50.4711	104.0744	15.5199	50.3209	102.1430	15.0723	50.0821	99.3065
	600	16.1393	50.8076	105.1369	16.0266	50.7496	104.3625	15.7283	50.5972	102.4111	15.2461	50.3544	99.5430
0.5	0	7.7837	14.6881	21.2563	7.7398	14.6431	21.1435	7.6214	14.5202	20.8386	7.4238	14.3127	20.3449
	100	7.2026	13.7153	19.8943	7.1748	13.6872	19.8012	7.0994	13.6100	19.5474	6.9733	13.4766	19.1255
	200	6.5704	12.6680	18.4319	6.5548	12.6527	18.3548	6.5126	12.6103	18.1435	6.4418	12.5358	17.7850
1	0	4.3182	7.6211	10.8300	4.2944	7.5940	10.7770	4.2294	7.5202	10.6338	4.1198	7.3964	10.4028
	100	3.0419	5.4530	7.7792	3.0424	5.4550	7.7508	3.0438	5.4609	7.6707	3.0461	5.4718	7.5260
	200	1.1785	1.9350	2.6263	1.1835	1.9277	2.6185	1.1983	1.9065	2.5987	1.2275	1.8657	2.5687
1	400	6.6694	11.6634	16.5351	7.0993	12.2607	16.7464	8.0572	13.8723	17.4086	8.7643	14.8493	18.1202
	600	7.5761	13.2292	18.7476	7.7945	13.5192	18.8106	8.3741	14.4573	19.0170	9.1640	15.9868	19.4641

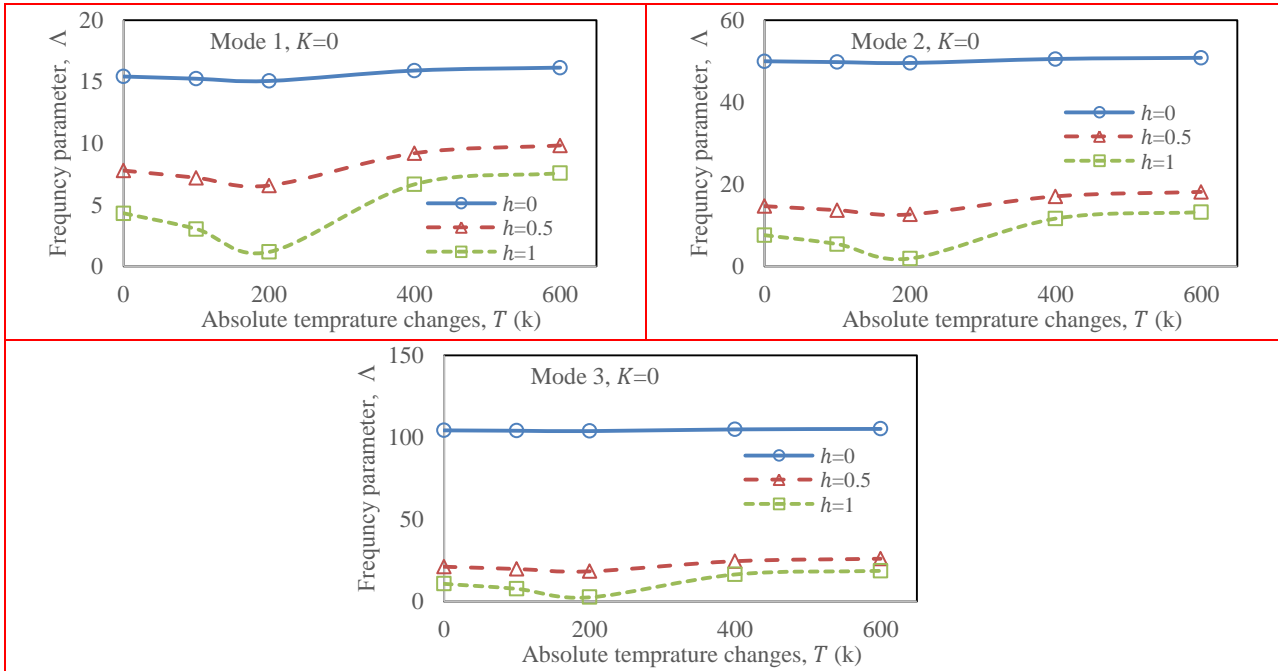


Figure 9. First three frequency parameters for a non-cracked CS beam versus temperature changes for different nonlocal parameters.

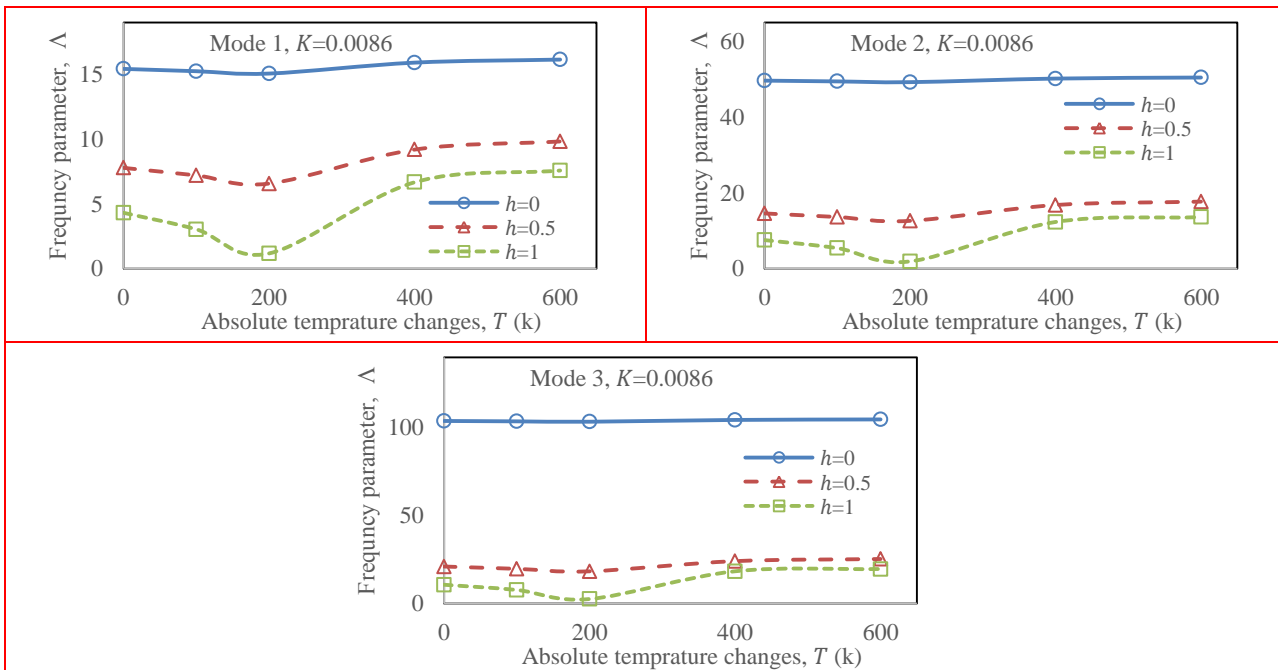


Figure 10. First three frequency parameters for a single-cracked CS beam versus temperature changes for different nonlocal parameters. ($K = 0.0086$ and $\zeta = 0.3$).

It is observed that the clamped-clamped nanomaterial beam is stronger than the simply supported and the clamped-simply supported beams and its frequencies are higher than the two other cases even when the crack severity and the nonlocal parameter reach to high values at any

temperature except the very low temperatures (i.e., $T = 200$). In the very low temperatures, approximately frequencies of all of the different beam supports approach each other as shown in Fig. 11.

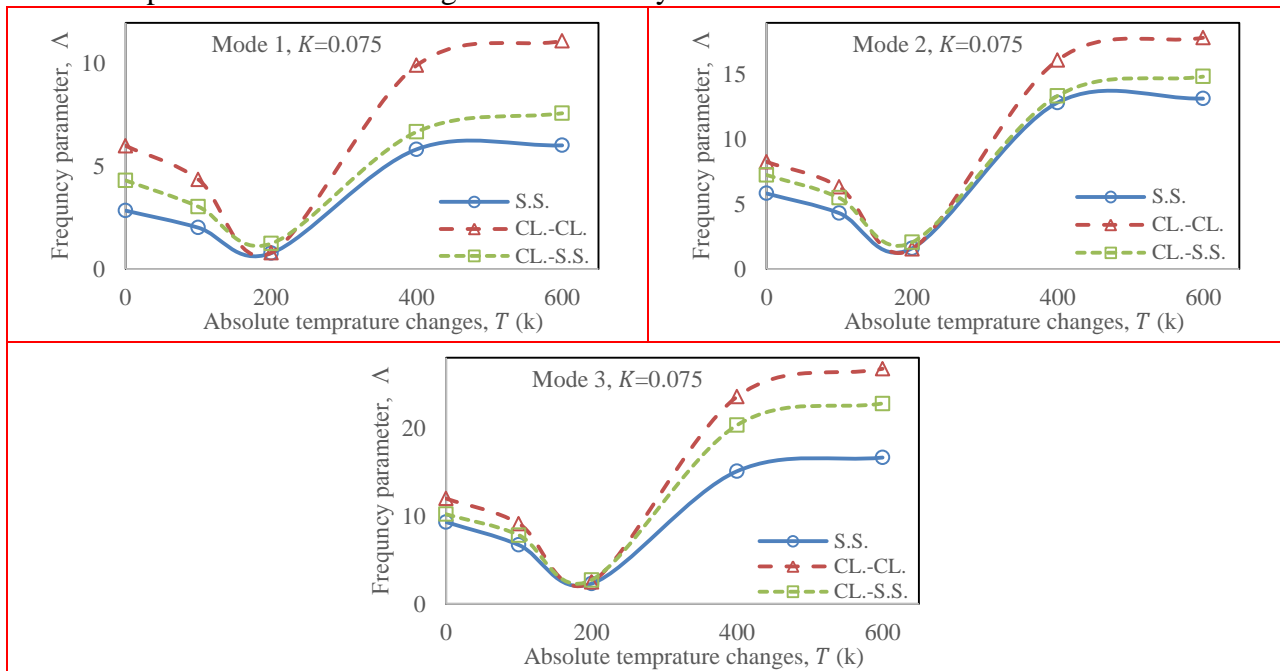


Figure 11. A comparison of first three frequency parameters of a single-cracked beam for different supports of SS, CC, and CS versus temperature changes. ($h = 1$, $K = 0.075$, and $\zeta = 0.3$).

There is an investigation performed by (Ebrahimi and Mahmoodi, 2018) in which the effect of the thermal load on the multi-cracked beams is determined. Their investigation includes some significant mistakes that will change all of the results. They have not considered the thermal load in the compatibility equations which belong to the continuity of the shear and the continuity of the

bending moment at the crack location. They have used the continuity equations of the bending moment and the shear force which belong to the cases in which the thermal load does not exist. The compatibility equations that have been used by them are as

- Continuity of the bending moment

$$\bar{W}_1''(b) + \Lambda^2 h^2 \bar{W}_1(b) = \bar{W}_2''(b) + \Lambda^2 h^2 \bar{W}_2(b) \tag{47}$$

- Continuity of the shear force

$$\bar{W}_1'''(b) + \Lambda^2 h^2 \bar{W}_1'(b) = \bar{W}_2'''(b) + \Lambda^2 h^2 \bar{W}_2'(b) \tag{48}$$

As it is seen in the Eqs. (47) and (48), there is not any parameter which belongs to the thermal load, that is the reason why their results were not sensitive to the temperature changes and they were not true. The true compatibility equations for the continuity of the bending moment and the continuity of the shear force are derived from the

equation of motion and they are already obtained as Eqs. (39) and (40) in which q is the dimensionless thermal load as

- Continuity of the bending moment

$$(h^2 q - 1) \bar{W}_1''(b) - \Lambda^2 h^2 \bar{W}_1(b) = (h^2 q - 1) \bar{W}_2''(b) - \Lambda^2 h^2 \bar{W}_2(b)$$

- Continuity of the shear force

$$(h^2 q - 1) \bar{W}_1'''(b) - (\Lambda^2 h^2 + q) \bar{W}_1'(b) = (h^2 q - 1) \bar{W}_2'''(b) - (\Lambda^2 h^2 + q) \bar{W}_2'(b)$$

2 4. CONCLUSIONS

Following conclusions have been made from the results obtained throughout the present study:

- For the temperature change values higher than the room temperature, the frequencies are increased. Vice versa, for the temperature change values lower than the room temperature, the frequencies are decreased.
- Increasing the crack severity does not always result in decreasing the frequencies, because of the temperature changes. As the crack severity is increased the frequencies decrease because the flexibility of the beam is increased. But when the nonlocal parameter h is reached to a very high value (i.e. $h = 1$), the frequencies increase with increasing the crack severity at the temperatures lower and higher than the room temperature but not at the room temperature.

It is concluded that a higher value of the nonlocal parameter does not always cause in decreasing the frequencies and the location of the crack is not always a tool to predict whether a certain frequency will be decreased or it will be increased because the temperature change has great effects on the frequencies.

The outcomes of the investigation demonstrate that the clamped-clamped beam is stronger than the simply supported and the clamped simply supported beams and its frequencies are higher than the two other cases even when the crack severity and the nonlocal parameter reach the high values at any temperature except the very low temperatures (i.e. $T = 200$) in which approximately frequencies of all of the different beam supports approach each other.

Acknowledgments

The authors are grateful to the University of Salahaddin-Erbil for supporting this work.

Conflict of interests

The author declares that they have no competing interests.

Funding

The author declares that this paper does not have any funder.

References

- ABDULLAH, S. S., HOSSEINI-HASHEMI, S., HUSSEIN, N. A. & NAZEMNEZHAD, R. 2020a. Effect of temperature on vibration of cracked single-walled carbon nanotubes embedded in an elastic medium under different boundary conditions. *Mechanics Based Design of Structures and Machines*, 1-26.
- ABDULLAH, S. S., HOSSEINI-HASHEMI, S., HUSSEIN, N. A. & NAZEMNEZHAD, R. 2020b. Thermal stress and magnetic effects on nonlinear vibration of nanobeams embedded in nonlinear elastic medium. *Journal of Thermal Stresses*, 1-17.
- AKBAS, S. D. 2018. Forced vibration analysis of cracked functionally graded microbeams. *ADVANCES IN NANO RESEARCH*, 6, 39-55.
- AKBAŞ, Ş. D. 2017. Forced vibration analysis of functionally graded nanobeams. *International Journal of Applied Mechanics*, 9, 1750100.
- EBRAHIMI, F. & BARATI, M. R. 2018. Vibration analysis of smart piezoelectrically actuated nanobeams subjected to magneto-electrical field in thermal environment. *Journal of Vibration and Control*, 24, 549-564.
- EBRAHIMI, F. & MAHMOODI, F. 2018. Vibration analysis of carbon nanotubes with multiple cracks in thermal environment. *Advances in nano research*, 6, 57-80.
- EBRAHIMI, F. & SALARI, E. 2015. Nonlocal thermo-mechanical vibration analysis of functionally graded nanobeams in thermal environment. *Acta Astronautica*, 113, 29-50.
- ELTAHER, M., MAHMOUD, F., ASSIE, A. & MELETIS, E. 2013. Coupling effects of nonlocal and surface energy on vibration analysis of nanobeams. *Applied Mathematics and Computation*, 224, 760-774.
- ERINGEN, A. C. 1972. Nonlocal polar elastic continua. *International journal of engineering science*, 10, 1-16.
- ERINGEN, A. C. 1983. On differential equations of nonlocal elasticity and solutions of screw dislocation and surface waves. *Journal of applied physics*, 54, 4703-4710.
- ERINGEN, A. C. & EDELEN, D. 1972. On nonlocal elasticity. *International Journal of Engineering Science*, 10, 233-248.
- HAGHSHENAS, A. & ARANI, A. G. 2014. Nonlocal vibration of a piezoelectric polymeric nanoplate carrying nanoparticle via Mindlin plate theory. *Proceedings of the Institution of Mechanical Engineers, Part C: Journal of Mechanical Engineering Science*, 228, 907-920.
- HOSSEINI-HASHEMI, S., KERMAJANI, M. & NAZEMNEZHAD, R. 2015. An analytical study on the buckling and free vibration of rectangular

- nanoplates using nonlocal third-order shear deformation plate theory. *European Journal of Mechanics-A/Solids*, 51, 29-43.
- HUSSEIN, N. A., RASUL, H. A. & ABDULLAH, S. S. 2020. The free vibration analysis of multi-cracked nanobeam using nonlocal elasticity theory. *Zanco Journal of Pure and Applied Sciences*, 32, 39-54.
- KARLIČIĆ, D., CAJIĆ, M., MURMU, T. & ADHIKARI, S. 2015a. Nonlocal longitudinal vibration of viscoelastic coupled double-nanorod systems. *European Journal of Mechanics-A/Solids*, 49, 183-196.
- KARLIČIĆ, D., JOVANOVIĆ, D., KOZIĆ, P. & CAJIĆ, M. 2015b. Thermal and magnetic effects on the vibration of a cracked nanobeam embedded in an elastic medium. *Journal of Mechanics of Materials and Structures*, 10, 43-62.
- LOGHMANI, M. & YAZDI, M. R. H. 2018. An analytical method for free vibration of multi cracked and stepped nonlocal nanobeams based on wave approach. *Results in Physics*, 11, 166-181.
- LOYA, J., LÓPEZ-PUENTE, J., ZAERA, R. & FERNÁNDEZ-SÁEZ, J. 2009. Free transverse vibrations of cracked nanobeams using a nonlocal elasticity model. *Journal of Applied Physics*, 105, 044309.
- LU, P., LEE, H., LU, C. & ZHANG, P. 2006. Dynamic properties of flexural beams using a nonlocal elasticity model. *Journal of applied physics*, 99, 073510.
- MURMU, T. & PRADHAN, S. 2009. Thermo-mechanical vibration of a single-walled carbon nanotube embedded in an elastic medium based on nonlocal elasticity theory. *Computational Materials Science*, 46, 854-859.
- MURMU, T. & PRADHAN, S. 2010. Thermal effects on the stability of embedded carbon nanotubes. *Computational Materials Science*, 47, 721-726.
- NAZEMNEZHAD, R. & HOSSEINI-HASHEMI, S. 2017. Exact solution for large amplitude flexural vibration of nanobeams using nonlocal Euler-Bernoulli theory. *Journal of theoretical and applied mechanics*, 55, 649-658.
- PEDDIESON, J., BUCHANAN, G. R. & MCNITT, R. P. 2003. Application of nonlocal continuum models to nanotechnology. *International Journal of Engineering Science*, 41, 305-312.
- PHADIKAR, J. & PRADHAN, S. 2010. Variational formulation and finite element analysis for nonlocal elastic nanobeams and nanoplates. *Computational materials science*, 49, 492-499.
- REDDY, J. 2007. Nonlocal theories for bending, buckling and vibration of beams. *International Journal of Engineering Science*, 45, 288-307.
- REDDY, J. & PANG, S. 2008. Nonlocal continuum theories of beams for the analysis of carbon nanotubes. *Journal of Applied Physics*, 103, 023511.
- ROOSTAI, H. & HAGHPANAHI, M. 2014. Vibration of nanobeams of different boundary conditions with multiple cracks based on nonlocal elasticity theory. *Applied Mathematical Modelling*, 38, 1159-1169.
- SOLTANPOUR, M., GHADIRI, M., YAZDI, A. & SAFI, M. 2017. Free transverse vibration analysis of size dependent Timoshenko FG cracked nanobeams resting on elastic medium. *Microsystem Technologies*, 23, 1813-1830.
- WANG, Q. 2005. Wave propagation in carbon nanotubes via nonlocal continuum mechanics. *Journal of Applied Physics*, 98, 124301.
- WANG, Q. & VARADAN, V. 2006. Vibration of carbon nanotubes studied using nonlocal continuum mechanics. *Smart Materials and Structures*, 15, 659.
- WANG, Q., ZHOU, G. & LIN, K. 2006. Scale effect on wave propagation of double-walled carbon nanotubes. *International Journal of Solids and Structures*, 43, 6071-6084.
- YAO, X. & HAN, Q. 2006. Buckling analysis of multiwalled carbon nanotubes under torsional load coupling with temperature change. *Journal of Engineering Materials and Technology*, 128, 419-427.
- ZHANG, Y., LIU, G. & XIE, X. 2005. Free transverse vibrations of double-walled carbon nanotubes using a theory of nonlocal elasticity. *Physical Review B*, 71, 195404.
- ZHANG, Y., LIU, X. & ZHAO, J. 2008. Influence of temperature change on column buckling of multiwalled carbon nanotubes. *Physics Letters A*, 372, 1676-1681.